

# Characterization of normal facial features and their association with genes



A thesis submitted in accordance with the conditions governing  
candidates for the degree of *Philosophiae Doctor* in Cardiff  
University

By

ARSHED M. TOMA  
BDS, MSc (Ortho.), MPhil

March 2014  
Cardiff University  
School of Dentistry  
Department of Applied Clinical  
Research and Public Health

Wales, UK

## ACKNOWLEDGEMENTS

The production of this thesis would not have been possible without the guidance and help of many people who shared their expertise in various ways through the course of the study.

First of all I would like to thank my principal supervisor, Professor Stephen Richmond, without him none of this would have happened. Also, I would like to deeply thank my supervisor, Dr Alexei Zhurov, who put me on the path towards the completion of this project.

I also like to convey my gratitude to my co-supervisors: Dr Rebecca Playle for her statistical guidance in the various stages of this project, and Professors David Marshall and Paul Rosin from the School of Computer Science and Informatics for their knowledge and guidance regarding the computational aspects of this work.

I also like to send special gratitude to Patricia Stewart (Grace) and Susan Bryant for their tremendous efforts in preparing the 3D images for analysis; and from ALSPAC, I would like to thank Kate Northstone for managing the data, and also Dr Lavinia Paternoster and Dr David Evans for their help and guidance regarding the genetic aspects of this project.

I also take the opportunity to thank Dr Hashmat Popat, who as a fellow PhD candidate shared ideas and expertise in 3D imaging and acted as support during the course of the study. I also like to thank my colleagues in work: Dr Jelena Djordjevic and Mr Jamie Deans for their kind support and continuous encouragement during my study. I would like to thank everybody in the School of Dentistry who keep asking about my PhD progress.

I am extremely grateful to all the participants who took part in this study, the midwives for their help in recruiting them, and the whole ALSPAC team.

Finally, I must thank my parents and brothers for their love and continuous support and encouragement during my study.

## ABSTRACT

*Background:* Craniofacial morphology has been reported to be highly heritable, but little is known about which genetic variants influence normal facial variation in the general population.

*Aim:* To identify facial variation and explore phenotype-genotype associations in a 15-year-old population (2514 females and 2233 males).

*Subjects and Methods:* The subjects involved in this study were recruited from the Avon Longitudinal Study of Parents and Children (ALSPAC). Three-dimensional (3D) facial images were obtained for each subject using two high-resolution Konica Minolta laser scanners. Twenty-one reproducible facial soft tissue landmarks and one constructed mid-endocanthion point (men) were identified and their coordinates were recorded. The 3D facial images were registered using Procrustes analysis (with and without scaling). Principal Component Analysis (PCA) was then employed to identify independent groups 'principal components, PCs' of correlated landmark coordinates that represent key facial features contributing to normal facial variation. A novel surface-based method of facial averaging was employed to visualize facial variation. Facial parameters (distances, angles, and ratios) were also generated using facial landmarks. Sex prediction based on facial parameters was explored using discriminant function analysis. A discovery-phase genome-wide association analysis (GWAS) was carried out for 2,185 ALSPAC subjects and replication was undertaken in a further 1,622 ALSPAC individuals.

*Results:* 14 (unscaled) and 17 (scaled) PCs were identified explaining 82% of the total variance in facial form and shape. 250 facial parameters were derived (90 distances, 118 angles, 42 ratios). 24 facial parameters were found to provide sex prediction efficiency of over 70%, 23 of these parameters are distances that describe variation in face height, nose width, and prominence of various facial structures. 54 distances associated with previous reported high heritability and the 14 (unscaled) PCs were included in the discovery-phase GWAS. Four genetic associations with the distances were identified in the discovery analysis, and one of these, the association between the common 'intronic' SNP (rs7559271) in *PAX3* gene on chromosome (2) and the nasion to mid-endocanthion 3D distance (n-men) was replicated strongly ( $p = 4 \times 10^{-7}$ ). *PAX3* gene encodes a transcription factor that plays crucial role in fetal development including craniofacial bones. *PAX3* contains two DNA-binding domains, a paired-box domain and a homeodomain. The protein made from *PAX3* gene directs the activity of other genes that signal neural crest cells to form specialized tissues such as craniofacial bones. *PAX3* different mutations may lead to non-functional *PAX3* polypeptides and destroy the ability of the *PAX3* proteins to bind to DNA and regulate the activity of other genes to form bones and other specific tissues.

*Conclusions:* The variation in facial form and shape can be accurately quantified and visualized as a multidimensional statistical continuum with respect to the principal components. The derived PCs may be useful to identify and classify faces according to a scale of normality. A strong genetic association was identified between the common SNP (rs7559271) in *PAX3* gene on chromosome (2) and the nasion to mid-endocanthion 3D distance (n-men). Variation in this distance leads to nasal bridge prominence.

## CONTENTS

<b>ABSTRACT.....</b>	<b>IV</b>
<b>CONTENTS.....</b>	<b>V</b>
<b>LIST OF FIGURES.....</b>	<b>XI</b>
<b>LIST OF TABLES.....</b>	<b>XIII</b>
<b>CHAPTER 1 (INTRODUCTION).....</b>	<b>1</b>
<b>1.1 Introduction.....</b>	<b>2</b>
<b>1.2 Aims and objectives of the study.....</b>	<b>6</b>
<b>1.2.1 Aim.....</b>	<b>6</b>
<b>1.2.2 Objectives.....</b>	<b>6</b>
<b>CHAPTER 2 (LITERATURE REVIEW).....</b>	<b>7</b>
<b>2.1 Facial morphology (historical overview).....</b>	<b>8</b>
<b>2.1.1 The enlightenment period.....</b>	<b>12</b>
<b>2.2 Analysis of facial morphology.....</b>	<b>14</b>
<b>2.2.1 Anthroposcopy (visual assessment).....</b>	<b>14</b>
<b>2.2.2 Anthropometry.....</b>	<b>16</b>
<b>2.3 Two-dimensional (2D) imaging techniques.....</b>	<b>24</b>
<b>2.3.1 Photographs.....</b>	<b>24</b>
<b>2.3.2 Lateral skull radiographs (cephalometry).....</b>	<b>26</b>
<b>2.4 Three-dimensional imaging techniques.....</b>	<b>27</b>
<b>2.4.1 Moiré topography and contour photography.....</b>	<b>29</b>
<b>2.4.2 Stereophotogrammetry.....</b>	<b>30</b>
<b>2.4.3 3D cephalometry.....</b>	<b>34</b>
<b>2.4.4 Morphanalysis.....</b>	<b>35</b>
<b>2.4.5 CT- assisted 3D imaging.....</b>	<b>35</b>
<b>2.4.6 Cone beam computed tomography (CBCT).....</b>	<b>36</b>
<b>2.4.7 Stereolithography.....</b>	<b>37</b>
<b>2.4.8 3D Laser scanning.....</b>	<b>38</b>
<b>2.4.9 3D facial morphometry.....</b>	<b>41</b>
<b>2.4.10 3D ultrasonography.....</b>	<b>41</b>
<b>2.5 General 3D concepts.....</b>	<b>42</b>

2.6	The use of three-dimensional imaging in.....	52
	orthodontics	
2.6.1	Optical surface scanning.....	52
2.6.2	Forensic science.....	55
2.6.3	Prediction of jaw surgery.....	56
2.6.4	Analysis of surface shape.....	56
2.6.5	Ultrasound.....	57
2.7	Facial dysmorphology.....	58
2.8	The role of 3D imaging in visualizing facial.....	59
	dysmorphology	
2.9	The clinical assessment of craniofacial.....	60
	dysmorphology	
2.10	The role of genes in human craniofacial variation....	65
2.10.1	Basic concepts.....	65
2.10.2	Genetic and environmental effects on craniofacial....	68
	morphology	
2.10.2.1	Genetic expression in craniofacial development.....	71
2.10.2.2	Recent advances in analysing the effects of.....	82
	genes on craniofacial morphology	
2.10.2.3	Studies that have identified hereditary, genetic &....	85
	environmental effects on craniofacial morphology	
2.11	Genotype-phenotype association analyses.....	90
2.12	The international HapMap project.....	95
2.13	General applications of human genome-wide.....	96
	association studies	
2.14	Principles of GWAS.....	99
2.14.1	Genotyping platforms.....	99
2.14.2	DNA pooling.....	99
2.14.3	SNP annotation.....	100
2.14.4	Genotype-calling algorithms.....	100
2.15	Hardware and software for quality control and.....	101
	statistical analysis	

2.15.1	Hardware.....	101
2.15.2	Software.....	102
2.15.3	Data structures.....	102
2.16	Quality control.....	103
2.16.1	Genotyping reproducibility and accuracy.....	103
2.16.1.1	Mendelian inconsistencies.....	103
2.17	Descriptive analyses of the GWAS data.....	104
2.17.1	Missingness.....	104
2.17.2	Allele frequencies.....	104
2.17.3	Genotype frequencies and HWE assessment.....	105
2.17.3.1	HWE (Hardy-Weinberg Equilibrium).....	105
2.18	Association analyses of GWAS data.....	105
2.19	Visualizing GWAS results.....	106
2.19.1	QQ plot.....	106
2.19.2	HaploView and genome graphs.....	106
2.20	GWAS discovery and replication phases.....	107
2.20.1	Linkage disequilibrium.....	109
2.21	Corrections for multiple testing.....	109
2.22	Statistical power.....	110
2.22.1	Factors influencing power.....	111
2.23	Summary of the GWAS process.....	112
<b>CHAPTER 3 (REPRODUCIBILITY OF FACIAL LANDMARKS).....</b>		<b>113</b>
3.1	Introduction.....	114
3.2	Subjects and methods.....	117
3.2.1	Project sample (cohort).....	117
3.2.1.1	Reproducibility sample.....	118
3.2.2	Image capture.....	118
3.2.3	Camera calibration.....	120
3.2.4	Processing the 3D facial scans.....	121
3.2.4.1	Removing extraneous data.....	121
3.2.4.2	Smoothing left and right shells.....	121
3.2.4.3	Registering left and right shells (alignment).....	122

3.2.4.4	Merging left and right shells, and filling holes.....	123
3.2.5	Identifying facial soft tissue landmarks.....	124
3.2.6	Statistical analyses.....	127
3.2.6.1	Reliability of the laser scanning procedure.....	127
3.2.6.2	Reliability of facial data capture.....	129
3.2.6.3	Assessment of reproducibility sample.....	129
3.2.6.4	Assessment of the reproducibility of facial landmarks	130
3.3	Results.....	131
3.3.1	Project sample.....	131
3.3.2	Reliability of facial data capture.....	132
3.3.3	Assessment of reproducibility sample.....	134
3.3.4	Assessment of the reproducibility of facial landmarks	135
3.4	Discussion.....	143
3.4.1	Reliability of the laser scanning procedure.....	143
3.4.2	Reproducibility of facial soft tissue landmarks.....	145
3.4.3	Summary.....	147
3.5	Conclusions.....	148
<b>CHAPTER 4 (EXPLORING FACIAL VARIATION).....</b>		<b>149</b>
4.1	Introduction.....	150
4.2	Subjects and methods.....	153
4.2.1	Sample.....	153
4.2.2	Statistical analyses.....	153
4.2.2.1	Analysis of 3D landmark data.....	153
4.2.2.1.1	Generalized Procrustes Analysis.....	153
4.2.2.1.2	Principal Component Analysis.....	158
4.2.2.1.3	Extracting parameters from PCs.....	163
4.2.2.1.3.1	Purposes of the PC parameters.....	163
4.3	Results.....	164
4.3.1	Analysis of 3D landmark data.....	164
4.3.1.1	Generalized Procrustes Analysis.....	164

4.3.1.2	PCA of the unscaled dataset.....	168
4.3.1.3	PCA of the scaled dataset.....	172
4.3.2	Normal ranges (scales) of facial variation.....	178
4.4	Discussion.....	181
4.4.1	Summary.....	181
4.4.2	Comparison with previous studies.....	182
4.4.3	PCA (unscaled dataset).....	184
4.4.4	PCA (scaled dataset).....	188
4.4.5	Impacts of the study.....	189
4.5	Conclusions.....	190
<b>CHAPTER 5 (VISUALIZING FACIAL VARIATION).....</b>		<b>192</b>
5.1	Introduction.....	193
5.2	Subjects and methods.....	197
5.2.1	Sample.....	197
5.2.2	Visualizing facial variation.....	197
5.2.2.1	Averaging facial images scaled based on the..... average centroid size	198
5.3	Results.....	202
5.3.1	Visualizing facial variation.....	202
5.4	Discussion.....	204
5.5	Conclusions.....	207
<b>CHAPTER 6 (GENDER PREDICTION).....</b>		<b>208</b>
6.1	Introduction.....	209
6.2	Subjects and methods.....	213
6.2.1	Sample.....	213
6.2.2	Facial parameters.....	213
6.2.3	Statistical analysis.....	214
6.2.3.1	Gender prediction efficiency.....	214
6.3	Results.....	216
6.3.1	Facial parameters.....	216
6.3.2	Gender prediction efficiency.....	216
6.4	Discussion.....	218

6.5	Conclusions.....	223
<b>CHAPTER 7 (FACIAL VARIATION AND GENETIC ASSOCIATION)...</b>		
7.1	Introduction.....	225
7.2	Subjects and methods.....	229
7.2.1	Sample.....	229
7.2.1.1	Genetic data.....	229
7.2.1.2	Facial data.....	229
7.2.2	Statistical analysis.....	230
7.2.2.1	Genome-wide association study (GWAS).....	232
7.2.3	Visualizing facial phenotypic variation.....	233
	influenced by genetic effect	
7.3	Results.....	234
7.3.1	Genome-wide association study (GWAS).....	234
7.3.2	Visualizing facial phenotypic variation.....	240
	influenced by genetic effect	
7.4	Discussion.....	244
7.5	Conclusions.....	249
<b>CHAPTER 8 (GENERAL DISCUSSION).....</b>		
8.1	Genome-wide association studies:.....	251
	failures and successes	
8.2	Pleiotropic nature of genes.....	255
<b>CHAPTER 9 (CONCLUSIONS).....</b>		
<b>CHAPTER 10 (FUTURE WORK).....</b>		
<b>CHAPTER 11 (REFERENCES).....</b>		
<b>CONTRIBUTIONS.....</b>		
<b>APPENDIX.....</b>		

## LIST OF FIGURES

Figure 2.1. The facial profiles of temperament.....	9
Figure 2.2. The twelve front facial types that describe personalities...	10
Figure 2.3. Anthropometric facial soft tissue landmarks.....	21
Figure 2.4. Types of facial anthropometric measurements.....	22
Figure 2.5. Manhattan plot.....	97
Figure 2.6. Summary of the GWAS process.....	112
Figure 3.1. Image capture.....	119
Figure 3.2. Camera calibration.....	120
Figure 3.3. Processing 3D facial scans.....	123
Figure 3.4. Normalisation of facial shells to natural head posture...	125
Figure 3.5. Facial soft tissue landmarks.....	126
Figure 3.6. Registration of the left and right facial shells.....	128
Figure 3.7. Project sample.....	132
Figure 3.8. Reproducibility of landmark identification.....	135
Figure 4.1. Generalized Procrustes Analysis.....	158
Figure 4.2. Two-standard-deviation envelopes for 21 facial landmarks (unscaled dataset)	165
Figure 4.3. Two-standard-deviation envelopes for 21 facial landmarks (scaled dataset)	166
Figure 4.4. Two-standard-deviation envelopes for 21 facial landmarks, superimposed unscaled versus scaled	167
Figure 4.5. Facial morphology variation revealed by the first three PCs extracted from the unscaled dataset	172
Figure 4.6. Facial morphology variation revealed by the first three PCs extracted from the scaled dataset	177
Figure 5.1. Registration of the facial shells.....	198
Figure 5.2. Point cloud generated by the averaging procedure.....	199
Figure 5.3. Constructed average face.....	201
Figure 5.4. Average faces constructed to illustrate variation revealed by PCs 1–3 (unscaled)	203
Figure 6.1. Assessment of gender prediction efficiency.....	215

- Figure 7.1. Facial landmarks and parameters analysed in.....231  
the genome-wide association study**
- Figure 7.2. Deconstruction of the 3D n-men phenotype into its.....239  
constituent dimensional distances**
- Figure 7.3. The average faces constructed to show the effect of.....242  
variation of the n-men 3D distance on the face shape**
- Figure 7.4. Superimposition of average phenotypes for *PAX3*.....243  
different genotypes (G allele)**

## LIST OF TABLES

Table 2.1. Classification of facial shape.....	19
Table 2.2. Genetic expression studies in craniofacial development...	74
Table 2.3. Hereditary, genetic, and environmental effects on.....	86
craniofacial morphology	
Table 3.1. Summary analysis of facial data capture (Group 1).....	133
Table 3.2. Summary analysis of facial data capture (Group 2).....	133
Table 3.3. Assessment of reproducibility sample.....	134
Table 3.4. Reproducibility of landmark identification.....	137
(summary analysis for total sample)	
Table 3.5. Reproducibility of landmark identification.....	140
(detailed analysis for sample divided by gender)	
Table 3.6. Ranking of facial landmarks according to the linear.....	142
distance between two spatial positions	
Table 4.1. PCA of unscaled landmark data.....	169
Table 4.2. Brief description of the principal components.....	170
extracted for the total sample (unscaled dataset)	
Table 4.3. PCA of scaled landmark data.....	173
Table 4.4. Brief description of the principal components.....	174
extracted for the total sample (scaled dataset)	
Table 4.5. Normal ranges (scales) of facial variation derived.....	179
from unscaled principal components	
Table 4.6. Normal ranges (scales) of facial variation derived.....	180
from scaled principal components	
Table 6.1. Gender prediction efficiency (>70%) provided by.....	217
24 facial parameters derived from the unscaled dataset	
Table 7.1. Discovery phase and replication phase results for.....	237
the four associations with $p < 5 \times 10^{-8}$	
Table 7.2. The association between rs7559271 and the.....	238
distances and angles relating to the n-men distance	
Table 7.3. The association between rs7559271 and the.....	240
scaled n-men distance in the combined sample	

# Chapter 1

## Introduction

## **1.1 Introduction**

The development of normal facial features and characteristics is a result of genetic and environmental interactions. There has been a longstanding debate of their relative contributions to facial development; some people suggesting greater influence from genetics (Lundström, 1948, 1954, 1984) while others proposing greater influence from environment (Corruccini, 1991, 1999; Rose and Roblee, 2009), and to some extent it depends on the feature or the anomaly that is under consideration.

Certain facial features have been reported to be highly heritable (60-70%) particularly face height and chin prominence (e.g. Hapsburgs chin) (Lundström, 1948, 1954, 1984; Lundström and McWilliam, 1987, 1988; Manfredi *et al.*, 1997; Hunter *et al.*, 1970; Watnick, 1972; Nakata *et al.*, 1973; Kohn, 1991; Savoye *et al.*, 1998; Johannsdottir *et al.*, 2005; Baydas *et al.*, 2007; Carels *et al.*, 2001). Surprisingly, at the time of this study there is no clear evidence associating genes with normal facial features in the general population.

The influence of the environment can be obvious in relation to trauma, fractures, burns and surgical intervention (scarring); each can have a major effect on facial growth and development depending on the severity and duration of the impact (James, 1985; Thaller and McDonald, 2004). Urban pollution (e.g. vehicle exhaust fumes and cleaning products) has also been reported to influence facial development via inhibiting nasal

airways and creating mouth breathing habit which results in a longer face (Linder-Aronson, 1970, 1979; Linder-Aronson *et al.*, 1986; McNamara, 1981; Kerr *et al.*, 1989; Corruccini *et al.*, 1985; and Bresolin *et al.*, 1983). However, the environmental effects on face shape are likely to be subtle as significant effects would be visually obvious and easily identifiable.

The interactions between genetic and environmental factors are more complex with the majority of research directed to the development of craniofacial anomalies (e.g. cleft lip and palate). The maternal environment is critical during foetal development. It is known that maternal diet (lack of zinc, reduced folic acid, and alcohol), smoking as well as air quality, allergens and noxious substances can have a major effect on foetus facial and holistic development (Zhu *et al.*, 2009; Jones and Smith, 1973).

Foetal development is split into three trimesters involving very rapid and complex developmental processes that can be affected by environmental and genetic interactions. It has been reported that viral infection in the first trimester may be associated with an increased risk of a cleft (Acs *et al.*, 2005). In addition, alcohol intake in the first trimester can affect educational attainment as well as facial features (Jones and Smith, 1973).

Twin studies provide an opportunity to explore the relative contributions of genetics and environment on the individuals' facial and holistic development. Monozygotic (MZ) twins share nearly 100% of their genes, which means

that differences between the twins may be as a result of the environment. Dizygotic (DZ) twins share about 50% of their genes. Heritability can be estimated by quantifying the extent of the genetic contribution to phenotypic variation, with proportions ranging from 0 (no heritability) to 1 (totally inherited).

In genetic epidemiology, genome-wide association studies (GWAS) examine the common genetic variants in different individuals to see if any variant is associated with a specific trait. GWAS typically focus on associations between single-nucleotide polymorphisms (SNPs) and traits like major diseases (Keith, 2007; Amos *et al.*, 2008).

Epigenetics can be defined as the study of heritable changes in gene expression that are not due to changes in DNA sequence. The discovery that differentiated cells can be artificially reprogrammed into induced pluripotent stem cells by a small set of transcription factors has opened up exciting medical prospects and provided good opportunity to investigate how stable epigenetic states are built and reversed. Diverse biological properties can be affected by epigenetic mechanisms. Epigenetic events at the local level during tooth formation can lead to quite major differences in the final appearance of the dentitions of MZ co-twins (Townsend *et al.*, 2005, 2012; Townsend and Brook, 2008, 2013). Epigenetic transcriptional enhancers, a major category of functional non-coding DNA - are likely involved in many developmental and disease-relevant processes (Visel *et al.*, 2009, 2013).

To examine the role of distant-acting enhancers in the craniofacial development, recent experiments on mice demonstrated the functional importance of enhancers in defining face and skull morphology (Attanasio *et al.*, 2013). Thousands of regions in the genome act like switches for the many genes that code for facial features, such as the shape of the skull or size of the nose.

In order to explore the influences of genetics and environment on facial variation it is important to standardise the capture and analysis of facial surface morphology. The important principles are to capture surface detail and this is best achieved using three-dimensional imaging (Moss *et al.*, 2003; Nute and Moss, 2000; Hennessy and Moss, 2001; McCance *et al.*, 1993; Kau and Richmond, 2008; Ferrario *et al.*, 1998a, b, 1999a, b, c; Hennessy *et al.*, 2002, 2004, 2005, 2007, 2010; Hammond *et al.*, 2004, 2005; Shaner *et al.*, 2000; Bugaighis *et al.*, 2010; Toma *et al.*, 2008, 2012); good definitions of facial landmarks to ensure accuracy and reliability (Coward *et al.*, 1997; Gwilliam *et al.*, 2006; Baik *et al.*, 2006, 2007; Toma *et al.*, 2009); and recruit a large population to investigate genetic and environmental influences on facial morphology (Paternoster *et al.*, 2012). The aim of this study is to identify facial variation and explore phenotype-genotype associations in a 15-year-old population.

## **1.2 Aims and objectives of the study**

### **1.2.1 Aim:**

- To identify facial variation and explore phenotype-genotype associations in a 15-year-old population

### **1.2.2 Objectives:**

- Objectively evaluate the feasibility of using laser scanning in a large population study
- Assess the reliability of facial surface landmarks
- Determine principal features of facial variation
- Identify appropriate methods to visualise and categorise facial variation
- Explore facial features which may be used to identify gender
- Explore phenotype/genotype associations related to facial features

## Chapter 2

### Literature Review

## **2. Literature Review**

### **2.1 Facial morphology (historical overview)**

The face is the body part that epitomises a human person and is required for identification of individuals. It can even be argued that the human face is a cultural construct that cannot be studied without taking into account cultural values (Berrios, 2003), and yet the human face is an anatomical entity that arose through biological processes during the course of human evolution and its structure is regulated by the same embryological, anatomical and physiological mechanisms that form all other parts of the body (Henneberg *et al.*, 2003).

Morphology as a system of diagnosis and therapeutics has been in existence for thousand years. A brief historical overview is useful in identifying the sources of morphology and describing its place in the development of current diagnostic approaches. The earliest depictions of morphology may be found in three sources: the Sphinx, the first book of Ezekiel, and Genesis. The study of facial morphology is believed to have originated in ancient Egypt more than 4500 years ago. The eastern morphology of India and China is different and may have a different origin. The evidence of an Egyptian origin can be seen in its Sphinxes. The Sphinxes have been categorized by type: criosphinx (lion body with ram head), hierocosphinx (lion body with hawk head), and androsphinx (lion body with human head, like the Great Sphinx). Thus they portray the four creatures (man, lion, eagle, and ram or ox) that are used in morphology to denote the four temperamental/humoral types, these are: bilious (man),

lymphatic (ox), sanguine (lion), and nervous (eagle). These humoral types are read by looking at the profile of the person (Figure 2.1).

References to morphology can be found in the Bible. The river that comes out of the Garden of Eden and parts into four (Genesis 2:10) is believed to refer to the four flows of energy, which is the most succinct way of defining temperaments. The creature with four faces, those of a man, a lion, an ox, and an eagle is also described in Ezekiel 1:10.

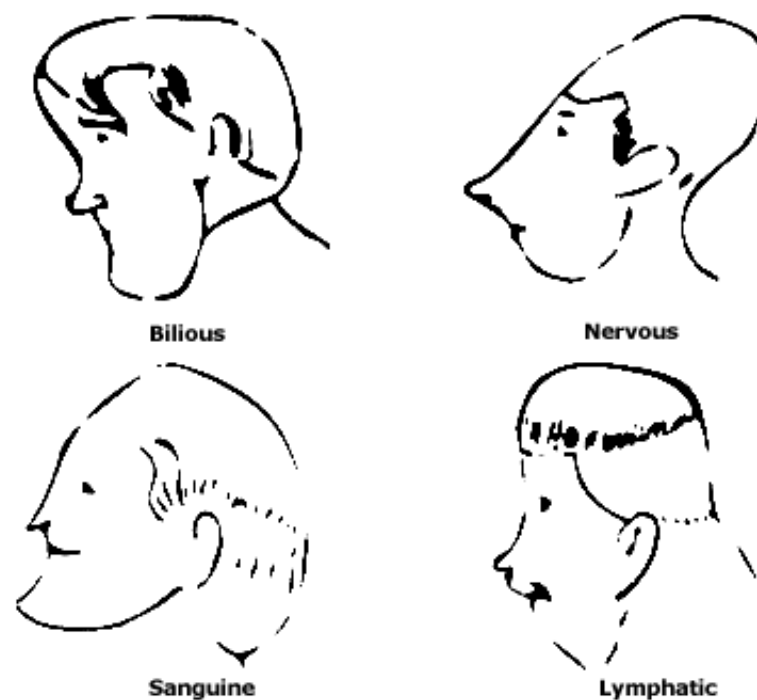


Figure 2.1. The facial profiles of temperament

Morphology holds that these four types, in various combinations, constitute the profiles of all human beings. It also holds that each type has invariable characteristics associated with it; that is any person who displays a predominance of one temperamental type must have certain behavioural, psychological and physiological characteristics.

As for the personality types, they are defined by the front shape of the face. According to morphology, there are twelve such shapes, all of geometrical design, that, like the temperamental types, are invariable throughout the world no matter what race. Ancient Greece has contributed the twelve geometrical faces that describe personalities. They were originally named with the names of Greek gods and later renamed by their Roman counterparts. The twelve front facial types that describe personalities are shown in Figure 2.2.

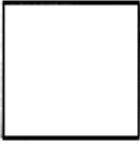
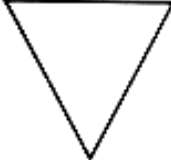
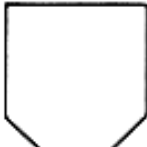
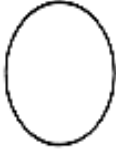
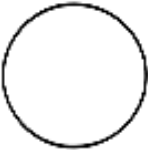
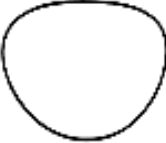
<b>Square</b>  Eos/Earth	<b>Rectangle</b>  Aries/Mars	<b>Short Triangle</b>  Hermes/Mercury	<b>Long Triangle</b>  Hermes/Mercury
<b>Trapezoid</b>  Chronos/Saturn	<b>Long Trapezoid</b>  Uranus	<b>Hexagon</b>  Pluto	<b>Reverse Trapezoid</b>  Zeus/Jupiter
<b>Oval</b>  Apollo/Sun	<b>Circle</b>  Ios/Moon	<b>Lozenge</b>  Aphrodite/Venus	<b>Oblong</b>  Poseidon/Neptune

Figure 2.2. The twelve front facial types that describe personalities

In modern times we don't see these "pure" facial types anymore because of admixture. In the ancient days, certain tribes and cultures shared a predominance of one facial type through inbreeding and intermarriage. The Greek sculptors carved these pure types and manifested them as the

gods and goddesses of ancient Greece, later adopted by the ancient Romans. The statues were placed in public view so as to remind the members of the population of the proper proportions and measures that obtained for each particular type.

The earliest recorded facial proportional analysis is in the Greek neoclassical canons (c. 450 BC). The neoclassical canons have been used for many years to describe the facial morphological features. However, the world is made up of many heterogeneous societies comprising multiple ethnic groups, and seeking orthodontic treatment, maxillofacial surgery and facial cosmetic surgery has become very popular within these societies. Facial proportional analysis is a critical component of the pre-operative assessment procedure. For surgical procedures, these “ideal” proportions derived from the Greek neoclassical perspective are not applicable for a significant portion of the world’s different ethnic groups. Several studies have found significant differences between the facial proportions described in the neoclassical canons and the mean values of these proportions in modern non-Caucasian ethnic populations (Farkas, 1994; Farkas and Munro, 1987; Farkas and Kolar, 1987a, b; Farkas *et al.*, 2000; Zacharopoulos *et al.*, 2012). These investigations into the applicability of the neoclassical facial canons have generated substantial amounts of data on the facial dimensions of numerous ethnic groups. Notably, Farkas and his associates (2005) compiled the single most comprehensive craniometric survey of ethnic groups from multiple regions around the world.

### **2.1.1 *The enlightenment period***

The age of enlightenment beginning in the 18<sup>th</sup> century brought interest in objective descriptions of the world, this included the human face. In the Netherlands, Peter Camper introduced the first system of measurements describing numerically variation of human faces. Camper (1770) was known for his theory of the “facial angle” originally in connection with two lectures he gave in Amsterdam to art students on beauty and portraiture, he determined that modern humans had facial angles between 70° and 80°, with African and Asian angles closer to 70°, and European angles closer to 80°. According to Camper’s new portraiture technique, the facial angle is formed by drawing two lines: one horizontally from the nostril to the ear; and the other perpendicularly from the advancing part of the upper jawbone to the most prominent part of the forehead.

Blumenbach (1776) followed soon thereafter by establishing the formal system of craniometry (analysis of human skulls). On the basis of his craniometrical research, Blumenbach divided the human species into five races: Caucasian or white race, Mongolian or yellow race, Malayan or brown race, Negroid or black race, and American or red race.

Blumenbach’s craniometric system has been largely used by physical anthropologists of the 19<sup>th</sup> century and was entrenched in the 20<sup>th</sup> century by Martin (1913) and Howells (1973). It provides a standardised set of diameters and angles based on several craniometric points which can be measured reliably by anyone familiar with the system.

The craniometric system is now universally accepted by physical (biological) anthropologists. It is also used, with modifications dictated by clinical needs, by orthodontists and other medical specialists. This ensures strict comparability of data collected by various scientists working in various countries and in various academic systems.

The craniometric system is also applicable to the fossils providing a record of human ancestry. In this way a large, uniform, quantitative database describing the variability of human faces across geographical space and through evolutionary and historical time has been provided by numerous craniometric publications (Farkas, 1994; Farkas *et al.*, 2005).

However, not all characteristics of the human face can be described by simple metrics, so a series of standardised categorical scales describing shapes of the entire face and its elements has been created within the broader range of descriptive scales (Farkas, 1994).

## **2.2 Analysis of facial morphology (current approaches)**

Facial morphology is the study of facial structures, form and shape. Analysis of the human face has a long tradition, as shown earlier, with different techniques applied to analyse facial morphology and assess growth of the face and jaws for the purposes of determining the aetiology, diagnosis, treatment planning and clinical outcome assessment of different kinds of malocclusion, facial asymmetry and dysmorphology.

### **2.2.1 Anthroposcopy (visual assessment)**

Anthroposcopy is the art of discovering or judging of a man's character, passions, and inclinations from a study of his visible features; it is a form of anthropology based upon visual observation or inspection of the physical characteristics of the human body as opposed to exact measurements carried out in *Anthropometry*. Anthroposcopy is one of the oldest methods of examination that is still in use in medicine today; in some instances the anthroposcopic observations are made relative to a set of reference values or standards. Hence, the method has a high degree of subjectivity (Farkas, 1994), although there is a trend toward more objective assessment of some characteristics. Skin colour; hair colour, form, and distribution; and eye colour are among the more common characteristics assessed by anthroposcopy. Colorimetric charts or scales are the reference for comparison, with most emphasis on skin pigmentation. Problems with such scales relate to intermediate shades or gradations. The use of photometric devices that identify spectral wavelengths has provided more objective assessment of skin, hair, and eye colour.

In addition, the assessment of physique is central to anthroposcopic studies. Physique refers to the body build or form, that is, the total configuration of the body. The most widely used classification is the assessment of an individual's somatotype, which is based on the varying contributions of three components: endomorphy (laterality, fatness), mesomorphy (musculoskeletal dominance), and ectomorphy (linearity).

The purposes of anthroposcopy can be summarized:

- The inspection of the physical features of a person with the purpose of judging his/her mental and moral characteristics.
- The determination of characteristics or personality from the human body shape and facial features.
- Anthroposcopic ratings have been used successfully in the evaluation of relationships between physique and physical performance, in documenting physique changes during maturation, growth, and adulthood, and in estimating morphological distances among neighbouring populations.

In other words, anthroposcopy is divination by observing body and facial features.

### 2.2.2 Anthropometry

Anthropometry is the systematic collection and correlation of various measurements of the human body. It is one of the principal techniques of physical anthropology that has gained attention in fields like forensic, socio-cultural, industrial and bio-medical applications. Anthropometry is a method recommended for quantitative analysis of craniofacial morphology using direct clinical measurements including distances, angles, ratios and proportions (Farkas, 1994). Anthropometry remains a simple, inexpensive, efficient and non-invasive method for describing craniofacial morphology. However, it lacks the details of more powerful technologies like 3D imaging systems, but it is better suited for population studies because of the availability of comparative, normal databases (Ward, 1989; Ward and Jamison, 1991; Borman *et al.*, 1999). Anthropometric data provides a good knowledge on the distribution of various measurements across human populations. For example, a known range for human measurements can help guide the design of products to fit most people, e.g. crash helmet (Dooley, 1982).

A quantitative comparison of anthropometric data before and after surgery enables objective assessment of surgical outcomes (Farkas, 1994). In forensic anthropology, average measures across a population may inform a likely appearance of victims from their remains (Farkas, 1994; Rogers, 1984; and Ackermann, 1997); and in the recovery of missing children, by aging their appearance taken from photographs (Farkas, 1994 and DeCarlo *et al.*, 1998).

In facial anthropometry, direct clinical measurements based on identifying specific facial landmarks allow the quantification of changes in facial morphology as a result of growth or healthcare intervention.

Facial landmarks can be divided into 3 broad categories (Shi *et al.*, 2006):

i) anatomical or anthropometric landmarks; ii) mathematical landmarks; and iii) pseudo-landmarks.

*i) Anatomical or anthropometric landmarks*, often used by scientists and clinicians, are biologically meaningful points defined as standard reference points on the face and head, such as: inner and outer canthi of the eyes, nasion, pronasale, subnasale, centre of the upper lip (labiale superius), centre of the lower lip (labiale inferius), outer corners of the mouth (cheilions), and a chin point (pogonion) (Farkas, 1994; Enciso *et al.*, 2003; Hammond *et al.*, 2004). They tend to be somewhat more abstract than other features of the skull (such as protuberances or lines). Anatomical landmarks are considered very important because they are useful in various scientific fields including anthropology, forensics, orthodontics, cosmetic surgery, and computer vision.

Three principal types of landmarks have been recognized based on their anatomical position on the face (Bookstein, 1991b):

- 1) Discrete juxtaposition or intersection of tissues (e.g., subnasale and cheilion)
- 2) Maxima of curvature (e.g., inner and outer canthi)
- 3) Extremal points (e.g., alare)

Some modifications regarding the above classification are noted below:

- Some facial landmarks can be a mixture of types (e.g. labiale superius, labiale inferius, and crista philtri can be classified as Type 1 and Type 2).
- Hard tissue Nasion is a Type 1 landmark (identified by the intersection of the bony sutures under the bridge of the nose), whereas soft tissue nasion is a Type 2 landmark (defined as the point of maximum concavity and maximum convexity on the bridge of the nose).
- Some Type 3 landmarks as defined by Farkas (1994) have been redefined as Type 2 landmarks (e.g., pronasale is defined as the point of maximum total curvature on the tip of the nose; pogonion is defined as the point of maximum Gaussian curvature on the anterior aspect of the chin; and sublabiale is defined as the extreme point of Gaussian curvature under the lower lip).
- Other types include landmarks located at the center of a structure or space (e.g., the cephalometric point "Sella").

*ii) Mathematical landmarks*, these points are defined according to certain mathematical or geometric properties of human faces, such as: middle point between two anatomical landmarks (for example, mid-endocanthion or mid-intercanthal point "men", this is the midpoint between left and right endocanthi); extreme point with respect to particular face region (for example, leftmost point of face contour); or centroid of a certain group of landmarks. A mathematical landmark may or may not coincide with an anatomical landmark, and it can be easily located using automated methods.

iii) *Pseudo-landmarks or semi-landmarks*, these points are identified based on two or more anatomical or mathematical landmarks (between landmarks), or around the outline of facial surface or hair contours. Unlike anatomical landmarks, semi-landmarks do not have specifically defined biological positions and can be approximately located using prior knowledge of anatomical or mathematical properties. Pseudo-landmarks are relatively easy to acquire using computational methods (Mercan *et al.*, 2013), and are generally accurate enough for appearance-based face recognition techniques applied in computer vision.

Farkas (1994) started with classifying the general shape of the face and facial profile into different categories outlined in Table 2.1.

Table 2.1. Classification of facial shape (Farkas, 1994)	
General Shape of the Face (x-y plane) - Frontal View	Facial Profile (y-z plane) - Lateral View
<ul style="list-style-type: none"> <li>- Proportionate in width and height (Normal)</li> <li>- Long-Narrow (Dolichofacial)</li> <li>- Short-Wide (Brachyfacial)</li> <li>- Square</li> <li>- Triangular</li> <li>- Trapezoid</li> </ul>	<ul style="list-style-type: none"> <li>- Normal (Straight Facial Profile)</li> <li>- Bird-like (Convex Facial Profile)</li> <li>- Dish-like (Concave Facial Profile)</li> <li>- Pseudoprognathic, Prognathic, other.</li> </ul>

The anthropometric evaluation of craniofacial morphology begins with the identification of landmarks. These landmarks, as explained above, are defined in terms of visible or palpable features (skin or bone) on the subject's head and face.

A series of measurements between these landmarks is then taken using carefully specified procedures and measuring instruments (such as callipers, levels and measuring tape). As a result, repeated measurements of the same individual are very reliable, and measurements of different individuals can be successfully compared (DeCarlo *et al.*, 1998).

Farkas (1994) described a widely used set of measurements to analyse the human face. Anthropometric data using this system is widely available (Farkas and Munro, 1987; Farkas, 1994). This system uses a total of (47) landmark points to describe the face; Figure 2.3 illustrates some of these points. The landmarks are typically identified by abbreviations of corresponding anatomical terms. For example, the inner canthus of the eye is 'en' for 'endocanthion', while the top of the flap of cartilage in front of the ear (tragus) is 't' for 'tragion'. Two of the landmarks determine a canonical horizontal orientation for the head. The horizontal plane is determined by the two lines (on either side of the head) connecting the landmarks 't' and 'or' for (orbitale), the lowest point of the eye socket on the skull. In measurements, anthropometrists actually align the head to this horizontal, in what is known as "Frankfurt Horizontal (FH)" position (Farkas, 1994; Kolar and Salter, 1996), so that measurements can be made easily and accurately. In addition to this, a vertical mid-line axis is defined by the landmarks 'n' for (nasion), a face feature roughly between the eyebrows; 'sn' for (subnasale), the centre point where the nose meets the upper lip; and 'gn' for (gnathion), the lowest point on the chin.

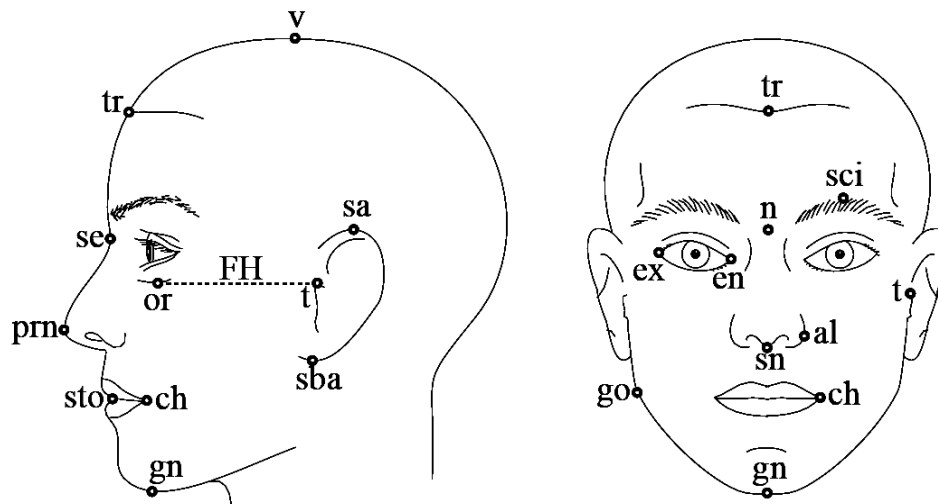


Figure 2.3. Anthropometric facial soft tissue landmarks

Five types of facial measurements have been described by Farkas (1994), as illustrated in Figure 2.4:

- The shortest distance between two landmarks. An example is en-ex, the distance between the landmarks at the corners of the eye.
- The axial distance between two landmarks, the distance measured along one of the axes of the canonical coordinate system, with the head in Frankfurt Horizontal (FH) position. An example is v-tr, the vertical distance (height difference) between the top of the head 'v' for (vertex) and hairline 'tr' for (trichion).
- The tangential (geodesic) distance between two landmarks, the distance measured along a prescribed (shortest) path on the surface of the face (curved surface). An example is ch-t, the surface distance from the corner of the mouth 'ch' for (cheilion) to the tragus.

- The angle of inclination between two landmarks with respect to one of the canonical axes. An example is the inclination of the ear axis with respect to the vertical.
- The angle between locations, such as mento-cervical angle at the chin.

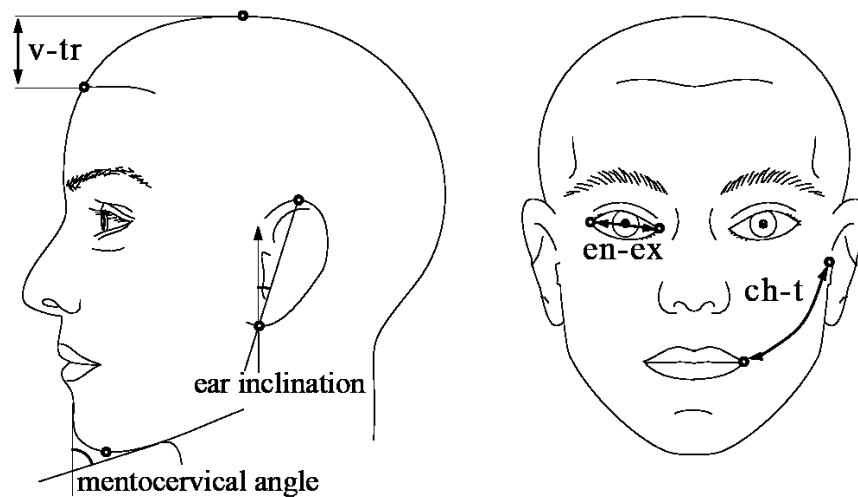


Figure 2.4. Types of facial anthropometric measurements

Farkas (1994) described a total of 132 measurements on the face and head. Some measurements are paired, where there is a corresponding measurement on the left and right sides of the face. Until recently, experienced anthropometrists could only carry out the measurement process by hand. However, scientists have investigated the 3D range scanners as an alternative to manual measurement (Farkas, 1994; Bush and Antonyshyn, 1996; Kolar and Salter, 1996). The systematic collection of anthropometric measurements has made possible a variety of statistical investigations of groups of subjects. Subjects have been grouped on the basis of their gender, race, age, attractiveness or the presence of a physical anomaly or syndrome. Means and variances of measurements within a group have been tabulated (Farkas, 1994 and Gordon, 1989).

Morecroft (2009) conducted a study based on analysing predefined anthropometric facial landmarks to evaluate 3D shape analysis for facial identification. 3000 subjects have been recruited for the study, and each face has been recorded using a 3D digital stereo-photographic Geomatrix scanner. The results showed that 27 reproducible facial landmarks are important for facial comparison and identification. Among these landmarks are: glabella, pogonion, endocanthion, exocanthion, cheilion, and stomion.

In addition to direct clinical measurements, the proportions between measurements have also been derived (Farkas and Munro, 1987). The description of the human form by proportions goes back to the ancient Greek neoclassical canons (c. 450 BC). Facial proportions provide useful information about the relationships between features and serve as more reliable indicators of group membership than simple measurements. The study of facial proportions has shown statistically significant differences across several population groups (Hrdlicka, 1972). Nasjletti and Kowalski (1975) looked for proportional changes over time with aging in the vertical dimensions of the front of the face. They found by examining 510 whites (20-86 years of age) that all the ages exhibited increases in total facial height and that these were always in constant proportions. The upper face was always very close to the same proportion of the entire face throughout the entire aging process. Kowalski and Nasjletti (1976) conducted a similar facial height study on a group of black American males, and they found that the facial proportions to be very close to constant in all ages even though there was growth occurring as with the white American group.

## **2.3 Two-dimensional (2D) imaging techniques**

### **2.3.1 Photographs**

Photography is a recognized aid in orthodontic diagnosis. It offers to orthodontists and maxillofacial surgeons an easy and satisfying method of recording existing conditions of teeth, occlusion, and facial form. A good knowledge of clinical photography is one of the required attributes of an orthodontist. However, this method faced some difficulties and limitations due to the varying degrees of resolution and accuracy acquired by different photographic techniques.

The basic aim of photography in orthodontics is to provide a visual record of a particular object or condition at a particular time. The photograph records the external manifestations of health, disease or deformity, as related to the teeth, gums, or adjacent tissues, and the development of facial characteristics. As applied by the orthodontist, photography falls into two categories of use (Graber, 1946): i) Diagnostic criteria; ii) Records.

The increased emphasis on the achievement of balanced facial harmony and smile aesthetics for our patients, in addition to the main orthodontic goals of a well-aligned dentition and functional occlusion, it has become essential to provide proper clinical photographic records of the orthodontic patient that can help to achieve proper treatment planning and follow-up procedure. Clinical photographs allow the orthodontist to carefully study the existing patient's soft tissue patterns during the treatment planning stage. We can assess lip morphology and tonicity, the smile arc and smile

aesthetics from various angles. We can also assess the degree of incisal show upon smiling. Thus, they allow us to study the patient in a so called “social setting”, and all that without the patient ever being present. Such information greatly aids the orthodontist in formulating the best possible treatment plan for each patient, and for monitoring in follow-up visits.

In addition, there has always been the need for photographic records for purposes of research and publication, and for teaching and presentations. Also, the growing importance of the need for such records for medico-legal reasons cannot be over-emphasized.

Photographs have also been used by researchers and clinicians to carry out facial morphology analysis via identifying certain landmarks on various facial structures and extracting measurements like distances, angles, and ratios. Such measurements (e.g. nose width, bizygomatic distance) have been used by researchers (Boehringer *et al.*, 2011; Liu *et al.*, 2012) to identify genes influencing facial variation. However, because of various types of distortions due to poor or variable image resolution, it is quite difficult to accurately extract anatomical landmarks from 2D face images, either manually or automatically, which may affect the conducted analyses.

### **2.3.2 Lateral skull radiographs (cephalometry)**

The introduction of Broadbent Cephalometer (Broadbent, 1931) enabled studies on the facial skeleton, and since that time, the diagnostic methods used in orthodontics were two-dimensional representations of patients' craniofacial morphology. These diagnostic methods remained essentially unchanged for over 80 years and are still in use today.

The two-dimensional cephalometric radiographs record mainly hard tissue information (Broadbent *et al.*, 1975; Popovich and Thompson, 1977). Today, however, the paradigm of our treatment goals has shifted from hard to soft tissue (Proffit, White and Sarver, 2003), and this shift requires the use of novel approaches for 3D imaging as well as creative diagnostic methods.

Although two-dimensional imaging techniques (facial photographs and lateral skull radiographs) are used routinely to measure the face and jaws in two dimensions, they tend to be imprecise as facial landmarks are subject to rotational, positional and magnification errors (Houston *et al.*, 1986; Benson and Richmond, 1997). In addition, the human face is a three-dimensional (3D) object whose features and underlying skeleton are not always accurately represented by projections onto a 2D surface.

## 2.4 Three-dimensional imaging techniques

Our understanding of facial morphology has greatly improved with the development of accurate, highly reliable, low cost, 3D acquisition systems (Toma *et al.*, 2012). The emergence of 3D imaging technologies in the 1970's and 1980's also facilitated realistic interactive surgical planning (Brewster *et al.*, 1984; Moss *et al.*, 1988). The use of 3D imaging technologies is becoming more and more widespread in a variety of commercial and healthcare fields. There are many systems available, although not all of them have the appropriate levels of resolution and accuracy. There are basically static and dynamic 3D acquisition systems. Orthodontists and maxillofacial surgeons routinely deal with the physical relationships among the components of the human head; therefore, the use of 3D imaging technologies for measurement and characterization of craniofacial morphology is fundamental to the objective analysis of facial normality and deformity.

The applications of 3D imaging technology in orthodontics include: pre- and post- orthodontic assessment of dento-skeletal relationships and facial aesthetics, auditing orthodontic outcomes with regard to soft and hard tissues, 3D treatment planning, and 3D soft and hard tissue prediction. Archiving 3D facial, skeletal and dental records for treatment planning and follow-up visits, research and medico-legal purposes are also among the benefits of using 3D models in orthodontics (Hajeer *et al.*, 2004a, b, c).

Many 3D imaging techniques have been utilized to register and analyse the face in three dimensions and avoid/reduce the shortcomings of the conventional 2D imaging techniques (photographs and radiographs). Each technique has advantages and disadvantages. These techniques include:

Anthropometry (Peyton and Ritchie, 1936; Farkas and Kolar, 1987a, b, Farkas *et al.*, 1993, Farkas, 1994), morphanalysis (Rabey, 1971), laser scanning (Cutting *et al.*, 1988; Moss *et al.*, 1989, 1994; McCance *et al.*, 1992a, b; Bush and Antonyshyn, 1996), 3D computed tomography (CT) (McCance *et al.*, 1992a), moiré stripes topography (Kawai *et al.*, 1990a, b; Chen and Iizuka, 1995) and contour photography (Leivesley, 1983), facial plaster modeling (Mishima *et al.*, 1996), video recording (Morrant and Shaw, 1996; Benson and Richmond, 1997), liquid crystal range finding (Yamada *et al.*, 1999), stereolithography (Bill *et al.*, 1995), 3D ultrasonography (Hell, 1995), 3D facial morphometry (Ferrario *et al.*, 1994b), and digigraph imaging (Nanda *et al.*, 1996). Recent innovations in computed stereophotogrammetry provided a useful technique for 3D recording of the face (Ayoub *et al.*, 1996, 1997, 1998, 2003; Bourne *et al.*, 2001).

The following is a brief review of the techniques that have been used to record the face in three dimensions.

### **2.4.1 Moiré topography and contour photography**

Rayleigh (1874) suggested that moiré patterns could be used for testing the performance of ruled diffraction gratings. The recent history of moiré interferometry reaches back 90 years or so when Occhialini and Ronchi first made use of gratings (optically transmitting, or reflecting black and white lines of even thickness) to test optical systems (Ronchi, 1923, 1927, 1964). During his research projects at the University of Florence, Occhialini noticed that overlapping two gratings formed fringes.

Moiré fringes have been also used by Pierson (1961) to determine body volume. In this case coloured acetate strips 1/8" wide were mounted to form a grid which was placed close to the subject, the coloured bands being projected by flashlights. The lines have been made closer on the grid (reduced lines spacing) in an attempt to reduce distortion. Takasaki (1970) reported a moiré method for observing contour lines for an object of medium or large size (e.g., face of a coin or car). Moiré topography has been utilized by Graham and Sampson (1973) to demonstrate typical change in shape of the female leg under dynamic conditions. They stated a few precautions to prevent inaccuracies.

Both Moiré topography and contour photography use grid projections during exposure, resulting in standardized contour lines on the face (Kawai *et al.*, 1990a, b; and Leivesley, 1983). Moiré topography delivers 3D information based on the contour fringes and fringe intervals. However, difficulties are encountered if a surface has sharp features, therefore these

two methods are more suitable to use on a smoothly contoured faces. In addition, great care is needed in positioning the head, as a small change in head position produces a large change in the fringe pattern. A 3D measuring system was proposed by (Motoyoshi *et al.*, 1992), but this system does not capture the normal facial texture, and subsequent landmark identification will be difficult. The authors did not propose any objective method for studying facial changes following surgery.

#### **2.4.2 Stereophotogrammetry**

Photogrammetry is as old as modern photography and can be dated to the mid-nineteenth century. Photogrammetry is the practice of determining the geometric properties of objects from photographic images; in other words, photogrammetry is the science or art of obtaining reliable measurements by means of photographs (Savara, 1965a; Thompson, 1966). Stereophotogrammetry refers to the special case where two cameras, configured as a stereo-pair, are used to recover the 3D distance to features on the surface of the face by means of triangulation. This technique has evolved to provide a more accurate evaluation of the face and may adopt one or more stereo-pair views to increase the number of 3D measurements obtained to compute a 3D face surface model (Hajeer *et al.*, 2002; 2004a).

In photogrammetry, the face is illuminated by either a structured or a speckled light pattern and in order to reduce inaccuracy due to movement, images are recorded simultaneously from several views. Then, the images are processed to calculate facial surface coordinates.

The duration of exposure has been reduced with improvement in the technology. Several stereophotogrammetric techniques were proposed before the introduction of contemporary digital stereophotogrammetry (Burke and Beard, 1967a, b; MacGregor, Newton and Gilder, 1971; Bjorn *et al.*, 1954; and Berkowitz and Cuzzi, 1977).

The incorporation of recent technology has given the ability to process complex algorithms to convert simple photographs to 3D measurements of facial surface changes that occur as a result of growth or healthcare interventions. In addition, the dynamic systems have a great potential in understanding, describing and quantifying facial changes as a result of function (e.g. studying lips movement) (Popat *et al.*, 2008a, b).

The clinical observation of the face remains an essential part of the clinical evaluation of the patients. Many congenital developmental abnormalities may arise from exogenous teratogens, chromosomal anomalies, or to a defect in a single gene. Numerous syndromes affecting facial morphology have been reported and a growing number of genes or chromosomal anomalies have been identified (Hammond *et al.*, 2005). Several studies have employed the stereophotogrammetric imaging technique to identify subtle influences on craniofacial morphology caused by many syndromes, such as “Noonan syndrome” (Hammond *et al.*, 2004).

One of the contemporary digital photogrammetric techniques is computed stereophotogrammetry (C3D). This is a 3D non-contact vision-based imaging system which is based on the use of stereo-pairs of digital cameras and special textured illumination (Siebert and Marshall, 2000). This system provides quick capture times and it is appropriate for imaging children and infants, as well as adults. C3D is a relatively new 3D imaging system that was developed to capture the 3D geometry of the face and it consists of two camera stations placed at each side of the face to take a stereo image. Each station contains a pair of monochrome digital cameras to capture a stereo image and a colour digital camera to capture the skin texture. The face is illuminated with a speckled flash that projects a random texture pattern onto the face. This textured illumination provides sufficient information in the images, captured by the monochrome cameras, to match the two sides of the face and accurately construct the 3D facial model (Ras *et al.*, 1996).

The accuracy of the system was evaluated by comparing the x, y, and z coordinates of specific landmarks digitized from on-screen 3D models for 21 plaster casts of cleft models, with the x, y, and z coordinates derived directly from these models using a previously validated 3D contact ultrasonic measuring system. The overall error between both measures was less than 0.6mm, which was acceptable for studying facial soft tissue changes (Ayoub *et al.*, 2003). With this imaging system, monochrome and colour stereo images are captured. The integration of these images produces

a dimensionally accurate 3D range model and a coloured photo realistic overlay. This system is not available commercially, and it is currently used for research purposes. This method is useful in studying facial soft tissue changes following orthognathic surgery and other types of facial surgery, as well as assessing facial soft tissue growth and development of the craniofacial complex (Hajeer *et al.*, 2002).

The main advantage of photogrammetry is its speed of data capture, typically less than 1 second (1.5 milliseconds at the highest resolution) (Hajeer *et al.*, 2002); whereas laser scanning takes approximately 5 to 10 seconds to scan the left and right sides of the face using two cameras. Therefore, the laser scanning technique requires a protocol to instruct the patient to remain still, presenting with no facial expressions. However, the resolution and accuracy of the 3D images produced in photogrammetry are less than those produced in laser scanning. The accuracy of facial surface scanning with Konica Minolta 900/910 laser scanners is in the range 0.3-0.5mm (Zhurov *et al.*, 2010); whereas the images obtained with a photogrammetric approach such as 3dMD (Atlanta, GA) cameras have been reported as 0.6-1.0 mm (Ayoub *et al.*, 2003; Kau *et al.*, 2005b). This is mainly due to the low density surface polygon meshes produced in photogrammetry as compared to laser scanning. This means that laser scanning has sufficient surface resolution and accuracy to detect the detailed morphology of facial structures, particularly the fine lines that form the inner and outer canthi (Toma *et al.*, 2012). Therefore, in this study we opted for laser scanning to analyse facial variation.

### **2.4.3 3D cephalometry**

Although the lateral cephalogram is considered the standard diagnostic tool, a number of researchers tried to develop further Broadbent's three-dimensional concept. For example, Baumrind and Moffitt (1972) proposed the "Coplanar Cephalometry". This technique generated a stereo image of the face, but it could not be measured or manipulated to satisfy the needs of the clinician, especially for the purposes of prediction of treatment outcome. It was also expensive and cumbersome to master. Cutting and his associates (1985) introduced the "Biplanar Cephalometry" to generate 3D tracings of the skeleton. This technique was later improved by Brown and Abbott (1989) who considered that the major obstacle to the derivation of three-dimensional data from lateral and coronal radiographs of the head is the lack of precision in locating the same landmarks on each of the biplanar images. Therefore, they described a method that uses radiographic equations based on the geometry of a biplanar system to predict the location of a reference point on one film from its location on the other. This technique, which differs from previously described systems, allows a pair of cephalometric films to be digitized by an on-line procedure controlled by a personal computer. Using this technique, the three-dimensional coordinates of reference points have been calculated and stored for subsequent retrieval when they can be used for metric analysis or for the display of simple wire-frame models of the skull. In addition, computing algorithms have been provided to aid software development.

3D cephalometry is simply based on abstracting 3D coordinate data from two biorthogonal head films, lateral and antero-posterior radiographs (Savara, 1965b; Baumrind *et al.*, 1983a, b; Grayson *et al.*, 1988; Bookstein *et al.*, 1991). The main drawbacks of this technique are patient exposure to radiation, difficulties in locating accurately the same landmarks in two biorthogonal radiographs, lack of soft tissue contour assessment, and the time-consuming nature of the procedure (Hajeer *et al.*, 2002).

#### **2.4.4 Morphanalysis**

Morphanalysis (analysis of form) was developed by Rabey (1968, 1971, 1977) to overcome the shortcomings of radiography and photography. The idea was to create a 3D reference grid using standardized 2D records (photographs and radiographs). The study casts could also be positioned in this 3D reference framework. The principle is to capture the frontal and lateral radiographs and photographs with the patient's head being in a fixed position. The equipment, however, was relatively expensive and time consuming and not very practical for every day use.

#### **2.4.5 CT- assisted 3D imaging**

In the mid-1980s, CT-assisted 3D imaging and modelling of the skeletal structures were introduced for use in maxillofacial surgery (McCance *et al.*, 1992a). Generally, this 3D imaging technique has been used occasionally for dental diagnosis and treatment planning; however, the conventional medical CT (Helical-CT) units were not developed originally for dental diagnostic use and the technique has gained considerable popularity and

applications in the medical field, but with regard to 3D facial imaging, its main disadvantages are considered to be as follows:

- Patient exposure to a high radiation dose (therefore, it is not suitable for long-term assessment following orthognathic surgery).
- Limited resolution of facial soft tissues due to slice spacing, which can be 5mm or more.
- Presence of artefacts due to metal objects such as dental restorations and fixed orthodontic appliances, because of the reduced penetrability.

Despite the obvious advantages of computed tomography (Marsh *et al.*, 1985; Lill *et al.*, 1992), it is not practical for routine use, mainly because of the high radiation exposure. Mapping of soft tissues requires that the image is captured, but this image must be conducive to measurements and to manipulation (Tuncay *et al.*, 2000).

#### **2.4.6 Cone beam computed tomography (CBCT)**

Cone beam computed tomography (CBCT) has been investigated in the past two decades due to its potential advantages over a fan beam CT. These advantages include: (a) great improvement in data acquisition efficiency, spatial resolution, and spatial resolution uniformity, (b) substantially better utilization of x-ray photons generated by the x-ray tube compared to a fan beam CT, and (c) significant advancement in clinical three-dimensional (3D) CT applications (Ning *et al.*, 2003; Kau *et al.*, 2005a; Palomo *et al.*, 2006).

Despite the considerable progress that has been made in diagnostic, medical imaging devices such as computed tomography, these devices are not used routinely in dentistry and orthodontics because of the high cost in comparison to lateral cephalometry, large space requirements and the high amount of radiation exposure. A device using computed tomography technology was developed for dental use called a limited cone beam dental compact-CT (3DX). The images provide useful information for orthodontic diagnosis and treatment planning (Nakajima *et al.*, 2005).

Current resources of computed tomography allow reconstruction of 3D images that improve the diagnosis, treatment planning and monitoring of treatments in maxillofacial surgery. Axial slices obtained from CT are used to generate 3D images that can be processed by means of different protocols — the 3D surface and 3D volume-rendering techniques (Cavalcanti and Antunes, 2002).

#### **2.4.7 Stereolithography**

Stereolithography (STL) is a method of organ-model-production based on computed tomography scans which enables the representation of complex 3D anatomical structures. Surfaces and internal structures of organs can be produced by polymerization of UV-sensitive liquid resin using a laser beam. In oral and maxillofacial surgery this technique is advantageous for reconstructing severe skull defects because a more accurate preoperative planning is possible.

With recently developed software, one can reconstruct unilateral bony defects by virtual mirror imaging of the contralateral side and production of an STL mirror model, as well as reconstruction of non-mirrorable defects by superimposition. The advantages of STL include: representation of complex anatomical structures, high precision and accuracy, and the option to sterilize the models for intraoperative use. More accurate planning using this method improves postoperative results, decreases risks and shortens treatment time (Bill *et al.*, 1995).

The obvious shortcomings of this technique are: (Ayoub *et al.*, 1996)

- Experienced and skilled operators are needed to get accurate 3D data
- Expense of the method
- Patient exposure to radiation for CT scans
- No production of soft tissue in machine-readable form

#### **2.4.8 3D Laser scanning**

In laser surface scanning, the face is traversed by a laser beam that captures depth information. Digital cameras monitor the illumination and triangulation geometry allows the construction of 3D shapes. The laser scanning unit can be either fixed or move across the human body/face to digitize its surface. Some systems require a trained operator to acquire optimal facial scans while others are automated (Hennessy *et al.*, 2005). This technology generally produces facial surfaces with high accuracy and resolution as it is capable of generating high-density surface polygon meshes in comparison to other techniques like the stereophotogrammetry.

Laser scanning techniques provide a non-invasive method for capturing the maxillofacial region in three dimensions. They have been used recently in clinical auditing of surgical outcome and measurement of surgical relapse (McCance *et al.*, 1992a, b; 1993; Moss *et al.*, 1994). A 3D laser scanning imaging system measures over 20,000 points on the surface of the face in 5 to 10 seconds using a completely non-hazardous technique (Arridge *et al.*, 1985; Moss *et al.*, 1987; 1988). The laser approach appears to have the greatest surface resolution and accuracy (Kau *et al.*, 2004a, b). The 3D data acquired by laser scanning is accurate to approximately 0.3-0.5mm (Zhurov *et al.*, 2010). Computer algorithms have been developed to handle the enormous quantity of 3D data produced. Programs (e.g. rapidform, geomagic) based on these algorithms form the basis of a practical, user-friendly, clinical system whose performance has been evaluated and is in routine use (Zhurov *et al.*, 2005).

Optical laser surface scanning accurately records the 3D shape of the face; it enables the clinician to assess changes in the face and jaws as a result of growth, treatment, or drug therapy and to study genetic effects. Average templates for groups of patients have been created to provide a comparison of treatment outcomes (Treil *et al.*, 2002). An average face has been obtained for groups of patients each year from 5 to 18 years (Moss and Hennessy, 2002) so that growth of an individual can be compared with the norm for that age to determine which areas of the face show abnormal growth. Moreover, prediction of facial form for forensic and surgical purposes is also possible.

Laser surface scanning has been successfully applied to human facial measurement (Toma *et al.*, 2012). This technique is valuable for its ease of application and generation of accurate 3D images enabling creation of valuable resources for normative populations (Yamada *et al.*, 2002), cross-sectional growth changes (Nute and Moss, 2000), and clinical outcomes in the surgical and non-surgical treatments in the head and neck regions (Ayoub *et al.*, 1998; and Moss *et al.*, 2003).

A shortcoming of this technique is a relatively slow data acquisition process; it takes approximately 5 to 10 seconds to scan the face. In addition, scanning the facial surface may produce a variety of artefacts in the vicinity of face edges (boundaries), e.g. the ears, bottom of the chin, and the forehead, where the laser beam hits these surfaces at different angles other than the perpendicular angle, this may also cause that these surfaces are not fully captured.

An additional issue that may pose problems in the scanning process is caused by head hair and facial hair (beard, eyebrows and eyelashes). These features are difficult to be captured by laser which results in noisy surfaces and voids at these areas. However, this problem can be solved by applying smooth filters or by manual editing these specific features.

#### **2.4.9 3D facial morphometry**

This system comprises two charge-coupled device (CCD) cameras that capture markers placed on the patient's face, and software for 3D reconstruction of landmarks (x, y, z) coordinates relative to a reference system (Ferrario *et al.*, 1994b, 1999a, b). The process of placing landmarks on the face is time- and labour-consuming and cannot be performed consistently due to movement of facial structures. Although the system has been used extensively to investigate facial changes, no life-like models were produced to show the natural soft tissue appearance of faces. This system cannot be used as a 3D treatment-planning tool or as a communication tool for use in orthognathic surgery patients.

#### **2.4.10 3D ultrasonography**

Ultrasonography was introduced recently to capture 3D data. This technique delivers a reflection picture, which is transformed into digital information (Hell, 1995). Ultrasonography waves do not visualize bone or pass through air, which acts as an absolute barrier during both emission and reflection. Therefore, a specific contact probe is required to generate a 3D database. This system records the 3D coordinates of the landmarks chosen, but it will not produce a 3D image. In addition, the procedure is time-consuming and necessitates a cooperative patient as well as a skilful operator. Motion of the head during data acquisition introduces errors, while touching facial soft tissues may cause distortions of their spatial positions.

## **2.5 General 3D concepts**

Generally, two-dimensional space (also called bi-dimensional space) is a geometric model of the planar projection of the physical universe in which we live. The two dimensions are commonly called length and width. Both directions lie in the same plane. The three-dimensional space is a geometric 3-parameters model of the physical universe (without considering time) in which all known matter exists. These three dimensions can be labelled by a combination of three chosen from the terms length, width, height, depth, and breadth. Any three directions can be chosen, provided that they do not all lie in the same plane. In mathematics, analytic geometry (also called Cartesian geometry) describes any point in three-dimensional space by means of three coordinates. Three coordinate axes are given, usually each perpendicular to the other two at the origin, the point at which they cross. They are usually labelled  $x$ ,  $y$ , and  $z$ . Relative to these axes, the position of any point in three-dimensional space is given by an ordered triple of real numbers, each number giving the distance of that point from the origin measured along the given axis, which is equal to the distance of that point from the plane determined by the other two axes. Other popular methods of describing the location of a point in three-dimensional space include cylindrical coordinates and spherical coordinates, though there is an infinite number of possible methods. The prototypical example of a coordinate system is the Cartesian coordinate system. In the plane, two perpendicular lines are chosen and the coordinates of a point are taken to be the signed distances to the lines. In three dimensions, three perpendicular planes are

chosen and the three coordinates of a point are the signed distances to each of the planes. This can be generalized to create  $n$  coordinates for any point in  $n$ -dimensional Euclidean space. In 2D photographs and radiographs, there are two axes (vertical and horizontal), while the Cartesian coordinates system in the 3D images has three axes: the x-axis (transverse, horizontal dimension), y-axis (vertical dimension), and z-axis (antero-posterior dimension, depth axis). The x-, y- and z- coordinates define a three-dimensional space in which multi-dimensional data are represented (Udupa and Herman, 1991).

3D computer graphics (in contrast to 2D computer graphics) are graphics that use a three-dimensional representation of geometric data (often Cartesian) that is stored in the computer for the purposes of performing calculations and rendering 2D images. Such images may be stored for viewing later or displayed in real-time. 3D computer graphics rely on many of the same algorithms as 2D computer vector graphics in the wire-frame model and 2D computer raster graphics in the final rendered display. 3D modeling is the process of developing a mathematical representation of any three-dimensional surface of an object (either inanimate or living) via specialized software. The product is called a 3D model. It can be displayed as a two-dimensional image through a process called 3D rendering or used in a computer simulation of physical phenomena. The model can also be physically created using 3D printing devices. Models may be created automatically or manually. The manual modeling process of preparing geometric data for 3D computer graphics is similar to plastic arts such as sculpting. New concepts in 3D modeling have started to emerge such as curve-controlled

modeling that emphasizes the modeling of the movement of a 3D object instead of the traditional modeling of the static shape (Huang and Yan, 2003). 3D modeling software is a class of 3D computer graphics software used to produce 3D models. Individual programs of this class are called modeling applications or modelers.

3D models represent a 3D object using a collection of points in 3D space, connected by various geometric entities such as triangles, lines, curved surfaces, etc. Being a collection of data (points and other information), 3D models can be created by hand, algorithmically (procedural modeling), or scanned. 3D models are widely used anywhere in 3D graphics. Actually, their use predates the widespread use of 3D graphics on personal computers. Many computer games used pre-rendered images of 3D models as sprites before computers could render them in real-time. Today, 3D models are used in a wide variety of fields. The medical industry uses detailed models of organs; these may be created multiple 2-D image slices from an MRI or CT scan. The two most common sources of 3D models are those that an artist or engineer originates on the computer with some kind of 3D modeling tool, and models scanned into a computer from real-world objects (either inanimate or living). Basically, a 3D model is formed from points called vertices (or vertexes) that define the shape and form polygons. A polygon is an area formed from at least three vertexes (a triangle). A four-point polygon is a quad, and a polygon of more than four points is an '*n*-gon'. The overall integrity of the model and its suitability to use in animation depend on the structure of the polygons.

3D rendering involves the computer calculations that are based on light placement, surface types, and other qualities to generate the 3D image (Seeram, 1997). Rendering converts a model into an image either by simulating light transport to get photo-realistic images, or by applying some kind of style as in non-photorealistic rendering. The two basic operations in realistic rendering are transport (how much light gets from one place to another) and scattering (how surfaces interact with light). This step is usually performed using 3D computer graphics software. Altering the scene into a suitable form for rendering also involves 3D projection, which displays a three-dimensional image in two dimensions.

Not all computer graphics that appear 3D are based on a wireframe model. 2D computer graphics with 3D photorealistic effects are often achieved without wireframe modeling and are sometimes indistinguishable in the final form. Some graphic art software includes filters that can be applied to 2D vector graphics or 2D raster graphics on transparent layers. Visual artists may also copy or visualize 3D effects and manually render photorealistic effects without the use of filters.

Almost all 3D models can be divided into two categories:

- *Solid* (acquired via *volumetric imaging* techniques, e.g. CT, holography or varifocal mirrors techniques) - These models define the *volume* of the object they represent (e.g. rock, skull). These are more realistic, but more difficult to build. Solid models are mostly used for non-visual simulations such as medical and engineering simulations, for CAD and specialized visual applications such as ray tracing and constructive solid geometry.

- *Shell/boundary* (acquired via *projective 'surface-based' imaging* techniques, e.g. laser surface scanning and stereophotogrammetry imaging techniques) - these models represent the *surface* of an object, not its volume (e.g. infinitesimally thin eggshell, facial surface). These are easier to work with than solid models. Almost all visual models used in games and film are shell models. Projective imaging is the most popular 3D imaging approach, but it does not provide a true 3D mode of visualization similar to what is offered by the volumetric imaging approach.

Because the appearance of an object depends largely on the exterior of the object, boundary representations are common in computer graphics. Two dimensional surfaces are a good analogy for the objects used in graphics, though quite often these objects are non-manifold. Since surfaces are not finite, a discrete digital approximation is required: polygonal meshes (and to a lesser extent subdivision surfaces) are by far the most common representation, although point-based representations have been gaining some popularity in recent years. Level sets are a useful representation for deforming surfaces which undergo many topological changes such as fluids.

The process of transforming representations of objects, such as the middle point coordinate of a sphere and a point on its circumference into a polygon representation of a sphere, is called tessellation. This step is used in polygon-based rendering, where objects are broken down from abstract representations (primitives) such as spheres, cones etc., to so-called meshes, which are nets of interconnected triangles. Meshes of triangles (instead of

e.g. squares) are popular as they have proven to be easy to render using *scanline* rendering (this is an algorithm for visible surface determination, in 3D computer graphics, that works on a row-by-row basis rather than a polygon-by-polygon or pixel-by-pixel basis). Polygon representations are not used in all rendering techniques, and in these cases the tessellation step is not included in the transition from abstract representation to rendered scene.

### *Modeling process*

There are three popular ways to build a model:

1. *Polygonal modeling* - points in 3D space, called vertices, are connected by line segments to form a polygonal mesh. The vast majority of 3D models today are built as textured polygonal models, because they are flexible and because computers can render them so quickly. However, polygons are planar and can only approximate curved surfaces using many polygons.
2. *Curve modeling* - surfaces are defined by curves, which are influenced by weighted control points. The curve follows (but does not necessarily interpolate) the points. Increasing the weight for a point will pull the curve closer to that point. Curve types include non-uniform rational B-spline (NURBS), splines, patches and geometric primitives.
3. *Digital sculpting* - still a fairly new method of modeling, 3D sculpting has become very popular in the few years it has been around. There are currently 3 types of digital sculpting: displacement, which is the most widely used among applications at this moment, volumetric and dynamic

tessellation. Displacement uses a dense model (often generated by subdivision surfaces of a polygon control mesh) and stores new locations for the vertex positions through use of a 32bit image map that stores the adjusted locations. Volumetric which is based loosely on 'Voxels' has similar capabilities as displacement but does not suffer from polygon stretching when there are not enough polygons in a region to achieve a deformation. Dynamic tessellation is similar to Voxel but divides the surface using triangulation to maintain a smooth surface and allow finer details. These methods allow for very artistic exploration as the model will have a new topology created over it once the models form and possibly details have been sculpted. The new mesh will usually have the original high resolution mesh information transferred into displacement data or normal map data if for a game engine.

The modeling stage consists of shaping individual objects that are later used in the scene. There are a number of modeling techniques, including:

- Constructive solid geometry
- Implicit surfaces, and
- Subdivision surfaces

The three-dimensional image acquisition systems are rapidly becoming more affordable, especially systems based on commodity electronic cameras. At the same time, personal computers with graphics hardware capable of displaying complex 3D models are also becoming inexpensive enough to be available to a large population. As a result, there is potentially an opportunity to consider new virtual reality applications as diverse as

cultural heritage and retail sales that will allow people to view realistic 3D objects on home computers. Although there are many physical techniques for acquiring 3D data including laser scanners, structured light and time-of-flight, there is a basic pipeline of operations for taking the acquired data and producing a usable numerical model, these are further detailed in the work published by Bernardini and Rushmeier (2002). Systems are available which output shape in the form of clouds of points that can be connected to form triangle meshes, and/or fitted with NURBS or subdivision surfaces. The 3D points are augmented by additional data to specify surface finish and colour. With the exception of surfaces with relatively uniform spatial properties, fine scale surface properties such as finish and colour are ultimately stored as image maps covering the geometry.

The shape of 3D objects may be acquired by a variety of techniques, with a wide range in the cost of the acquisition hardware and in the accuracy and detail of the geometry obtained. On the high cost end, an object can be CAT scanned (Rocchini *et al.*, 1999), and a detailed object surface can be obtained with isosurface extraction techniques. On the low cost end, models with relatively sparse 3D spatial sampling can be constructed from simple passive systems such as video streams by exploiting structure from motion (Pollefeys *et al.*, 1999), or by observing silhouettes and using space carving techniques (Zheng, 1994). Also there are the scanning systems that capture range images (that is an array of depth values for points on the object from a particular viewpoint). While these scanners span a wide range of cost, they are generally less expensive and more

flexible than full 3D imaging systems such as CAT scanners, while obtaining much more densely sampled shapes than completely passive systems. Fundamentally, there are two streams of processing for building models from a range scanning system, one for the geometry and one for the fine scale surface appearance properties (Bernardini and Rushmeier, 2002). The geometric and surface appearance information can be exchanged between the two processing streams to improve both the quality and efficiency of the processing of each type of data. In the end, the geometry and fine scale surface appearance properties are combined into a single compact numerical description of the object.

Many different devices are commercially available to obtain range images. To build a model, a range scanner can be treated as a “black box” that produces a cloud of 3D points. It is useful however to understand the basic physical principles used in scanners. Characteristics of the scanner should be exploited to generate models accurately and efficiently. The most common range scanners are triangulation systems. A lighting system projects a pattern of light onto the object to be scanned, possibly a spot or line produced by a laser, or a detailed pattern formed by an ordinary light source passing through a mask or slide. A sensor, frequently a CCD camera, senses the reflected light from the object. Software provided with the scanner computes an array of depth values, which can be converted to 3D point positions in the scanner coordinate systems, using the calibrated position and orientation of the light source and sensor. The depth calculation may be made robust by the use of novel optics, such as the

laser scanning systems (Beraldin *et al.*, 1995). Alternatively, calculations may be made robust by using multiple sensors (Zitnick and Webb, 1996). A fundamental limitation of what can be scanned with a triangulation system is having an adequate clear view for both the source and sensor to see the surface point currently being scanned. Surface reflectance properties affect the quality of data that can be obtained. Triangulation scanners may perform poorly on materials that are shiny, have low surface albedo, or that have significant subsurface scattering. An alternative class of range scanners are time-of-flight systems. These systems send out a short pulse of light, and estimate distance by the time it takes the reflected light to return. These systems have been developed with near real time rates, and can be used over large (e.g. 100 m) distances. Time-of-flight systems require high precision in time measurements, and so errors in time measurement fundamentally limit how accurately depths are measured.

Basic characteristics to know about a range scanner are its scanning resolution, and its accuracy. Accuracy is a statement of how close the measured value is to the true value. The absolute accuracy of any given measurement is unknown, but a precision that is a value for the standard deviation that typifies the distribution of distances of the measured point to true point can be provided by the manufacturer. Resolution is the smallest distance between two points that the instrument measures. The accuracy of measured 3D points may be different than the resolution. For example, a system that projects stripes on an object may be able to find the depth at a particular point with submillimeter accuracy. However, because the stripes

have some width, the device may only be able to acquire data for points spaced millimetres apart on the surface. Resolution provides a fundamental bound on the dimensions of the reconstructed surface elements, and dictates the construction of intermediate data structures used in forming the integrated representation.

Generally, for medical and dental purposes, there are two main geometrical strategies for measuring scanned objects in three dimensions: orthogonal measurement and measurement by triangulation (Baumrind, 2001). The orthogonal measurement means that the object is sliced into layers. The x and y dimensions are measured directly on the slice surface, and the z dimension is measured by tallying the number of slices in the area of interest. An example of this method is the ordinary CT scanning. The measurement by triangulation is analogous to the geometry of mammalian stereoscopic vision (Baumrind, 2001). Simply, two images of the object need to be captured from two different views simultaneously or in rapid succession. Stereophotogrammetry depends on this method of measurement, as well as both biplanar and coplanar stereo x-ray systems.

## **2.6 The use of three-dimensional imaging in orthodontics**

### **2.6.1 *Optical surface scanning***

Surface digitization technologies have emerged on an experimental basis over the past 30 years, but commercial systems based on several optical principles have become increasingly available for a variety of biological and anatomical applications. In orthodontics, two remarkable techniques are now commonly employed for digitizing the facial surface, namely laser scanning and photogrammetry.

An optical surface scanning system was first tested in 1981 to produce a non-invasive 3D image of the face. This system was subsequently modified, improved, and re-tested (Arridge *et al.*, 1985; Moss *et al.*, 1987; Aung *et al.*, 1995). Since that time, the system has also been developed to scan models of teeth (Stern and Moss, 1994). In 1996, a hand-held scanner was designed to make the system mobile (McCallum *et al.*, 1996). This system can be used for scanning many parts of the body.

The recent introduction of a probe that records the 3D coordinates of any point means that many of the points used by Farkas (1994) can now be recorded. Many recent scanners, which take instant pictures, have the problem of the scarcity of data at the periphery of the scan which makes joining of the two scans difficult and not very accurate. In contrast, the hand-held scanner overcomes this problem and can collect over 120 000 points around the head. It is important to have sufficient data over all the surfaces for the analysis of changes in facial morphology, and especially of surface shape changes (Harrison *et al.*, 2004; Park *et al.*, 2006).

Over the years, the value of the 3D imaging systems in the diagnosis and management of patients has been demonstrated. 3D material has been obtained for various types of craniofacial anomalies including cleft palate, hemifacial microsomia and cherubism (Moss and James, 1984; Moss *et al.*, 1990, 1996; McCance *et al.*, 1997a,b,c,d; Duffy *et al.*, 2000). Craniofacial patients, who were treated surgically, have been recorded before and after

treatment (Kobayashi *et al.*, 1990; Moss *et al.*, 1987, 1991; and McCance *et al.*, 1993), and there is also a large database of patients who have undergone various types of orthodontic treatment (Moss *et al.*, 1997). A database of untreated children and adults divided into males and females provides useful control group data (Nute and Moss, 2000). A group of untreated Class II patients and a collection of twins and families for genetic studies provide further useful information (McCulley, 2000).

Several other studies have reported and assessed the three-dimensional soft tissue facial changes due to growth and development of the face and jaws (Ferrario *et al.*, 1997, 2003; Kau, 2007). Recently, the efforts have been directed to analyse facial morphology variation using 3D imaging and geometric morphometric techniques with specific anatomical landmarks being identified on the 3D facial scans. The reproducibility of identifying facial landmarks has been considered (Coward *et al.*, 1997; Gwilliam *et al.*, 2006; Baik *et al.*, 2006, 2007; Toma *et al.*, 2009).

Moss (2006) reported a study on a series of patients at different ages to distinguish between facial forms of males and females. For this study, 43 (5 to 6 year old), 41 (11 year old), and 42 (17 year old) patients were selected together with a random group of (131) adults from Ireland. The facial surfaces of the subjects were recorded in 3D using either a fixed laser scanner (Moss *et al.*, 1987) or a hand-held scanner (McCallum *et al.*, 1996, 1998) and between 60 000 and 120 000 points were recorded for each patient.

Landmarks were then identified on each facial scan as described by Farkas (1994), and the x, y, and z coordinates were recorded for statistical shape analysis. The landmarks were analysed following suitable scaling and alignment (rotation and translation) using generalized Procrustes analysis to produce a mean shape for the sample. The results show that the adult female face was wider and the eyes were more lateral and anterior, with nasion being posteriorly positioned as compared to the adult male face. The nose was smaller, narrower, and less protrusive. The distance between the lower and upper margins of the lips was greater, and the upper lip was located more posteriorly. The mouth width was similar but the chin point (pg) was situated more posteriorly. Similar analysis was applied to the groups of males and females (5-6, 11, and 17 years of age) and the results of these analyses show that there were statistically significant differences between males and females at all age groups and the difference between males and females were similar at all ages.

### **2.6.2 Forensic science**

In forensic science, the optical surface scanning has proved valuable in assisting in identification by building faces over dry skulls that have been found. Programs have been written using the depth of soft tissues over the underlying bone from CT scans, which can be used to determine the position of the surface of the soft tissues relative to the bone surface (Vanezis *et al.*, 1989; De Greef and Willems, 2005). Optical surface scanning has also proved useful in identifying suspected criminals from video footage or photographs (Linney and Coombes, 1998).

In medicine, optical surface scanning has been used as a mean of studying certain diseases such as investigations into the developmental model of schizophrenia (Waddington *et al.*, 1999; Hennessy *et al.*, 2002). It has also been used to identify changes in facial morphology as a result of drug therapy.

### **2.6.3 Prediction of jaw surgery**

Programs (e.g., Amira<sup>®</sup>) may also demonstrate the change in the surface of the face following movement of the jaws after orthognathic surgery (Moss *et al.*, 1988 and McCance *et al.*, 1993). The image can be viewed from any aspect, thus it is possible to allow the patient to see the potential 3D effects of surgery before it is undertaken (Moss, 2006).

### **2.6.4 Analysis of surface shape**

This method allows a description of the surface, which is independent of surface orientation (rotation and translation), and is thus the same from any viewpoint. A 3D rendered face can be segmented into nine surface types via the Shape Index (SI) values which was introduced in (1992) by Koenderink and Van Doorn. The points on the face are colour-coded based on the surface type to which they belong, in order to produce a surface type image which is a readily understandable way of displaying the data. The nine different surface shapes distinguished by their colour are: spherical cap (red), dome (pink), ridge (green), saddle ridge (dark blue), saddle (light blue), saddle rut (brown), rut (dark grey), trough (light grey), and spherical cup (white).

These programs have been used to identify differences in the shape of the face due to treatment (Ismail and Moss, 2002; Ismail *et al.*, 2002; Moss *et al.*, 2003). One other area in which these programs are proving useful is in facial genetics where attempts are being made to determine which features of the face are inherited and which are environmentally affected (McCulley, 2000). Moreover, 3D face shape analysis has been applied to the design and construction of protective equipments (Coblentz *et al.*, 1991).

### **2.6.5 Ultrasound**

Ultrasound is improving rapidly and resulting in some excellent 3D images of the face and underlying structures. The work has now progressed so that images can be displayed adding the 4<sup>th</sup> dimension "Time". Recently, the lips have been recorded in four dimensions and the movements of the muscles of the lips have been demonstrated (Deng *et al.*, 2000; Popat *et al.*, 2008a, b).

Ultimately, non-invasive ultrasound may provide an image of the hard tissues of teeth and jaws, thus dispensing with radiation. The advances in 3D imaging of the face and skull enable the results of treatment to be viewed from any perspective and to analyse the changes that have occurred more efficiently (Moss, 2006).

## **2.7 Facial dysmorphology**

Clinical dysmorphology is a medical discipline based on the assessment of patients presenting with congenital developmental abnormalities that can be isolated malformations or syndromes associated with developmental delay. A number of developmental anomalies are the result of a single anomaly in morphogenesis leading to a cascade of subsequent defects defining a sequence (Jones, 1997). Four categories of developmental anomalies have been described (Dollfus and Verloes, 2004):

- Malformation as a single morphogenetic defect
- Deformation resulting from mechanical constraints on a normal embryo
- Disruption sequence resulting from a destruction of a normal structure
- Dysplasia, defined as a primary defect in the differentiation and organization of a given tissue

There are various aetiologies associated with congenital anomalies and they include in utero exposure to exogenous teratogens (i.e., a drug, an infectious agent, or alcohol) or to an obstetrical hazard (i.e., leakage of amniotic fluid); chromosomal anomalies (i.e., trisomy, monosomy, or structural rearrangement as deletion, duplication, or translocation) or a defect at the level of genes implied in development (Elliott and Maher, 1994; Epstein, 1995; Opitz, 1982). More than 2,000 syndromes are assumed to be the result of alterations (mutations) of specific genes (Winter, 1998). The dramatic advances in molecular biology have opened the field to molecular investigations and a wide variety of genes have been identified as responsible for many developmental syndromes.

However, the clinical approach to these syndromes remains essential. Examination of the face is of great importance in this field as major or minor facial anomalies can be relevant for diagnosis. Morphological features are often so characteristic that it is well known that patients with the same syndrome can resemble each other more than their own non-affected siblings.

Phenotypic anomalies can be subdivided roughly into two subgroups: qualitative and quantitative. Qualitative anomalies are relatively easy to define as present or absent compared to an “ideal” human phenotype. Morphological measurements can be easily performed with transparent ruler derived measurements. However, these are less reliable than calliper-derived measurements, which are rarely used in practice. The measurements are compared to normal, such as the reference measures published by Feingold and Bossert (1974).

### **2.8 The role of 3D imaging in visualizing facial dysmorphology**

Many genetic syndromes involve a facial gestalt that suggests a preliminary diagnosis to an experienced clinical geneticist even before a clinical examination and genotyping are undertaken. Using visualization and pattern recognition, Hammond *et al.* (2004) showed that 3D dense surface models “DSM” of the full face characterize facial dysmorphology in Noonan syndrome and in 22q11 deletion syndrome.

Later on, Hammond *et al.* (2005) conducted a larger study involving 696 individuals. This study managed to extend the use of dense surface models to establish accurate discrimination between controls and subjects with Williams, Smith-Magenis, 22q11 deletion, or Noonan syndromes and between individuals with different syndromes in these groups. However, the full power of the DSM approach is demonstrated by the comparable discriminating abilities of localized facial features, such as periorbital, perinasal, and perioral patches, and the correlation of DSM-based predictions and molecular findings. This study demonstrated the potential of face shape models to assist clinical training through visualization, to support clinical diagnosis of affected individuals via pattern recognition, and to enable objective comparison of individuals sharing other phenotypic or genotypic properties.

### **2.9 The clinical assessment of craniofacial dysmorphology**

Size and shape variations of the craniofacial bones compared with the size of teeth are the significant underlying aetiology of the various kinds of malocclusions. Many orthodontic patients have mild to moderate skeletal discrepancies that are associated with unfavourable facial aesthetics, occlusion, as well as psychosocial complications (Birkeland *et al.*, 2000). Although human maxillofacial and dental morphology appears to be influenced by both genetic and environmental factors, an estimated 40% or more of the dental and skeletal variations that lead to malocclusion may be ascribed to hereditary factors (Lauweryns *et al.*, 1993; Townsend *et al.*, 1998; Eguchi *et al.*, 2004).

These malocclusions are usually associated with craniofacial imbalances due to retrognathic or prognathic maxillae (Proffit *et al.*, 1998). Early studies with longitudinal cephalometric radiographs and dental casts of siblings showed that facial skeletal features had stronger heritability when compared with pure dental features. Therefore, it was concluded that the skeletal contribution of a malocclusion has a significant hereditary component, as opposed to the more environmentally determined dental contribution (Harris and Johnson, 1991).

The association of facial dysmorphogenesis with various genetic disorders has increased information in the field of craniofacial genetics. However, the genetic component of subtle dysmorphisms commonly seen in orthodontic patients, such as prognathic or retrognathic maxillae, remains unclear. The structural variations of the face appear polygenic in origin (Shum *et al.*, 2000). Linkage of quantitative measurements on genetic traits, i.e., phenotypic differences with genomic differences, is a basic strategy for mapping quantitative trait loci (QTL).

The clinical assessment of craniofacial features is based on the overall subjective clinical evaluation of the face and body, in addition to the objective measurements that are important to validate the clinical impression. The face is methodically evaluated by regions: forehead, mid-face (periocular region, nose, and ears), and lower part of the face (mouth and chin).

Clinical photographs (the patient standing, the face and both profiles) should be a standard of any evaluation in dysmorphology of craniofacial features. Those pictures are useful for reviewing purposes, for off-consultation discussion, and for appreciation of the phenotypic evolution in the long term (DiLiberti and Olson, 1991; Dollfus and Verloes, 2004).

In order to help the clinician to diagnose the syndrome, databases are available that are based on the systematic morphological analysis of the patient, guiding the clinician by submitting a list of possibly corresponding syndromes. Many genetic syndromes involve craniofacial abnormalities (Gorlin *et al.*, 2001), a single facial feature, such as nose shape, may even be sufficient to suggest a particular syndrome. Experienced geneticists can often make an immediate diagnosis by recognizing characteristic facial features of a syndrome. Inexperienced clinicians may struggle to make such a gestalt diagnosis, e.g., in a very young children or when they had limited exposure to a particular syndrome or to an affected individuals of the same age or ethnic group.

Thus, the objective analysis of dysmorphic facial growth is potentially useful in training clinical geneticists and in assisting clinical diagnosis (Ward *et al.*, 2000; Hammond *et al.*, 2004). Several objective techniques for analysing craniofacial morphology, e.g., anthropometry of the head and face, cephalometry, and photogrammetry, have been reported (Allanson, 1997).

Anthropometric studies of the face have documented characteristic features and their change over time for a number of dysmorphic syndromes, e.g., Down syndrome (Allanson *et al.*, 1993), Rubinstein-Taybi syndrome (Allanson and Hennekam, 1997), and Sotos syndrome (Allanson and Cole, 1996). An early study of the Noonan syndrome (NS) phenotype documented changes in facial form causing some characteristic features to become more subtle with age (Allanson *et al.*, 1985). This remodelling of the face was reconfirmed later in a 2D photogrammetric study (Sharland *et al.*, 1993).

A study of lateral cephalometric radiographs of children with Williams syndrome identified important skeletal features contributing to facial appearance but it was not possible to use them to characterize the facial morphology conclusively (Mass and Belostoky, 1993). A photogrammetric study on children under 10 years of age with Williams syndrome has established soft tissue craniofacial indices outside normal ranges (Hovis and Butler, 1997).

Until recently, most studies of facial morphology have concentrated on the delineation of characteristic features and not on the construction and testing of computational models of face-shape variation, to be used to visualize and discriminate facial differences between or within syndromes, or between groups with specific syndromes and the general population.

The application of 2D face-shape analysis in Fetal Alcohol Syndrome (FAS) has resulted in a diagnostic protocol that is used in a number of clinical centers (Sokol *et al.*, 1991; Astley and Clarren, 1996; Sampson *et al.*, 2000). Studies using 2D images have achieved an accuracy of 74% in inter-syndrome discrimination comparing five syndromic groups, each with 6-13 individuals (Loos *et al.*, 2003).

Recently, rapid and non-invasive 3D imaging of the face has become available. The clinical usability of 3D images is considerable because the face is viewable from any angle and at closer proximity than most children, or even adults, would tolerate. Each 3D image comprises a surface of > 20,000 points. Unlike 2D images, the 3D surfaces are robust to changes in illumination. It is possible to retrieve 3D data from a single 2D image, but this requires standard lighting conditions or a previously constructed lighting model (Arridge *et al.*, 1985; Ayoub *et al.*, 1998).

Stereophotogrammetry using multi-images to calculate 3D measurements has proved more consistent than direct measurements to analyse facial dysmorphology of children in the diagnosis of fetal alcohol syndrome (Meintjes *et al.*, 2002). The 3D full face surface analysis has proven successful in delineating facial morphology in Noonan syndrome, 22q11 deletion syndrome, Bardet-Biedl syndrome, and Smith-Magenis syndrome, and discriminating between controls and subjects with Noonan syndrome and 22q11 deletion syndrome (Beales *et al.*, 1997; Hammond *et al.*, 2003a, b, 2004 and 2005).

## **2.10 The role of genes in human craniofacial variation**

### **2.10.1 *Basic concepts***

Cells are the fundamental working units of every living system. All the instructions needed to direct their activities are contained within the chemical DNA (deoxyribonucleic acid). DNAs from all organisms are made up of the same chemical and physical components. The DNA sequence is the particular side-by-side arrangement of bases along the DNA strand. This order spells out the exact instructions required to create a particular organism with its own unique traits.

The genome is an organism's complete set of DNA. Genomes vary widely in size; the smallest known genome for a free-living organism (bacterium) contains about 600,000 DNA base pairs, while the human and mouse genomes have some 3 billion. Except for mature red blood cells, all human cells contain a complete genome.

DNA in the human genome is arranged into chromosomes, physically separate molecules that range in length from about 50 million to 250 million base pairs. Human cells have 23 pairs of chromosomes (22 pairs of autosomes and one pair of sex chromosomes), giving a total of 46 per cell. A few types of major chromosomal abnormalities, including missing or extra copies or gross breaks and re-joinings (translocations), can be detected by microscopic examination. Most changes in DNA, however, are more subtle and require a closer analysis of the DNA molecule to find perhaps single-base differences (illustrating Figures 1-4 in the Appendix).

Each chromosome contains many genes, the basic physical and functional units of heredity. Genes are specific sequences of bases that encode instructions on how to make proteins. Genes comprise only about 2% of the human genome; the remainder consists of non-coding regions, whose functions may include providing chromosomal structural integrity and regulating where, when, and in what quantity proteins are made. The human genome is estimated to contain 20,000-25,000 genes. Although genes get a lot of attention, it's the proteins that perform most life functions and even make up the majority of cellular structures.

The word '*intron*' is derived from the term intragenic region, i.e. a region inside a gene. An intron is any nucleotide sequence within a gene that is removed by RNA splicing while the final mature RNA product of a gene is being generated. The term intron refers to both the DNA sequence within a gene and the corresponding sequence in RNA transcripts. Sequences that are joined together in the final mature RNA after RNA splicing are exons. Introns are found in the genes of most organisms and many viruses, and can be located in a wide range of genes, including those that generate proteins, ribosomal RNA (rRNA), and transfer RNA (tRNA). When proteins are generated from intron-containing genes, RNA splicing takes place as part of the RNA processing pathway that follows transcription and precedes translation. Introns are now known to occur within a wide variety of genes throughout organisms and viruses within all of the biological kingdoms. The frequency of introns within different genomes is observed to vary widely across the spectrum of biological organisms. For example,

introns are extremely common within the nuclear genome of higher vertebrates (e.g. humans and mice), where protein-coding genes almost always contain multiple introns, while introns are rare within the nuclear genes of some eukaryotic microorganisms. In contrast, the mitochondrial genomes of vertebrates are entirely devoid of introns, while those of eukaryotic microorganisms may contain many introns.

The term '*exon*' derives from the expressed region, an exon is any nucleotide sequence encoded by a gene that remains present within the final mature RNA product of that gene after introns have been removed by RNA splicing. The term exon refers to both the DNA sequence within a gene and to the corresponding sequence in RNA transcripts. In RNA splicing, introns are removed and exons are covalently joined to one another as part of generating the mature messenger RNA. In many genes, each of the exons contain part of the open reading frame (ORF) that codes for a specific portion of the complete protein. However, the term exon is often misused to refer only to coding sequences for the final protein. This is incorrect, since many non-coding exons are known in human genes (Zhang, 1998).

Exonization is the creation of a new exon, as a result of mutations in intronic sequences (Sorek, 2007).

### **2.10.2 Genetic and environmental effects on craniofacial morphology**

Despite the morphological diversity of human skulls being the basis of innumerable studies, relatively little is known about the genes and molecular processes which control skull growth and how variation in these may lead to the diversity of human facial phenotypes. Generally, any two copies of the human genome differ from one another by approximately 0.1% of nucleotide sites, that is, one variant per 1,000 bases on average (Li and Sadler, 1991; Wang *et al.*, 1998; Cargill *et al.*, 1999; Halushka *et al.*, 1999). The most common type of variant, a SNP (single nucleotide polymorphism, pronounced `snip'), is a difference between chromosomes in the base present at a particular site in the DNA sequence. For example, some chromosomes in a population may have a C at that site "C allele", whereas others have a "T allele". An allele is one of a number of alternative forms of the same gene or same genetic locus (a group of genes). It is the alternative form of a gene for a character producing different effects. Sometimes different alleles can result in different observable phenotypic traits, such as different pigmentation. However, many genetic variations result in little or no observable variation.

It has been estimated that, in the world's human population, about 10 million sites (that is, one variant per 300 bases on average) vary such that both alleles are observed at a frequency of  $\geq 1\%$ , and that these 10 million common SNPs constitute 90% of the variation in the population (Kruglyak and Nickerson, 2001; Reich, Gabriel and Altshuler, 2003). The remaining 10% is due to a vast array of variants that are each rare in the population.

The presence of particular SNP alleles in an individual is determined by testing (genotyping) a genomic DNA sample.

*Intronic SNP* is a single nucleotide polymorphism in intronic sequences consists of a variation at an appreciable frequency between individuals of a single interbreeding population of a single nucleotide.

*Exonic SNP* is a single nucleotide polymorphism which occurs in an exon, and may affect the amino acid sequence of the protein when translated.

The recent completion of the human genome sequence has shifted research efforts in genomics toward understanding the function of the human genome, its regulation, and how sequence variation contributes to human different phenotypes. Large numbers of sequence variants throughout the human genome have been identified, and efforts are currently underway to understand the overall relationship between sequence variation on a genomic level, and the goal of identifying a subset of single nucleotide polymorphisms (SNPs) that will capture the vast majority of genetic diversity found in the human population. The hope is that this subset could then be used to identify genomic regions and SNPs, in genome-wide analyses, which may predispose human beings to common disorders such as obesity, diabetes, or cardiovascular disorders, or contribute to human complex physical traits.

Using SNP data to examine human phenotypic differences, genetic variation among human races can be observed in almost any trait, from the physical and biochemical, to disease resistance. Humans are identical

over most of their genomes. Thus, only a relatively small number of genetic differences have resulted in the striking variation seen among individuals of our species. When we think of variation between people, we often think of differences in height, weight, face shape, and skin colour. Each of these characteristics is only partially controlled by genes. The complex interaction between genes and the environment, as well as between multiple genes, makes trying to understand and quantify human phenotypic variation difficult. Therefore, instead of looking at complex human traits, several researchers went straight to the source and looked for nucleotide sequences in the genome that could tell them about individual human variation. For these studies, the identification of single base changes (single nucleotide polymorphisms) was considered ideal.

Many genes are regarded as master genes for head and face development, controlling pattern, induction, and epithelial-mesenchymal interactions during development of the craniofacial complex (Klingenberg *et al.*, 2001). Malocclusion should be regarded not as abnormal or as a disease, but as a variation of occlusion in a continuous, multi-factorial trait (Mossey, 1999a, b). Most genetic studies of shape characterize in terms of the relative sizes of parts and use a set of linear distances for measurement (Klingenberg *et al.*, 2001). Moreover, as clinicians we need to have a clear and in-depth understanding of the mechanisms of both normal and abnormal facial growth and the subsequent effects on occlusion and facial morphology. This requires having a good knowledge of the contributed genes and the hereditary effects on the development of the face.

### 2.10.2.1 Genetic expression in craniofacial development:

The vertebrate head is a highly complex composite structure whose morphological characteristics are controlled at the level of the gene (Cobourne, 2000). The embryonic vertebrate face is composed of similarly sized buds of neural crest-derived mesenchyme encased in epithelium. These buds or facial prominences grow and fuse together to give the postnatal morphological characteristics of each species. Many signals and genes have been shown to play an important role in facial morphogenesis via controlling the development of facial prominences to the skeletal structure of the face. Richman and Lee (2003) examined two experiments, one at the genetic level and one at the signal level, in which transformation of facial prominences and subsequent change of jaw identity was induced. They proposed that signals such as retinoids, and transcription factors such as distal-less related genes specify jaw identity.

There is now increasing evidence for the role of gene families that encode transcription factors in determining the embryonic plan of the developing craniofacial complex. These genes act as regulators of gene transcription being intimately involved with the control of complex interactions between multiple downstream genes. Combinatorial expression of the *Hox* genes (a family of highly conserved master regulatory genes related to the homeotic genes of the fruitfly *Drosophila*) have been shown to play a definitive role in patterning distinct regions of the craniofacial complex (Cobourne, 2000).

Much of the fascination regarding the neural crest lies within its ability to generate a diverse array of cell types throughout the vertebrate body. These cells originate at the border of the neural and non-neural ectoderm, and later delaminate from the dorsal neural tube. In the chick, neural crest migration occurs after the neural tube has closed; however, in both the human and mouse, cranial neural crest cells (NCCs) have been shown to migrate from the unfused neural folds (Nichols, 1981; O’Rahilly and Müller, 2007). Once free from the neural tube, NCCs move throughout the body. Depending on their origin, cranial NCCs will either migrate through the facial mesenchyme and into the frontonasal process, or will populate the branchial arches (Noden, 1975; Lumsden *et al.*, 1991; Serbedzija *et al.*, 1992) to generate multiple derivatives, including: the majority of the cranial connective tissue and skeletal elements, neurons and glia of the peripheral nervous system, and cells contributing to the valves of the heart, secretory cells, and melanocytes.

The expression and function of several genetic markers during neural crest development have been integrated into operational models as a cascade, genetic network, or neural crest gene regulatory network (NC-GRN). These models link the expression and function of signaling molecules, transcription factors and other neural crest markers from early NCC induction events, specification, migration and eventual differentiation. According to the NC-GRN, signaling molecules (*BMP*, *FGF*, *Notch*, *RA*, and *Wnt*) participate in both induction and later steps of neural crest development. This induction triggers the expression of a specific set of

transcription factors collectively known as border specifier genes (*Msx1*, *Msx2*, *Pax3*, *Pax7*, and *Zic1*), which – along with signaling molecules – direct the expression of neural crest specifiers (*AP-2*, *FoxD3*, *Snail2*, *Sox9* and *Sox10*). Specific roles for some of these genes in neural crest development have been illustrated through functional assays in a variety of model systems, including *Xenopus*, zebrafish, chick and mouse. For instance, *Pax3*, *Pax7*, *Sox10* and *AP-2* mutant mice all demonstrate neural crest defects. These manifest as deformities of the nose and jaw in both *Pax3* (*Spotch*) and *Pax7* mutants; *Pax3* mutants additionally exhibit malformations of ganglia of the peripheral nervous system (Tremblay *et al.*, 1995, 1998; Mansouri *et al.*, 1996).

On the other side, the role of muscles in the aetiology and development of facial deformity, particularly in the vertical dimension has also been investigated in several ‘gene expression studies’. Following the publication of the human genome it has now become possible to examine the total gene expression in a particular body tissue using micro-array technology, rather than multiple investigations of single structural components. RNA extracted from a muscle biopsy can be amplified through a process of reverse transcription, and following fluorescent labelling can be hybridized to the DNA on a microchip. The varying levels of fluorescence emitted from the individual array gives the relative expression of a particular gene sequence. This can then be read by a computer to give the relative gene expression of a tissue from one subject compared to another (Hunt *et al.*, 2006).

Table 2.2 summarises some of the genetic expression studies in craniofacial development.

<b>Table 2.2. Genetic expression studies in craniofacial development</b>			
<b>N</b>	<b>Genetic Expression</b>	<b>Effect</b>	<b>Reference</b>
1	<i>IIX</i> myosin heavy chain protein " <i>MHC</i> "	"Long face" 2-4 fold reduction in gene expression as compared with "normal" facial form	Hunt <i>et al.</i> , 2006
2	$\alpha$ 6 integrin expression		
3	Fibronectin		
4	$\alpha$ cardiac <i>MHC</i>	"Long face" 4-6 fold increase in gene expression as compared with "normal" facial form	
5	Perinatal <i>MHC</i>		
6	Developmental <i>MHC</i>		
7	Growth hormone gene receptor	Mandibular height	Zhou <i>et al.</i> , 2005
8	Chromosome 12	Maxillary shape	Oh <i>et al.</i> , 2007
9	Chromosome 10/11	Mandibular size	Dohmoto <i>et al.</i> , 2002
10	<i>FGF</i> signaling <i>Fgfr2&amp;3</i> , <i>Fgf8</i> regulates expression of <i>Tbx2</i> , <i>Erm</i> , <i>Pea3</i> , <i>Pax3</i>	Mandible and maxilla, Normal development of the nasal region	Nie <i>et al.</i> , 2006 Firnberg and Neubüser, 2002
11	<i>Dlx-2</i> and <i>Dlx-3</i>	Mandible and maxilla	Robinson and Mahon, 1994
12	Orthodontical-related homeobox " <i>Otx2</i> "	Mandible and forebrain	Hide <i>et al.</i> , 2002
13	Paired-box <i>PAX3</i>	Ear, eye and facial development	Goulding <i>et al.</i> , 1991 Gruss and Walther, 1992 Stuart <i>et al.</i> , 1994 Gerard <i>et al.</i> , 1995 Read and Newton, 1997 Terzic and Saraga-Babic, 1999
14	Paired-box <i>PAX6</i>	Eye development	Walther and Gruss, 1991 Nishina <i>et al.</i> , 1999 Terzic and Saraga-Babic, 1999
15	Paired-box <i>PAX9</i>	Mandible and maxilla, Tooth agenesis (Oligodontia)	Stockton <i>et al.</i> , 2000
16	Paired Homeobox ( <i>Hox</i> ) <i>Pitx/Ptx1/Brx2</i> , <i>Pitx2/Otx2/RIEG/Brx1</i>	Mandible and maxilla	Cobourne, 2000 Lanctot <i>et al.</i> , 1999
17	<i>Basic helix-loop-helix Twist</i>	Facial prominence Facial asymmetry	Bourgeois <i>et al.</i> , 1998
18	<i>MAFB</i>	Palatal development	Beaty <i>et al.</i> , 2010

Among the world's most common congenital malformations are cleft lip and cleft palate which occur in one in every 700 births. An international consortium of scientists, led by researchers at 'Johns Hopkins University Bloomberg School of Public Health' has identified two genes that when altered are closely associated with cleft lip and/or cleft palate. This finding is the result of a large family-based, genome-wide association study of cleft lip and/or cleft palate (Beaty *et al.*, 2010). This study identified four different regions of the human genome likely to contain genes controlling risk for cleft lip and/or cleft palate. Two of these regions, the *IRF6* gene on chromosome 1 and a region on chromosome 8, were previously identified in other studies (Park *et al.*, 2007). Moreover, this study identified genes (*MAFB*) on chromosome 20 and (*ABCA4*) on another part of chromosome 1 as being associated with cleft lip and/or cleft palate. In addition to findings in humans, the investigators showed that *MAFB* gene was active in the developing head and mouth of embryonic mice, which further argues this gene plays some role in normal facial development.

Some of the paired-box (*PAX*) genes have been identified to influence craniofacial development. *PAX* genes are a family of genes coding for tissue specific transcription factors containing a paired domain and usually a partial or complete homeodomain. An octapeptide may also be present. *PAX* proteins are important in development for the specification of specific tissues. The murine *Pax* gene family consists of nine members (Walther *et al.*, 1991; Wallin *et al.*, 1993) which are grouped into six different classes (Callaerts *et al.*, 1997).

The classification of *Pax* genes is based on the presence of gene products containing the obligatory paired domain, additional content of octapeptide, and complete or partial homeodomain (Callaerts *et al.*, 1997).

The expression of human *PAX6* and *PAX3* genes was investigated in 6 human (6-9 week old) conceptuses by in situ hybridization (Terzic and Saraga-Babic, 1999). *PAX6* expression was detected in both layers of the optic cup, optic stalk and prospective corneal epithelium, while transcripts of *PAX3* were observed in the ventricular zone at the mesencephalic-rhombencephalic border, and in the dorsal part of the ventricular zone and the roof plate of the medulla oblongata and the spinal cord. *PAX3* gene characterized ectomesenchyme of the upper and lower jaw, and tongue. During early human development, *PAX6* and *PAX3* genes seem to be involved in the brain regionalization and establishment of dorso-ventral polarity of the spinal cord. Additionally, *PAX6* participates in organogenesis of the eye and the pituitary gland, and *PAX3* in the development of face and neck mesenchyme.

The role of different *PAX* genes is given below (with emphasis on *PAX3* and *PAX9* as these two genes have been shown to influence craniofacial development):

- *PAX1* has been identified in mice with the development of vertebrate and embryo segmentation, and some evidence this is also true in humans. It transcribes a 440 amino acid protein from 4 exons and 1,323bps (binding proteins) in humans.

- *PAX2* has been identified with kidney and optic nerve development. It transcribes a 417 amino acid protein from 11 exons and 4,261bps in humans.
- *PAX3* has been identified with ear, eye and facial development (Gerard *et al.*, 1995; Read and Newton, 1997; Terzic and Saraga-Babic, 1999). This gene was formerly known as *splotch*. It belongs to a family of genes called homeobox (*homeoboxes*). It also belongs to the paired box (*PAX*) family of transcription factors. It transcribes a 479 amino acid protein in humans. *PAX3* plays a critical role in the formation of tissues and organs during embryonic development. Generally, *PAX* gene family is important for maintaining normal function of certain cells after birth. To carry out these roles, *PAX* genes provide instructions for making proteins that attach to specific areas of the DNA. By attaching to critical DNA regions, *PAX* proteins help control the activity of particular genes. On the basis of this action, *PAX* proteins are called transcription factors. During embryonic development, *PAX3* is active in cells called neural crest cells. These cells migrate from the developing spinal cord to specific regions in the embryo. The protein made from *PAX3* gene directs the activity of other genes that signal neural crest cells to form specialized tissues or cell types such as some nerve tissue, bones in the face and skull (craniofacial bones), and pigment-producing cells called melanocytes. Melanocytes produce the pigment melanin, which contributes to hair, eye, and skin colour. Melanocytes are also found in certain regions of the brain and inner ear. *PAX3* protein is also necessary for the formation of muscle tissue (myogenesis) early in development.

Craniofacial-deafness-hand syndrome is caused by mutations in the *PAX3* gene. At least one *PAX3* gene mutation has been identified in individuals with craniofacial-deafness-hand syndrome, a condition characterized by distinctive facial features, profound hearing loss, and abnormalities of the hand muscles that can restrict movement. The mutation replaces a single protein building block (amino acid) called asparagine with another amino acid called lysine at position 47 in the *PAX3* protein. This mutation appears to affect the ability of the *PAX3* protein to bind to DNA. As a result, the *PAX3* protein cannot control the activity of other genes and cannot direct the neural crest cells to form specialized tissues. A lack of specialization of neural crest cells leads to the impaired growth of craniofacial bones, nerve tissue, and muscles seen in craniofacial-deafness-hand syndrome. In addition, several *PAX3* gene mutations have been identified in people with Waardenburg syndrome (WS), types I and III (Waardenburg, 1951; Read and Newton, 1997; Tsukamoto *et al.*, 1992; Pingault *et al.*, 2010). Some of these mutations change single amino acids used to make the *PAX3* protein. Other mutations lead to an abnormally small version of the *PAX3* protein. Researchers believe that all *PAX3* gene mutations have the same effect: they destroy the ability of the *PAX3* protein to bind to DNA and regulate the activity of other genes. As a result, melanocytes do not develop in certain areas of the skin, hair, eyes, and inner ear, leading to hearing loss and the patchy loss of pigmentation that are characteristic features of Waardenburg syndrome. Additionally, loss of *PAX3* protein function disrupts development of craniofacial bones and

certain muscles, producing the limb and facial features that are unique to Waardenburg syndrome, types I and III.

Biologically, *PAX3* is expressed longitudinally down the length of the neural tube from the hindbrain, but only in mitotically active cells of the alar and roof plates, dorsal to the sulcus limitans. These cells are the source of the neural crest. Among neural crest derivatives, *PAX3* expression was seen in the spinal ganglia and some craniofacial cells (*nasal process* and some first and second branchial arch derivatives). It is also expressed in early embryonic phases in dermatomyotome of paraxial mesoderm which helps to demarcate. In that way *PAX3* contributes to early striated muscle development since all myoblasts are derived from dermatomyotome of paraxial mesoderm. In addition, *PAX3* is frequently expressed in melanomas (Medic and Ziman, 2010) and contributes to tumor cell survival (Scholl *et al.*, 2001).

In a recent experiment on mice (Guo *et al.*, 2010), the authors identified a novel nonsense mutation in *PAX3* gene in *N*-ethyl-*N*-nitrosourea (ENU)-derived white belly spotting (wbs) mice and its genetic interaction with the *c-Kit*. This novel mutation (*K107X*) in the *PAX3* coding region in wbs mice caused loss of *PAX3* protein in the homozygous mutant. The identification of two novel mutant lines on white belly spotting provides not only new lines of murine models for Waardenburg syndrome (WS) and piebaldism but also hints for the functional studies of the two proteins, *PAX3* and *c-Kit*. The interaction between *PAX3* and *c-Kit* during melanocyte development

provides new clue to the dissection of the complexity of the regulatory network of melanocyte development.

During embryonic development, *PAX3* is active in neural crest cells and plays a critical role in the formation of tissues and organs, such as limb muscles, melanocytes, craniofacial bones, and nerve tissue (Machado *et al.*, 2001). Recently, it has been reported that *PAX3* gene acts as a nodal point in melanocyte stem cell differentiation by repressing the dopachrome tautomerase (*Dct*) promoter (Lang *et al.*, 2005). In humans, loss of function with *PAX3* leads to WS1 and WS3, while translocation of *PAX3* with *FKHR* leads to rhabdomyosarcoma (Barr *et al.*, 1993). The first identified loss-of-function mouse model of *PAX3* was named *Spotch* (Epstein *et al.*, 1993), which highly resembled the hypopigmentation phenotype in WS. Epstein and his associates (1993) identified a mutation within intron 3 of the *PAX3* gene that produces aberrantly spliced mRNA transcripts in the *spotch* mouse mutant, which eventually lead to the generation of non-functional *PAX3* polypeptides. Murine *PAX3* (479 amino acids) contains two DNA-binding domains, a paired-box domain (PD) and a homeodomain (HD) (Goulding *et al.*, 1991). The *wbs* mutation (Guo *et al.*, 2010) is located at the 3' end of exon 2 (of 8 exons in *PAX3* gene), this nonsense mutation (*K107X*) within the highly conserved *motif* of the pairedbox domain lead to truncation of the paired-box domain and loss of the homeodomain. A western blot analysis using an antiserum raised against the N-terminal part of the *PAX3* detected no normal-size or truncated *PAX3* protein in the homozygous mutant embryo, indicating that the mutation is a null mutation.

Similar to previously reported *PAX3* null alleles, homozygous *wbs* mutants displays spina bifida and embryonic lethality. Thus, the *wbs* mutation identified in this study serves as an appropriate model for WS.

- *PAX4* has been identified with pancreatic islet beta cells. It transcribes a 350 amino acid protein from 9 exons and 2,010bps in humans.
- *PAX5* has been identified with neural and spermatogenesis development and b-cell differentiation. It transcribes a 391 amino acid protein from 10 exons and 3,644bps in humans.
- *PAX6* is the most researched and appears throughout the literature as a “master control” gene for the development of eyes and sensory organs (Walther and Gruss, 1991; Terzic and Saraga-Babic, 1999), certain neural and epidermal tissues as well as other homologous structures, usually derived from ectodermal tissues.
- *PAX7* has been possibly associated with myogenesis. It transcribes a protein of 520 amino acids from 8 exons and 2,260bps in humans. *PAX7* directs postnatal renewal and propagation of myogenic satellite cells but not for the specification.
- *PAX8* has been associated with thyroid specific expression. It transcribes a protein of 451 amino acids from 11 exons and 2,526bps in humans.
- *PAX9* has been associated with a number of organ and other skeletal developments, particularly teeth (Stockton *et al.*, 2000). *PAX9* is a member of the paired box family of transcription factors. It transcribes a protein of 341 amino acids from 4 exons and 1,644bps in humans. It has been also found in mammals contributing to tooth development (Pereira *et al.*, 2006).

*PAX9* may more generally involve development of stratified squamous epithelia as well as various organs and skeletal elements. *PAX9* plays a role together with other genes (*AXIN2* and *MSX1*) in the absence of wisdom teeth in some human populations (Pereira *et al.*, 2006), and in oligodontia cases (congenital absence of 6 teeth or more) (Mu *et al.*, 2013). More recently, *PAX9* polymorphism has been reported for susceptibility to sporadic non-syndromic severe anodontia (congenital absence of all teeth) in a case-control study in the south-west China (Wang *et al.*, 2013). In addition, genetic associations have been identified between *PAX9* single-nucleotide polymorphisms and non-syndromic cleft lip with or without cleft palate (Lee *et al.*, 2012a), and common *PAX9* variants with permanent tooth size variation in non-syndromic East Asian populations (Lee *et al.*, 2012b). This gene has been also found amplified in lung cancer. The amplification covers three tissue developmental genes – *TTF1*, *NKX2-8*, and *PAX9* (Kendall *et al.*, 2007).

#### **2.10.2.2** *Recent advances in analysing the effects of genes on craniofacial morphology:*

Epigenetics can be defined as the study of heritable changes in gene expression that are not due to changes in DNA sequence. The discovery that differentiated cells can be artificially reprogrammed into induced pluripotent stem cells by a small set of transcription factors has opened up exciting medical prospects and provided good opportunity to investigate how stable epigenetic states are built and reversed. Diverse biological properties can be affected by epigenetic mechanisms. Epigenetic events

at the local level during tooth formation can lead to quite major differences in the final appearance of the dentitions of MZ co-twins (Townsend *et al.*, 2005, 2012; Townsend and Brook, 2008, 2013).

Epigenetic transcriptional enhancers, a major category of functional non-coding DNA - are likely involved in many developmental and disease-relevant processes (Visel *et al.*, 2009, 2013). To examine the role of distant-acting enhancers in the craniofacial development, recent experiments on mice demonstrated the functional importance of enhancers in defining face and skull morphology (Attanasio *et al.*, 2013). Thousands of regions in the genome act like switches for the many genes that code for facial features, such as the shape of the skull or size of the nose.

A recent study (Claes *et al.*, 2014) attempted modeling 3D facial shape from DNA. The authors used spatially dense quasi-landmarks to measure face shape in population samples with mixed West African and European ancestry from three locations (United States, Brazil, and Cape Verde). Using bootstrapped response-based imputation modeling (BRIM), they uncovered the relationships between facial variation and the effects of sex, genomic ancestry, and a subset of craniofacial candidate genes. The facial effects of these variables were summarized as response-based imputed predictor (RIP) variables, which were validated using self-reported sex, genomic ancestry, and observer-based facial ratings (femininity and proportional ancestry) and judgments (sex and population group). By jointly modeling sex, genomic ancestry, and genotype, the independent

effects of particular alleles on facial features can be uncovered. The results on a set of 20 genes showing significant effects on facial features provide support for this approach as a novel mean to identify genes affecting normal-range facial features and for approximating the appearance of a face from genetic markers.

Moreover, a recent genome-wide association study of primary tooth eruption identified pleiotropic loci to be associated with height and craniofacial distances (Fatemifar *et al.*, 2013). In this study, the authors identified a total of 15 independent loci, with 10 loci reaching a genome-wide significance ( $P < 5 \times 10^{-8}$ ) for 'age at first tooth' and 11 loci for 'number of teeth'. The identified loci included eight previously unidentified loci, some containing genes known to play a role in tooth and other developmental pathways. Three of these loci, containing the genes *HMGA2*, *AJUBA* and *ADK*, also showed evidence of association with craniofacial distances, particularly those indexing facial width. Their results suggest that the genome-wide association approach is a powerful strategy for detecting variants involved in tooth eruption, and potentially craniofacial growth and more generally organ development.

**2.10.2.3** *Studies that have identified hereditary, genetic and environmental effects on craniofacial morphology:*

For generations, clinicians and scientists have argued as to the respective contribution of genetics and so called environmental factors in influencing the ultimate facial form and associated malocclusion. Table 2.3 lists some of the work that has identified hereditary, genetic (association studies) and environmental effects on craniofacial morphology.

Table 2.3. Hereditary, genetic, and environmental effects on craniofacial morphology

Hereditary Effects						
Sample		Method	Facial Parameters	Effect	(Sig level) p-value/ correlation coefficients	Reference
Ethnicity	N					
Different families examined at the University of Illinois, Chicago, United States.	65 members (28 parents and 37 offspring) of 15 families, 13 of which included same sex twins	Cephalometry	12 angular measurements	None of the measurements showed significant genetic variation. Twins showing pronounced outward similarity may show dissimilarity in the craniofacial pattern.	(Non Sig) Low correlation coefficients	Wylie, 1944
“Mount Holyoke” college students with their sisters, and families lived near the college (United States).	275 subjects	Cephalometry	9 angular measurements	Significant positive correlation in several instances, particularly between sisters. The angle formed by the palatine plane relative to the upper part of the face shows the highest degree of correlation.	0.01 0.05	Stein, Kelley and Wood, 1956
Turkish Anatolian siblings	138 subjects (70 women) (68 men)	Cephalometry	6 facial proportions and 6 soft tissue measurements	The genetic determination significantly higher in the soft-tissue measurements (except upper lip) than in the facial proportions.	0.001 0.01 0.05	Baydas <i>et al.</i> , 2007
Twins from the East Flanders Prospective	79 pairs (33 MZ) (46 DZ)	Cephalometry	5 facial proportions based on 4 vertical and 5 horizontal measurements	All facial proportions were controlled by additive genes and the specific environment. The highest genetic component was 71% for upper to lower facial height.	0.05	Savoie <i>et al.</i> , 1998
Twins from Italy	10 pairs MZ, 10 pairs DZ same sex twins, and 10 pairs of same sex singletons	Cephalometry	39 lateral view cephalometric parameters	The 39 cephalometric variables are under strong genetic control, especially the vertical ones. Heritability more expressed anteriorly than posteriorly. Mandibular shape more genetically determined than mandibular size.	(Sig) High correlation coefficients	Manfredi <i>et al.</i> , 1997
Children and their parents from Iceland	363 children (assessed at 6 and 16 years old)	Cephalometry	33 linear and angular parameters	Cephalometric data can support predictions. Analysis of parental data can have predictive value for offspring.	0.001 0.01 0.05	Johannsdottir <i>et al.</i> , 2005
Twins including white, Asian, and Afro-Caribbean	52 subjects (10 pairs MZ) (16 pairs DZ)	3D optical surface scanning	28 linear distances	Significant genetic determination for mid-facial parameters (left eye width, intercanthal width, nose height, and nose width).	0.05	Naini and Moss, 2004

Genetic Effects (association studies)							
Sample		Method	Gene/SNP	Facial Parameters	Effect	(Sig level) P-value	Reference
Ethnicity	N						
Chinese	(Stage 1) 158 cases 147 controls (Stage 2) 211 cases 224 controls	Clinical examination, cephalometry (diagnostic aid)	<i>EPB41</i> /rs4654388	ANB angle (diagnostic aid)	Mandibular prognathism	Stage 1 (0.03, 0.05)  Stage 2 (0.008)	Xue <i>et al.</i> , 2010a, b
Chinese	211 cases 224 controls	Clinical examination, cephalometry (diagnostic aid)	<i>COL2A1</i> /rs1793953	ANB angle (diagnostic aid)	Mandibular prognathism	Genotype F. (0.025)  Allele Freq. (0.031)	Xue <i>et al.</i> , 2014
White, Asian, African American, and Hispanic	44 cases 36 controls	Clinical examination, cephalometry (diagnostic aid)	<i>MYO1H</i> /rs10850110	ANB angle, A-B plane (diagnostic aid)	Mandibular prognathism	0.03	Tassopoulou-Fishell <i>et al.</i> , 2012
White (UCL Hospital and Whipps Cross University Hospital/ UK, and Riyadh Military Hospital/ Saudi Arabia)	29 subjects (8 males) (21 females)  Age Range (16-36) Years	Clinical examination, cephalometry	<i>MYH</i> genes ( <i>MYH1</i> , <i>MYH2</i> , <i>MYH3</i> , <i>MYH6</i> , <i>MYH7</i> , and <i>MYH8</i> )	ANB angle, Lower anterior face height	Prognathic and retrognathic facial phenotypes have different masseter muscle gene expressions	0.05	Moawad <i>et al.</i> , 2012
Chinese	92	Clinical examination, cephalometry	<i>CYP19A1</i> /rs2470144 and rs2445761	ANB angle (diagnostic aid); Maxillary and mandibular sagittal lengths (condyion to anterior nasal spine, condyion to hard-tissue pogonion).	Pubertal sagittal jaw growth (males)	Maxillary (.003, .002)  Mandibular (0.0001)	He <i>et al.</i> , 2012
Japanese Hispanics Chinese Euro-Americans African American	167 24 24 24 24	Cephalometry	Growth Hormone polymorphisms <i>P561T</i> and <i>C422F</i>	Cranial base length, Maxillary length, Total mandibular length, Mandibular corpus length, Mandibular ramus height.	Mandibular ramus height	0.03	Tomoyasu <i>et al.</i> , 2009
German European Dutch European	529 2497	2D photos 3D MRI	<i>GREM1</i> /rs1258763 <i>CCDC26</i> /rs987525	Nose width, Bizygomatic distance	Nose width, Bizygomatic distance	6x10 <sup>-4</sup> 0.017	Boehringer <i>et al.</i> , 2011

(Europeans from several countries) Netherlands Germany Australia Canada UK	(Total 10,000) Discovery Phase 5,388 (Dutch, German, and Australian) Replication Phase (2,337 Australian, 568 Canadian, and 1,530 UK)	2D photos 3D MRI	<i>PRDM16</i> /rs4648379 <i>PAX3</i> /rs974448 <i>TP63</i> /rs17447439 <i>C5orf50</i> /rs6555969 <i>COL17A1</i> /rs805722	48 facial phenotypes including the centroid size, 36 inter-landmark distances and 11 shape PCs.	AlrL-Prn AlrR-Prn EyeR-N EyeL-N EyeR-EyeL ZygR-N ZygL-N	Discovery All SNPs ( $5 \times 10^{-8}$ )  Replication Highest Association ( $7.5 \times 10^{-5}$ )	Liu <i>et al.</i> , 2012
North Europeans	Discovery phase (2,185) Replication phase (1,622)	3D laser scanning	<i>PAX3</i> /rs7559271	54 facial distances 14 principal components	Nasal bridge prominence	Discovery ( $2.2 \times 10^{-10}$ )  Replication ( $4 \times 10^{-7}$ )	Paternoster <i>et al.</i> , 2012
People of European ancestry from the customer base of 23andMe	Over 55,000	Self-reported morphological traits	<i>ZEB2</i>	Chin dimple, nose shape, dimples, earlobe attachment, nose-wiggling ability, and central diastema	Chin dimple	$4 \times 10^{-5}$	Eriksson <i>et al.</i> , 2012
<b>Environmental Effects</b>							
Sample		Method	Medical Condition	Facial Parameters	Effect	(Sig level) P-value/ confidence interval	Reference
Ethnicity	N						
Egyptians (Caucasians)	20 cases 20 controls (males)	Cephalometry	Juvenile Diabetes (Type I)	33 cephalometric linear and angular measurements	The diabetics had decreased linear/angular measurements as compared to the controls	0.01 0.05	El-Bialy <i>et al.</i> , 2000
Patients were examined at the University of British Columbia, Canada.	25 cases (adult males)	Cephalometry	Obstructive Sleep Apnea (OSA)	22 variables including 16 craniofacial, 2 airway, 2 tongue, and 2 hyoid.	OSA subjects showed several alterations in the craniofacial form	0.05	Lowe <i>et al.</i> , 1986
White, North American children	25 pairs (cases and their normal siblings), and other 14 controls.	Cephalometry	Perennial Allergic Rhinitis	28 cephalometric linear and angular measurements	The allergic children had longer, more retrusive faces than controls.	0.05	Trask <i>et al.</i> , 1987

African American	73 cases (42 males) (31 females)  69 controls (35 males) (34 females)	Anthropometry (direct clinical measurements using a manual caliper)	Schizophrenia	7 facial measurements to cover facial depth, upper facial height, mid-facial height, lower facial height, and total facial height.	Gender-specific differences between cases and controls in mid-facial depth and upper and lower facial heights.	0.001	Compton <i>et al.</i> , 2007
British Caucasians	418 cases 3010 controls	3D laser scanning	Asthma	9 facial parameters (5 linear and 4 angular)	Mid-face height was shorter and inter-ala (nose) width was wider in asthmatic females only	95% CI	Al Ali <i>et al.</i> , 2012
British Caucasians	734 cases 2829 controls	3D laser scanning	Atopy	8 facial parameters (7 linear and 1 angular)	Total anterior face height and mid-face height were longer in atopic children	95% CI	Al Ali <i>et al.</i> , 2013

**MZ: monozygotic; DZ: dizygotic; CI: confidence interval**

## 2.11 Genotype-phenotype association analyses

There are two primary analytic methods for mapping genes involved in human traits: linkage and association. Association methods provide greater power and resolution than linkage analyses (Risch and Merikangas, 1996), and they have become increasingly popular for mapping genes involved in complex phenotypes. This popularity derives from the rapidly increasing catalogue of DNA sequence variants across the genome that can be used as markers in genetic analyses. In addition to knowing the variation across the genome, the cost and time to parse such variation has been steadily decreasing (Palmer and Cardon, 2005). Association analyses are useful for assessing potential candidate genes, fine-mapping linkage regions, and more recently, for genome-wide analyses.

### *Linkage vs. Association*

Comparing (older, low-resolution) linkage and (more modern, high-resolution) association techniques for identifying candidate genes for disorders and physical traits:

Linkage analysis was a very popular method for detecting genes of major effect particularly in psychiatry (e.g. schizophrenia) and genes contributing to distinct facial features (e.g. eye colour, dimpled/cleft chin) and craniofacial anomalies (e.g. cleft lip and palate). It was used mostly in the '80s and perhaps early 1990s usually based on within-family design either sibling pairs or large multiplex pedigrees. It is really optimally designed for disorders in which their genes have major effect. One of the things that came out of that generation of linkage studies was that it is relatively clear that if there

are genes of major effect they are relatively rare and relatively isolated populations within schizophrenia. Association studies take the opposite approach. In general, there are case-control association studies, though there are family-based approaches also, which hopefully are going to find genes that have less of a strong effect and thus maybe multiple genes of lesser effect can be detected. With the association approach, where we essentially compare allele frequencies between cases and controls and then examine whatever number of genes or number of polymorphisms in individual study.

The principle of a linkage study is the following: if a disease runs in a family, one could look for genetic markers that run exactly the same way in the family (from grandmother/grandfather, to father/mother, to individual siblings within the family). If we find one, we assume the gene that causes the disease is somewhere in the same area of the genome as the marker. In theory, one could genotype generations and generations of a family, and follows the inheritance of the disease. That is, however, not practical, as people tend to do bothersome things like die, and digging up bodies to get DNA samples is unlikely to get past an ethical review (and even if it were ethical, it's tough to know the phenotype of a long-dead great-aunt).

In practice, a popular design is to genotype affected siblings and use the following logic: for a given bit/region of chromosome, each sibling gets two copies, one from biological mother and one from biological father (Mendelian Inheritance). If the two have inherited the same bits/regions from each parent, the area is more likely to be involved in the disease than if each sibling inherits different bits/regions. So, in linkage studies, we are

not testing specific alleles, but investigating chromosomal regions. That brings us to the first limitation of linkage mapping, the resolution is low. That is, the chunks of chromosome are millions and millions of base pairs long (recombination over a couple generations doesn't break chromosomes up that much). So even after getting a strong signal, there are generally a number of genes in the area that must be painstakingly tested. This could take years. Another limitation is that the strongest linkage signals tend to come from recessive and highly-penetrant (and thus generally rare) diseases. This is because the goal is to find regions where affected siblings have received the same chromosomal segments from each parent, and these are the conditions that ensure the strongest linkage signals. So, linkage is the best approach to detect regions involved in recessive, highly penetrant diseases, and can narrow down the search for causal variants to a few million base pairs, in general.

On the other side, the principle of an association study is to gather samples: some people with a disease (case group) and some people without a disease (control group), and look to see if a certain allele (or genotype) is present more often in the cases than in the controls. If the allele plays a role in causing the disease, or is correlated with a causal allele, it will have a higher frequency in the case population than the control population.

Generally, after a linkage study, one nominates "candidate genes" in the region under the linkage signal, and performs an association study on alleles in the genes. In this way, a specific gene, or even a specific allele, can be identified as playing a possible causal role in the disease. The resolution is much higher, but it was previously implausible to perform

these sorts of studies on regions much larger than a couple genes. However, with the HapMap project and the technology to genotype hundreds of thousands of alleles in parallel, it is now possible to perform association studies on the level of the whole genome. This would essentially skip the step of a linkage scan.

The limitations of the 'association' approach: first, many different mutations in a gene might lead to a disease. In linkage studies, this doesn't pose a problem, the different mutations still in the same region. But in population-level association studies, the effect of each mutation is diluted by the presence of the others. Further, case-control studies are always subject to problems like population substructure that family-based studies don't have. But to detect low-penetrance alleles in complex disease (or any complex phenotype), then genome-wide association studies will doubtless provide unprecedented views of the contributions of genetic factors.

One of the most advanced association approaches is to conduct genome-wide association studies (GWAS). This strategy is intended to combine the advantage of linkage studies, that they can systematically search the genome without any a priori knowledge about the location of potential susceptibility alleles, with the advantages of association methods, namely that they are more powerful at detecting genes of small effect, that they can more tightly localize genes of interest like disease genes, and that simpler sample structures can be used (e.g., unrelated individuals for case-control versus densely affected families).

Several challenges have to be addressed while performing genome-wide association studies. Certain analytic methods are needed to deal with the large multiple tests associated with hundreds of thousands of markers across the genome (Cardon and Bell, 2001). This is compounded by the fact that the SNPs being tested are not independent, which makes direct analytic correction approaches highly conservative. In addition, the sheer volume of genotypic data that will be generated will create unique computational demands, both in terms of data storage and analysis.

Until very recently, the association analyses were restricted to candidate genomic regions, either prioritized via linkage analysis or candidate gene studies. Technologically, surveying the whole genome at the density required for association analysis was impossible. This is no longer the case, as whole-genome SNP panels can now be genotyped across many samples at an affordable and constantly decreasing cost.

GWAS is a genetic association study design in which a sample of cases and controls, or a collection of families, is genotyped for a large number of genetic markers – usually single nucleotide polymorphisms (SNPs) due to their relative ease of multiplexing. Unlike the traditional genetic association studies of the past few decades, which considered only specific regions of the genome (typically those previously identified by linkage analysis or containing functional candidate genes), the ultimate aim of the GWAS design is to capture all common genetic variation across the genome and to relate this variation to disease risk.

### **2.12 The international HapMap project**

In October (2002), the International Haplotype Map Project (HapMap) was initiated. HapMap is a collaboration of scientists in Japan, the UK, Canada, China, Nigeria, and the USA, with the goal of developing a haplotype map of the human genome to describe the common patterns of human DNA sequence variation. Haplotypes consist of a series of ordered markers along a chromosome, and refer to the alleles carried at each of these markers based on the chromosomes inherited from one's parents.

Because the frequencies of common haplotypes differ across populations, several populations have been genotyped by the HapMap. A total of 269 DNA samples were genotyped from four populations: (i) the Yoruba people in Ibadan, Nigeria; (ii) Japanese in Tokyo, Japan; (iii) Han Chinese in Beijing, China; and (iv) individuals from Utah, USA. By analyzing DNA from populations with African, Asian, and European ancestry HapMap researchers aimed to identify most of the common haplotypes that exist in broad human subpopulations. All of the information generated by the HapMap Project is freely available on the Web.

The HapMap project has dramatically aided the design of association studies by revealing many features about genetic variation across the genome. Historically, association studies were used largely to examine candidate genes of interest, chosen based on hypothesized biological relevance to the disease under study. These studies were often limited to

testing for association with a known functional polymorphism in the candidate gene or with a single or small number of polymorphic markers in the gene. With data from the HapMap project, it is now possible to select tag SNPs to cover the genetic variation present across a candidate gene of interest. The exact number of SNPs needed for any given gene will depend on the size of the gene and the pattern of variation across the region.

### **2.13 General applications of human genome-wide association studies**

Genome-wide association studies (GWAS) are a powerful method for identifying disease susceptibility genes for common diseases, offering the promise of novel targets for therapeutic intervention that act on the root cause of a disease. GWAS involve scanning thousands of samples, either as case-control cohorts or in family trios, utilizing hundreds of thousands of SNP markers located throughout the human genome. Algorithms are applied that compare the frequencies of single SNP alleles, genotypes, or multi-marker haplotypes between disease and control cohorts. This analysis identifies regions (loci) with statistically significant differences in allele or genotype frequencies between cases and controls, pointing to their role in the disease (Keith, 2007).

As an example for the above studies, a genome-wide association scan of tag SNPs has identified a susceptibility locus for lung cancer at 15q25.1 (Amos *et al.*, 2008).

Furthermore, genome-wide association analyses have been also used to identify the genes underlying normal variation of the population general features. A genome-wide association analysis has identified 20 loci that influence adult height (Weedon *et al.*, 2008). In this study, a Manhattan plot (Figure 2.5) was obtained for the SNPs from the genome-wide association meta-analysis of several studies. The red dots represent the SNPs that reached a significant level in a joint analysis of samples.

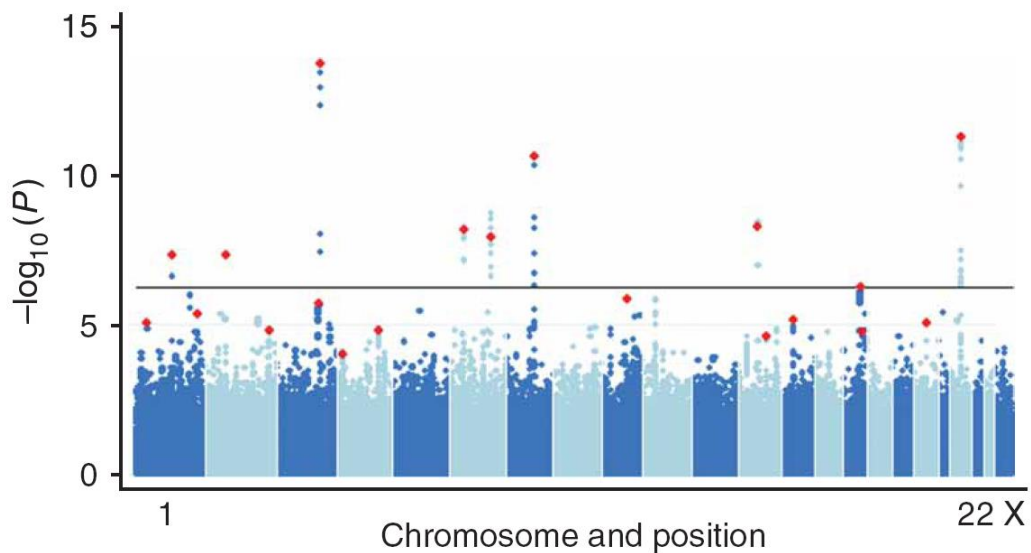


Figure 2.5. Manhattan plot

The clinical observation of facial structures remains an essential part of the clinical evaluation of the patient's general condition. Many congenital developmental abnormalities, syndromes and diseases were recognized due to having exogenous teratogens, chromosomal anomalies, or genetic defects. Numerous syndromes affecting facial morphology have been reported and a growing number of genes or chromosomal anomalies have been identified. Moreover, the normal variation of the general features of the human face and body were also found to be controlled by genes.

In genetic epidemiology, a genome-wide association study (GWAS) is an examination of genetic variation across a given genome, designed to identify genetic associations with observable traits. In human studies, this may include traits like blood pressure or weight, or why some people get a disease or condition. Recently, GWAS have been used to successfully dissect a variety of complex traits, ranging from discrete clinical outcomes such as asthma and diabetes (Moffatt *et al.*, 2007; Scott *et al.*, 2007; WTCCC, 2007) to continuous traits as diverse as height, weight, global gene expression and blood lipid levels (Dixon *et al.*, 2007; Frayling *et al.*, 2007; Sanna *et al.*, 2008; Scuteri *et al.*, 2007; Willer *et al.*, 2008).

The amount of information generated in these studies is staggering and interpreting their results requires efficient computational tools for data analysis and visualization. A diverse set of statistical methods can be used to examine the association between phenotypes of interest and single nucleotide polymorphism (SNP) data. For example, p-values, effect size estimates and their standard errors, as well as SNP-specific heritability estimates are all commonly reported in GWAS studies. When there are thousands of phenotypic outcomes and hundreds of thousands SNPs, the result set is usually very large, containing several million statistics and easily totalling several gigabytes. These datasets can be integrated into specialized local databases for further investigation, but it can be also challenging for researchers without extensive database or programming skills to access the results (Chen, Liang and Abecasis, 2009; Cookson *et al.*, 2009; Guan *et al.*, 2009).

## **2.14 Principles of GWAS**

### **2.14.1 Genotyping platforms:**

Several companies market GWAS platforms. Each company has multiple different platforms that are targeted for differing scientific uses, and each of these platforms has advantages, disadvantages, technical limitations, and cost considerations. For example, a platform may perform better in samples of European ancestry than in samples with substantial proportions of individuals with African ancestry, and another platform may allow the inclusion of a large number of additional SNPs of interest. Genotyping is based on the presence of a SNP in a DNA segment of about 200-1200 bases that is flanked by specific restriction enzyme sites. Thus, the SNP content is somewhat opportunistic, and SNPs are selected based on genomic context.

### **2.14.2 DNA pooling:**

Some groups have conducted GWAS on DNA pools whereby small aliquots of DNA from each case are combined to create one or more case pools with a similar procedure for control pools. Each pool is then genotyped on a GWAS platform, and the statistical comparison is of aggregate allele frequencies in case versus control pools. The obvious advantage of DNA pooling is cost, instead of individual GWAS genotyping of hundreds or thousands of cases and controls, only a handful of pools need to be genotyped. However, these substantial cost savings come at the considerable price of loss of information, as well as less-accurate measures of case and control allele frequencies.

### **2.14.3 SNP annotation:**

There is a knowledge gap in human genetics; we know basic information about millions of SNPs in the human genome but we understand the functional significance of only a small fraction. There are many examples of synonymous coding SNPs or intronic SNPs that are not predicted to be of functional importance and yet variation in these regions leads to profound alterations in gene expression or function. Moreover, there may be important errors in the annotation files for a GWAS platform, where the stated location of a SNP on a chromosome could be assigned wrongly. Moreover, SNPs may be located in different genes or transcripts than indicated in the GWAS annotation file.

### **2.14.4 Genotype-calling algorithms:**

The basic readout of all major GWAS platforms is fluorescence intensities for each of the 2 alleles for a SNP for each subject. Scatter plots for each GWAS SNP (minor allele versus major allele fluorescence intensities) typically yield 3 clusters corresponding to subjects homozygous for the major allele, homozygous for the minor allele, and heterozygotes along with “no-call” or missing genotypes. The quality of a genotype call is a measure of the confidence of genotype assignment (e.g., high confidence for a subject whose intensities are at the centroid of a well-defined cluster and low confidence for a subject with intensities intermediate between two loose clusters). Quality scores can be computed for SNPs which may be useful for determining whether a SNP might be included in an analysis.

A genotype-calling algorithm is a software program that converts raw intensity values to three level genotypes. A number of details are critical for the analysis of GWAS data. First, the number of subjects called at one time. The calling software will likely yield better calls if thousands of subjects are considered simultaneously instead of dozens, as there will be a greater number of subjects forming the cluster representing minor allele homozygotes. Second, the genotype for each subject has an associated quality score, or the confidence with which a genotype is assigned, along with a threshold below which genotypes are set to missing. In summary, GWAS technologies and calling algorithms are very good but caution is needed when dealing with GWAS data as some proportion of SNPs simply will not work unless being properly detected and corrected.

## **2.15 Hardware and software for quality control and statistical analysis**

### **2.15.1 *Hardware:***

The computing challenges posed by GWAS studies are not necessarily that severe. Many quality control operations and statistical analyses are readily completed with affordable desktop computers. There are three basic features to consider independently of the operating system and computer manufacturer. First, it is always better to have more and faster processors. Secondly, a key bottleneck for GWAS operations is Random Access Memory (RAM). Third, a large hard drive is essential to store GWAS genotype files.

**2.15.2 Software:**

The “PLINK” software is specifically designed and optimized for GWAS analyses. However, there is definitely more than one way to perform quality control and to analyse GWAS genotype data. Possibilities include writing custom code to conduct all required analytic procedures, using “R Package” for statistical computing, or using an existing commercial package (e.g., SAS, SPSS, or JMP/Genetics). Moreover, other groups have developed their own software for GWAS.

**2.15.3 Data structures:**

It is critical that all data files be handled with care and with great attention to the details. In particular, errors can occur when merging files; therefore, data management must be conducted with caution and intelligence.

Genotypes are often given as a string of two alleles either as combinations of the four bases (A: *adenine*, C: *cytosine*, G: *guanine*, and T: *thymine*) or as minor allele-major allele (e.g., AA, AB, BB). Missing genotypes may be referred to as 00, NN, or a blank.

The quality score for each SNP or for each genotype call is given. It is worth investigating the impact of more stringent quality control thresholds on the overall SNP call rate.

## **2.16 Quality control**

### **2.16.1 Genotyping reproducibility and accuracy:**

The investigators usually choose to genotype additional samples so that they can monitor the genotyping process, and to enable calculations of the genotyping reproducibility, error (via Mendelian inconsistencies) and accuracy. The genotyping reproducibility can be estimated by genotyping the same randomly selected sample twice. Mendelian inconsistencies are one way to detect genotyping error and require family data (an important caveat is that the SNP cannot be in a copy number variant region where Mendelian errors may in fact be expected).

The genotyping accuracy can be estimated by genotyping a sample where “gold standard” genotypes are available – a HapMap CEU sample can arguably be used for this purpose. Estimates of genotyping reproducibility, error (via Mendelian inconsistencies) and accuracy are essential to understand whether the GWAS genotyping is problematic. These should be noted for the entire sample. These QC metrics are essential for scientific reports and to assure the investigator that the data are of sufficient quality.

#### **2.16.1.1 Mendelian inconsistencies:**

A Mendelian error in the genetic analysis of a species, describes an allele in an individual which could not have been received from either of its biological parents by Mendelian inheritance. Inheritance is defined by a set of related individuals who have the same or similar phenotypes for a locus of a particular gene. A Mendelian error means that the very structure of the

inheritance as defined by analysis of the parental genes is incorrect: one parent of one individual is not actually the parent indicated; therefore the assumption is that the parental information is incorrect. The possible explanations are multiple and can be due to experimental genotyping errors or to the erroneous assignment of the individuals as relatives. Mendelian error is established by demonstrating the existence of a trait which is inconsistent with every possible combination of genotype compatible with the individual.

### **2.17 Descriptive analyses of the GWAS data**

Descriptive data include missingness, minor allele frequency, genotype frequencies, and HWE (Hardy-Weinberg equilibrium) P-values.

#### **2.17.1 *Missingness:***

This option produces files containing missingness information for each subject (the number of missing SNPs/total number of SNPs) and for each SNP (the number of missing individuals /total number of individuals).

#### **2.17.2 *Allele frequencies:***

This option computes allele frequency data for each SNP. These data should be stored as important descriptors for the GWAS platform. Allele frequency data can also be compared to reference samples. A1 and A2 refer to minor and major alleles. MAF (Minor Allele Frequency) is the number of occurrences of the minor allele divided by the number of non-missing chromosomes.

### **2.17.3 Genotype frequencies and HWE assessment:**

This PLINK command yields genotype frequencies and HWE information via an exact test (Wigginton and Abecasis, 2005).

#### **2.17.3.1 HWE (Hardy-Weinberg Equilibrium):**

The “Hardy-Weinberg Equilibrium” states that both allele and genotype frequencies in a population remain constant, that is, they are in equilibrium from generation to generation unless specific disturbing influences are introduced. Those influences include non-random mating, mutations, selection, limited population size, "overlapping generations", random genetic drift and gene flow. It is important to understand that outside the lab, one or more of these “disturbing influences” are always in effect. That is, HWE is impossible in nature.

### **2.18 Association analyses of GWAS data**

Following quality control and descriptive analyses, the association analyses are the heart of the GWAS study to know which genomic region or regions show evidence of association with the variation of interest.

PLINK software can produce five tests of association for each SNP in the final GWAS dataset. The five tests are:

- 1) Allelic association-ALLELIC.
- 2) Cochran-Armitage trend test-TREND.
- 3) Genotypic association-GENO.
- 4) Dominant gene action-DOM.
- 5) Recessive gene action-REC.

Exactly what tests are best in which circumstances is a matter of some debate. Some investigators focus on a single test like the general test of association, whereas others prefer the Cochran-Armitage trend test plus tests assuming dominant and recessive gene action. What is clear, however, is that whichever of these tests are used, keeping track of the total number of statistical comparisons is essential.

## **2.19 Visualizing GWAS results**

### **2.19.1 QQ plot:**

A QQ Plot is a very useful graphic technique to assess whether observed ( $P$ -values) deviate from the expected values. These graphs plot the observed  $-\log_{10}(P)$  by the expected  $-\log_{10}(i/(L+1))$ , where  $i$  is rank order of the SNP in the dataset sorted by  $P$ -value in ascending order, and  $L$  is the number of SNPs successfully genotyped (Balding, 2006).

### **2.19.2 HaploView and genome graphs:**

Both HaploView (Barrett *et al.*, 2005) and the “Genome Graphs” tool of the UCSC Genome Browser (Hinrichs *et al.*, 2006) offer ways to plot GWAS results in their genomic context. The HaploView has the ability to read PLINK files directly. Genome Graphs allow access to the rich set of additional information integral to the UCSC browser. With HaploView, one plots the chromosomes along the x-axis and the  $P$ -values along the y-axis. One also changes the scale of the y-axis to show the  $-\log_{10}$  of the values. The  $-\log_{10}$  of the  $P$ -value transforms the  $P$ -value such that larger values indicate more significance.

Generally, the information conducted from the GWAS results include the marker name, chromosome position, and the value being plotted.

## **2.20 GWAS discovery and replication phases**

For a successful GWAS study, the genetic association results have to be validated before being published. This can be achieved through carrying out a genome-wide discovery analysis to identify any genetic association with the phenotype of interest, then trying to replicate the results. The gold standard for validation of any genetic study is replication in an additional independent sample. There are a variety of criteria involved in establishing a positive replication of a GWAS result (Chanock *et al.*, 2007). Replication studies should have sufficient sample size to detect the effect of the susceptibility allele. This means that replication samples should ideally be larger to account for the over-estimation of effect size.

With replication, it is important for the study to be well-powered to identify spuriously associated SNPs where the null hypothesis is most likely true. Replication studies should be conducted in an independent dataset drawn from the same population as the GWAS discovery analysis, in an attempt to confirm the effect in the target population. Once an effect is confirmed in the target population, other populations may be sampled to determine if the SNP has an ethnic-specific effect. Replication of a significant result in an additional population is sometimes referred to as generalization, meaning that the genetic effect is of general relevance to multiple human populations.

Identical phenotype criteria should be used in both GWAS discovery and replication studies. Replication of a GWAS result should be thought of as the replication of a specific statistical model, a given SNP predicts a specific phenotype effect. However, using even slightly different phenotype definitions between GWAS discovery and replication studies can cloud the interpretation of the final result.

A similar effect should be seen in the replication set from the same SNP, or a SNP in high LD (linkage disequilibrium) with the GWAS discovery identified SNP. Because GWAS typically use SNPs that are markers that were chosen based on LD patterns, it is difficult to say what SNP within the larger genomic region is mechanistically influencing disease risk. With this in mind, the unit of replication for a GWAS should be the genomic region, and all SNPs in high LD are potential replication candidates.

However, continuity of effect should be demonstrated across both studies, with the magnitude and direction of effect being similar for the genomic region in both datasets.

In brief, the general strategy for a replication study is to repeat the ascertainment and design of the initial GWAS as closely as possible, but examine only specific genetic effects found significant in the initial GWAS. Effects that are consistent across the two studies can be labeled replicated effects.

### **2.20.1 Linkage disequilibrium:**

In population genetics, the term “linkage disequilibrium” is the non-random association of alleles at two or more loci that may or may not be on the same chromosome. It is also referred to as “gametic disequilibrium”. In other words, linkage disequilibrium is the occurrence of some combinations of alleles or genetic markers in a population more often or less often than would be expected from a random formation of haplotypes from alleles based on their frequencies.

### **2.21 Corrections for multiple testing (Bonferroni correction)**

A p-value, which is the probability of seeing a test statistic equal to or greater than the observed test statistic if the null hypothesis is true, is generated for each statistical test. This effectively means that lower p-values indicate that if there is no association, the chance of seeing this result is extremely small.

Statistical tests are generally called significant and the null hypothesis is rejected if the p-value falls below a predefined alpha value, which is nearly always set to 0.05. This means that 5% of the time, the null hypothesis is rejected when in fact it is true and we detect a false positive. This probability is relative to a single statistical test; in the case of GWAS, hundreds of thousands to millions of tests are conducted, each one with its own false positive probability. The cumulative likelihood of finding one or more false positives over the entire GWAS analysis is therefore much higher.

One of the simplest approaches to correct for multiple testing is the “Bonferroni correction”. The Bonferroni correction adjusts the alpha value from  $\alpha = 0.05$  to  $\alpha = (0.05/k)$  where  $k$  is the number of statistical tests conducted. For a typical GWAS study using 500,000 SNPs, statistical significance of a SNP association would be set at  $1e-7$ . This correction is the most conservative, as it assumes that each association test of the 500,000 is independent of all other tests – an assumption that is generally untrue due to linkage disequilibrium among GWAS markers.

## **2.22 Statistical power**

The power of a statistical test is the probability that the test will reject the null hypothesis when the null hypothesis is false (i.e. the probability of not committing Type II error, hence the probability of confirming the alternative hypothesis when the alternative hypothesis is true). The power is in general a function of the possible distributions, often determined by a parameter, under the alternative hypothesis. As the power increases, the chances of a Type II error occurring decrease. The probability of a Type II error occurring is referred to as the false negative rate ( $\beta$ ). Power analysis can be used to calculate the minimum sample size required so that one can be reasonably likely to detect an effect of a given size. Power analysis can also be used to calculate the minimum effect size that is likely to be detected in a study using a given sample size. In addition, the concept of power is used to make comparisons between different statistical testing procedures: for example, between a parametric and a nonparametric test of the same hypothesis.

### **2.22.1 Factors influencing power**

Statistical power may depend on a number of factors. Some of these factors may be particular to a specific testing situation, but at a minimum, power nearly always depends on the following three factors:

- *The statistical significance criterion used in the test*

A significance criterion is a statement of how unlikely a positive result must be, if the null hypothesis of no effect is true, for the null hypothesis to be rejected. The most commonly used criteria are probabilities of 0.05, 0.01, and 0.001.

- *The magnitude of the effect of interest in the population*

The magnitude of the effect of interest in the population can be quantified in terms of an effect size, where there is greater power to detect larger effects. In statistics, an effect size is a measure of the strength of a phenomenon. An effect size can be a direct estimate of the quantity of interest, or it can be a standardized measure that also accounts for the variability in the population.

- *The sample size used to detect the effect*

The sample size determines the amount of sampling error inherent in a test result. Other things being equal, effects are harder to detect in smaller samples. Increasing sample size is often the easiest way to boost the statistical power of a test.

In addition to the above factors, the *precision* with which the data are measured also influences statistical power. Consequently, power can often be improved by reducing the measurement error in the data. A related concept is to improve the “reliability” of the measure being assessed.

Moreover, the *design* of an experiment often influences the power. For example, in a two-sample testing situation, it is optimal to have equal numbers of observations from the two populations being compared (as long as the variances in the two populations are the same).

### 2.23 Summary of the GWAS process

Figure 2.6 is a diagram illustrating the essential steps of the GWAS process.

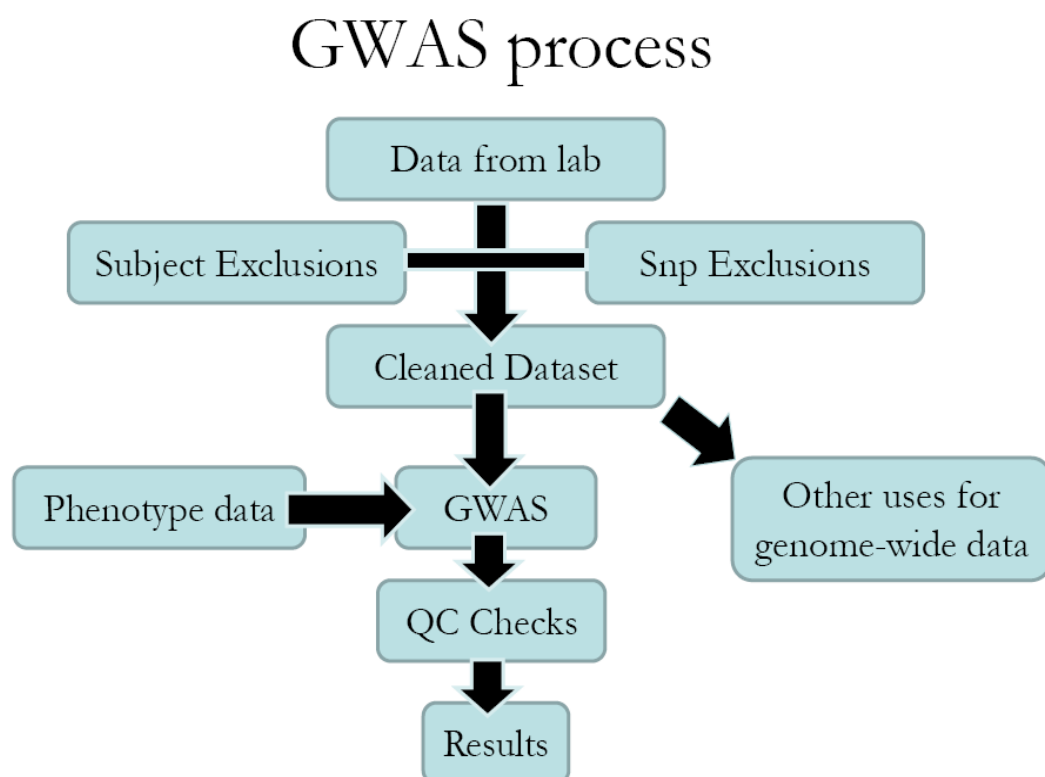


Figure 2.6. Summary of the GWAS process

## Chapter 3

# Reproducibility Of Recording Facial Soft Tissue Landmarks On The 3D Laser Scans

## **Reproducibility Of Recording Facial Soft Tissue Landmarks On The 3D Laser Scans**

### **3.1 Introduction**

Different methods have been utilized to assess facial morphology and detect morphological changes over time, in order to diagnose genetic and acquired malformations, to plan and evaluate surgery, to study normal and abnormal growth patterns and to evaluate the results of treatment. Surface anthropometry refers to the measurement of facial surface features using direct clinical measurements, while cephalometry refers to the analysis of craniofacial features from x-ray images of the head (cephalograms).

The anthropometric and cephalometric studies in orthodontics are based on biological homology, i.e. spatial correspondence between definable points on structures in individuals, and geometric variation in the relative location or pattern of these points or landmarks (Bookstein, 1986, 1991b). Craniofacial form is defined by size and shape, and both can be analysed using specifically defined landmarks. Quantitatively, identifying the extent of deviation of an individual's facial pattern from the normal state requires the collection of data on normal individuals in order to establish numerical descriptions of normal measurement ranges. Syndrome diagnosis requires the definition of characteristic abnormal patterns associated with a given syndrome. Growth studies require facial pattern changes to be monitored over time. Surgical planning requires visualization and quantification of dysmorphic features and the ability to model the changes that surgery is expected to bring about. For all these purposes, in order to have valid and reliable results, it is important that the reproducibility of recording facial landmarks is clinically acceptable.

The reproducibility of facial landmarks has been studied at length in two dimensions through the role of cephalometrics in orthodontics (Mitgard *et al.*, 1974; Richardson, 1966); however, as the face is a three-dimensional structure, the need to record and analyse its morphological features in three dimensions has been emphasized (Ferrario *et al.*, 1996a, b; Hajeer *et al.*, 2002).

Using 3D human face data to measure facial features is of great practical importance in craniofacial research and orthodontic practice. Traditionally, direct anthropometry using callipers has been the standard technique for quantifying craniofacial dysmorphology, as well as for surgical planning and outcome assessment (Wong *et al.*, 2008). However, some of the major downsides to direct anthropometry include the excessive time of the method, the amount of training required, the extent of measurement error, and limitations in the kinds of data that can be collected.

Following the introduction of cost-effective 3D surface imaging solutions, computerized anthropometry has largely replaced more traditional direct methods for collecting quantitative 3D information on human faces (Heike *et al.*, 2009). These systems are capable of capturing the full 3D geometry of the human face in just a fraction of a second. While computerized 3D anthropometry represents a major advance, to obtain measurements, points on the face and head corresponding to traditional anthropometric landmarks must still be captured manually through the use of software. This can be a time consuming process, requiring a fair amount of training.

Efficiency is particularly crucial when dealing with very large 3D facial database. Recognizing the need to move beyond manual data collection, more recently, computer scientists have tried to develop automatic methods to detect landmarks from 3D facial surfaces (Deli *et al.*, 2010; Tie and Guan, 2013; Perakis *et al.*, 2010; Guo *et al.*, 2013; Yu and Moon, 2008; Nair and Cavallaro, 2009; Romero-Huertas and Pears, 2008). However, these methods require that the resulting automatically-generated landmarks to be located in the correct anatomical positions and the process to be extendable to as many landmarks as needed.

Many studies have evaluated the errors in obtaining measurements from lateral skull cephalograms and the pattern of error in identifying most cephalometric landmarks is well established (Richardson, 1966; Baumrind and Frantz, 1971a, b). In cephalometric studies, errors can also arise due to variations in head position when radiographs are obtained, even when a cephalostat is used (Ahlqvist *et al.*, 1986).

In three-dimensional studies, recent investigations into the reproducibility of different facial landmarks have shown variable levels of reproducibility depending on the anatomical position of the landmarks being assessed; the number of examiners and their visual acuity, experience and skills in identifying landmarks using different tools and software programmes; and the accuracy of the systems used to obtain and process 3D facial images (Coward *et al.*, 1997; Gwilliam *et al.*, 2006; Baik *et al.*, 2006, 2007; Toma *et al.*, 2009; Othman *et al.*, 2013).

The aim of this study was to assess the reproducibility of identifying soft tissue landmarks on 3D facial scans that can be used to analyse normal facial variation in a large population cohort.

An objective is to evaluate the feasibility of using laser scanning in a large population cohort.

## **3.2 Subjects and methods**

### **3.2.1 *Project sample (cohort)***

The children involved in this project were recruited from the Avon Longitudinal Study of Parents and Children (ALSPAC) which was designed to explore how environmental factors interact with genes to influence development, health, and behaviour of children (Golding *et al.*, 2001). The initial ALSPAC sample consisted of 14541 pregnancies. This was the number of pregnant women enrolled in the ALSPAC study with an estimated date of delivery between April 1991 and December 1992. Out of the initial 14541 pregnancies, all but 69 had known birth outcome. Of these 14472 pregnancies, 195 were twins, three were triplets and one was a quadruplet pregnancy; meaning that there were 14676 fetuses in the initial ALSPAC sample. Of these 14676 fetuses, 14062 were live births and 13988 were alive at 1 year.

The children were re-called at the age of 15 years. Invitations were sent to 9985 participants who reported that they were interested to take part in the clinics. Ethical approval for this study was obtained from the ALSPAC Law and Ethics Committee and the Local Research Ethics Committees.

### **3.2.1.1 Reproducibility sample**

The reproducibility of recording facial soft tissue landmarks was assessed for 60 subjects (30 males and 30 females, 15 year old) who were randomly selected from the ALSPAC cohort (random sample of cases using SPSS).

### **3.2.2 Image capture**

A laser scanning system was used to capture the 3D facial images of the children recruited for this study. This system consisted of two high-resolution Konica Minolta vivid 900 optical digitizers. Each of these cameras emits an eye safe Class I laser (FDA)  $\lambda = 690 \text{ nm}$  at 30 mW, with a reported manufacturing accuracy of 0.1mm for a static surface scanning (e.g. cube or mannequin head). The operating accuracy for facial surface scanning is in the range 0.3-0.5 mm (Zhurov *et al.*, 2005, 2010). For facial surface scanning, a Minolta medium range lens with focal length 14.5 mm was used. Each scanner was placed at a distance of 1350 mm from the subject's head. Two Bowen's tri-lite lamps were used to ensure consistent lighting in a daylight free room. As the subjects were normally of different heights and in order to maintain a natural head posture, the subjects sat on a self-adjustable stool and were asked to look straight ahead at a "heart-shaped symbol" hanging from the ceiling and levelled with the optical lenses of the cameras. Reference marks were placed on the floor to ensure a standardized position of the subjects in relation to the cameras. The subjects were also instructed to swallow hard and to keep their jaws in a relaxed position, trying to stay still during the scanning procedure (Figure 3.1).

The laser cameras were connected in serial via a SCSI cable to a desktop computer workstation. The laser cameras were angled at approximately 45 degrees to facilitate an overlap of the images taken for the two sides of the face, so that they can be later processed, registered and merged to form a composite 3D single image that represents the whole scanned face of a subject. Multi-Scan™ software (Cebas Computer, Eppelheim, Germany) was used to control the cameras to work sequentially. The scan time for each side of the face was 3.5 seconds with a total scan time for both sides of the face being approximately 7 seconds. The set of left and right 3D facial scans for each individual were saved separately as a vivid file format in an appropriate directory. The 3D data was then transferred to a reverse modelling software package Rapidform® 2006 (INUS Technology Inc, Seoul, Korea) for image processing and analysis.

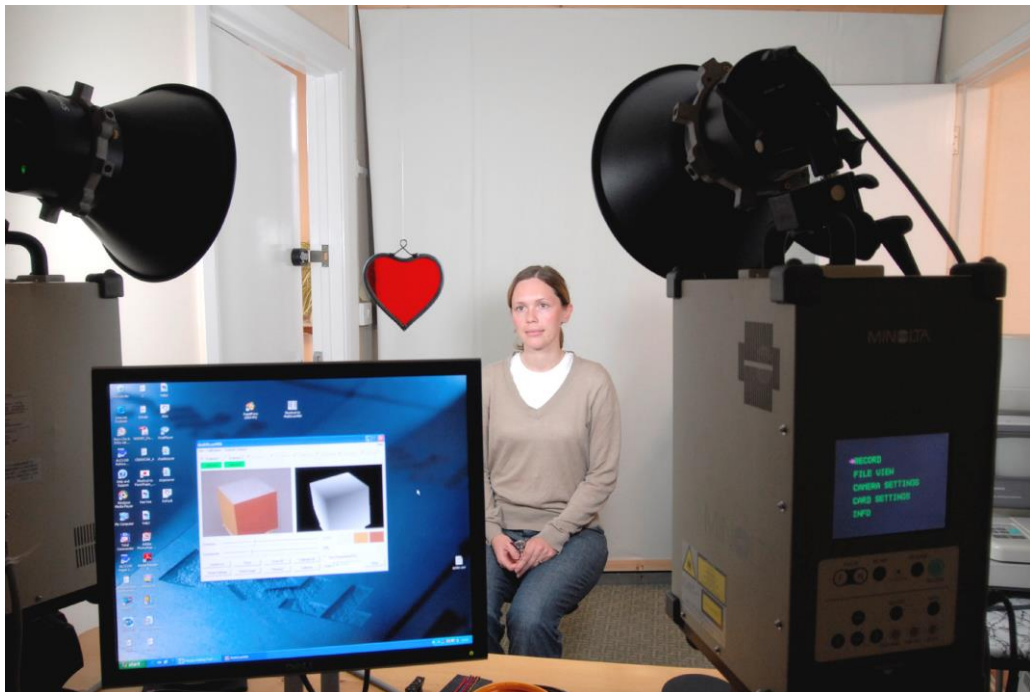


Figure 3.1. Image capture

### 3.2.3 Camera calibration

A calibration procedure was performed prior to each scanning session. In this procedure, a calibration cube of known fixed dimensions and coloured surfaces was placed in the space where the subject's head would be (Figure 3.2). The cube was fixed to a tripod, which in turn was placed on fixed markings on the floor to ensure standardized positioning. For a successful camera calibration, three faces of the cube need to be equally visible on both camera screens, so that the cube faces and consequently the subject's facial scans are accurately captured with a reasonable degree of alignment in the three dimensions of space.



Figure 3.2. Camera calibration

### **3.2.4 Processing the 3D facial scans**

The left and right 3D facial scans of each participant were imported into Rapidform software and the following steps were performed using a locally developed algorithm implemented as a macro in Rapidform (Zhurov *et al.*, 2005). These steps are essential in order to obtain a workable 3D facial image for each participant that is suitable for landmarking and further analysis. Figure 3.3 illustrates an individual's 3D facial scans (before and after processing):

- Removing extraneous data
- Smoothing left and right shells (surface scans)
- Registering left and right shells (alignment)
- Merging left and right shells followed by filling holes and removing mesh defects

#### **3.2.4.1 Removing extraneous data**

Extraneous information like hair, bits of clothes and scanning equipment were removed.

#### **3.2.4.2 Smoothing left and right shells**

The raw scans initially captured by the cameras are fairly rough (Figure 3.3, left), this is due to scanning noise; therefore, the facial surfaces need to be smoothed to reduce the noise using a suitable software technique. Rapidform offers three methods of smoothing: Laplacian, Loop and Curvature. In this study, in order not to distort the source image, we opted for the "Laplacian" method with shape and volume preservation.

### **3.2.4.3** *Registering left and right shells (alignment)*

One may think that this stage is of little importance in image processing, since the calibration procedure of the cameras should guarantee accurate alignment of the right and left facial scans. However, this is not exactly true. Calibration can be done as explained earlier with a special object, e.g., calibration cube, placed where the subject's face will be scanned later; this can provide a fairly good initial alignment of the left and right facial scans. In reality, the positions of the calibration cube and that of the subject's face never coincide exactly. This can cause a misalignment error (usually about 1 or 2 mm) in the resulting positions of the left and right facial scans, which, if proceeded with merging, may result in a slightly distorted and imprecise face that will affect the landmarking accuracy and future analyses.

Therefore, software registration of the left and right facial scans, based on the iterative closest point algorithm (ICP), was very important in this study to compensate for such error. The deviation between the left and right facial shells of each subject was displayed using a colour deviation map. The mean, standard deviation, maximum and minimum distances were recorded. The average distance between the left and right facial shells, prior to merging, should not exceed an error of 0.3-0.5 mm (with the aim to obtain a combined facial shell accurate to within 0.5-1 mm). Poor registration and scanning errors due to subject movement can lead to a distorted final image that is not suitable for landmarking and analyses. With laser scanning, this can happen for some subjects due to relatively long scanning time (approximately

7 seconds). To avoid or minimise this issue, the participants' attention was drawn to the fact that they should remain as still as possible during the scanning. In addition, a minimum of three pairs of facial scans were taken for each individual so that we could select the best scans. However, a small number of scans required careful manual editing to improve its mesh quality without disturbing facial features.

#### **3.2.4.4 Merging left and right shells, and filling holes**

The final stage of image processing included merging the left and right shells to form a whole face, followed by filling holes which normally appear in the regions of eyebrows, eyes, and nose, where the reflection of laser light was lost and therefore not recorded (Figure 3.3).



Figure 3.3. Processing 3D facial scans, before processing (left) and after processing (right)

### **3.2.5 Identifying facial soft tissue landmarks**

The facial shells were aligned to a common reference frame to facilitate consistency in lighting and orientation prior to undertaking landmark identification (Figure 3.4).

The reference planes had their origin at the mid-endocanthion (or mid-intercanthal) point “men”, the midpoint between left and right endocanths; this point does not lie on the facial surface and it was shown previously to be the most reliable landmark of the face and stable over time (Zhurov *et al.*, 2010).

The sagittal plane (yz) runs vertically through the midline of the face; it is defined as the symmetry plane of the combined structure consisting of the facial shell and its mirror reflection. The transverse plane (xz) is horizontal and is determined by a vertical cylinder that best fits the combined face. The coronal plane (xy) is vertical and perpendicular to the sagittal and transverse planes. The x axis lies horizontally from left to right eye, the y axis is directed vertically upward, and the z axis points forward (Toma *et al.*, 2009; Zhurov *et al.*, 2010).

This choice of the frame of reference defines a natural head posture purely from analysing the face geometry.

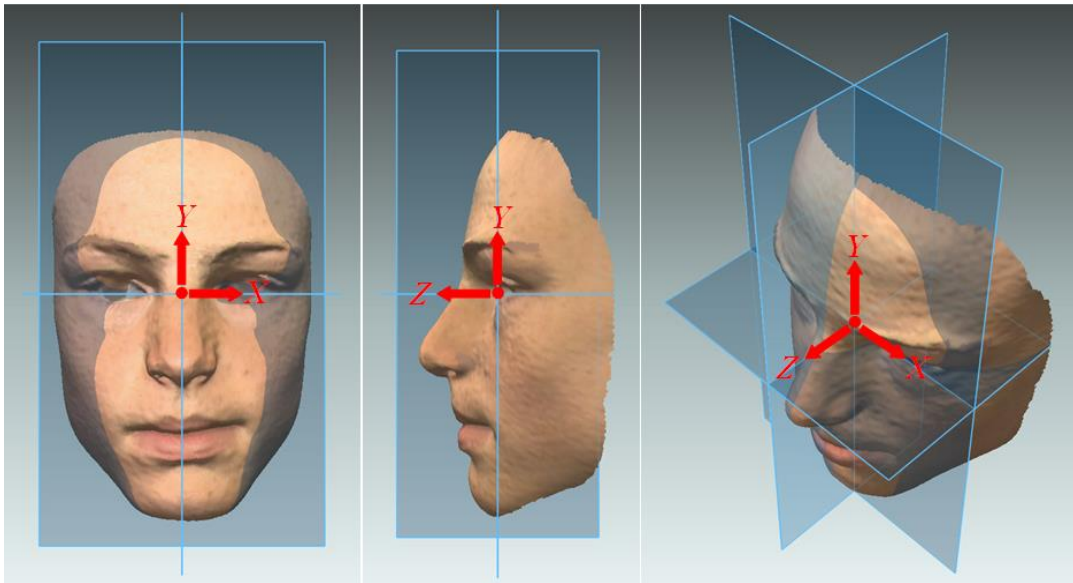
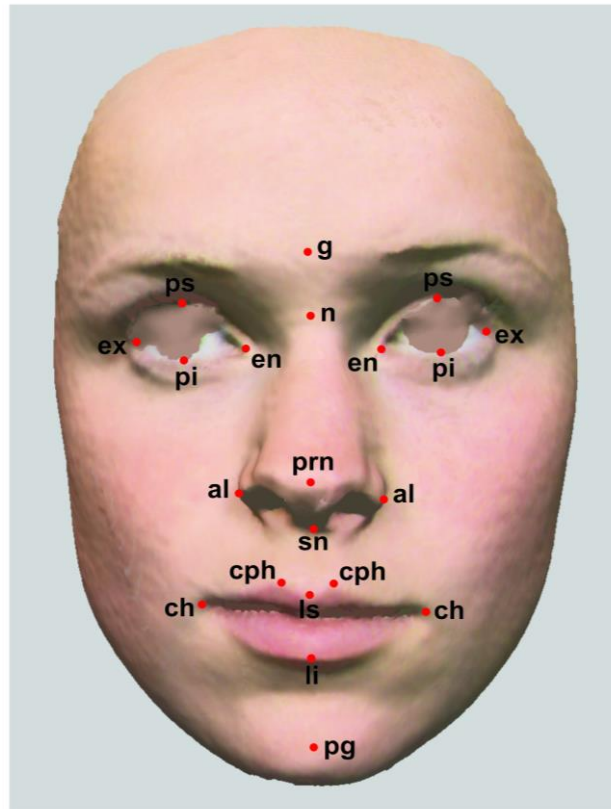


Figure 3.4. Normalisation of facial shells to natural head posture (NHP) The x-axis (horizontal); y-axis (vertical); z-axis (depth of field); the coronal, sagittal and transverse planes were taken as the xy, yz and xz planes, respectively.

The 21 facial surface landmarks chosen for this study (Figure 3.5) have been used previously by several researchers and regarded as being the most reproducible soft tissue landmarks that define the main facial features contributing to facial variation (e.g. height, width, and prominence of various facial structures: the forehead, the eyes, the nose, the lips and mouth, and the chin) (Farkas, 1994; Hennessy and Moss, 2001; Hennessy *et al.*, 2002, 2005, 2007). In addition, landmarking these structures (with 21 landmarks) can be performed with a reasonable degree of reproducibility giving promise of valid and reliable results, i.e. the reproducibility error in facial landmarking should be reasonably much smaller than the true facial variation observed within the sample.

The x, y, and z coordinates of each landmark were recorded (63 coordinates in total).



<u>Landmarks</u>	<u>Definition</u>
- Glabella (g)	Most prominent midline point between eyebrows
- Nasion (n)	Deepest point of nasal bridge
- Endocanthion (en) L/R	Inner commissure of the left and right eye fissure
- Exocanthion (ex) L/R	Outer commissure of the left and right eye fissure
- Palpebrale superius (ps) L/R	Superior mid-portion of the free margin of upper left and right eyelids
- Palpebrale inferius (pi) L/R	Inferior mid -portion of the free margin of lower left and right eyelids
- Pronasale (prn)	Most protruded point of the apex nasi
- Subnasale (sn)	Mid-point of angle at columella base
- Alare (al) L/R	Most lateral point on left and right alar contour
- Labiale superius (ls)	Mid-point of the upper vermilion line
- Labiale inferius (li)	Mid-point of the lower vermilion line
- Crista philtri (cph) L/R	Point on left and right elevated margins of the philtrum just above VL
- Cheilion (ch) L/R	Point located at left and right labial commissure
- Pogonion (pg)	Most anterior mid-point of the chin

Figure 3.5. Facial soft tissue landmarks

### **3.2.6 Statistical analyses**

#### **3.2.6.1 Reliability of the laser scanning procedure in the ALSPAC study**

The reliability of the laser scanning procedure was assessed based on the registration quality of the left and right facial scans taken for each individual; this represents the scan quality.

The precision to which the registered left and right facial shells coincide across the overlapping area was used to determine the quality of the facial scans (Figure 3.6). A scan was considered to be of good quality if 70–100% of its overlapped left and right facial shells coincided with each other to within 0.5 mm. From practical considerations, three quality categories were determined according to the percentage of overlap between the left and right sides of the face with a tolerance level set as 0.5 mm:

- Good: 70–100% of the overlapped left and right facial shells coincide with each other to within 0.5 mm.
- Fair: 60–69% of the overlapped left and right facial shells coincide to within 0.5 mm.
- Poor: <60% of the overlapped left and right facial shells coincide to within 0.5 mm.

In addition, the average distance between the overlapped left and right facial shells as well as the standard deviation, maximum and minimum distances were recorded. The average distance should not exceed an error of 0.3-0.5 mm to ensure an accurate merged face.

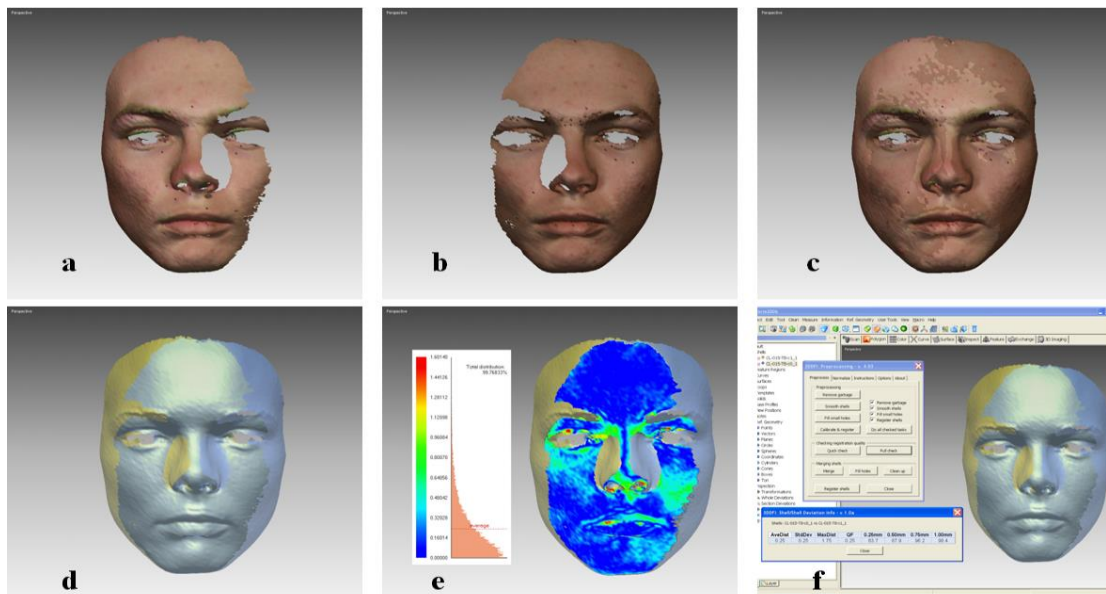


Figure 3.6. Registration of the left and right facial shells (scan quality)  
a) Right shell, b) left shell, c) overlapped shells/texture view,  
d) overlapped shells/transparent view, e) deviation colour map,  
f) records taken.

The following sorts of unsuitable scans were excluded from the sample of the study:

- Faces with poor quality of registration, indicating that the subject was not still enough during the scanning procedure; the assessment was made using deviation colour maps as described above.
- Faces with fair or good quality of registration that were found to have a noticeable smile or open mouth (as these do not meet the requirement of neutral facial expression).
- Scans with significant defects or holes that were difficult to compensate by manual editing (moustache, beard or too much hair over the forehead).

**3.2.6.2** *Reliability of facial data capture (facial posture adoption study)*

Two groups were randomly selected as part of the study to assess their ability to adopt the same facial expressions over two scanning occasions. The first group was made of 120 subjects who had their facial scans taken twice at the same scanning session (1 minute interval). The second group was made of 20 subjects who had their facial scans taken twice at two different occasions over a period of time ranging from 15 to 42 days, with an average interval of 32 days between the scanning sessions. For each participant, two 3D full-face images were created as described previously by merging each pair of the left and right facial scans. Records including the average distance, standard deviation and percentage of overlap (deviation) between the shells were taken to assess the scan quality. The two full-face images of each participant were superimposed one over the other and registered using best-fit technique so as to assess the deviation (level of agreement, precision or coincidence) between them at tolerance levels set as 0.5mm, 0.75mm and 1.0mm.

**3.2.6.3** *Assessment of reproducibility sample*

To determine whether the random sample of 60 subjects selected for reproducibility assessment was representative of the ALSPAC population cohort recruited for this project, the average facial height of the 60 subjects was compared to the average facial height of the total ALSPAC sample. The facial height of each individual was measured as a linear distance between nasion (n) and pogonion (pg).

#### **3.2.6.4 Assessment of the reproducibility of facial landmarks**

The reproducibility of identifying facial landmarks was assessed for one examiner (intra-examiner) at a two-week interval between the first and second readings so as to exclude memory bias. The reproducibility of identifying landmarks was also assessed between two examiners (inter-examiner). Bland-Altman plots (Bland and Altman, 1986, 2010) were used to assess and visualise errors in landmarks identification in the three spatial dimensions. The reproducibility of each landmark in each dimension was classified into 4 categories: <0.5mm (very good), <1mm (good), <1.5mm (fair), and >1.5mm (poor).

In addition, the errors were expressed as the “Euclidean” distance between two points (combining the differences in the x, y, and z coordinates) using the following formula:

$$D = \sqrt{(\Delta x)^2 + (\Delta y)^2 + (\Delta z)^2}$$

$D$  = 3D (Euclidean) distance

$\Delta x$  = difference in the x-axis

$\Delta y$  = difference in the y-axis

$\Delta z$  = difference in the z-axis

For each landmark, the average and standard deviation of each measurement were calculated for the total sample (60 subjects) for both intra- and inter-examiner reproducibility assessments.

### **3.3 Results**

#### **3.3.1 Project sample**

A total of 5235 (15-year-old) children attended the laser scanning sessions. 399 out of them were excluded for several reasons: (i) facial images were not recorded at all, (ii) faces had obvious dysmorphology, (iii) scans had significant defects or holes, and (iv) subjects smiled or had their mouth open during the scanning.

The scan quality was assessed (based on the registration quality of the left and right facial shells) for 4836 subjects. A further 89 faces (2%) were found to have poor quality of registration. So, a total of 488 subjects were excluded from the sample.

The final sample represented normal variation in 4747 British adolescents (2514 females and 2233 males); 92% of these individuals were white northern Europeans (Caucasians), and the remaining subjects (8%) were a mixture of different ethnic groups other than white.

78% of the subjects had good quality facial scans and 20% had fair quality facial scans. The mean “average distance” between the left and right facial shells obtained for 4747 individuals was 0.34mm.

Figure 3.7 shows a flow chart illustrating the process of obtaining the final project sample.

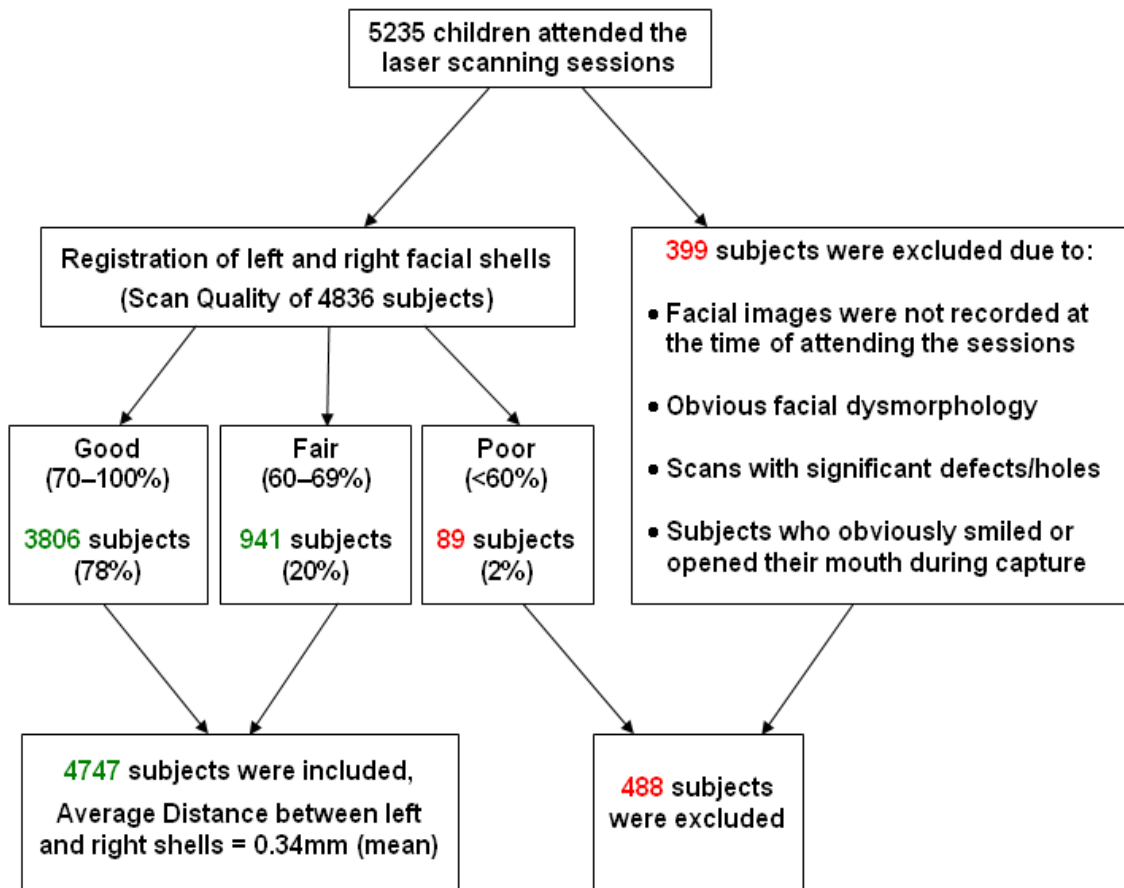


Figure 3.7. Project sample

### 3.3.2 Reliability of facial data capture (facial posture adoption study)

Tables 3.1 and 3.2 show the average precision (percentage of coincidence to within a set tolerance level) between the full-face scans taken for group 1 (120 subjects) and group 2 (20 subjects), respectively. For the first group, the precision was (on average) 85%, 94%, and 97% at the tolerance levels of 0.5mm, 0.75mm and 1.0mm, respectively. The minimum percentage of coincidence was 70.2% at 0.5mm tolerance level, while the maximum percentage of coincidence was 100% at 0.75mm and 1.0mm tolerance levels.

For the second group, the precision was (on average) 77%, 88%, and 93% at the tolerance levels of 0.5mm, 0.75mm and 1.0mm, respectively. The minimum percentage of coincidence was 64.3% at 0.5mm tolerance level, while the maximum percentage of coincidence was 98.1% at 1.0mm tolerance level.

Tables 1 and 2 of the Appendix show the registration data of the left and right facial shells of each participant scans for group 1 (120 subjects) and group 2 (20 subjects), respectively, and display the degree of coincidence between the two full-face scans of each subject at the tolerance levels of 0.5mm, 0.75mm and 1.0mm.

<b>Sample (n=120)</b>	<b>Tolerance Levels for Face/Face Deviation</b>		
	<b>0.5mm (%)</b>	<b>0.75mm (%)</b>	<b>1.0mm (%)</b>
<b>Mean</b>	84.64	93.51	96.88
<b>SD</b>	7.86	5.04	3.52
<b>Min</b>	70.2	77.7	80.9
<b>Max</b>	99.5	100.0	100.0

<b>Sample (n=20)</b>	<b>Tolerance Levels for Face/Face Deviation</b>		
	<b>0.5mm (%)</b>	<b>0.75mm (%)</b>	<b>1.0mm (%)</b>
<b>Mean</b>	77.05	87.91	92.75
<b>SD</b>	7.37	5.34	3.90
<b>Min</b>	64.3	78.3	85.6
<b>Max</b>	90.4	96.4	98.1

### 3.3.3 Assessment of reproducibility sample

Table 3.3 shows the average face heights obtained for the 60 subjects (30 females, 30 males) selected to assess reproducibility as well as for the total ALSPAC sample of 4747 individuals (2514 females, 2233 males).

<b>Table 3.3. Assessment of reproducibility sample</b>										
	<b>Reproducibility Sample</b>					<b>ALSPAC Sample</b>				
	<b>N</b>	<b>AFH (n-pg)</b>	<b>SD</b>	<b>min</b>	<b>max</b>	<b>N</b>	<b>AFH (n-pg)</b>	<b>SD</b>	<b>min</b>	<b>max</b>
<b>Males</b>	30	104.41	5.60	93.9	118.6	2233	104.82	6.02	84.0	127.6
<b>Females</b>	30	99.38	5.63	88.1	110.7	2514	98.98	5.18	82.8	117.0
<b>Total</b>	60	102.14	6.02	88.1	118.6	4747	101.73	6.31	82.8	127.6

**AFH: Average Face Height (measurements in mm)**

We can see that Table 3.3 shows almost the same average face heights of the reproducibility sample and the full ALSPAC sample for males, females, and total samples, with a difference less than 0.5mm and similar standard deviations. This indicates that the sample selected for the reproducibility assessment of facial landmarks is representative of the population cohort recruited for this project.

### 3.3.4 Assessment of the reproducibility of facial landmarks

Bland-Altman plots were used to assess and visualise errors in landmarks identification, as shown in Figure 3.8 (a, b, c, and d). This figure shows examples of different landmark coordinates to illustrate the four levels of agreement used to classify landmarking errors.

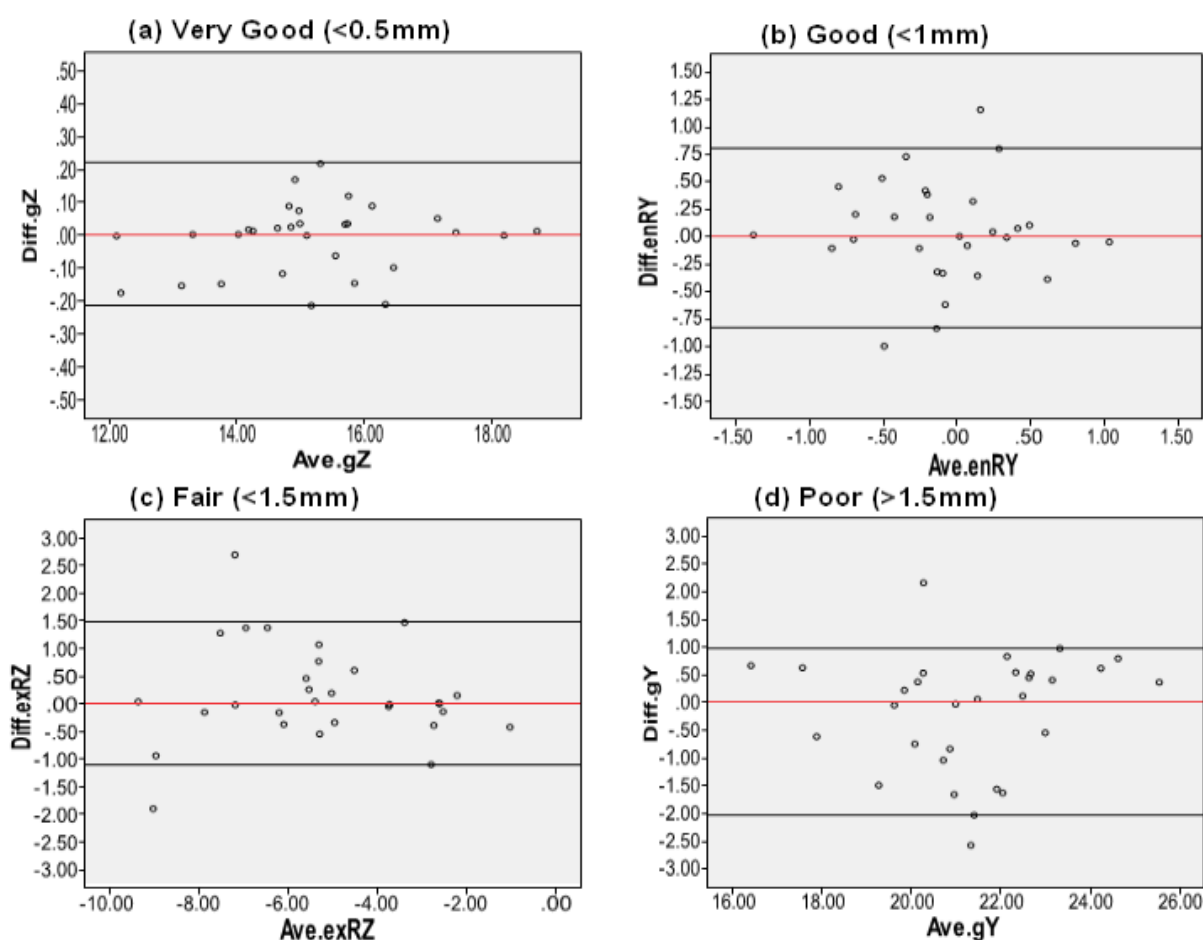


Figure 3.8. Reproducibility of landmark identification (Bland-Altman plots)

**Note:**

As the Bland-Altman method suggests, 95% limits of agreement between measurements can be used to indicate the reproducibility level. Provided that the mean and standard deviation are constant and the differences between measurements have an approximately normal distribution, the 95% of such differences should lie between the mean minus 1.96 SD and mean plus 1.96 SD.

- a) Illustrates an example for a Bland-Altman plot obtained to assess the reproducibility of the landmark glabella (g) in the z-axis for 30 females involved in the intra-examiner reproducibility assessment. The vertical axis of the plot (Diff.gZ) shows the difference between readings taken for the landmark glabella for each of the 30 individuals; whereas the horizontal axis (Ave.gZ) shows the average of the readings. The (zero) red line refers to the subjects where the difference between readings was equal to zero (highest reproducibility). This plot indicates that the landmark coordinate (glabella, z) has very good reproducibility level, as the difference between readings for all subjects was  $<0.5\text{mm}$  (error).
  
- b) Shows another example of a Bland-Altman plot obtained to assess the reproducibility of endocanthion (right) in the y-axis for 30 females involved in the intra-examiner reproducibility assessment. This plot indicates that the landmark coordinate (endocanthion, right, y) has good reproducibility level, as the 95% limits of agreement (indicated by black lines) include differences between readings  $<1\text{mm}$  (error).
  
- c) Shows another example of a Bland-Altman plot obtained to assess the reproducibility of exocanthion (right) in the z-axis for 30 females involved in the intra-examiner reproducibility assessment. This plot indicates that the landmark coordinate (exocanthion, right, z) has fair reproducibility level, as the 95% limits of agreement (indicated by black lines) include differences between readings  $<1.5\text{mm}$  (error).
  
- d) Shows another example of a Bland-Altman plot obtained to assess the reproducibility of glabella in the y-axis for 30 males involved in the inter-examiner reproducibility assessment. This plot shows that the landmark coordinate (glabella, y) has poor reproducibility level, as the 95% limits of agreement (indicated by black lines) include differences between readings  $>1.5\text{mm}$  (error).

Table 3.4 gives a summary of the results obtained for the intra- and inter-examiner reproducibility assessments for the total sample (60 subjects). The numbers of landmark coordinates and percentages were given for each of the four reproducibility levels (<0.5mm, <1mm, <1.5mm, and >1.5mm). The majority of landmark coordinates were reproducible to less than 1mm (intra-examiner 51%, inter-examiner 45%). The very good reproducibility level coordinates (<0.5mm) make up 33% (intra-examiner) and 30% (inter-examiner); whereas the fair reproducibility level coordinates (<1.5mm) make up 11% (intra-examiner) and 19% (inter-examiner). The poorest reproducibility level coordinates (>1.5mm) make up 5% (intra-examiner) and 6% (inter-examiner).

Table 3.4. Reproducibility of landmark identification (summary analysis for total sample)								
Method of Assessment	Intra-examiner (n=60)				Inter-examiner (n=60)			
Reproducibility Level	<0.5mm	<1mm	<1.5mm	>1.5mm	<0.5mm	<1mm	<1.5mm	>1.5mm
Number of Coordinates	21	32	7	3	19	28	12	4
Percentages	33%	51%	11%	5%	30%	45%	19%	6%

**Total Number of Coordinates = 63**

The intra- and inter- examiner reproducibility assessments of landmarks identification in the three dimensions are detailed further in Table 3.5 for the sample divided by gender (30 males and 30 females).

Table 3.5 gives the following findings:

- Fair and poor reproducibility coordinates were more frequent in the inter-examiner assessment than intra-examiner assessment, whereas very good and good reproducibility coordinates were noticed more in the intra-examiner assessment than inter-examiner assessment.
- The coordinates showing consistent poor reproducibility in both intra- and inter- examiner reproducibility assessments include: glabella (g) and nasion (n) in the y-axis and alare (al) in the z-axis.
- The chin point pogonion (pg) in the y-axis showed poor reproducibility in the inter-examiner reproducibility assessment (males only), whereas the right eye points exocanthion (ex) and palpebrale superius (ps) in the y-axis showed poor reproducibility in the inter-examiner reproducibility assessment (females only).
- Most of the eye points showed fair reproducibility in both intra- and inter- examiner reproducibility assessments.
- The following landmark coordinates showed consistent very good reproducibility in both intra- and inter- examiner assessments:
  - glabella (g) in the z-axis
  - nasion (n) in the z-axis
  - palpebrale inferius (pi) in the z-axis
  - pronasale (prn) in the x- and z- axes
  - alare (al) in the x-axis
  - labiale superius (ls) in the x-, y-, and z- axes
  - labiale inferius (li) in the y- and z- axes

- crista philtri (cph) in the y- and z- axes
- pogonion (pg) in the z-axis
- Other landmark coordinates showed consistent good reproducibility in both intra- and inter- examiner assessments.

Table 3.5. Reproducibility of landmark identification (detailed analysis for sample divided by gender)															
Intra-examiner								Inter-examiner							
Females (n=30)				Males (n=30)				Females (n=30)				Males (n=30)			
<0.5mm n=21	<1mm n=31	<1.5mm n=8	>1.5mm n=3	<0.5mm n=21	<1mm n=32	<1.5mm n=7	>1.5mm n=3	<0.5mm n=18	<1mm n=29	<1.5mm n=11	>1.5mm n=5	<0.5mm n=20	<1mm n=27	<1.5mm n=12	>1.5mm n=4
gX	nX	enRZ	gY	gZ	gX	enLX	gY	gZ	gX	exLX	gY	gZ	gX	enLX	gY
gZ	enLX	exRX	nY	nX	enLY	enLZ	nY	nZ	nX	exRX	nY	nX	enLY	enLZ	nY
nZ	enLY	exRZ	alLZ	nZ	enRX	exRX	alLZ	piLZ	enLX	exRZ	exRY	nZ	enRX	exLX	alLZ
psLZ	enLZ	psLY		piLY	enRY	exRZ		piRZ	enLY	psLY	psRY	piLY	enRY	exLY	pgY
piLZ	enRX	psRY		piLZ	enRZ	psRY		prnX	enLZ	piRY	alRZ	piLZ	enRZ	exRX	
piRZ	enRY	prnY		piRY	exLX	alRZ		prnZ	enRX	prnY		piRZ	exLZ	exRY	
prnX	exLX	snY		piRZ	exLY	pgY		alLX	enRY	alLZ		prnX	exRZ	psLY	
prnZ	exLY	alRZ		prnX	exLZ			alRX	enRZ	chLX		prnZ	psLX	psLZ	
snX	exLZ			prnZ	exRY			lsX	exLY	chRX		alLX	psRX	prnY	
alLX	exRY			snZ	psLX			lsY	exLZ	chRZ		alRX	psRY	alRZ	
alRX	psLX			alLX	psLY			lsZ	psLX	pgY		lsX	psRZ	chLX	
lsX	psRX			alRX	psLZ			liY	psLZ			lsZ	piLX	chRX	
lsY	psRZ			lsY	psRX			liZ	psRX			liX	piRX		
lsZ	piLX			lsZ	psRZ			cphLY	psRZ			liY	piRY		
liY	piLY			liY	piLX			cphLZ	piLX			liZ	snX		
liZ	piRX			liZ	piRX			cphRY	piLY			cphLY	snY		
cphLY	piRY			cphLY	prnY			cphRZ	piRX			cphLZ	snZ		
cphLZ	snZ			cphLZ	snX			pgZ	snX			cphRY	alY		
cphRY	alLY			cphRY	snY				snY			cphRZ	alRY		
cphRZ	alRY			cphRZ	alLY				snZ			pgZ	lsY		
pgZ	liX			pgZ	alRY				alLY				cphLX		
	cphLX				lsX				alRY				cphRX		
	cphRX				liX				liX				chLY		
	chLX				cphLX				cphLX				chLZ		
	chLY				cphRX				cphRX				chRY		
	chLZ				chLX				chLY				chRZ		
	chRX				chLY				chLZ				pgX		
	chRY				chLZ				chRY						
	chRZ				chRX				pgX						
	pgX				chRY										
	pgY				chRZ										
					pgX										

Notation: g, glabella; n, nasion; ps, palpebrale superius; pi, palpebrale inferius; prn, pronasale; sn, subnasale; al, alare; ls, labiale superius; li, labiale inferius; cph, crista philtri; ch, cheilion; pg, pogonion; en, endocanthion; ex, exocanthion; L, left; R, right; X, x-axis; Y, y-axis; Z, z-axis (e.g., enLY stands for endocanthion left, y-coordinate).

Reproducibility levels: <0.5mm (very good), <1mm (good), <1.5mm (fair), and >1.5mm (poor).

Table 3.6 ranks the 21 facial landmarks from the most to least reproducible for both intra- and inter- examiner assessments. This ranking is based upon assessing each landmark according to the linear distance between the landmark positions. The accuracy of identifying different landmarks ranged from 0.29mm to 1.26mm (error in landmark positioning). 17 landmarks were reproducible to less than 1mm for intra-examiner assessment, and 14 landmarks were reproducible to less than 1mm for inter-examiner assessment.

The lip points labiale superius (ls) and labiale inferius (li) were the most reproducible facial landmarks (<0.5mm) for both intra- and inter- examiner assessments, followed by the landmarks crista philtri (cph), palpebrale inferius (pi), pronasale (prn), subnasale (sn), palpebrale superius (ps), endocanthion (en), and alare (al) with less than 1mm reproducibility errors for both intra- and inter- examiner assessments. The landmarks nasion (n), glabella (g), and exocanthion (ex) followed with reproducibility errors more than 1mm for both intra- and inter- examiner assessments.

The least reproducible facial landmarks were glabella (g) for intra-examiner assessment and nasion (n) for inter-examiner assessment. Landmarks showed differences in their reproducibility level between intra- and inter- examiner assessments: cheilion (ch) and pogonion (pg) were reproducible to less than 1mm in intra-examiner assessment and more than 1mm in inter-examiner assessment.

Table 3.6. Ranking of facial landmarks according to the linear distance between two spatial positions						
Rank	Intra-examiner (n=60)			Inter-examiner (n=60)		
	Landmark	Average	SD	Landmark	Average	SD
1	ls	0.29	0.17	ls	0.41	0.23
2	li	0.39	0.20	li	0.47	0.25
3	cphR	0.50	0.34	cphR	0.57	0.40
4	cphL	0.52	0.30	cphL	0.58	0.42
5	piL	0.58	0.37	piL	0.62	0.48
6	prn	0.59	0.34	piR	0.66	0.43
7	sn	0.59	0.52	prn	0.67	0.38
8	piR	0.61	0.41	sn	0.76	0.46
9	chL	0.77	0.41	enR	0.81	0.49
10	pg	0.80	0.56	alL	0.84	0.54
11	psR	0.82	0.57	alR	0.85	0.49
12	psL	0.84	0.56	psL	0.92	0.57
13	enR	0.85	0.59	enL	0.93	0.58
14	exL	0.85	0.71	psR	0.98	0.61
15	chR	0.89	0.41	chL	1.02	0.51
16	enL	0.90	0.57	g	1.05	0.62
17	alR	0.90	0.42	chR	1.08	0.52
18	alL	1.01	0.53	exL	1.12	0.77
19	n	1.04	0.76	pg	1.13	0.59
20	exR	1.09	0.67	exR	1.26	0.75
21	g	1.11	0.69	n	1.26	0.91

Notation: g, glabella; n, nasion; ps, palpebrale superius; pi, palpebrale inferius; prn, pronasale; sn, subnasale; al, alare; ls, labiale superius; li, labiale inferius; cph, crista philtri; ch, cheilion; pg, pogonion; en, endocanthion; ex, exocanthion; L, left; R, right; SD, Standard Deviation.

Cells highlighted in green colour indicate landmarks with reproducibility <0.5mm error; cells highlighted in blue colour indicate landmarks with reproducibility >0.5mm and <1mm error; and cells highlighted in yellow colour indicate landmarks with reproducibility >1mm error.

### **3.4 Discussion**

#### **3.4.1 Reliability of the laser scanning procedure**

Fifty-two percent of the invited children attended the recall, and 91 percent of these had suitable facial scans. Although the acquisition time for the laser cameras was relatively long (approximately 7 seconds), the reliability of the laser scanning procedure in this study was remarkably good. The mean “average distance” between the registered left and right facial scans obtained for 4747 individuals was 0.34mm. In addition, the reliability of facial soft tissue capture (ability of the scanned subjects to present the same facial expressions or facial posture over time) was also assessed in this study. High percentages of coincidence were recorded between the facial scans taken for individuals at different scanning occasions (short and long terms intervals). Few studies have assessed the reliability of capturing facial soft tissues over time. Kau (2007) analysed facial changes in children aged 11–14 year old using 3D laser-scan imaging technology, and he reported that a high level of soft tissue reproducibility can be achieved upon using a standardized approach for capturing facial morphology.

In our study, similar findings were observed. The superimposed facial shells were found to show the greatest deviation in the lower jaw area, and this finding was not unexpected as the lower jaw is freely movable. However, this deviation was limited to certain zones near the lips, corners of the mouth and/or the chin area; the difference did not exceed 1–1.5mm.

Other deviation zones were observed mostly in the eye region; this is due to the complex geometry of this area, which makes it difficult to capture using a laser-based acquisition system. This may influence the mesh generation during computerized processing of the 3D facial scans. Although these areas were quite small, patchy, non-systematic and not detrimental to the overall reproducibility of facial soft tissue morphology, they had relatively influenced the accuracy in identifying the eye landmarks in some subjects where the mesh showed large polygons, and landmarks placed over these areas were not as precise as those placed over areas with high density of polygons. This may have also been reflected on the reproducibility level exhibited by these landmarks. Therefore, some precautions should be taken when processing these areas of the face to ensure that a dense mesh is produced, making the identification of landmarks easier and more accurate.

In general, we can say that capturing facial soft tissue morphology with a laser-scan imaging system shows a high level of reproducibility; any level of deviation observed between the superimposed facial scans is clinically acceptable and non-significant, making this technique feasible for studying facial morphology.

### **3.4.2 Reproducibility of facial soft tissue landmarks**

This study investigated the reproducibility of identifying 21 soft tissue landmarks on the 3D facial scans of 60 randomly selected individuals from the ALSPAC cohort. The selected sample was proved representative of the population cohort by comparing the average facial height obtained for the reproducibility sample (102.14mm) with that obtained for the total ALSPAC sample (101.73mm). The average facial heights were similar with the difference not exceeding 0.4mm. The reproducibility of recording facial landmarks was assessed in each of the three dimensions. The majority of the x, y, and z coordinates of the 21 facial landmarks were reproducible to less than 1mm (51% intra-examiner, 45% inter-examiner), which is considered clinically acceptable (Gwilliam *et al.*, 2006).

The coordinates with fair reproducibility level (<1.5mm) were mainly associated with the eyes as explained above. The relatively poor reproducibility level (>1.5mm) shown by only a few landmarks (y-coordinates of glabella, nasion, and pogonion and z-coordinate of alare) was mainly due to difficulties in accurately locating these landmarks over flat areas of the associated facial features (forehead, bridge of the nose, sides of the nose, and chin), making it easy to misplace these points too high/low vertically (glabella, nasion, and pogonion) or too far in/out horizontally (alare). However, the reproducibility of these landmarks was much better in the other dimensions.

Only a few coordinates exhibited differences in their reproducibility level between males and females. For example, the landmark subnasale (sn) in the y-axis was relatively more reproducible in males (<1mm) than females (<1.5mm) for their intra-examiner assessment only. This could be due to the fact that where the “nasolabial angle” is found with curved contour, accurately locating the point can be quite difficult. This angle should ideally be about 100–110° for a woman and 90–100° for a man. In this study, the nasolabial angle was slightly smaller in males than females. On the other side, females tend to exhibit well-defined lip contours as compared to males, making it relatively easier to locate the landmark labiale superius (ls) in all three coordinates, with a very good reproducibility level being reported in both intra- and inter- examiner assessments. However, the inter-examiner assessment of both males and females showed fair reproducibility of the left/right cheilions in the x-axis as compared to their good reproducibility in the intra-examiner assessment.

The lip points labiale superius (ls) and labiale inferius (li) were ranked the most reproducible facial landmarks (<0.5mm) with respect to the distance between two landmark positions for both intra- and inter- examiner assessments; this was due to the well-defined contours at the areas of the upper and lower lips, making it easier to accurately locate these points. On the other side, the landmarks glabella (g) and nasion (n) were ranked the least reproducible for the intra- and inter- examiner assessments, respectively. The reason was explained above. Similar findings have been reported by Gwilliam *et al.* (2006).

The least reproducible facial landmarks (glabella and nasion) were due to having poor reproducibility level in the y-axis only. These landmarks showed good to very good reproducibility levels in the x-axis for different reproducibility assessments (intra- and inter-examiner) of males and females, and constant very good reproducibility level in the z-axis for all reproducibility assessments of males and females. Beside, these are considered the most important facial landmarks that can be used to study facial variation at the areas of forehead (between the eyebrows) and nasal bridge (Farkas, 1994).

### **3.4.3 Summary**

The results showed different levels of reproducibility, which could be affected by the following factors:

1. Clarity of description/definition of the landmarks.
2. Clarity of morphological details, which may be gender specific. A landmark associated with a pointed feature, such as labiale superius (ls) or crista philtri (cph), is more likely to produce a smaller error compared to a landmark placed on a locally flat surface, such as glabella (g) or alare (al).
3. Examiner factors: e.g. visual acuity, self-discipline, organization skills and ability to follow the landmark definition exactly.
4. Computer screen resolution.
5. Visualisation of the three planes of space (x, y, and z) identifying the position of each particular landmark on the face.

### **3.5 Conclusions**

- The reproducibility of identifying facial landmarks varies between landmarks. For good reproducibility, a landmark must be unambiguously defined and its definition well understood by the examiner. Landmarks placed on clearly defined contours show higher reproducibility than those placed on flat areas; this may be gender specific.
- To be of clinical use, it must be ensured that the reproducibility of each landmark in all three spatial dimensions (x, y, and z) is sufficiently high.
- Poorer reproducibility was observed in the inter-examiner assessment than intra-examiner assessment.
- The examiner must become familiar with the software program used to view and process the 3D facial scans in order to improve reproducibility of some landmarks (e.g. those associated with the eyes).
- The majority of the x, y, and z coordinates were reproducible to less than 1mm (51% intra-examiner, 45% inter-examiner), which is clinically acceptable. The precision of identifying the 21 facial landmarks ranged from 0.29mm to 1.26mm (error).
- The fact that different facial landmarks show different reproducibility levels should be considered when analysing facial morphology variation. Also landmark variation will affect sample size estimation in determining various differences between population groups.

## Chapter 4

# Exploring Facial Variation In Large Population

## Exploring Facial Variation In Large Population

### 4.1 Introduction

Facial morphology attracts interest from a wide variety of research disciplines (e.g., anthropology, developmental anatomy, orthodontics, maxillofacial surgery, cosmetic surgery, genetics, and psychology). Many studies have been undertaken to analyse the variation of facial hard and soft tissues that occur as a result of growth and clinical interventions (Moss *et al.*, 2003; Nute and Moss, 2000; Hennessy and Moss, 2001; McCance *et al.*, 1992a, b, 1993, 1997a, b, c, d; Kau and Richmond, 2008; Ferrario *et al.*, 1998a, b, 1999a), and in individuals with various kinds of syndromes, developmental anomalies, genetic and medical disorders (Hennessy *et al.*, 2002, 2004, 2007, 2010; Hammond *et al.*, 2004, 2005; Shaner *et al.*, 2000; Bugaighis *et al.*, 2010). However, less attention has been paid to the analysis of normal facial variation and to the identification of the genetic basis for this variation.

The characterization of the human face in three dimensions is fundamental to the objective analysis of facial normality and deformity. Recently, several researchers focused on the three-dimensional analysis of variation of facial features associated with dysmorphic anomalies (e.g., cleft lip and palate) through analysing the variation in the relative positions of facial landmarks associated with these features (Shaner *et al.*, 2000; Bugaighis *et al.*, 2010); however, it has to be realised that many malformations due to genetic and medical disorders are subtle and difficult to recognize even by experienced clinical geneticists. Slight variations in facial morphological features or a

combination of minor distinct features in the face are far more difficult to detect, but may be decisive in a syndrome diagnosis. Therefore, understanding normal variation of the face is fundamental to identify the minor physical anomalies associated with various genetic and medical conditions and affecting the relative positions of facial landmarks.

A few studies have tried to analyse normal facial variation using either 2D or 3D records. In these studies, facial landmarks have been extracted and their coordinates subjected to geometric morphometric analysis. This involved superimposing the individual landmark configurations and then subjecting the resulting shape coordinates to a principal component analysis (PCA). PCA is a statistical technique used commonly by researchers in order to highlight similarities and differences within a sample. In facial morphology analysis, several researchers used PCA to identify the main components explaining the majority of facial variation within a sample. In these studies, the extracted principal components (PCs) explained the variation in height, width, and prominence of the face and its main structures: the forehead, the eyes, the nose, the lips and mouth, and the chin.

Using the x and y coordinates of 12 facial landmarks extracted from 2D profile photographs of 110 Caucasian adult patients, Krey and Dannhauer (2008) identified 6 principal components responsible for 86.5% of the total variance in facial profile variation.

A recent study (Weinberg *et al*, 2013) investigated the heritability of face shape in a set of 10 monozygotic and 11 same-sex dizygotic twin pairs who were comprised of Caucasian boys and girls between the ages of 5 and 12 years. Using a 3D stereophotogrammetric imaging technique and geometric morphometric analysis of 13 surface landmarks, a total of 17 PCs were extracted; the first 9 PCs accounted for approximately 90% of the total variance in face shape. Three of the derived shape PCs displayed evidence of moderate to high heritability.

A comparison between the results of the above studies (in addition to other studies) and the current study is outlined in the discussion section of this chapter. Generally, the studies that have been undertaken so far to analyse normal facial variation used small samples for its analyses, which may have not explained enough the total variance in facial morphology.

The *aim* of this study is to identify the key facial features contributing to normal facial variation in a large population of British adolescents.

The *objectives* of this study include:

- Determining the principal features of facial variation with respect to facial form (size + shape) and facial shape only.
- Define normality of the face (normal ranges/scales of facial variation, including normal variation in symmetry of different facial features).

## 4.2 Subjects and methods

### 4.2.1 Sample

The final ALSPAC sample of 4747 British adolescents (2514 females and 2233 males) was used for this study.

### 4.2.2 Statistical analyses

#### 4.2.2.1 Analysis of 3D landmark data

##### 4.2.2.1.1 Generalized Procrustes Analysis (GPA):

Morphometrics is a field concerned with studying variation and change in the size and shape of organisms or objects in the simplest possible fashion by removing extraneous information and thereby facilitating comparison between different objects. There are several methods for extracting data from shapes, each with its own benefits and weaknesses. Traditional methods include measuring distances, angles, areas and volumes and it enables us to describe complex shapes and permits numerical comparison between different forms (Zelditch *et al.*, 2004).

In the last three decades, more advanced methods have been developed such as geometric morphometrics which is a collection of approaches for the multivariate statistical analysis of coordinate data, usually (but not always) limited to landmark point locations. An example of a geometric morphometric technique is Generalized Procrustes Analysis (GPA) which is a method to register landmarked shapes, whose results are further used to analyse the distribution and changes of a set of shapes as a result of growth, experimental treatment or evolution (Dalal and Phadke, 2007).

Shape and landmarks are important concepts involved with generalized Procrustes analysis. Landmarks have been defined as a finite set of points on a shape surface that accurately describe the shape. Shape is defined as all the geometrical information that remains when location, scale and rotational effects are filtered out from an object (Bookstein, 1991b).

As is known from geometric morphometrics, prior to comparing shapes or faces, they need to be fitted into a reference framework that places them in the same virtual space. This can be achieved by Procrustes registration of the landmark sets through translation, rotation and scaling to minimize overall deviations between the landmarks sets (Hennessy and Moss, 2001).

Procrustes analysis (also called ordinary Procrustes analysis) is a form of statistical shape analysis used to superimpose two landmarked shapes. The Procrustes distance provides a metric to minimize, in order to align, a pair of shape instances annotated by landmark points. GPA employs ordinary Procrustes analysis to align a population of shapes instead of only two shape instances (Bookstein, 1991b).

The algorithm outline is the following:

- 1) Choose a reference shape among the training set instances.
- 2) Align all other instances on current reference.
- 3) Compute the mean shape of the current training set.
- 4) If the Procrustes distance between the mean shape and the reference is above a threshold, set reference to mean shape and continue to step 2.

Generally, the shape of an object can be considered as a member of an equivalence class formed by removing the translational, rotational and scaling (size) components. In order to compare the faces and observe facial variation, they need to be fitted into a common reference framework including a common origin that places them in the same virtual space and assigns an equal weight to each facial landmark, i.e., the translational components can be removed from an object by translating the object so that the mean of all the points lies at the origin (for the face, it is facial centroid).

*Mathematically*, suppose we have  $N$  faces each defined by 21 facial landmarks (points) in three dimensions ( $x, y, z$ ). So each facial shape is represented by 63 coordinates:

$$((x_1, y_1, z_1), (x_2, y_2, z_2), \dots, (x_{21}, y_{21}, z_{21}))$$

The centroid of a shape is the point  $(\bar{x}, \bar{y}, \bar{z})$  with the mean coordinates:

$$\bar{x} = \frac{x_1 + x_2 + \dots + x_{21}}{21}, \quad \bar{y} = \frac{y_1 + y_2 + \dots + y_{21}}{21}, \quad \bar{z} = \frac{z_1 + z_2 + \dots + z_{21}}{21}$$

The centroid is taken to be the origin of coordinates and all shapes are now translated to the origin:

$$(x, y, z) \rightarrow (x - \bar{x}, y - \bar{y}, z - \bar{z}), \text{ giving the points:}$$

$$(x_1 - \bar{x}, y_1 - \bar{y}, z_1 - \bar{z}), \dots$$

The size of a face is defined as its centroid size, which is the root square deviation of all landmarks from the centroid:

$$S = \sqrt{(x_1 - \bar{x})^2 + (y_1 - \bar{y})^2 + \dots + (y_{21} - \bar{y})^2 + (z_{21} - \bar{z})^2}$$

Once the sizes  $S_1, \dots, S_N$  of all faces have been calculated, the scale or size component is removed by scaling each object uniformly in all dimensions to the 'average size' by the factor  $\bar{S} / S_i$ ,  $i = 1, \dots, N$ , where:

$$\bar{S} = \frac{S_1 + S_2 + \dots + S_N}{N}$$

As a result, smaller faces are scaled up and bigger faces are scaled down. This is an optional step, which is only relevant when size of the face is of no interest and the focus is on face shape variation. Because face size is an important factor in many clinical applications, such as analysis of facial morphology, GPA was performed in this study to analyse facial form (size + shape) as well as facial shape separately.

Rotation is another non-shape attribute that must be removed (standardised) from the dataset prior to interpretation. In GPA, this is performed by minimizing the Procrustes distance between the current shape and mean shape, i.e., the square root of the sum of squared distances between the respective landmarks. Removing the rotational component is mathematically much more complex because it involves a sophisticated matrix analysis.

A relatively simple example can only be given in a two-dimensional case. Suppose the current shape and mean shape are defined by their landmark coordinates  $(x_1, y_1), \dots, (x_n, y_n)$  and  $(\bar{x}_1, \bar{y}_1), \dots, (\bar{x}_n, \bar{y}_n)$ , respectively, where  $n$  is the number of landmarks. If the current shape is rotated about the origin by an angle  $\theta$ , its new coordinates will be expressed as:

$$(u_i, v_i) = (x_i \cos \theta - y_i \sin \theta, x_i \sin \theta + y_i \cos \theta), \quad i = 1, \dots, n$$

The Procrustes distance is:

$$d = \sqrt{(u_1 - \bar{x}_1)^2 + (v_1 - \bar{y}_1)^2 + \dots + (u_n - \bar{x}_n)^2 + (v_n - \bar{y}_n)^2}$$

The distance can be minimized by using a *least squares* technique to find the angle  $\theta$  that provides the minimum of  $d$ . This technique yields the angle:

$$\theta = \arctan \frac{(x_1 \bar{y}_1 - \bar{x}_1 y_1) + \dots + (x_n \bar{y}_n - \bar{x}_n y_n)}{(x_1 \bar{x}_1 + y_1 \bar{y}_1) + \dots + (x_n \bar{x}_n + y_n \bar{y}_n)}.$$

Summary:

In this study, all facial shells were initially normalised to a natural head posture (NHP) with the origin set at mid-endocanthion point, as described earlier in Chapter 3.

Generalized Procrustes Analysis (GPA) was performed to register (align) the sets of the 21 facial landmarks by removing translation and rotation (Bookstein, 1991b):

- without scaling to analyse facial form (size + shape), and
- with scaling to analyse facial shape only.

Apart from the registered sets, GPA provided mean shapes for both unscaled and scaled datasets. For each of the 21 landmarks of either mean shape, the standard deviations were calculated for all individuals and plotted as ellipsoids. Each ellipsoid covered two standard deviations from the mean in the x, y and z dimensions, and so represented 95% of the variability.

Figure 4.1 illustrates an example for registering (aligning) three sets of 21 facial landmarks (displayed in red, green, and blue) obtained for three individuals of the ALSPAC sample, using generalized Procrustes analysis.

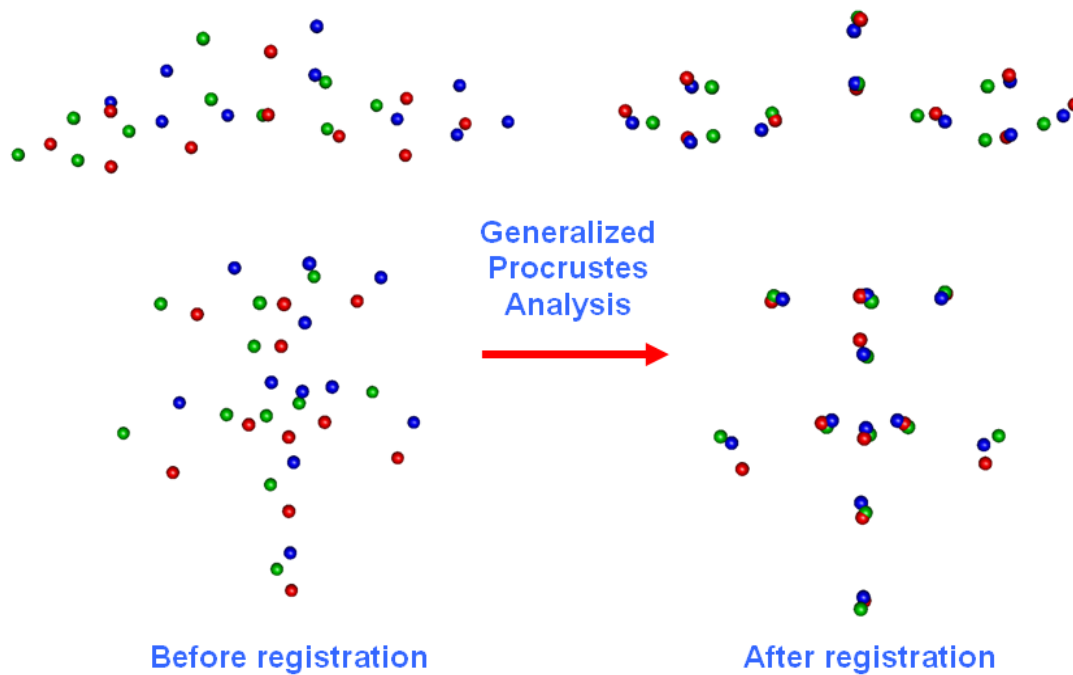


Figure 4.1. Generalized Procrustes Analysis (GPA)

#### 4.2.2.1.2 Principal Component Analysis (PCA):

PCA is a way of identifying patterns in data, and expressing the data in a way so as to highlight their similarities and differences (Pearson, 1901). Since patterns can be hard to find in data of high dimension, where the luxury of graphical representation is not available, PCA is considered a powerful tool for analysing data, and it is a statistical technique that has found many applications in fields such as face recognition and image compression where data of high dimension needs to be analysed (Hennessy *et al.*, 2002, 2004; Hammond *et al.*, 2004, 2005).

In other words, PCA is a technique used to reduce multi-dimensional data sets to lower dimensions for analysis so as to generate predictive models by analyzing the multidimensional data sets obtained for a particular study.

PCA was first invented in 1901 by Karl Pearson, as an analogue of the principal axes theorem in mechanics; it was later independently developed (and named) by Harold Hotelling (1933, 1936). The method is mostly used as a tool in exploratory data analysis and for making predictive models. PCA can be done by eigenvalue decomposition of a data covariance (or correlation) matrix or singular value decomposition of a data matrix, usually after mean centering (and normalizing or using Z-scores) the data matrix for each attribute (Abdi and Williams, 2010). The results of a PCA are usually discussed in terms of component scores, sometimes called factor scores (the transformed variable values corresponding to a particular data point), and loadings (the weight by which each standardized original variable should be multiplied to get the component score) (Shaw, 2003).

PCA is defined as an orthogonal linear transformation that transforms the data to a new coordinate system such that the greatest variance by any projection of the data comes to lie on the first coordinate (called the first principal component), the second greatest variance on the second coordinate, and so on. This involves the computation of the eigenvalue decomposition of a data set; this step gives us the components in order of significance from highest to lowest. It also helps us to discriminate between significant and non-significant components. Generally, for a good PCA, a few components should explain most of the variance and the rest explain relatively small amounts of the variance observed in the sample.

*Mathematically*, PCA is a statistical procedure that uses an orthogonal transformation to convert a set of observations of possibly correlated variables into a set of values of linearly uncorrelated variables called principal components. The number of principal components is less than or equal to the number of original variables. This transformation is defined in such a way that the first principal component has the largest possible variance (that is, accounts for as much of the variability in the data as possible), and each succeeding component in turn has the highest variance possible under the constraint that it is orthogonal to (i.e., uncorrelated with) the preceding components. Principal components are guaranteed to be independent if the data set is jointly normally distributed. PCA is sensitive to the relative scaling of the original variables.

PCA is the simplest of the true eigenvector-based multivariate analyses. Often, its operation can be thought of as revealing the internal structure of the data in a way that best explains the variance in the data. If a multivariate dataset is visualised as a set of coordinates in a high-dimensional data space (1 axis per variable), PCA can supply the user with a lower-dimensional picture, a projection or 'shadow' of this object when viewed from its most informative viewpoint. This is done by using only the first few principal components so that the dimensionality of the transformed data is reduced. PCA defines a new orthogonal coordinate system that optimally describes variance in a single dataset.

Given a set of points in Euclidean space, the first principal component corresponds to a line that passes through the multidimensional mean and minimizes the sum of squares of the distances of the points from the line. The second principal component corresponds to the same concept after all correlation with the first principal component has been subtracted from the points. The singular values (in  $\Sigma$ ) are the square roots of the eigenvalues of the matrix. Each eigenvalue is proportional to the portion of the 'variance' (more correctly of the sum of the squared distances of the points from their multidimensional mean) that is correlated with each eigenvector. The sum of all the eigenvalues is equal to the sum of the squared distances of the points from their multidimensional mean. PCA essentially rotates the set of points around their mean in order to align with the principal components. This moves as much of the variance as possible (using an orthogonal transformation) into the first few dimensions. The values in the remaining dimensions, therefore, tend to be small and may be dropped with minimal loss of information. PCA is often used in this manner for dimensionality reduction. PCA has the distinction of being the optimal orthogonal transformation for keeping the subspace that has largest 'variance'.

Such dimensionality reduction can be a very useful step for visualising and processing high-dimensional datasets, while still retaining as much of the variance in the dataset as possible. For example, selecting  $L = 2$  and keeping only the first two principal components finds the two-dimensional plane through the high-dimensional dataset in which the data is most spread out, so if the data contains clusters these too may be most spread

out, and therefore most visible to be plotted out in a two-dimensional diagram; whereas if two directions through the data (or two of the original variables) are chosen at random, the clusters may be much less spread apart from each other, and may in fact be much more likely to substantially overlay each other, making them indistinguishable.

In this study, PCA was used to identify key factors that contribute to facial variation using the 21 facial landmarks. This technique aims to explore the many variables in the data matrix so that the new components of variables are derived and correlated with the original variables but not with each other; so they are now independent of each other. It is a data reduction technique used to highlight important features of a data set (Mao *et al.*, 2006).

Summary:

PCA of the unscaled and scaled datasets of 21 facial landmarks (63 x, y, and z coordinates) was employed using 'SPSS' to identify independent principal components, representing important combinations of correlated variables. In this study, the 'Kaiser–Guttman criterion' (Guttman, 1954; Cliff, 1988; Jackson, 1993) was used as the stopping rule to identify critical principal components (PCs). According to this rule, the components with eigenvalues greater than the average eigenvalue should only be retained. The rotation method used for PCA was the varimax technique with Kaiser normalization (Kaiser, 1958).

#### 4.2.2.1.3 *Extracting parameters from principal components:*

A parameter characterizing each principal component was derived. These parameters (which are described below) are based on only those coordinates that make the greatest contribution to the corresponding principal component. A parameter can be one of the following three kinds: (i) a *centroid* of the group of most significant coordinates contributing to a particular component, (ii) the *distance* between two centroids if the group of the most significant coordinates naturally splits into two subgroups, or (iii) the *ratio* between two distances.

It should be emphasized that these parameters are not the component scores that result from PCA but are artificially created quantities that, unlike the component scores, are associated with actual facial features and are physically meaningful.

##### 4.2.2.1.3.1 *Purposes of the PC parameters:*

- To assign a physical meaning to a PC.
- To identify meaningful normal ranges of facial variation associated with a PC.
- To help visualize the facial variation associated with each PC (see Chapter 5).

## 4.3 Results

### 4.3.1 Analysis of 3D landmark data

#### 4.3.1.1 Generalized Procrustes Analysis (GPA):

Figures 4.2 and 4.3 visualize facial variation for the unscaled and scaled datasets, respectively, (ALSPAC sample, 4747 subjects) displayed as ellipsoid envelopes at the 21 landmarks against an average face; Figure 4.4 shows the superimposition of the results presented in Figures 4.2 and 4.3. Each ellipsoid represents a variation of two standard deviations in all dimensions around the mean position of the respective landmark and so defines a 95% confidence region of landmark positions. For the method of construction of average faces, see Chapter 5. It is apparent from the figures that pogonion shows the largest variation in the y and z axes for both unscaled and scaled datasets. The inner canthi as well as the left and right alari exhibit the least variation in the unscaled dataset, while the inner canthi and upper lip landmarks (labiale superius, left and right crista philtri) show the least variation in the scaled dataset.

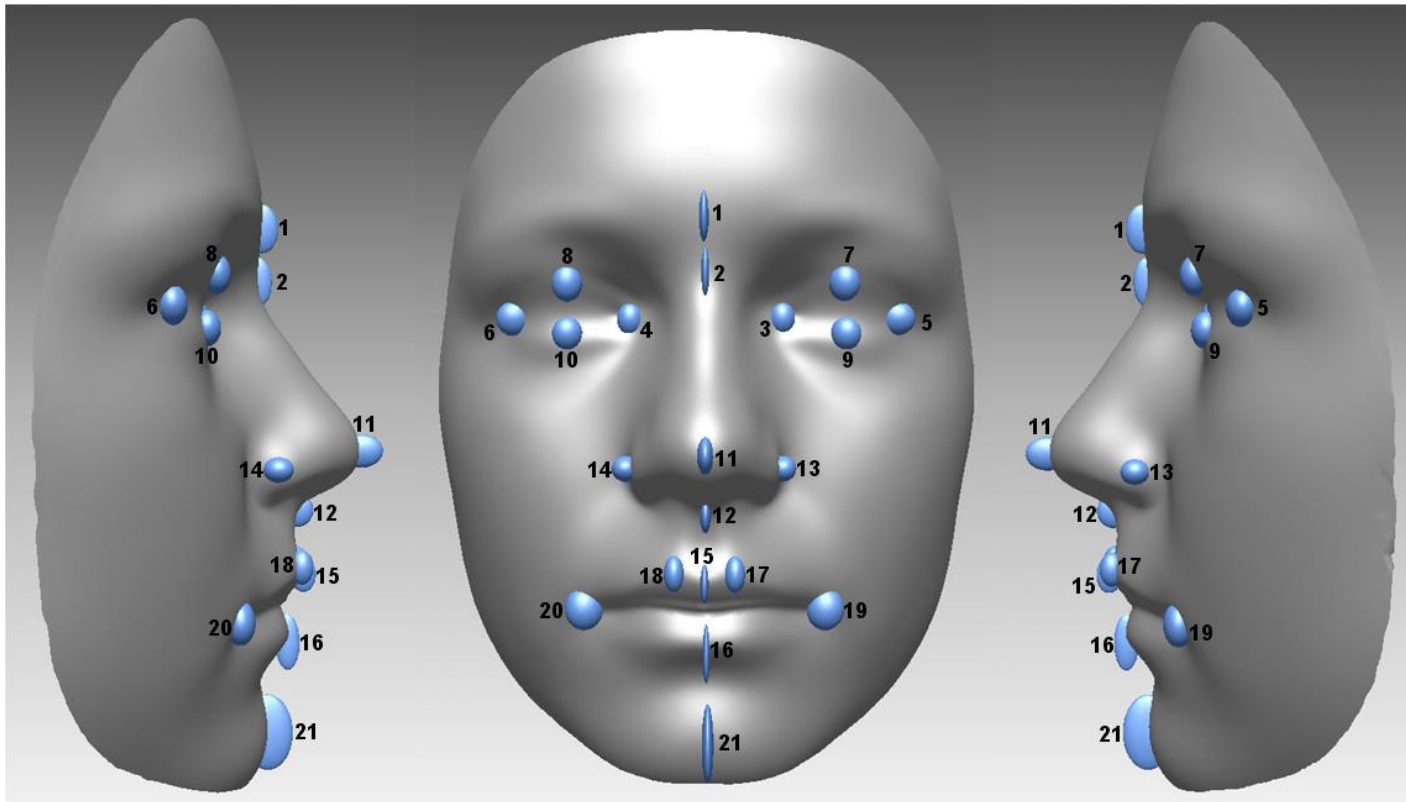


Figure 4.2.

Two-standard-deviation envelopes for 21 facial landmarks (unscaled dataset, ALSPAC sample of 4747 subjects), *Facial Landmarks*: 1, glabella; 2, nasion; 3 and 4, endocanthion (left and right); 5 and 6, exocanthion (left and right); 7 and 8, palpebrale superius (left and right); 9 and 10, palpebrale inferius (left and right); 11, pronasale; 12, subnasale; 13 and 14, alari (left and right); 15, labiale superius; 16, labiale inferius; 17 and 18, crista philtri (left and right); 19 and 20, cheilion (left and right); 21, pogonion.

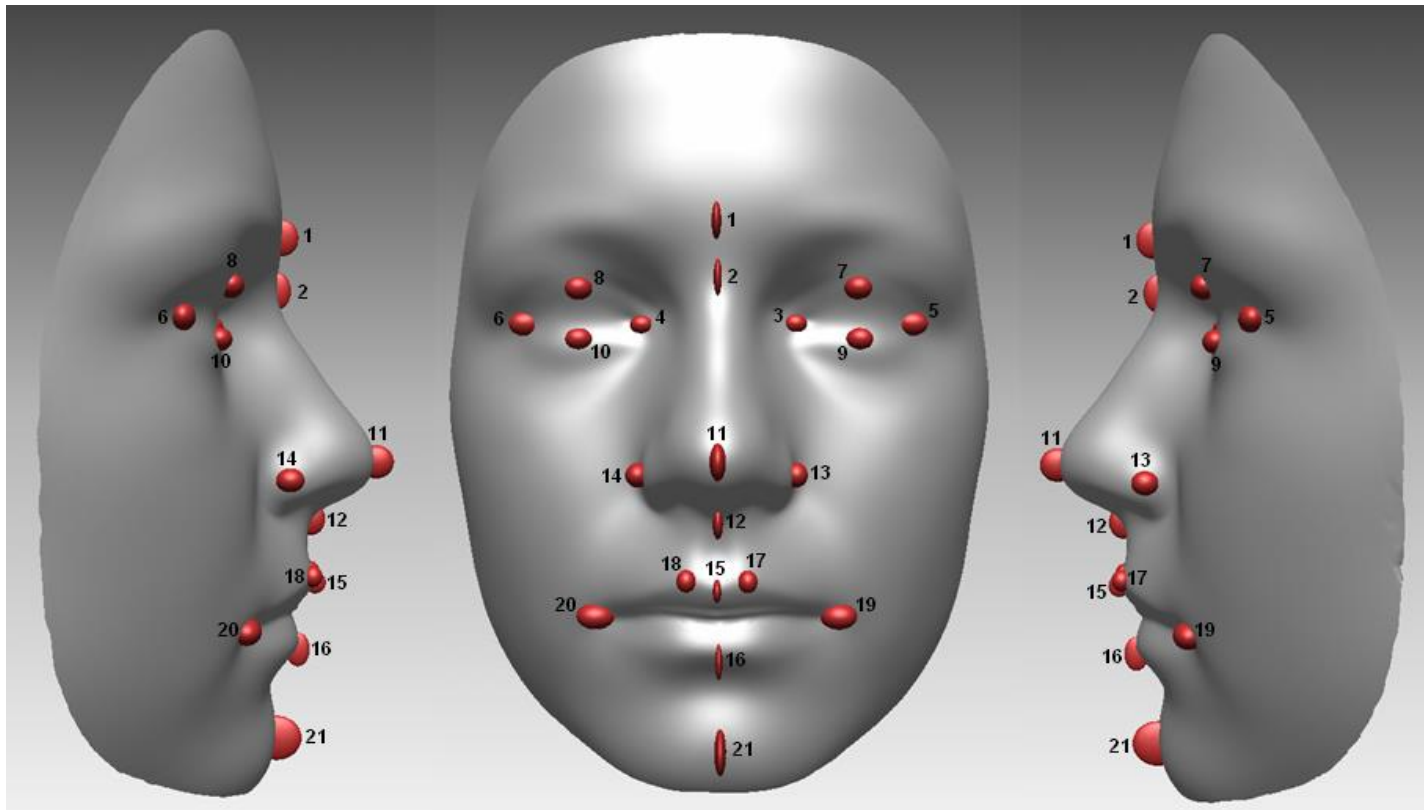


Figure 4.3.

Two-standard-deviation envelopes for 21 facial landmarks (scaled dataset, ALSPAC sample of 4747 subjects), *Facial Landmarks*: 1, glabella; 2, nasion; 3 and 4, endocanthion (left and right); 5 and 6, exocanthion (left and right); 7 and 8, palpebrale superius (left and right); 9 and 10, palpebrale inferius (left and right); 11, pronasale; 12, subnasale; 13 and 14, alari (left and right); 15, labiale superius; 16, labiale inferius; 17 and 18, crista philtri (left and right); 19 and 20, cheilion (left and right); 21, pogonion.

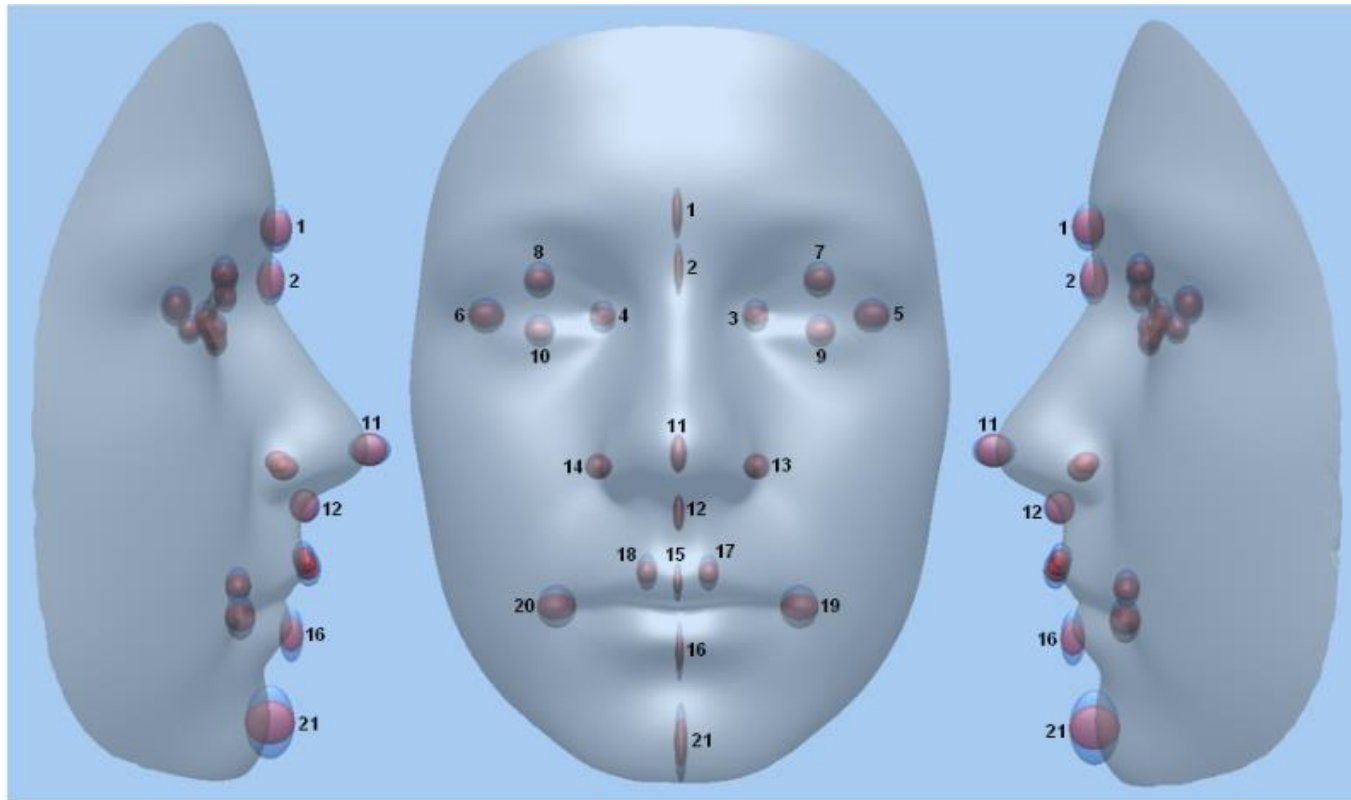


Figure 4.4.

Two-standard-deviation envelopes for 21 facial landmarks, superimposed unscaled (blue) versus scaled (red).

*Facial Landmarks:* 1, glabella; 2, nasion; 3 and 4, endocanthion (left and right); 5 and 6, exocanthion (left and right); 7 and 8, palpebrale superius (left and right); 9 and 10, palpebrale inferius (left and right); 11, pronasale; 12, subnasale; 13 and 14, alari (left and right); 15, labiale superius; 16, labiale inferius; 17 and 18, crista philtri (left and right); 19 and 20, cheilion (left and right); 21, pogonion.

#### 4.3.1.2 PCA of the unscaled dataset:

For the total ALSPAC sample of 4747 individuals, 14 principal components were identified by PCA (Table 4.1). This table lists the factor loadings (coefficients) for each coordinate in all extracted principal components. These coefficients indicate the relative importance of different landmark coordinates to the variation associated with each component.

Each component includes a group of landmark coordinates (highlighted cells) that have high loadings (coefficients  $>0.5$  in magnitude) in the rotated component matrix. These landmark coordinates contribute greatly to the facial variation accounted for by each component. The non-highlighted cells within each component (coefficients  $<0.5$  in magnitude) indicate landmark coordinates that have less effect on facial variation (coefficients in the range 0.1–0.49 in magnitude are presented and coefficients  $<0.1$  in magnitude are not shown).

#### Note:

Although there is no gold standard for factor loadings, requiring a loading to be 0.5 is asking that 25% of the variance on the variable be shared with the factor, which is pretty stringent. Some researchers use a cut-off level of 0.4 (16% shared variance), or even 0.3 or 0.35. However, the inclination to use a more stringent criterion (0.5) is usually preferred when the analysis is based on principal components, because the estimated loadings would be higher.

PCs	X-Y-Z	Principal Components													
		1	2	3	4	5	6	7	8	9	10	11	12	13	14
PC1	lsY	-.851		.260							.186				
	cphRY	-.843		.243			.102			.126					
	cphLY	-.841		.240			.107			.137					
	enLY	.834	.138	-.112	.165	-.200	-.155								-.105
	enRY	.829	.160	-.108	.153	-.176	-.180						.106		.116
	pgY	-.822	-.155				-.187								
	chRY	-.816	-.190		-.214										
	chLY	-.814	-.180		-.221			-.100							
	piRY	.810			.154	-.151	-.256							.125	-.121
	piLY	.808			.165	-.170	-.254							-.137	-.104
	psLY	.792					-.278							-.123	.332
	psRY	.783					-.276							-.112	.335
	liY	-.769	-.124		-.386										
	exRY	.759			.189	-.210	-.309							.145	.197
exLY	.748			.194	-.173	-.313							-.184	-.220	
gY	.644	.223			.308	-.130									
nY	.620	.132	-.468		.123								-.192	-.145	
PC2	psLX	.143	.939							-.125					
	psRX	-.139	-.939							-.116					
	piLX	.144	.933							-.135					
	piRX	-.150	-.932							-.127				-.126	
	enRX		-.837			.129				-.168				.219	
	enLX	.102	.830			-.108				-.126				-.225	
	exRX	-.192	-.810											-.391	
	exLX	.184	.768						.123	-.148				.432	
PC3	alLZ	.209		-.798		-.101	-.171	-.130							
	alRZ	.220		-.786			-.152	-.144							
	snZ	.347		-.706	.260	-.144		-.150							
	prnZ	.404		-.690		-.253	-.138	-.204							
	liZ	.295		.562				-.239							
PC4	lsZ	.368			.863						-.163				
	cphRZ	.391			.861	-.112									
	cphLZ	.388			.861	-.117								-.109	
	pgZ	-.151		.271	-.788		-.195	-.321							
PC5	gZ	-.103	.198	.176		-.858									
	nZ	.157	.157	-.163		-.822	.103								
	piRZ	-.374		.352	-.245	.673					.114			.158	
	piLZ	-.376		.349	-.242	.659				.117	.105			.167	
	enLZ	-.469		.244	-.191	.521	.154		.111		.105		.119	.274	
enRZ	-.458		.250	-.185	.485	.167							.321		
PC6	prnY					.120	.821								
	alLY	-.284					.791								
	alRY	-.299					.768		-.108						
	snY	-.226		.184			.722						.162		
PC7	chRX	-.123	-.128								.196				
	chLX	.139	.145								-.205				
	chLZ	.203		.230										-.124	
	chRZ	.195		.225										.145	
PC8	snX								.940						
	prnX								.906						
PC9	gX									.167					
	nX									.974					
PC10	cphRX	-.164						.183						.312	
	cphLX	.147						-.199						.422	
	alLX	.266	.321		.158	-.163		-.219	.266				.188		
	alRX	-.275	-.332		-.162	.158		.219	.265				-.189		
PC11	psLZ	-.275		.207		.101	.219		.109				.805	.109	
	psRZ	-.288		.237		.209	.209		-.116				.784	-.125	
PC12	lsX													.942	
PC13	exLZ	-.307	-.252	.278	-.172	.369			.166	.105				.161	
	exRZ	-.320	-.290	.287	-.186	.368	.109		-.129	-.118				-.146	
PC14	pgX								-.180					-.153	
	liX								-.104					.486	
														.926	
														.775	

The highlighted cells (coefficients >0.5 in magnitude) indicate landmark coordinates that contribute greatly to the facial variation; non-highlighted cells (coefficients <0.5 in magnitude) indicate landmark coordinates that have less effect on facial variation (coefficients in the range 0.1–0.49 in magnitude are presented and coefficients <0.1 in magnitude are not shown).

The 14 principal components explain 82.1% of the total variance in facial form (Table 4.2), with the first 3 components accounting for 45.9% of the total variance (PC1 28.8%, PC2 10.4%, PC3 6.7%). The other principal components account for considerably smaller portions of the total variance (PC4 5.3%, PC5 4.8%, PC6 4.4% etc.). Separate PCAs of the male and female subsamples were also carried out and the results are included in Table 4.2.

<b>Total Sample (N=4747)</b>		<b>Males (N=2233)</b>		<b>Females (N=2514)</b>	
<b>Brief description of principal components</b>	<b>%</b>	<b>PC</b>	<b>%</b>	<b>PC</b>	<b>%</b>
<b>PC1</b> , Face height	28.8	PC1	24.2	PC1	21.9
<b>PC2</b> , Inter-eye distance (face width)	10.4	PC2	11.0	PC2	11.1
<b>PC3</b> , Prominence of the nose	6.7	PC3	7.4	PC3	7.6
<b>PC4</b> , Protrusion of the upper lip relative to the chin	5.3	PC4	5.4	PC4	5.7
<b>PC5</b> , Eyes depth relative to the nasal bridge	4.8	PC6	4.5	PCs 7, 9	4.4 + 3.3
<b>PC6</b> , Vertical height of the nose	4.4	PC5	5.1	PC6	4.4
<b>PC7</b> , Ratio of mouth width to mouth depth	4.0	PC7	4.4	PC5	5.0
<b>PC8</b> , Deviation of the nasal tip and columella base	3.6	PC8	3.8	PC8	3.9
<b>PC9</b> , Horizontal asymmetry of the nasal bridge	3.2	PC10	2.7	PC10	2.9
<b>PC10</b> , Philtrum-to-nose width ratio	2.7	PCs 14,15	1.8 + 1.7	PCs 15, 16	1.7 + 1.6
<b>PC11</b> , Upper eyelids depth	2.4	PC12	2.3	PC13	2.0
<b>PC12</b> , Horizontal asymmetry of the upper lip (philtrum)	2.3	PC11	2.5	PC11	2.7
<b>PC13</b> , Facial flatness (outer canthi depth)	1.9	PC9	3.4	PC14	1.8
<b>PC14</b> , Horizontal asymmetry of the chin and lower lip	1.7	PC13	2.0	PC12	2.4

**% (Percentage of variance explained)**

- The order of principal components (1-14) for the total sample is based on their percentage of variance explained (descending order), PC1 has the highest percentage of variance and PC14 has the least percentage of variance.
- Principal components 14 and 15 (males) describe variation in philtrum and nose width, respectively; principal components 7 and 9 (females) describe variation in depth of lower eyelids (relative to nasal bridge) and inner canthi, respectively; principal components 15 and 16 (females) describe variation in nose and philtrum width, respectively.
- Principal component 6 (total sample), associated with variation of vertical height of nose, coincides with PC5 (males) and PC6 (females).
- Principal component 7 (total sample), associated with variation of the mouth width to mouth depth ratio, coincides with PC7 (males) and PC5 (females).

The first principal component includes two subsets of landmarks grouped around the eyes and mouth (highlighted by red rectangles in Figure 4.5). The first subset represents the y coordinates of 10 upper face landmarks including 8 landmarks around the eyes (3–10) as well as glabella and nasion. The second subset includes the y coordinates of 7 lower face landmarks (15–21). The loadings of the two subsets have opposite signs; which indicates statistical variation in opposite (upward-downward) directions. Therefore, PC1 essentially describes variation in face height.

The second principal component (enclosed in yellow rectangles) consists of the x coordinates of 8 landmarks around the eyes (3–10). Loadings with opposite signs correspond to variation in opposite (outward-inward) directions. Therefore, this component essentially describes variation in inter-eye width.

The third principal component (indicated by green rectangle) represents a single group of the z coordinates of four landmarks associated with the nose (11–14); consequently this component characterises the prominence of the nose.

In the gender-specific PCAs, fifteen principal components were identified for males and sixteen for females. Brief component definitions and variances explained are listed in Table 4.2. The first eight principal components for males and the first four components for females were nearly the same as those of the total sample. Subtle gender differences were noticed in the sequence of some principal components as compared with the total sample; for example, PC14 (related to asymmetry of the chin in the total sample) was positioned as PC13 and PC12 in males and females, respectively.

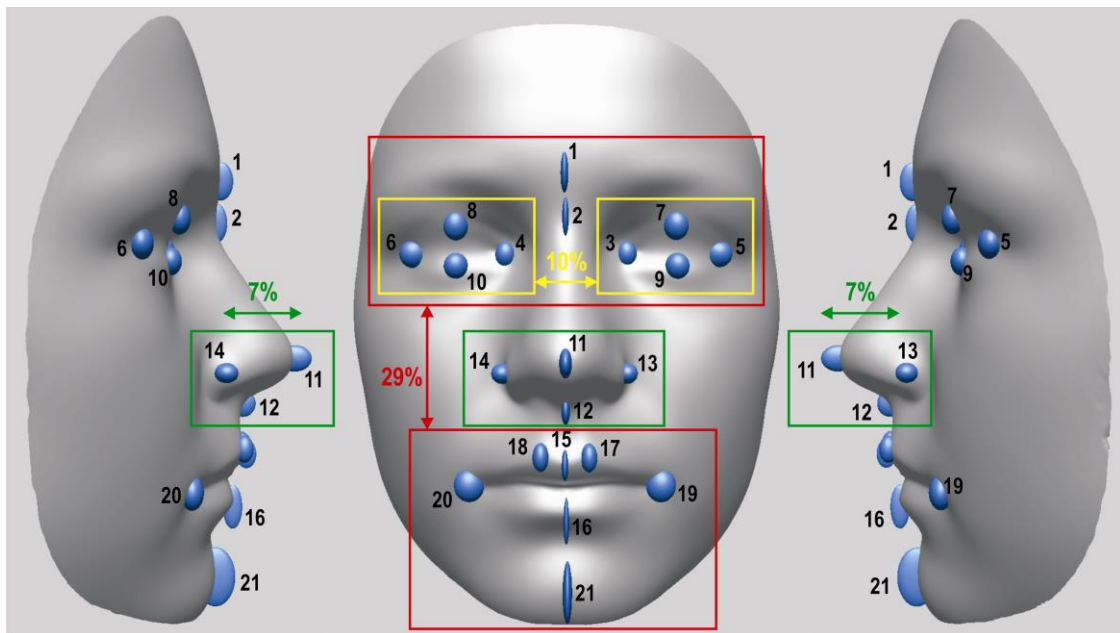


Figure 4.5.

Facial morphology variation revealed by the first 3 principal components extracted from the unscaled dataset of 21 facial landmarks: PC1 (red, explains 29% of total variance), PC2 (yellow, 10%) and PC3 (green, 7%). *Facial Landmarks:* 1, glabella; 2, nasion; 3 and 4, endocanthion (left and right); 5 and 6, exocanthion (left and right); 7 and 8, palpebrale superius (left and right); 9 and 10, palpebrale inferius (left and right); 11, pronasale; 12, subnasale; 13 and 14, alari (left and right); 15, labiale superius; 16, labiale inferius; 17 and 18, crista philtri (left and right); 19 and 20, cheilion (left and right); 21, pogonion.

#### 4.3.1.3 PCA of the scaled dataset:

For the total ALSPAC sample, 17 principal components were identified by PCA (Table 4.3).

The 17 principal components explain 81.6% of the total variance in facial shape (Table 4.4), with the first 3 components accounting for 34.8% of the total variance (PC1 18.3%, PC2 9.3%, PC3 7.2%). The other PCs account for considerably smaller portions of the total variance (PC4 5.7%, PC5 5.4%, PC6 4.7% etc.). Separate PCAs of the male and female subsamples were also carried out and the results are included in Table 4.4.

Table 4.3. Principal component analysis of scaled landmark data – 4747 Individuals

PCs	X-Y-Z	Principal Components																	
		1	2	3	4	5	6	7	8	9	10	11	12	13	14	15	16	17	
PC1	psLX	<b>-906</b>		.109					.155										
	piLX	<b>-894</b>	.125	.113					.154										
	psRX	<b>.890</b>	-.143	-.110		.119			-.162										
	piRX	<b>.888</b>	-.121	-.124		.112			-.153										
	enRX	<b>.812</b>							-.128										
	enLX	<b>-.803</b>						.105	.115	.151	-.135								
	exRX	<b>.697</b>	-.275	-.142	.164	.141			-.159	.355	-.110				-.246				
	exLX	<b>-.648</b>	.276	.134	-.168	-.138			.162	-.388	-.151				.272				
	psLY	<b>.489</b>	.383		.114				-.371	-.139	-.221								
	pgY	<b>-.474</b>		-.119	-.235	.217			-.468	-.311	-.249								
psRY	<b>.464</b>	.410	.106	.130				-.368	-.131	-.216	.104	.270							
liY	<b>-.452</b>	-.105		-.243	-.423			-.226	-.273	-.177									
PC2	enLZ	-.161	<b>.726</b>	.111					.112	.127									
	enRZ	-.104	<b>.716</b>	.116					.125	.141									
	piRZ	-.114	<b>.706</b>	.295	-.107	-.164				.281	-.115								
	piLZ	-.102	<b>.695</b>	.287	-.117	-.169				.289	.120								
	nZ	-.146	<b>-.563</b>			-.143			.159	.119	-.524								
	gZ	-.209	<b>-.562</b>	.258					.111	.116	-.554								
	enLY	.334	<b>-.518</b>		.308				-.151	-.114	.239								
	enRY	.294	<b>-.482</b>		.324				-.192	-.117	.271								
PC3	aiRZ	.136		<b>-.824</b>															
	aiLZ	.118		<b>-.823</b>															
	prnZ	.135	-.284	<b>-.733</b>	-.163				-.121	-.104									
	snZ	.150	-.189	<b>-.700</b>	-.101	.245			-.104										
liZ	.169		<b>.579</b>																
PC4	chRX			-.111	<b>.841</b>														
	chLX			.106	<b>-.837</b>														
	chLZ	.101		.249	<b>.811</b>														
	chRZ			.238	<b>.808</b>														
PC5	cphRZ	.101	-.159																
	cphLZ	.112	-.154																
	lsZ	.121	-.121																
	pgZ	-.137		.280	-.406	<b>-.758</b>													
PC6	aiLY	-.160																	
	prnY		.159																
	aiRY	-.155																	
	snY			.136															
PC7	cphLY	-.269		.110	-.112														
	cphRY	-.266		.153	-.109														
	lsY	-.307	.102		-.121														
PC8	exRZ			.265															
	exLZ			.240															
PC9	snX																		
	prnX																		
PC10	pgX																		
	liX																		
PC11	gX																		
	nX																		
PC12	psLZ			.221				.187											
	psRZ	-.106		.249				.179											
PC13	lsX																		
PC14	gY	.101	.327	.152		-.104	-.203		.265										
	nY	.211		-.473	.147				.211										
	piLY	.349	-.261		.213				.262										
	piRY	.340	-.227		.223				.270										
	exLY	.344	-.141	.142	.104	.138	-.311	-.262											
exRY	.348	-.220	.124	.126	.136	-.303	-.264												
PC15	aiLX	-.110			-.152														
	aiRX	.118			-.153														
PC16	chRY	-.239		-.133	-.265	-.125	-.173												
	chLY	-.253		-.142	-.291	-.133	-.161												
PC17	cphRX				.194														
	cphLX				-.192														

The highlighted cells (coefficients >0.5 in magnitude) indicate landmark coordinates that contribute greatly to the facial variation; non-highlighted cells (coefficients <0.5 in magnitude) indicate landmark coordinates that have less effect on facial variation (coefficients <0.1 in magnitude are not shown).

Table 4.4. Brief description of the principal components extracted for the total sample (scaled dataset) and their corresponding positions in male and female samples					
Total Sample (N=4747)		Males (N=2233)		Females (N=2514)	
Brief description of principal components	%	PC	%	PC	%
PC1, Ratio of inter-eye distance (face width) to face height (chin to eyes)	18.3	PC1	17.4	PC1	17.5
PC2, Ratio of nasion/glabella prominence (relative to eyes) to inner canthi height	9.3	PCs 6, 10	4.9 + 3.4	PCs 7, 10	4.6 + 3.3
PC3, Prominence of the nose relative to the lower lip	7.2	PC2	9.5	PC2	8.8
PC4, Ratio of mouth width to mouth depth	5.7	PC5	5.4	PC4	5.8
PC5, Prominence of the upper lip relative to the chin	5.4	PC4	6.1	PC3	6.8
PC6, Vertical height of the nose	4.7	PC3	6.7	PC5	5.6
PC7, Vertical height of the upper lip	4.6	PC7	4.7	PC8	4.2
PC8, Facial flatness (outer canthi depth)	4.5	PC6	4.9	PC7	4.6
PC9, Deviation of the nasal tip and columella base	3.7	PC8	4.2	PC9	3.8
PC10, Horizontal asymmetry of the chin and lower lip	3.3	PC11	2.7	PC11	2.8
PC11, Horizontal asymmetry of the nasal bridge	2.7	PC12	2.6	PC13	2.2
PC12, Upper eyelids depth	2.6	PC14	2.0	PC14	2.1
PC13, Horizontal asymmetry of the upper lip (philtrum)	2.2	PC13	2.1	PC12	2.7
PC14, Eye-to-nasion/glabella height	2.0	PCs 9, 15	3.8 + 1.9	PCs 6, 15	4.8 + 2.0
PC15, Nose width	1.9	PC16	1.8	PC16	1.8
PC16, Vertical height of the mouth	1.8	PC17	1.8	PC17	1.8
PC17, Philtrum width	1.7	PC18	1.7	PC18	1.7

% (Percentage of variance explained)

The first principal component, extracted from the scaled dataset, includes 3 subsets of landmarks grouped around the eyes and mouth (highlighted by red rectangles in Figure 4.6). The first subset represents the x coordinates of 8 landmarks around the eyes (3–10), loadings with opposite signs for left and right eyes correspond to variation in opposite (outward-inward) directions, which indicates variation in inter-eye width (face width). The second subset includes the y coordinates of 2 upper face landmarks (7, 8). The third subset includes the y coordinates of 2 lower face landmarks (16, 21). Loadings of the second and third subsets have opposite signs; which indicates statistical variation in opposite (upward-downward) directions that describes variation in face height. Therefore, PC1 essentially describes variation in the ratio between face width and face height.

The second principal component (enclosed in yellow rectangles) consists of two subsets of landmarks. The first subset represents the z coordinates of 6 landmarks, 4 of them around the eyes (3, 4, 9, and 10) as well as glabella and nasion. Loadings with opposite signs correspond to variation in opposite (forward-inward) directions, which describes variation of the nasion/glabella prominence relative to the eyes. The second subset represents the y coordinates of 2 landmarks (3, 4). Therefore, this component essentially describes variation in the ratio of nasion/glabella prominence (relative to eyes) to inner canthi height.

The third principal component (indicated by green rectangles) represents a single group of the z coordinates of four landmarks associated with the

nose (11–14), and the z coordinate of the lower lip landmark (16). Loadings with opposite signs correspond to variation in opposite (forward-inward) directions, which describes variation in the prominence of the nose relative to the lower lip.

In the gender-specific PCAs, 18 principal components were identified for males and females. Brief component definitions and variances explained are listed in Table 4.4. The first principal component (ratio of face width to face height) and the last three components (nose width, vertical height of the mouth, and philtrum width) were the same for all groups (total, males and females). Gender differences were noticed in the sequence of several principal components as compared with the total sample; however, PCs 1, 2, 10, 11, 14, 15, 16, 17, and 18 were similar in males and females.

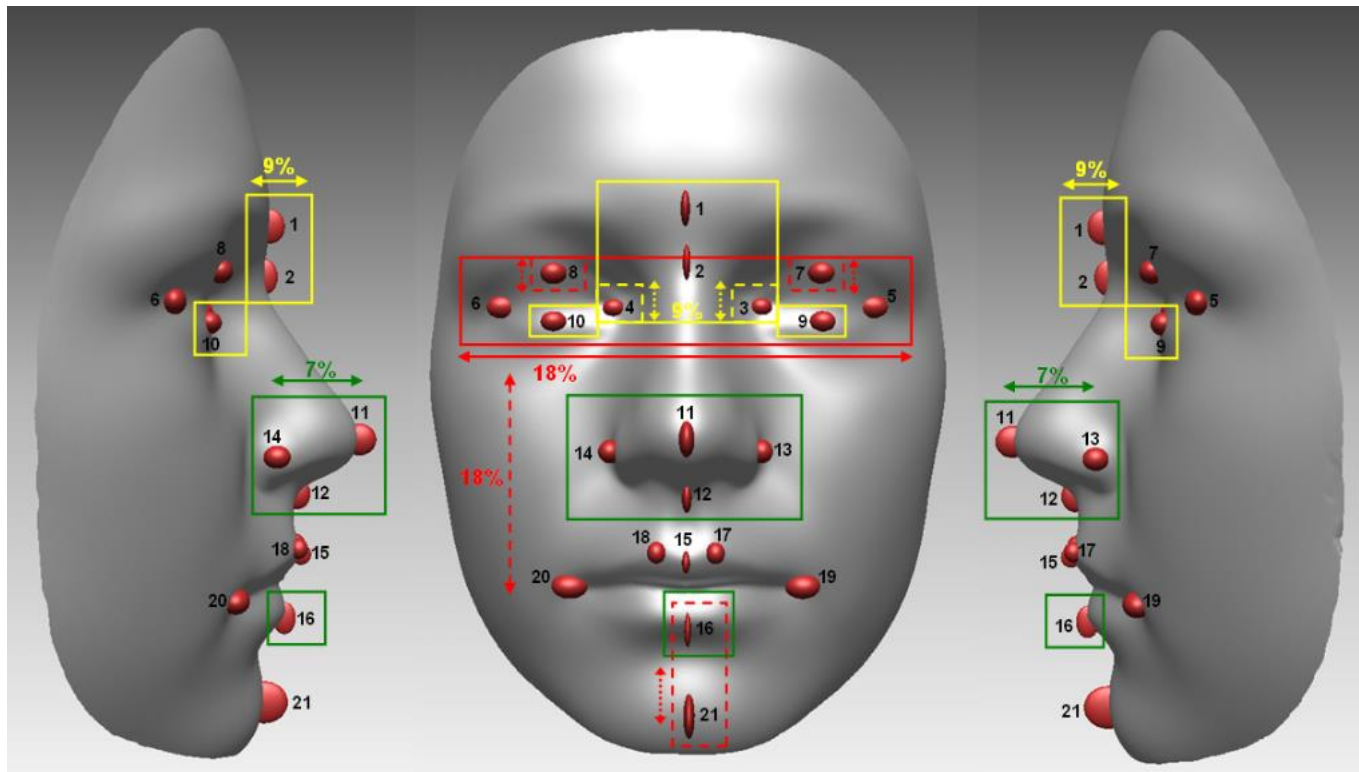


Figure 4.6.

Facial morphology variation revealed by the first 3 principal components extracted from the scaled dataset of 21 facial landmarks: PC1 (red, explains 18% of total variance), PC2 (yellow, 9%) and PC3 (green, 7%).

*Facial Landmarks:* 1, glabella; 2, nasion; 3 and 4, endocanthion (left and right); 5 and 6, exocanthion (left and right); 7 and 8, palpebrale superius (left and right); 9 and 10, palpebrale inferius (left and right); 11, pronasale; 12, subnasale; 13 and 14, alari (left and right); 15, labiale superius; 16, labiale inferius; 17 and 18, crista philtri (left and right); 19 and 20, cheilion (left and right); 21, pogonion.

### **4.3.2 Normal ranges (scales) of facial variation**

Tables 4.5 and 4.6 list the normal ranges (scales) of facial variation based on parameters derived from principal components—unscaled and scaled, respectively. In addition, the average and standard deviation of each derived parameter for each principal component was also obtained for the male, female, and total samples.

The first three principal components extracted from the unscaled dataset (Figure 4.5) explained the majority (46%) of facial variation in the sample. Three parameters (P1, P2 and P3) characterising the first three principal components were defined and calculated as follows:

- P1: vertical distance between the centroids of the upper and lower sets of landmarks (1 to 10 and 15 to 21), highlighted in Figure 4.5;
- P2: horizontal distance between the centroids of the left and right sets of landmarks associated with the eyes;
- P3: z coordinate of the centroid of the landmarks associated with the nose (11 to 14).

The above derived parameters are shown here as examples; the same principle was applied to all extracted components.

Principal Components (unscaled)	Total Sample (N=4747)			Males (N=2233)			Females (N=2514)		
	Range	Ave	SD	Range	Ave	SD	Range	Ave	SD
<b>PC1</b> , Face Height	59.802 - 91.571	74.100	4.067	62.972 - 91.571	76.300	3.744	59.802 - 83.006	72.146	3.267
<b>PC2</b> , Inter-Eyes Distance (Face Width)	50.496 - 72.867	61.463	3.175	53.516 - 72.867	62.147	3.198	50.496 - 72.797	60.857	3.030
<b>PC3</b> , Prominence of the nose	-5.769 - 17.308	6.132	2.442	-5.769 - 14.861	6.790	2.488	-3.814 - 17.308	5.548	2.244
<b>PC4</b> , Protrusion of the upper lip relative to the chin	-5.630 - 23.952	8.402	3.873	-3.297 - 23.952	9.727	3.830	-5.630 - 18.883	7.225	3.514
<b>PC5</b> , Eyes depth relative to the nasal bridge	6.065 - 23.702	14.337	2.459	6.065 - 23.702	15.707	2.224	6.109 - 19.689	13.119	1.967
<b>PC6</b> , Vertical height of the nose	-14.894 - -2.2	-8.482	1.443	-14.894 - -2.2	-8.612	1.535	-13.546 - -3.703	-8.367	1.345
<b>PC7</b> , Ratio of mouth width to mouth depth	-0.177 - 0.38	0.132	0.065	-0.177 - 0.323	0.113	0.064	-0.104 - 0.380	0.148	0.062
<b>PC8</b> , Deviation of the nasal tip and columella base	-3.492 - 3.78	0.002	0.686	-3.374 - 3.78	-0.012	0.734	-3.492 - 2.584	0.014	0.640
<b>PC9</b> , Horizontal asymmetry of the nasal bridge	-2.370 - 1.89	-0.179	0.522	-2.365 - 1.57	-0.197	0.537	-2.370 - 1.890	-0.163	0.508
<b>PC10</b> , Philtrum-to-nose width ratio	1.504 - 8.696	2.669	0.403	1.504 - 8.696	2.633	0.419	1.641 - 5.087	2.701	0.385
<b>PC11</b> , Upper eyelids depth	1.269 - 19.97	10.456	2.426	1.269 - 19.97	11.130	2.472	1.848 - 17.448	9.858	2.219
<b>PC12</b> , Horizontal asymmetry of the upper lip (philtrum)	-2.303 - 2.514	-0.167	0.465	-2.303 - 2.039	-0.175	0.470	-2.278 - 2.514	-0.161	0.460
<b>PC13</b> , Facial flatness (outer canthi depth)	-0.010 - 0.133	0.059	0.018	0.000 - 0.108	0.056	0.017	-0.010 - 0.133	0.061	0.018
<b>PC14</b> , Horizontal asymmetry of the chin and lower lip	-2.462 - 3.253	0.338	0.492	-2.462 - 2.405	0.361	0.498	-1.822 - 3.253	0.317	0.486

**Ave: Average value of parameter; SD: Standard deviation**

<b>Table 4.6. Normal ranges (scales) of facial variation derived from scaled principal components</b>									
<b>Principal Components (scaled)</b>	<b>Total Sample (N=4747)</b>			<b>Males (N=2233)</b>			<b>Females (N=2514)</b>		
	<b>Range</b>	<b>Ave</b>	<b>SD</b>	<b>Range</b>	<b>Ave</b>	<b>SD</b>	<b>Range</b>	<b>Ave</b>	<b>SD</b>
<b>PC1</b> , Ratio of inter-eye distance (face width) to face height (chin to eyes)	1.191 - 1.890	1.470	0.094	1.195 - 1.890	1.492	0.097	1.191 - 1.780	1.451	0.087
<b>PC2</b> , Ratio of nasion/glabella prominence (relative to eyes) to inner canthi height	0.072 - 1.496	0.568	0.172	0.072 - 1.371	0.479	0.131	0.219 - 1.496	0.646	0.166
<b>PC3</b> , Prominence of the nose relative to the lower lip	7.759 - 19.666	13.985	1.465	9.008 - 19.666	14.380	1.468	7.759 - 18.817	13.635	1.370
<b>PC4</b> , Ratio of mouth width to mouth depth	-0.177 - 0.380	0.132	0.065	-0.177 - 0.323	0.113	0.064	-0.104 - 0.380	0.148	0.062
<b>PC5</b> , Prominence of the upper lip relative to the chin	-5.833 - 21.658	8.363	3.745	-3.26 - 21.658	9.472	3.656	-5.833 - 19.688	7.378	3.543
<b>PC6</b> , Vertical height of the nose	48.332 - 73.810	58.513	3.191	48.719 - 73.81	58.900	3.332	48.332 - 68.647	58.169	3.020
<b>PC7</b> , Vertical height of the upper lip	26.231 - 47.997	36.476	2.901	26.23 - 47.539	36.499	3.062	28.275 - 47.997	36.456	2.751
<b>PC8</b> , Facial flatness (outer canthi depth)	11.800 - 29.756	20.503	2.403	11.80 - 29.563	21.080	2.403	12.198 - 29.756	19.990	2.285
<b>PC9</b> , Deviation of the nasal tip and columella base	-3.569 - 3.595	0.003	0.685	-3.266 - 3.595	-0.010	0.715	-3.569 - 2.516	0.015	0.656
<b>PC10</b> , Horizontal asymmetry of the chin and lower lip	-2.503 - 3.223	0.338	0.492	-2.503 - 2.256	0.352	0.486	-1.906 - 3.223	0.325	0.497
<b>PC11</b> Horizontal asymmetry of the nasal bridge	-2.473 - 1.917	-0.179	0.523	-2.473 - 1.561	-0.192	0.525	-2.409 - 1.917	-0.168	0.521
<b>PC12</b> , Upper eyelids depth	1.466 - 19.182	11.071	2.247	1.466 - 19.173	11.462	2.268	2.694 - 19.182	10.723	2.170
<b>PC13</b> , Horizontal asymmetry of the upper lip (philtrum)	-2.383 - 2.592	-0.168	0.466	-2.383 - 1.882	-0.171	0.460	-2.207 - 2.592	-0.165	0.471
<b>PC14</b> , Eye-to-nasion/glabella height	9.118 - 24.862	16.713	2.132	9.118 - 23.529	16.157	2.126	10.795 - 24.862	17.207	2.013
<b>PC15</b> , Nose width	25.639 - 44.327	33.651	2.381	25.64 - 44.327	34.139	2.389	25.999 - 42.110	33.217	2.288
<b>PC17</b> , Philtrum width	4.317 - 22.452	12.849	1.861	4.317 - 22.452	13.225	1.908	7.073 - 19.634	12.514	1.752

**Ave: Average value of parameter; SD: Standard deviation**

## 4.4 Discussion

### 4.4.1 Summary:

The human face is a highly complex geometric surface. The simple inter-landmark distances used in previous 2D studies may have over-simplified the common variation of human faces. As the high throughput acquisition of high content 3D image data becomes easier, methods based on shape geometric information, especially of high definition, become increasingly necessary to enable comprehensive and fully quantitative analyses of the complex facial features.

The present study assessed normal variation of facial morphology in a large population of 15-year-old Caucasian adolescents. The results can be considered specific to this particular population, and the methodology used in this study can form the basis to analyse and compare facial morphology of other population groups.

In this study, 14 and 17 principal components were extracted from the unscaled and scaled datasets, respectively, describing the majority (82%) of facial soft tissue variation, with the first three PCs (unscaled) accounting for 46% of the total variance in facial form (size + shape), and the first three PCs (scaled) accounting for 35% of the total variance in facial shape only. The sample was registered using Procrustes analysis; with this technique the 3D coordinates of the landmarks were placed in the same space reducing confounding errors (rotation and translation).

#### 4.4.2 Comparison with previous studies:

There have been a number of studies using principal component analysis on either lateral skull radiographs or photographs. One of these studies assessed craniofacial form in 622 individuals and identified 6 principal components that explained 68 percent of the variation. The study did not use Procrustes analysis to register the landmarks and arguably resulted in a rather complex array of facial parameters forming each principal component (Cleall *et al.*, 1979). However, the first and third principal components were broadly similar to the findings in the present study, the first representing face height and the third convexity (mid-face and dental protrusion). The second component related to antero-posterior aspects of facial morphology which is recorded in PC4 in the present study.

Photographs were used to identify 6 components explaining 86.5 percent of the variance (Krey and Dannhauer, 2008). The first principal component (33.9%) described scaling along an axis from Porion to the chin (a combination of vertical and horizontal vectors); the second component (28.6%) characterized the vertical dimension of the lower face.

The soft tissue profile of 170 patients aged 7 to 17 years were assessed (Halazonetis, 2007). The first 8 principal components explained 90% of the total shape variability. The first component (36%) related to lip, nose, and chin prominence, the second component (18%) related to facial convexity, and the next 2 components mainly related to lower lip shape. The overall shape differences between average profiles of boys and girls were minor.

There were some similarities and differences identified when making a comparison with previous studies. The present study was undertaken on a large population of the same age, whereas previous studies included subjects ranging from 7 years of age to adulthood. In addition, previous studies used 2D records, whereas the 3D data utilised in this study should eliminate projection problems commonly found in radiographs and photographs (Houston *et al*, 1986; Benson and Richmond, 1997).

The chin prominence feature reported by Halazonetis (2007) and Krey and Dannhauer (2008) would be reported as a positive change in the z axis for the upper lip landmarks relative to the chin in PC4 of the current study, although this component only explains 5.3% of the total variance.

The study by Weinberg *et al.* (2013) used a 3D stereophotogrammetric imaging technique and geometric morphometric analysis of 13 surface landmarks in order to identify the heritability of face shape in 21 pairs of Caucasian twins (10 monozygotic, 11 dizygotic) aged between 5 and 12 years. This study identified a total of 17 PCs with the first 9 PCs accounted for approximately 90% of the total shape variance. Three of the derived shape PCs displayed evidence of moderate to high heritability (PC4, PC5, and PC7). PC4 was associated with a complex suite of shape variations including variation in the lateral position of the left and right endocanthion points, variation in nasal breadth, height, and projection, and variation in the width of the philtrum and vertical height of the upper lip. PC5 was associated mainly with the vertical and anterior-posterior position of nasion,

the anterior-posterior position of the orbits, and the breadth of the nasal floor and philtrum. PC7 was related to the vertical position of landmarks defining the inter-orbital septum and variation in the nasolabial angle. The first few PCs, accounting for the majority of shape variation in the sample, did not demonstrate strong evidence of heritability. Instead, shape variation along these PCs was related more to sex and age/maturity related factors.

#### **4.4.3 PCA (unscaled dataset):**

In this study, as the 3D coordinate data was registered in a common space using Procrustes analysis, the extracted principal components should be more valid based on the relative importance of independent landmark coordinates in space. The fourteen principal components derived in the current study reflect the complexity of facial morphology. The first three components describe face height, width and convexity, while the other 11 components contribute to subtle changes in the face that makes the face unique via describing the variation of its complex geometry.

The first principal component (face height) explained 29 per cent of the total variance in facial form and this evidence gives support to previous facial classifications as long/thin and short/wide face types (Schendel *et al.*, 1976; Opdebeeck and Bell, 1978; Opdebeeck *et al.*, 1978; Farkas, 1994). In this study, the average distance between the upper and lower facial centroids (parameter P1, Table 4.5) was 74.1 mm (ranging from 59.8 to 91.6 mm), with the nasion to pogonion distance being 101.7 mm (ranging from 82.8 to 127.6 mm), and male faces were on average 6 mm longer than female

faces (n-pg distance: Table 3.3, Table 3/Appendix). This distance is slightly less than 8 mm reported for 50 fifteen-year-old Caucasians assessed by Farkas (1994) and higher than 1.8 mm for approximately 40 norms, 8 to 12-year-old, studied by Bugaighis *et al.* (2013). In addition, previous clinical studies of long and short face types also reported limited samples which reflect face height differences equivalent to two standard deviations from the mean (Schendel *et al.*, 1976; Opdebeeck and Bell, 1978).

For PC2, the average distance between the left and right centroids of the landmarks associated with the left and right eyes (parameter P2) was 61.5 mm (range 50.5 – 73 mm) with the average distance between the inner canthi of the eyes being 34.2 mm (range 24.0 – 46.5 mm). The intercanthal distance (enL-enR: Table 3/Appendix) was on average 1.2 mm larger in males compared to females. Similar findings were reported in smaller samples (Laestadius *et al.*, 1969; Farkas, 1994; Bugaighis *et al.*, 2013).

Many syndromes exhibit an inter-eye distance whose deviation from the mean may even exceed 2SD (Cohen *et al.*, 1995; Farkas *et al.*, 1989; Feingold and Bossert, 1974; Miamoto *et al.*, 2011). Hypertelorism can be seen in 1q21.1 duplication syndrome, Apert syndrome, Basal Cell Nevus syndrome, Crouzon syndrome, DiGeorge syndrome, Noonan syndrome, and LEOPARD syndrome (Kreiborg and Cohen, 2010; Randolph *et al.*, 2011; Mann, 1957); hypotelorism can be seen in trigonocephalic patients (Nagasao *et al.*, 2011) and in Schilbach-Rott syndrome (Joss *et al.*, 2002).

For PC3, the prominence of the nose centroid (parameter P3) was on average 6.1 mm (ranging from -5.8 to 17.3 mm). The nasal tip protrusion (sn-prn: Table 3/Appendix) was on average slightly less in females (19.4 mm) compared to males (20.1 mm). Similar findings were reported elsewhere (Zankl *et al.*, 2002; Farkas, 1994).

The parameters P1, P2 and P3 associated with the first three principal components can be used to characterise the face as a three-dimensional statistical continuum, where each coordinate corresponds to the standard deviation from the mean value of the respective parameter. For example, a face with coordinates (-1.38, -0.15, 1.97) indicates the deviation from the mean values of P1, P2 and P3 by -1.38, -0.15 and 1.97 SD, respectively. For quick characterisation, the fractional values of the coordinates can be rounded to the nearest integer, so that the above face can be represented as (-1, 0, 2), which indicates that the face is slightly shorter than normal, has a normal width and a quite protruded nose. In a similar way, more coordinates can be used which are associated with more principal components, allowing one to characterise the face as a multidimensional statistical continuum. A method for visualizing this 3D face continuum will be described in Chapter 5.

Although male faces size is generally larger than female faces size (Ferrario *et al.*, 1998a, b, 1999a), the principal component analysis for males and females show similar relative importance of facial parameters which will be useful in facial classification.

In this study, fifteen PCs were identified for males and sixteen for females. The first eight principal components for males and the first four components for females were nearly the same as those of the total sample. However, slight sex differences were observed in the sequence of some PCs (e.g., PCs 11, 13, and 14) as compared with the total sample, suggesting different levels of significance of the variation exhibited by different facial features for males and females.

Facial asymmetry was suggested to arise from random variation or genetic and environmental influences (Waddington, 1957). The present study showed that minor facial asymmetry is relatively common in both sexes with similar patterns (PC8, nasal tip/columella base; PC9, nasal bridge; PC12, upper lip/philtrum; PC14, lower lip/chin). A mild degree of facial asymmetry has been reported elsewhere (Lu, 1965; Vig and Hewitt, 1975; Shah and Joshi, 1978; Alavi *et al.*, 1988; Peck *et al.*, 1991; Pirttiniemi, 1992; Ferrario *et al.*, 1993). Differences in facial asymmetry have been reported between the sexes; however, most of these studies have been undertaken on relatively small samples (Ercan *et al.*, 2008; Smith, 2000; Hardie *et al.*, 2005, Farkas and Cheung, 1981; Severt and Proffit, 1997; Shaner *et al.*, 2000; Ferrario *et al.*, 1994a, 2001; Haraguchi *et al.*, 2002).

In this study, the chin point (pogonion) deviated between -5.6 mm and 5.2 mm from the sagittal plane; nasal tip (pronasale), -4.7 mm and 4.9 mm compared to the columella base (subnasale), -3.1 mm and 2.6 mm; glabella, -2.9 mm to 2.0 mm; nasion, -2.2 mm to 1.9 mm; upper lip (labiale superius), -2.3 mm and 2.5 mm; lower lip (labiale inferius), -1.5 mm to 2.8 mm.

In previous studies, the degree of asymmetry was attributed to discernible imbalances in the development of skeletal, dental and soft tissues (Williamson and Simmons, 1979; Alavi *et al.*, 1988; Schmid *et al.*, 1991; Pirttiniemi *et al.*, 1990; Pirttiniemi, 1992). Unfortunately, the methods employed in these studies describe details of local imbalances of certain facial features with less emphasis on systematic assessment of facial asymmetry.

#### 4.4.4 PCA (scaled dataset):

With respect to the scaled data analyses, it was obvious that scaling has removed size variation within the sample. Therefore, a few first components (PCs 1, 2, and 4) can essentially be characterised as ratios of different measurements.

PC1 (responsible for 18% of the shape variance) explained facial variation as the ratio of inter-eye distance (face width) to face height (chin to eyes). PC2 (responsible for 9% of the variance) explained facial variation as the ratio of nasion/glabella prominence (relative to eyes) to inner canthi height. PC4 (responsible for 6% of the variance) explained facial variation as the ratio of mouth width to mouth depth (prominence). PC3 (responsible for 7% of the variance) explained facial variation as the prominence of the nose relative to the lower lip (the same as PC3, unscaled dataset).

Eighteen principal components were identified for males and females. The first principal component (ratio of face width to face height) and the last three components (nose width, vertical height of the mouth, and philtrum width) were the same for all groups (total, males and females). Again gender

differences were observed in the positions of several PCs as compared with the total sample; however, PCs 1, 2, 10, 11, 14, 15, 16, 17, and 18 were practically the same in males and females.

#### **4.4.5 Impacts of the study:**

In this study, the amounts of reproducibility error in placing various soft tissue landmarks on the face (Tables 3.4, 3.5 and 3.6) were reasonably much smaller than the true facial variation observed within the sample as shown in Figures (4.2, 4.3, and 4.4), which justifies that the accuracy of different landmarks' placement is sufficient enough to study the variations across different faces using the 3D landmark data.

In this study, the principal component analysis of the 21 facial landmarks (63 x, y, and z coordinates) identified 14 PCs explaining 82% of the total variance in facial form, which is considered reasonable as compared to a study reported by Hammond and Suttie (2012) who found that 50–100 modes (PCs) are required to cover 99% of shape variation in a set of faces using all face points of a 3D image (20,000-50,000 points). This suggests that as few as 21 landmarks or so defining main facial features can be considered good enough to explain the majority of facial variation within the sample. Furthermore, in this study, parameters were derived based on the principal components. Each parameter represents the facial variation identified by each component. These parameters were used to divide the sample into appropriate statistical groups to carry out facial averaging where all face points were used to visualize facial variation (this will be explained in Chapter 5).

The current study provides a comprehensive range of soft tissue facial parameters for a large population of 15-year-old adolescents. The levels of deviation from the mean for the various parameters provide a basis for future assessment of subjects using craniofacial landmarks. Moreover, facial height and width have been reported to show strong genetic components (Savoye *et al.*, 1998; Baydas *et al.*, 2007). The current dataset was used to investigate genotype/phenotype associations via a genome-wide association study; this will be discussed in Chapters (7, 8).

However, there are many projects underway around the world such as the FaceBase Consortium (Hochheiser *et al.*, 2011) collecting both 3D facial images and genetic data with the intention to undertake genome-wide association studies. It is important that the face data collected is standardised with matching age groups to allow analyses within and across population groups.

#### 4.5 Conclusions

- 14 PCs were identified for the total ALSPAC sample of 4747 subjects (unscaled dataset), which explained 82% of the total variance in facial form, with the first three components accounting for 46% of the variance and describing face height, width and convexity.
- 15 PCs were identified for males and 16 for females (unscaled dataset). The results generally showed that males and females had similar modes or patterns of facial variation, suggesting that the major components of facial variation do not differ between the genders. However, different PCs positions between males and females indicate different levels of significance

of the variation exhibited by different facial features for males and females, though both genders present the same components of facial variation. In addition, size variation between genders was obvious for most derived facial parameters specially face height.

- 17 PCs were identified for the total ALSPAC sample of 4747 subjects (scaled dataset), which explained 82% of the total variance in facial shape, with the first three components accounting for 35% of the variance. Ratios explained most of the shape variance revealed by the first few components (PCs 1, 2, and 4). 18 PCs were identified for males and females, separately.
- PC3 was the same for both unscaled and scaled datasets, explaining variation in nose prominence/face convexity (7% of the total variance).
- The variation in facial form and shape can be accurately quantified and described as a multidimensional statistical continuum.
- This method of facial assessment may be useful to identify and classify faces and facial changes that occur as a result of growth and inform clinicians of appropriate healthcare interventions for specific facial types.

## Chapter 5

# Exploring The Methods To Visualize Facial Variation

## Exploring The Methods To Visualize Facial Variation

### 5.1 Introduction

In orthodontics, a gender, age and ethnicity specific facial average, also known as facial norm, is an essential visualizing tool for the diagnosis and treatment planning of any orthodontic case involving dentofacial deformities. Such facial averages help estimate the changes required by the orthodontic and/or surgical treatment procedures. Traditionally, these facial averages are developed based on clinical photographs or a set of radiographs 'lateral cephalograms and panoramic views' (Kau *et al.*, 2011). However, these methods are confined to the 2D representation of patients' 3D facial structures; hence they lose important information and are prone to clinical inaccuracy (Caloss *et al.*, 2007). Advancement in modern 3D imaging technology would enable the construction of accurate 3D facial averages that could be used in the assessment of facial variation.

Facial averaging is an important component of research, which has found a number of applications in different disciplines including:

- psychology, for the purposes of analysing facial attractiveness (Langlois and Roggman, 1990; Langlois *et al.*, 1994; Rhodes *et al.*, 1999) and evaluating facial characteristics and their association with anti-social behaviour and psychosis (Farrell, 2011);
- biometrics for face recognition purposes (Gnanaprakasam *et al.*, 2010; Zhao *et al.*, 2008);

- orthodontics and other craniofacial applications to study various facial anomalies (e.g., oral clefts) in comparison to normal facial morphology (Bugajhis *et al.*, 2012; Djordjevic *et al.*, 2012), and variation in facial soft tissues associated with different orthodontic malocclusions (e.g., Class III malocclusion) as compared to normal individuals (Bozic *et al.*, 2010; Krneta *et al.*, 2012);
- evaluating average facial growth in a cohort of subjects (Nute and Moss, 2000; Kau and Richmond, 2008);
- comparing facial morphology for different ages (Moss, 2006), gender (Toma *et al.*, 2008; Bugajhis *et al.*, 2013), and ethnicity (Bozic *et al.*, 2009; Kau *et al.*, 2010); and
- studying the effects on facial morphology caused by various medical disorders, such as asthma (Al Ali *et al.*, 2012) and atopy (Al Ali *et al.*, 2013), and syndromes, such as Noonan syndrome (Hammond *et al.*, 2004) and Binder syndrome (Kau *et al.*, 2007).

Generally, the methods that have been used recently to visualize facial variation in three dimensions can be classified into three basic approaches: the first approach is based purely on facial landmarks and is used to visualize variation in certain locations of the face that have been marked with facial landmarks (e.g., forehead, eyes, nose, lips, and chin). An example for this technique is the use of ellipsoids as described earlier in Chapter 4. The second and third approaches are based on extracting information from the whole face in order to construct the average face which is considered an excellent tool

to visualise facial phenotypes of homogeneous groups. These two approaches are defined as: landmark-based and surface-based.

With the landmark-based approach, a set of landmark points is selected on each image, the sets of landmarks are appropriately aligned together, and the three-dimensional coordinates (x, y and z) of the respective landmarks are averaged across all images. This averaged landmark configuration is then used as a template onto which each image is warped. A texture image can be produced by averaging the grey-scale or colour values. This way of representing a three-dimensional object may hold problems of altered facial parameters due to warping. Since the face is reduced to a smaller number of data points, facial topography cannot be fully evaluated (Souccar and Kau, 2012).

With the surface-based approach, the facial average may represent the average of the z (depth) coordinates of all pixels of the facial images instead of a limited number of landmark points (Kau *et al.*, 2006) or may be constructed using more sophisticated algorithms (Zhurov *et al.*, 2010). The facial images are first pre-aligned (standardized) to be in an upright position with a common origin of coordinates and then are finely aligned using a best-fit algorithm. The averaging procedure produces a dense point cloud, which is then triangulated to obtain the 3D average face.

Different techniques have been utilized to analyse the variation in facial morphology. The traditional methods include measuring linear distances, angles, areas and volumes. Recently, more advanced methods have been

developed to identify the change in facial form and shape using geometric morphometrics, which is based on the analysis of facial landmarks. In general, a morphometric study aims to describe a biological shape in the simplest possible way, removing extraneous information and facilitating comparison between different objects. With this technique, the whole set of data describing the shape of an object is essentially replaced by a relatively small number of landmarks, which are further analysed by statistical methods such as principal component analysis and others.

Although very powerful, the techniques of morphometrics have some deficiencies. Most notably, nearly all quantitative data defining the shape is discarded and just a small number of points are retained. For example, facial scans obtained with Konica Minolta 900/910 laser cameras or 3dMD optical scanning devices are represented by approximately 50,000 data points, whereas only 20 to 40 landmarks are typically used to describe a face. It is clear that most information about the shape is not fully represented. Therefore, to have a more comprehensive assessment and visualization of facial morphology variation, using average faces is more beneficial.

Different techniques have been introduced to average three-dimensional facial images to take into account all facial information available. Landmarks and methods of morphometrics can also be used in some of the stages to enhance the accuracy of the average faces produced. This chapter will discuss one of the averaging methods used to visualize facial variation.

The aim of this study is to visualize facial morphology variation revealed by the principal components (explained earlier in Chapter 4) using a novel, surface-based method of facial averaging.

## **5.2 Subjects and methods**

### **5.2.1 Sample**

The final ALSPAC sample of 4747 British adolescents (2514 females and 2233 males) was used for this study.

### **5.2.2 Visualizing facial variation**

In order to visualize facial morphology variation revealed by the principal component analysis of the 3D landmark data, a parameter characterizing each principal component was derived as described earlier in Chapter 4. The unscaled PCs 1-3 (Figure 4.5) are presented in this chapter as these components explained almost half (46%) of the variation within the sample. The same principle can be applied to all other PCs (unscaled and scaled). The three parameters (P1, P2 and P3) characterizing the first three unscaled PCs explained variation in facial height (PC1, 29%), inter-eye distance (PC2, 10%), and nose prominence (PC3, 7%). All faces were split into seven groups in each of the parameters (for each PC) corresponding to -3 through +3 standard deviations from the mean value. The resulting 21 groups were then averaged using an in-house developed algorithm (Zhurov *et al.*, 2010) implemented as a Rapidform® macro.

The following pages illustrate the averaging method used in this study.

### 5.2.2.1 Averaging facial images scaled based on the average centroid size:

The steps required to produce an average face are described below:

#### 1) Spatial registration of the facial shells.

The faces are first landmarked. Prior to averaging, the facial shells need to be fitted into a common frame of reference. This is achieved through the removal of translation, rotation and size differences by scaling the shells to the average centroid size (calculated from the landmark representation, as described in Chapter 4). The faces are all aligned so that their mid-endocanthion points coincide as well as their sagittal, coronal, and transverse planes, as shown in Figure 5.1 (see section 3.2.5 “Identifying facial soft tissue landmarks” in Chapter 3 for more details).

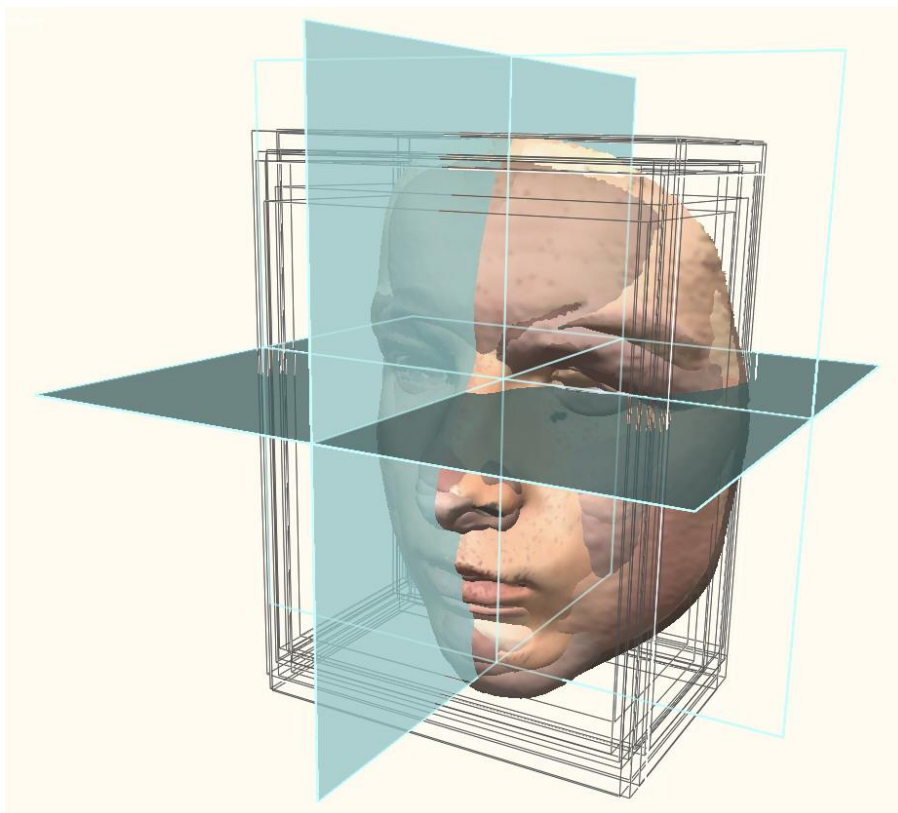


Figure 5.1. Registration of the facial shells in the three planes of space (15 randomly selected faces were aligned on mid-endocanthion point)

2) Averaging in spherical radial direction (first step of averaging).

This method uses spherical coordinates  $R, \varphi, \psi$  and the averaging is performed in the radial coordinate  $R$ . The origin of the spherical coordinate system is taken to be the average centre of the spheres that fit all facial data points and are constructed for each face. The main formulas of the method are the following:

$$R_{ij}^{\text{ave}} = \frac{R_{ij}^1 + \dots + R_{ij}^K}{K}, \quad R_{ij}^k = h_k(\varphi_i, \psi_j),$$

$$X = R \cos \varphi \sin \psi + S_X, \quad Y = R \sin \varphi \sin \psi + S_Y, \quad Z = R \cos \psi + S_Z,$$

with  $(S_X, S_Y, S_Z)$  being the coordinates of the centre of the average sphere. The average face is defined by the point cloud (Figure 5.2), a set of unconnected points, whose  $X$ ,  $Y$  and  $Z$  coordinates are expressed as:

$$\{R_{ij}^{\text{ave}} \cos \varphi_i \sin \psi_j + S_X, R_{ij}^{\text{ave}} \sin \varphi_i \sin \psi_j + S_Y, R_{ij}^{\text{ave}} \cos \psi_i + S_Z\}$$

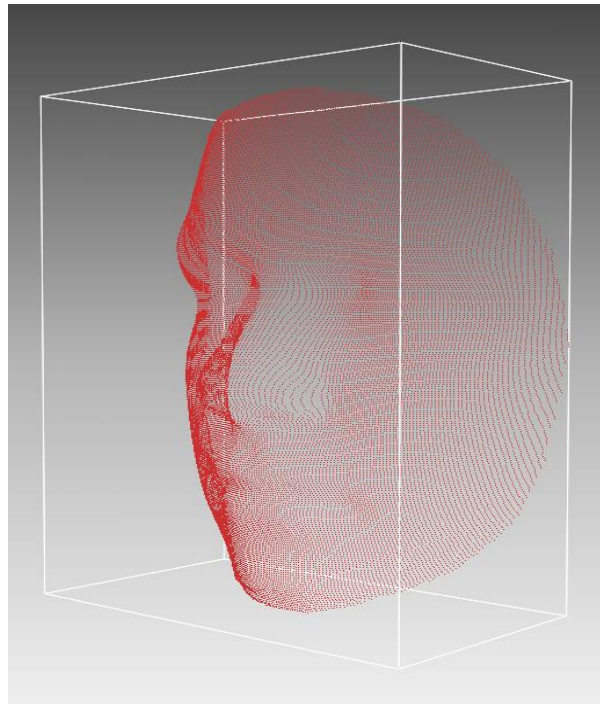


Figure 5.2. Point cloud generated by the averaging procedure

**3) Averaging using a template (second step of averaging).**

Suppose there is a surface, which we call a template, defined by a discrete set of points  $\{\mathbf{R}_i\}$  with coordinates  $\mathbf{R}_i = (X_i, Y_i, Z_i)$ . Let  $\mathbf{N}_i$  denote a unit vector perpendicular (normal) to the surface at the point  $\mathbf{R}_i$  and let  $d_i^k$  denote the signed distance from  $\mathbf{R}_i$  to facial shell  $k$  along the vector  $\mathbf{N}_i$ ; the distance  $d_i^k$  is assumed positive if shell  $k$  is outside the template (at the point where the distance is measured) and negative otherwise. This surface can be used to compute an average face according to the formula:

$$\mathbf{R}_i^{\text{ave}} = \mathbf{R}_i + \frac{d_i^1 + \dots + d_i^K}{K} \mathbf{N}_i$$

The highest accuracy is achieved if the line along which the averaging is performed meets the facial shell at the right angle. A straight single line cannot meet all the shells (that need to be averaged) at the right angles, but we can try to provide that all these angles are close to the right angle “on average”; in this case, our target will be reached and the accuracy of averaging will be the highest. The ideal candidate for a template possessing this property would be the average face. This vicious circle leads us to the idea of organising the following iterative procedure. In the first step, we calculate an average shell (e.g., by averaging in the radial direction; see Step 2) and then use this shell as the template and calculate another average, which can further be used as the template for the next step, and so on. This procedure can be continued until the desired accuracy is attained, that is, when the average shell obtained in the current step becomes practically indistinguishable from that obtained in the previous step.

#### 4) Triangulation.

The final point cloud is then triangulated to create an average shell; this means that the points are organized in the form of triangles to create the average 3D facial shell (Figure 5.3). The average face may need further improvement by filling in small holes and removing possible mesh defects. The main distinction of the above algorithm from that described in Zhurov *et al.* (2010) is that all faces are first scaled to the average centroid size, calculated from their landmark representations. This improvement allows us to achieve sharper average images, with greater details around the eyes, nose and lips.

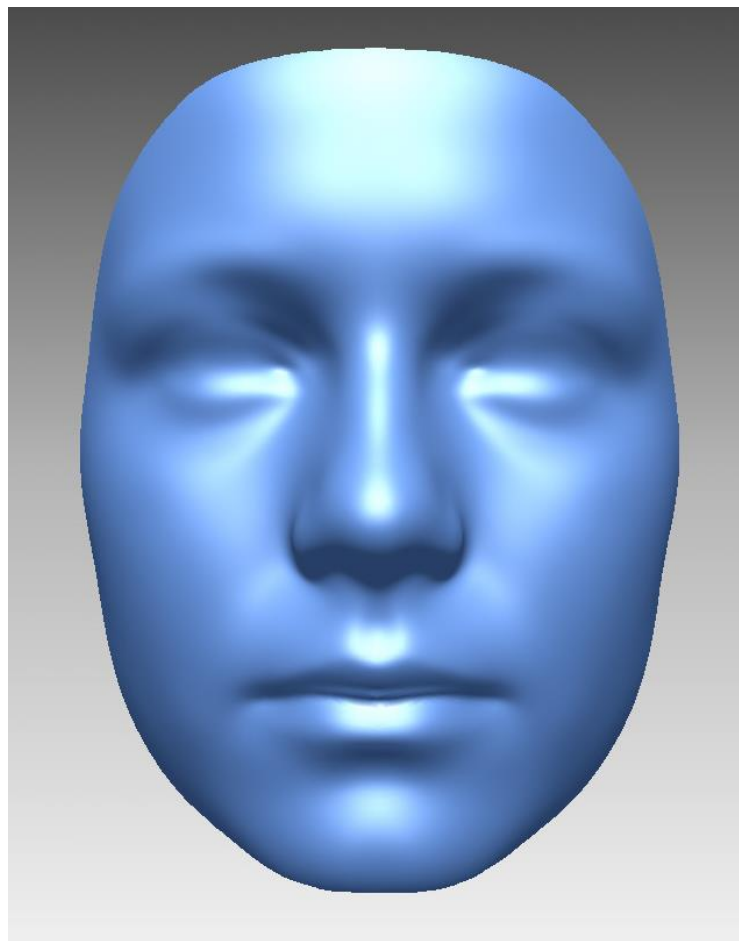


Figure 5.3. Constructed average face for 1785 individuals making the normal/average PC1 group (mean face height,  $P1 \pm 0.5SD$ ), see Figure 5.4

## 5.3 Results

### 5.3.1 Visualizing facial variation

A total of 21 average faces were constructed (see section 5.2.2 Visualizing facial variation) to visualize facial morphology variation identified by the first three principal components extracted from the unscaled dataset (Figure 5.4).

In addition, 28 average faces were constructed for PCs 4–7 (unscaled), and short videos were generated for PCs 1–7 (unscaled) showing the mode of variation represented by each component as explained in Table 4.2. In these videos, each frame corresponds to a 0.1 SD change in each component parameter, from –3 to +3 SDs; an in-house developed macro was used to generate nine intermediate frames between each pair of average faces.

**PC1**, face height (29%)

**PC2**, inter-eye distance (10%)

**PC3**, nose prominence (7%)

**PC4**, protrusion of upper lip relative to chin (5%)

**PC5**, eye depth relative to nasal bridge (5%)

**PC6**, vertical height of the nose (4%)

**PC7**, ratio of mouth width to mouth depth (4%)

Note: *The videos are saved on a CD and enclosed with this thesis. The same principle can be applied to the scaled PCs.*

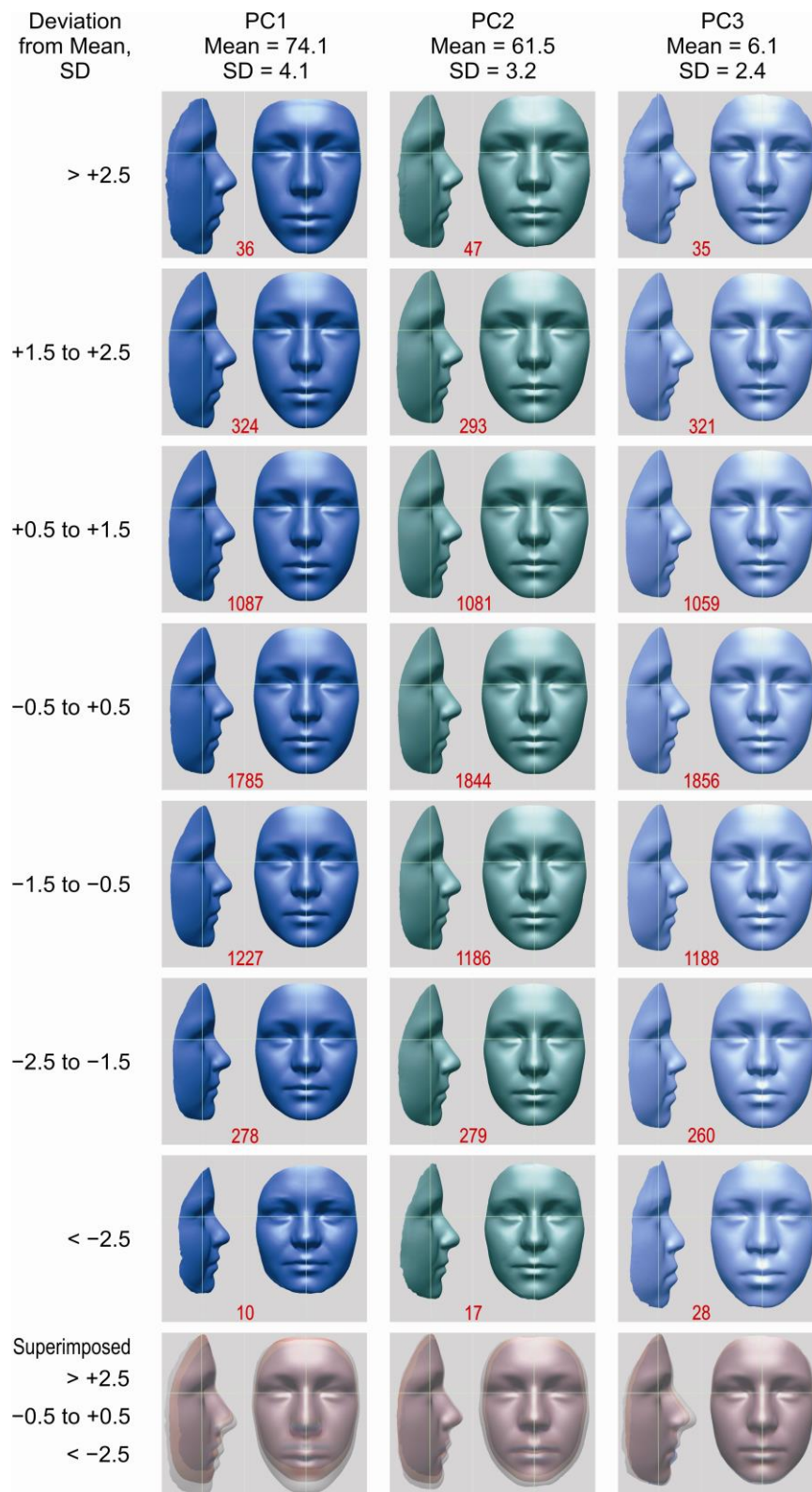


Figure 5.4.

Average faces constructed to illustrate variation revealed by PCs 1–3 (unscaled): face height (left column, PC1), inter-eye width (middle column, PC2) and nose prominence (right column, PC3). The numbers shown in red colour, each indicate the number of individuals contributed to each average face. Total sample = 4747.

## 5.4 Discussion

The present study visualized normal variation in facial morphology for 4747 British adolescents using a novel method of facial surface averaging, with the landmarks utilised to evaluate the centroid sizes and the faces scaled to the average centroid size. The parameters derived for the different PCs (see Chapter 4) were used to characterize facial variation as a multidimensional statistical continuum, and facial averaging allowed visualizing this variation.

Generally in 3D face classification studies, the most frequently employed registration approaches prior to averaging included a best-fit alignment (rotation and translation) that uses the iterative closest point (ICP) algorithm, which establishes a dense correspondence between two point clouds in a rigid manner (Kau *et al.*, 2006).

In dense registration, the points on the *test* surface and the points on the *reference* surface (template) are put into one-to-one correspondence. The ICP algorithm achieves this by iteratively locating the closest point on the test surface for each point on the reference surface, and rigidly moving the aligned surface to minimize the total point-to-point distances (Besl and McKay, 1992). Upon convergence, the distances between the points can be summed up to find a total distance to the reference face. Usually the reference face is cropped and cleansed from all clutter, and the number of correspondences equals the number of points on the reference surface.

Whereas with the thin-plate splines (TPS) based non-rigid registration method (landmark-based), landmarks are identified on the test face, and these drive the registration (Bookstein, 1989, 1991a, b). The TPS method describes a mathematical transformation that aligns the landmarks on the test face with the landmarks on the reference face exactly, and all other points are interpolated. Although this method is considered much faster than the ICP alignment, the facial topography cannot be fully evaluated and the facial parameters may be altered due to warping.

The averaging method used in this study enabled accurate construction of average faces via scaling different individual faces based on the average centroid size, thus minimizing the effects of the variation in face size on the accuracy of the average faces produced. Prior to averaging, the 3D facial shells were aligned (registered) so that their mid-endocanthion points coincide as well as the sagittal, coronal, and transverse planes. The average faces produced using this method allowed accurate visualization and comparisons of facial morphology variation revealed by the principal components.

To clarify whether the spherical coordinates are suitable for averaging in this study and why not using the cylindrical coordinates (as the initial step of averaging): as suggested in the work published by Zhurov *et al.* (2010), iterative averaging on a template (T-averaging) should be performed to achieve the best possible results whether the initial template used was constructed by averaging in the Z-coordinate (Z-average), in the cylindrical

radial direction (CR-average) or in the spherical radial direction (SR-average). Three iterations have to be performed in order to achieve the best results when one can visually see that all facial features have become cleaner and sharper (accurate). In T-averaging, using any of the initial templates mentioned above will lead to a final average face (after three iterations) that is clean, sharp, and accurate. The third-iteration (T3) average may be treated as the 'true' average for the selected method of superimposition. It can be further used to assess other methods of averaging as illustrated in the work published by Zhurov *et al.* (2010), where deviation colour maps between the Z and T3, CR and T3, and SR and T3 averages showed that all the first three methods of averaging have artefacts commensurable with those of the superimposition technique (Figure 5, Appendix). Therefore, it can be concluded that the method of superimposition does not have a significant effect on the average face in case the Z-, CR- or SR-averaging method is used, because all of them have approximately the same level of errors. It is only important if the final average is constructed using the iterative template method with two or three iterations. However, by looking at the deviation colour maps between the CR and T3, and SR and T3 averages, we can see that the CR vs T3 colour map shows obvious deviation of 0.5mm at the periphery, this does not exist with the SR vs T3, therefore, in this study we opted for the spherical radial direction (SR-average) to use as the initial template (method of averaging).

## **5.5 Conclusions**

- This study presented a novel surface-based method to visualize facial morphology variation using accurate average faces where the individual faces, prior to averaging, were scaled based on the average centroid size.
- Variation in facial morphology can be accurately quantified and visualized as a multidimensional statistical continuum with respect to the principal components.
- This method of facial assessment has the potential to identify and classify faces and facial changes that occur as a result of physical anomalies affecting the growth and development of the face, and inform clinicians of appropriate healthcare interventions for specific facial types.

# Chapter 6

## Gender Prediction

## Gender Prediction

### 6.1 Introduction

The human face provides a range of information about the given individual regarding his or her sex, age, ethnicity, personality, health, and emotional state of mind. Human beings have an intuitive ability that allows them to easily distinguish between a male and a female face. Though males and females differ in many characteristics, the face plays a significant role in differentiation between genders. However, a viewer often cannot describe the exact reason of how he/she could determine if a person is a male or a female. It is difficult to specify exactly the features and the reasons which enable the viewer to make the distinction.

Previous studies utilized different methods for gender discrimination. Experiments have been made (Bruce *et al.*, 1993) based on perceptual abilities of the subjects to recognize faces. Subjects were considerably less accurate in identifying the sex from three-dimensional representations of faces obtained by laser-scanning, compared with a condition where 2D photographs were taken with hair concealed and eyes closed. This suggests that cues from features such as eyebrows and skin texture play an important role in decision-making.

Psychological and physiological studies (Palmer, 1977; Burton *et al.*, 1993; Bruce *et al.*, 1993; and Abdi *et al.*, 1995) also support the theory for parts-based representation for faces and gender in the brains of human beings. Edelman *et al.* (1998) compared human performance against a computer

model in classifying gender of 160 adult individuals (80 males, 80 females) using their frontal face images. The classification procedure was based on the upper half of the face that comprised the forehead, eyebrows and eye region against lower half of the face that comprised the mouth, chin, and jaw line. Their study revealed that human performance is decisively better in classifying females on the basis of the upper half of the face, whereas the accuracy for male classification improved with the lower half of the face. Moreover, these studies also showed that general gender information is encoded in hairstyle, nose, eyebrows, eyes and chin region. This is due to the fact that males have thicker eyebrows and bigger nose and mouth as compared to their female counterparts, which is in congruence with several forensic and anthropometric studies that showed female faces, nose, and mouth are generally smaller than those of males (Farkas, 1994).

In orthodontics, the role of cephalometric parameters in the identification of gender has been thoroughly investigated. The lateral skull cephalogram reveals architectural and morphological details of the skull on a single radiograph, thereby providing additional characteristics and multiple measurements for comparison. Many studies, using lateral skull radiographs and discriminant function analysis, have been carried out for the determination of sex and claimed accuracy of 77 to 100% (Biggerstaff, 1977; Patil and Mody, 2005; Naikmasur *et al.*, 2010; Hsiao *et al.*, 1996; Badam *et al.*, 2012; Binnal and Devi, 2012; and Kumar *et al.*, 2013). Among facial parameters that have proven useful in the discrimination of sex: upper facial height, length of cranial base, total face height, and mastoid height (Patil and Mody, 2005;

Binnal and Devi, 2012); bizygomatic width, ramus height, depth of face, and upper facial height (Naikmasur *et al.*, 2010); maximum head length, maximum head breadth, morphological facial length, and bigonial diameter (Kumar *et al.*, 2013). Studies performed to identify the sex of individuals using direct anthropometric measurements of their craniofacial bones have claimed an accuracy of 77 to 92% (Biggerstaff, 1977; Steyn and Iscan, 1998; Kranioti *et al.*, 2008; Robinson and Bidmos, 2009).

Other studies employed different techniques for automatic recognition of faces (Mäkinen and Raisamo, 2008a, b; Wu *et al.*, 2010, 2011; Cao *et al.*, 2011; Shih, 2013); however, as yet no procedure has been developed which comes near to human capacity. Several attempts have been made for this purpose; these range from techniques based upon the explicit measurement of different facial characteristics, through to the statistical analysis of facial patterns via methods of geometric morphometrics. Generally speaking, gender classification methods can be divided into two main categories:

i) geometry-based, and ii) appearance-based.

The geometry-based approach is focused on extracting the geometric feature points from the facial image and describes the shape structure of the face. The appearance-based methods are divided into two categories: texture-oriented and statistics-oriented. The texture-oriented approach utilizes different texture descriptors to characterize the gender of a facial image, and utilizes a machine learning strategy to recognize the gender. The statistics-based approach usually acquires satisfactory results for the classification scheme,

and it focuses on using different features that are quantified into a probability to characterize a facial image as to gender using its visual characteristics.

Enlow (1982) suggested a number of features that distinguish between male and female faces. In general, the nose and nasopharynx are larger in men than in women. This is because men in general have a greater body mass than women, and require larger lungs and larger passages to supply the lungs with air. As a consequence of the larger nasopharynx, men in general have more prominent brows, more sloping foreheads, and more-deep-set eyes than woman. Shepherd (1989) points out that women appear to have fuller cheeks than men. This is in part due to the less protrusive nose, but also to a pad of adipose tissue over the bone.

Generally, if the dimorphic nature of the human face is well understood and clearly specified, it should be relatively straightforward to specify an automatic procedure to discriminate between male and female faces.

In this study, using explicit facial measurements, we *aim* to identify the facial features that are most different in male and female faces, and can be used in the prediction of gender, as well as provide a good source of different facial characteristics that can be used in the future for automatic recognition of faces.

## 6.2 Subjects and methods

### 6.2.1 Sample

The final ALSPAC sample of 4747 British adolescents (2514 females and 2233 males) was used for this study.

### 6.2.2 Facial parameters

The x, y, and z coordinates of the 21 facial landmarks (unscaled dataset), in addition to mid-endocanthion point (men), were used to generate a set of facial parameters, including:

- Distances
- Angles
- Ratios between two distances

*Mathematically* a distance between points A and B in three dimensions, defined by their coordinates:

$$(X_A, Y_A, Z_A), (X_B, Y_B, Z_B)$$

is calculated using the formula:

$$d_{AB} = \sqrt{(X_B - X_A)^2 + (Y_B - Y_A)^2 + (Z_B - Z_A)^2}$$

Angles were calculated as follows. Given three points, A, B and C, defined by their coordinates:

$$(X_A, Y_A, Z_A), (X_B, Y_B, Z_B), (X_C, Y_C, Z_C)$$

We wish to measure the angle  $\alpha$  ( $\angle BAC$ ) between two vectors  $\overrightarrow{AB}$  and  $\overrightarrow{AC}$  in three dimensions. From vector calculus it is known that:

$$\cos \alpha = \frac{(X_B - X_A)(X_C - X_A) + (Y_B - Y_A)(Y_C - Y_A) + (Z_B - Z_A)(Z_C - Z_A)}{d_{AB} d_{AC}}$$

$$\sin \alpha = \sqrt{1 - \cos^2 \alpha}$$

$$\tan \alpha = \frac{\sin \alpha}{\cos \alpha} = \frac{\sqrt{1 - \cos^2 \alpha}}{\cos \alpha}$$

$$\alpha = \arctan(\tan \alpha) \quad \text{.....in radians}$$

$$\alpha = \frac{180}{\pi} \arctan(\tan \alpha) \quad \text{.....in degrees}$$

$$\pi = 3.141693, \quad 1 \text{ rad} = \frac{180^\circ}{\pi} = 57.29578^\circ$$

The ratio between the distances from A to B and C to D is calculated as:

$$r_{ABCD} = d_{AB} / d_{CD}$$

### 6.2.3 Statistical analysis

#### 6.2.3.1 Gender prediction efficiency:

The gender prediction efficiency of the derived facial parameters was assessed using a valid statistical technique 'Discriminant Function Analysis' carried out in 'SPSS'.

This is a statistical analysis used to predict a categorical dependent variable (called a grouping variable: gender) by one or more continuous or binary independent variables (called predictor variables: facial parameters).

*Mathematically*, this technique is based upon calculating the means and standard deviations for all derived facial parameters (distances, angles and ratios). Each subject is assigned as being either a male or female based on his/her measured values. For each parameter, gender is predicted by comparing each individual measure with its respective male and female means. For example, if an individual measure lies closer to its female mean, then that subject will be assigned as being a female. Figure 6.1 illustrates an example for one of the derived facial parameters (Is-men) that was used to predict gender based on this method.

For each parameter, percentages of males and females as well as total prediction efficiency were recorded.

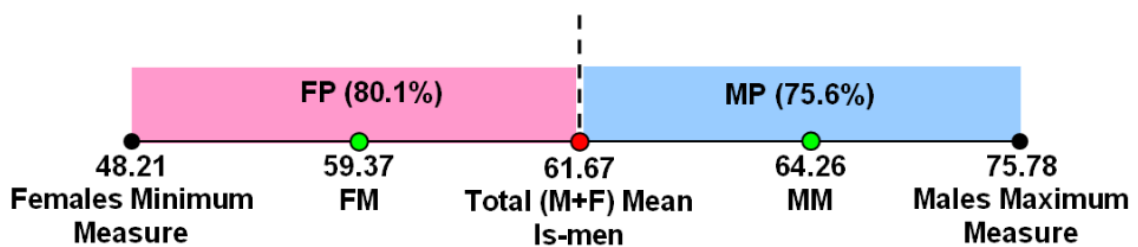


Figure 6.1. Assessment of gender prediction efficiency provided by the facial parameter (Is-men);

**FM:** Females Mean

**MM:** Males Mean

**FP:** Females Prediction

**MP:** Males Prediction

## 6.3 Results

### 6.3.1 Facial parameters

250 facial parameters were derived (Table 3, Appendix), including:

- 90 Distances
- 118 Angles
- 42 Ratios

### 6.3.2 Gender prediction efficiency

Out of the 250 facial parameters, only 24 parameters (Table 6.1) provided gender prediction efficiency of over 70%. The highest prediction efficiency was provided by the 3D distance ls-men: 80.1% (females), 75.6% (males), and 78% (total prediction efficiency).

Out of the 24 parameters, 13 were distances related to mid-endocanthion point (men). For example, we had total prediction efficiency of 72.6% for pg-men, 73.1% for n-men in the z-axis, 73.5% for li-men, 75.4% for sn-men in the z-axis, and 76.7% for ls-men in the z-axis. Obviously these parameters describe variation in different facial heights (total, upper, and lower facial heights), and prominence of facial structures (forehead, nasal bridge, tip of the nose, lips and mouth, and chin).

Other parameters (alL-alR, prn-alL, prn-alR) describe variation in nose width; and parameters like (enL-XZ, enR-XZ, enL-XY, enR-XY) describe prominence of eye landmarks with respect to the facial planes (mid-sagittal, coronal and transverse).

None of the angles provided prediction efficiency of over 70%, and only 1 ratio (sn-ls/g-n.y) gave prediction efficiency of 73.2% in females only.

No	Facial Parameters	Females (Average)	Females (SD)	Males (Average)	Males (SD)	Females (Pred.)	Males (Pred.)	Total (Pred.)
1	men-g.z	14.76	2.12	17.23	2.37	72.0%	70.4%	71.2%
2	men-n.z	13.54	1.93	16.00	2.17	73.8%	72.2%	73.1%
3	men-alL.x	15.84	1.35	17.12	1.50	70.1%	66.9%	68.6%
4	men-prn.z	35.61	2.58	39.23	3.06	76.3%	73.6%	75.0%
5	mal-men.z	15.88	1.93	18.19	2.16	73.3%	71.4%	72.4%
6	sn-men.z	21.10	2.07	24.03	2.38	76.1%	74.6%	75.4%
7	ls-men.z	22.14	1.75	24.80	2.00	78.6%	74.5%	76.7%
8	mcph-men.z	21.25	1.69	23.85	1.91	77.9%	75.1%	76.6%
9	mch-men.z	6.63	1.81	8.42	1.80	67.7%	70.0%	68.8%
10	exR-XZ	-0.53	1.68	1.45	1.92	72.2%	70.0%	71.2%
11	enL-XZ	-0.91	1.46	1.29	1.66	77.0%	74.9%	76.0%
12	enR-XZ	-1.11	1.46	0.98	1.66	76.1%	72.5%	74.4%
13	enL-XY	0.57	1.13	-1.01	1.19	75.8%	74.5%	75.2%
14	enR-XY	0.87	1.10	-0.60	1.22	75.7%	72.5%	74.2%
15	sn-men	46.55	2.79	50.03	3.30	73.3%	70.0%	71.7%
16	alL-alR	32.44	2.30	35.00	2.56	73.0%	69.0%	71.1%
17	prn-alL	25.70	1.51	27.60	1.78	74.6%	70.5%	72.7%
18	prn-alR	25.95	1.52	27.77	1.77	73.9%	70.5%	72.3%
19	ls-men	59.37	2.97	64.26	3.42	80.1%	75.6%	78.0%
20	li-men	72.52	3.80	77.55	4.36	75.2%	71.6%	73.5%
21	pg-men	90.92	4.47	96.76	5.32	74.4%	70.6%	72.6%
22	pg-n	98.98	5.18	104.82	6.02	70.5%	68.0%	69.3%
23	pg-sn	48.86	3.96	52.78	4.61	70.2%	65.9%	68.2%
24	sn-ls/g-n.y	1.1398	0.3142	1.4163	0.4186	73.2%	58.2%	66.1%

## **6.4 Discussion**

Without explicit training, all of us can easily recognize individual faces as being males or females, even when cues from hairstyle, makeup, and facial hair are minimized; however, the exact facial measurements which allow us to tell each individual face gender are yet not fully covered. In this study, we used a large set of 250 different facial measurements including distances, angles, and ratios to investigate which of these parameters can predict gender in a large population of 4747 British adolescents (2514 females and 2233 males).

The dictionary meaning of 'dimorphism' is 'difference of form between members of the same species'. Sexual dimorphism, in general, refers to the differences between males and females of the species in terms of size, appearance, and behaviour. Dimorphism exists in various forms in all humans. Studies have shown that parts of human anatomy exhibit sexual dimorphism. Factors and the features responsible for dimorphism in humans are still under research. The aim of this study was to identify the features of the face that most contribute to sexual dimorphism. Research on sexual dimorphism can be used in conjunction with face recognition systems in several ways. It can be used as a mechanism to reduce the search space by half, if the gender of the face is known in advance or can be determined automatically. In large databases this could result in significant reduction in search time. Furthermore, the research can be used for analysing the facial expressions and determining the gender of the subject in the photograph.

Several studies have contributed to the body of knowledge in sexual dimorphism, providing quantitative results that measure sexual dimorphism in human faces in order to develop a basis to differentiate between male and female faces. Researchers used both direct measurements and measurements from photographic images for their analyses. They also studied how sexual dimorphism changes as a function of age and which features are more significant in the expression of sexual dimorphism. In addition, they analysed the features to determine which ones are likely to be most useful in automated analyses with the goal is to fundamentally understand the degree and extent of sexual dimorphism in the human face. Scientists, for a long time, have relied on measurements obtained directly or indirectly from the human face by manual methods. However, there is an active research community in extracting features automatically and develop a fully automated system to accurately classify faces into males and females, in the sense that the most important features of the face that distinguish between males and females are identified (Mäkinen and Raisamo, 2008a, b; Wu et al., 2010, 2011; Cao et al., 2011; Shih, 2013).

Facial distances describe variation in size, whereas angles and ratios give information mainly about shape and asymmetries. The current study found that facial parameters which describe variation in size can predict gender. A total of 24 facial parameters were found to provide gender prediction efficiency of over 70%, 23 of these parameters were distances that describe variation in facial height, nose width, and prominence of facial structures (forehead, eyes, nasal bridge, tip of the nose, lips and mouth, and chin).

None of the angles were found to predict gender, and only 1 ratio gave prediction efficiency of over 70%, that was in females only.

Similar results were obtained in previous studies. Meerdink *et al.* (1990) performed a study where college students were requested to qualitatively assess several male and female faces based on 12 facial features, such as face width (narrow/wide) or nose size (small/large). It was found that both male and female subjects had similar assessments of the male and female faces. Statistical analysis revealed that among metric features, subjects were found to assess gender on the basis of size, e.g., face width and face length, mouth size, and eye size. In addition, judgments of male faces relied on eye spacing and a combination of nose size and eyebrow shape while female faces relied on nose size in isolation and the compound eye-eyebrow. Even though the metric properties used in this study were limited in number and qualitatively assessed, the results clearly suggest that facial gender discrimination may be achieved on the basis of some “rules” shaped by experience and evolution, which in turn may be based on objective precise metric differences between male and female faces.

Another attempt was made by Ferrario *et al.* (1993) to use facial metric measurements for the assessment of male and female faces. They utilized Euclidean distance matrix analysis to determine sexual dimorphism in the human face. The method employed a two-step procedure: (a) calculate all the possible Euclidean distances between the selected points on a face; and (b) compare the two faces by calculating the matrix of ratios of

corresponding linear Euclidean distances measured on the faces. The analysis was conducted on a small sample made of 108 healthy young adults (57 men, 51 women) aged (20-27 year old) who were screened from a group of 160 healthy white Caucasian dental students by a detailed questionnaire and verified through clinical examination. 22 facial points were extracted from the subjects' photographs, and 231 distances were then extracted and ratios were derived from these distances. The results showed significant sexual dimorphism among adult faces. In most of the cases it was observed that the female face is shorter when compared to her male counterpart. Most of the size differences involved vertical distances, where the chin point (pogonion) was one of the most frequent endpoints. Therefore, the middle and lower thirds of the face expressed the majority of gender variation.

Fellous (1997) used a set of 24 horizontal and vertical measurements derived from 40 facial points individually extracted for a set of 109 pictures of young adults, subdivided into two groups: the first set of pictures (training set) consisted of 52 pictures acquired from 26 males and 26 females (47 Caucasians and 5 Asians) who displayed a neutral facial expression; the second set made of 57 frontal pictures acquired from 26 females and 31 males (54 Caucasians and 3 Asians) exhibiting various facial expressions and was used as a (test set) to assess gender prediction. The horizontal distances were normalized with respect to the interpupillary distance, whereas the vertical distances were normalized with respect to the distance from the eyes midpoint to the philtrum ridges midpoint. Discriminant analysis

showed that 5 distances explain over 95% of gender differences and predict gender of 90%. The results showed that “femaleness” relies on large distances between external eye corners, a measure of overall eye extent, large distance between the eyes and eyebrows, a small nose, narrow and round face; whereas “maleness” relies on the presence of a large nostril-to-nostril width, wide cheek bones, lengthy face, small extent of the eyes and small distances between the eyebrows and eyes.

In summary, comparing the findings of the present study with those identified in previous studies (mentioned above), we found that face gender can be predicted efficiently based on facial parameters that describe mainly variation in the relative size of various facial structures between males and females. The previous studies recruited quite small samples (about 100 young adults) for their gender prediction analyses. The high gender prediction efficiency (90%) achieved by Fellous (1997), though it is impressive, his technique was applied on a small sample of young adults (mixed ethnicity) who were tested based on displaying various facial expressions. Whereas the present study applied discriminant function analysis on a large population cohort of 4747 (15-year-old) Caucasian adolescents who displayed neutral facial expression, therefore, the gender prediction efficiency of 70%-80% identified in this study for 24 facial parameters can be considered reasonably good.

### **6.5 Conclusions**

- This study has demonstrated to what extent gender prediction can be achieved on the sole basis of facial metric information.
- 24 facial parameters were found to provide gender prediction efficiency of over 70%, 23 of these parameters are distances that describe variation in facial height, nose width, and prominence of facial structures (forehead, eyes, nasal bridge, tip of the nose, lips and mouth, and chin). 13 of these distances are related to mid-endocanthion point (men), which suggests it is an important landmark.
- The highest prediction efficiency was provided by the 3D distance *Is-men*: 80.1% (females), 75.6% (males), and 78% (total prediction efficiency).
- None of the angles were found to predict gender, and only 1 ratio gave prediction efficiency of over 70% in females only.
- These parameters provide a good source of different facial characteristics that can be used in the future for automatic recognition of faces.

## Chapter 7

# Exploring The Association Between Facial Features And Genes

## Exploring The Association Between Facial Features And Genes

### 7.1 Introduction

A gene is the molecular unit of heredity of a living organism. It is widely accepted by the scientific community as a name given to some stretches of deoxyribonucleic acids (DNA) and ribonucleic acids (RNA) that code for a polypeptide or for an RNA chain that has a function in the organism, though there still are controversies about what plays the role of the genetic material (Sarkar and Plutynski, 2008). Genes hold the information to build and maintain an organism's cells and pass genetic traits to offspring. All organisms have genes corresponding to various biological traits, some of which are immediately visible, such as eye color or number of limbs, and some of which are not, such as blood type, increased risk for specific diseases, or the thousands of basic biochemical processes that comprise life. The word 'gene' is derived from the Greek word *genesis* meaning 'birth', or *genos* meaning 'origin'.

A modern working definition of a gene is “a locatable region of genomic sequence, corresponding to a unit of inheritance, which is associated with regulatory regions, transcribed regions, and/or other functional sequence regions” (Pearson, 2006; Pennisi, 2007). Where a 'gene' is the basic instruction unit — a sequence of nucleic acids (DNA or, in the case of certain viruses RNA), an 'allele' is one variant of that gene. In most cases, all people would have a gene for the trait in question, but certain people will have a specific allele of that gene, which results in the trait variant.

The term 'phenotype' refers to the "outward, physical manifestation" of the organism. These are the physical parts, the sum of the atoms, molecules, macromolecules, cells, structures, metabolism, energy utilization, tissues, organs, reflexes and behaviors; anything that is part of the observable structure, function or behavior of a living organism.

The term 'genotype' refers to the "internally coded, inheritable information" carried by all living organisms. This stored information is used as a set of instructions to build and maintain a living creature. These instructions are found within almost all cells, they are written in a coded language known as the genetic code, and they are copied at the time of cell division or reproduction and passed from one generation to the next (inherited). These instructions are intimately involved with all aspects of the life of a cell or an organism. They control everything from the formation of protein macromolecules, to the regulation of metabolism and synthesis.

Gene-environment interaction is a term used to indicate that a phenotypic effect is due to a mixture of environmental factors (nurture) and genetic factors (nature). Most traits, including facial traits, show gene-environment interactions; however, the extent to which both genetic and environmental factors influencing facial variation is typically not addressed. Researchers have been trying to investigate the relative contribution of genes and the environment to the etiology of malocclusion. Genetic mechanisms are clearly predominant during embryonic craniofacial morphogenesis, but environment is also thought to influence facial morphology postnatally,

particularly during facial growth. Orthodontists and maxillofacial surgeons use different techniques in the treatment of malocclusion and other dentofacial deformities, but with limited effectiveness. The key to the determination of the etiology of malocclusion lies in the ability to differentiate the effect of genes and environment on the craniofacial skeleton in a particular individual. Our ability to do this is limited by our lack of knowledge of the genetic effects on craniofacial morphology, and lack of scientific evidence for the influence of environmental factors on human craniofacial morphogenesis.

Any two human genomes differ in millions of different ways. There are small variations in the individual nucleotides of the genomes (SNPs) that may cause alterations in an individual's traits, or phenotype, which can be anything from disease risk to physical properties such as height.

In genetic epidemiology, a genome-wide association study (GWAS) is an examination of many common genetic variants in different individuals to see if any variant is associated with a trait. GWAS typically focus on associations between single-nucleotide polymorphisms (SNPs) and traits like face height, eye colour, or major diseases.

Craniofacial morphology has been reported to be highly heritable, as demonstrated by twin and family studies (Table 2.3. Literature Review); however, the individual genetic variants which affect normal variation in human facial features have yet to be identified. The heritability of different facial features has been investigated in several cephalometric studies that

suggest a number of potential parameters to have a genetic association. Higher heritabilities have been found for several vertical variables than for horizontal ones (Lundström and McWilliam, 1987; Carels *et al.*, 2001; Manfredi *et al.*, 1997).

Among craniofacial parameters that have been reported to be inheritable and have potential for strong genetic associations, there are the proportions with high heritability estimates: upper-to-lower facial height (71%) and anterior-to-posterior facial height (66%), and the vertical distance: total facial height (62%) (Savoye *et al.*, 1998).

Manfredi *et al.* (1997) also investigated the heritability of 39 cephalometric parameters in their study on twins. In this study, the analysis of variance for each cephalometric parameter was first performed to determine the within-pair variance. The observed variance was then used to calculate Pearson's intraclass correlation coefficients and hence genetic heritability ( $h^2$ ). According to their analyses, high heritability values (coefficients of genetic heritability,  $h^2$ ) were obtained for total anterior facial height ( $h^2 = 1.5$ ) and lower anterior facial height ( $h^2 = 1.56$ ).

In another study on twins (Carels *et al.*, 2001), sex differences in genetic determination were found for anterior facial height, showing a significantly higher genetic component (heritability estimates) for boys (91%) than for girls (68%), and no genetic influence was found for the angular measurements; only environmental influences common to both members of each pair of twins could be demonstrated.

In this project we conducted, to the best of our knowledge, the first genome-wide association study of three-dimensional facial morphology in a large population of British adolescents.

The aim of this study was to explore 'facial' phenotype-genotype associations in a 15-year-old population.

An objective of this study was to visualize facial morphology variation influenced by genetic effects.

## **7.2 Subjects and methods**

### **7.2.1 Sample**

#### **7.2.1.1 Genetic data:**

Biological samples (including DNA) were collected for 10,121 of the ALSPAC children.

#### **7.2.1.2 Facial data:**

The facial data extracted for the final ALSPAC sample of 4747 British adolescents (2514 females, 2233 males) forms the basis for this study and future analyses. This data includes the following facial parameters:

- Principal components (14 unscaled, 17 scaled), highlighted in Chapter 4.
- 250 facial measurements (90 distances, 118 angles, and 42 ratios), highlighted in Chapter 6 (Table 3, Appendix).

### 7.2.2 Statistical analysis

- i. Pertinent to the current study, the 14 (unscaled) principal components and a set of 54 facial parameters including *unscaled* 3D and 2D distances (Figure 7.1) characterizing main facial features and have previously shown strong heritability in several 2D cephalometric studies (e.g., facial height, width, convexity, as well as prominence of landmarks with respect to the facial planes) were selected for inclusion in the first round GWAS study. The reason why we didn't include all facial parameters in the GWAS study was to avoid being accused of data dredging (sometimes referred to as data fishing), a data mining practice in which large volumes of data are analysed seeking every possible relationships between data that may lead to premature conclusions.
- ii. Variation in the 3D distance can be influenced in any dimension (x, y, or z) or plane (xy, yz, or xz). Therefore, the 3D distances identified with genetic associations were further investigated to determine in which dimension(s) and plane(s) the associations were having an effect.
- iii. The *unscaled* 3D distances identified with genetic associations were further investigated by generating *scaled* distances (to exclude size effect) and try replicating the associations.

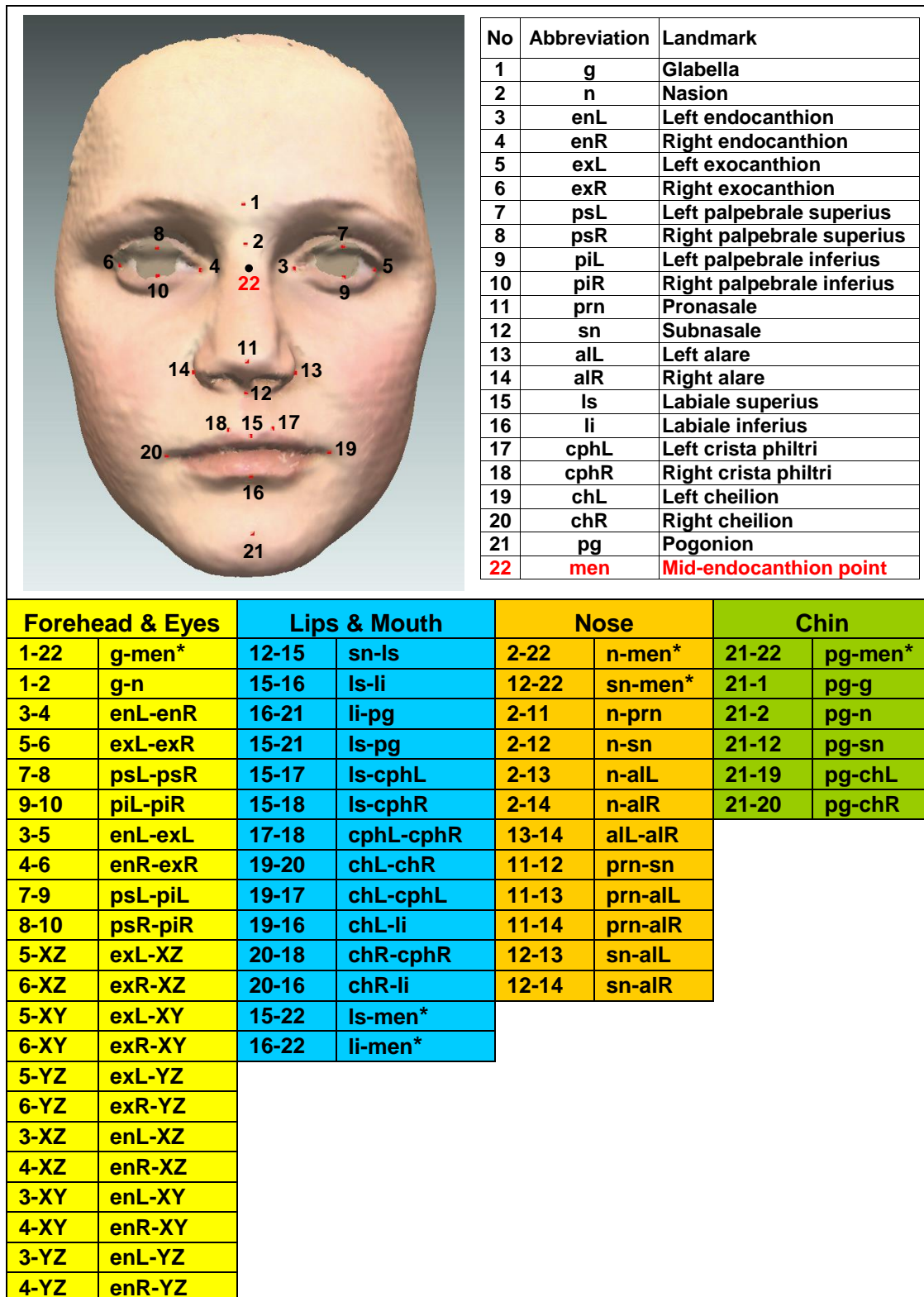


Figure 7.1.

Facial landmarks and parameters analysed in the genome-wide association study. Parameters with pairs of numbers denote direct 3D distance between pairs of landmarks. Those with “xz” “xy” or “yz” denote the prominence of landmarks from the xz, xy, or yz planes. \* “men” (point 22) denotes the mid-endocanthion or mid-intercanthal point (the midpoint between left and right endocanthi); this point does not lie on the facial surface.

### 7.2.2.1 Genome-wide association study (GWAS):

A discovery-phase genome-wide association analysis for the 14 principal components and 54 facial parameters was first conducted. At this phase 3,714 participants were genotyped with either the Illumina 317K or 610K genome-wide SNP (single nucleotide polymorphism) genotyping platforms by the Wellcome Trust Sanger Institute (Cambridge, UK) or the Centre National de Génotypage (Evry, France).

The identified associations in the discovery phase were followed up in a replication phase that included 9,912 individuals from the same population cohort but were not included in the discovery sample, with additional imputed genome-wide data available. At this phase the participants were genotyped with the Illumina HumanHap550 quad genome-wide SNP genotyping platform by 23andMe subcontracting the Wellcome Trust Sanger Institute (Cambridge, UK) and the Laboratory Corporation of America (Burlington, NC, US).

For both analyses (discovery and replication phases) a common set of SNPs present in the genotyping platforms were extracted and the resulting raw genome-wide data was subjected to standard quality control methods.

Individuals were excluded on the basis of having:

- Incorrect sex assignments
- Minimal or excessive heterozygosity
- Disproportionate levels of individual missingness
- Evidence of cryptic relatedness
- Evidence of population stratification

The exclusion criteria are further detailed (Paternoster *et al.*, 2012).

(*Bonferroni* correction method for multiple testing was applied in this study)

### **7.2.3 Visualizing facial phenotypic variation influenced by genetic effect**

To visualize facial phenotypic variations influenced by genes, average faces were constructed using a locally developed algorithm implemented as a Rapidform® macro (Zhurov *et al.*, 2010). The averaging procedure is described in Chapter 5.

- i) Average faces were constructed for females and males showing the effect of variation of the parameter identified with genetic association on the face shape. The female and male faces were split into seven groups corresponding to  $-3$  through  $+3$  SDs from the mean value of the parameter. In addition, short videos were generated for females and males showing the parameter variation effect on the face shape. In these videos, each frame corresponds to a 0.1 SD change in the identified parameter, from  $-3$  to  $+3$  SDs; an in-house developed macro was used to generate nine intermediate frames between each pair of average faces.
- ii) Average faces were constructed for all individuals with different genotypes of the gene associated with a facial parameter.

## 7.3 Results

### 7.3.1 Genome-wide association study (GWAS)

*Discovery-phase:* standard quality control methods were applied and individuals were excluded accordingly. The final dataset consisted of 3,233 subjects, each with 2,543,887 imputed autosomal markers. Of these 3,233 with genetic data, 2,185 participants (1,080 males, 1,105 females) also had facial data available. So, the discovery-phase genome-wide association analysis was conducted ( $n=2,185$ ) for the 54 facial distances and 14 PCs with 2,543,887 imputed autosomal markers (SNPs).

Four genetic associations were identified (Table 7.1) that reached the traditional threshold for genome-wide significance (defined as  $p < 5 \times 10^{-8}$ ) with three of the 3D distances (enR.yz, n-men, prn-all). One of these associations (rs7559271 and n-men, association 'Manhattan' plot is shown in Figure 6 of the Appendix) reached a stringent *Bonferroni* corrected threshold of  $p < 9 \times 10^{-10}$  after adjusting for the 54 facial distances tested. Although we analysed 54 different distances, many of these are correlated, so a *Bonferroni* correction would be conservative.

No genome-wide significant associations were observed for any of the principal components.

*Replication-phase:* following standard quality control methods, the final dataset consisted of 8,365 individuals. Of the 8,365 ALSPAC genotyped individuals, 1,622 (750 males, 872 females) also had facial data and were not included in the discovery sample. We attempted to replicate all four associations with  $p < 5 \times 10^{-8}$  that were identified in the discovery-phase.

The association between nasion to mid-endocanthion distance (n-men) and the genetic marker (SNP) rs7559271 in *PAX3* gene on chromosome 2q36.1 replicated strongly ( $p = 4.0 \times 10^{-7}$ ), as shown in Table 7.1. Because 4 associations were tested in replication, applying a *Bonferroni* correction for this phase would yield  $\alpha = 0.0125$ .

Table 7.2 shows the association between rs7559271 and the distances and angles relating to n-men distance in the combined sample of 3,807 participants. A strong genetic association was observed in the y distance ( $p = 5.3 \times 10^{-8}$ ), which reflects height of nasion relative to men, and the z distance, reflecting prominence of nasion relative to men ( $p = 4.4 \times 10^{-9}$ ). In contrast, there was much weaker association between rs7559271 in the x distance ( $p = 0.006$ ), which reflects lateral distance of nasion relative to the mid-endocanthion. In this analysis, combining discovery and replication samples, the G allele of rs7559271 was strongly associated with the 3D distance n-men ( $p = 4.1 \times 10^{-16}$ ).

rs7559271 is an intronic SNP (common genetic variant) in *PAX3* (paired box 3, MIM 606597). This gene encodes a transcription factor that plays crucial role in fetal development including craniofacial bones (as explained in details in the Literature Review, section **2.10.2.1** Genetic expression in craniofacial development). Murine *PAX3* (479 amino acids) contains two DNA-binding domains, a paired-box domain (PD) and a homeodomain (HD) (Goulding *et al.*, 1991). The protein made from *PAX3* gene directs the activity of other genes that signal neural crest cells to form specialized

tissues or cell types such as some nerve tissue, bones in the face and skull (craniofacial bones), and pigment-producing cells called melanocytes. *PAX3* gene mutations, e.g. mutations leading to truncation of the paired-box domain (PD) or loss of the homeodomain (HD) (Guo *et al.*, 2010) and mutations producing aberrantly spliced mRNA transcripts (Epstein *et al.*, 1993), eventually may lead to non-functional *PAX3* polypeptides and destroy the ability of the *PAX3* proteins to bind to DNA and regulate the activity of other genes to form bones and other specific tissues.

Table 7.1. Discovery phase and replication phase results for the four associations with $p < 5 \times 10^{-8}$ in the discovery phase							Discovery Phase (n=2185)		Replication Phase (n=1622)	
Distance	Mean	SD	SNP	Chr: position	Gene	Effect: Alt allele	SE	p-value	SE	p-value
enR.yz	17.081	1.510	rs10862567	12:81946438	<i>TMTC2</i>	T:A	0.033	$4.4 \times 10^{-8}$	0.035	0.506
<b>n-men</b>	<b>17.505</b>	<b>2.341</b>	<b>rs7559271</b>	<b>2:222776530</b>	<b>PAX3</b>	<b>G:A</b>	<b>0.027</b>	<b><math>2.2 \times 10^{-10}</math></b>	<b>0.032</b>	<b><math>4.0 \times 10^{-7}</math></b>
prn-alL	26.596	1.896	rs1982862	3:55039780	<i>CACNA2D3</i>	C:A	0.046	$1.8 \times 10^{-8}$	0.049	0.167
prn-alL	26.596	1.896	rs11738462	5:61046695	<i>C5orf64</i>	G:A	0.036	$1.8 \times 10^{-8}$	0.039	0.527

Means and standard deviations (SDs) are in mm; SE: standard error

<b>Phenotype</b>	<b>D/Plane</b>	<b>Mean</b>	<b>SD</b>	<b>Interpretation</b>	<b>SE</b>	<b>P-value</b>
n-men (3D dist)	xyz	17.507	2.343	3D distance between nasion and men	0.047	4.1x10 <sup>-16</sup>
n-men (1D dist)	x	0.573	0.452	absolute lateral distance of nasion from men	0.011	0.006
n-men (1D dist)	y	9.184	2.324	height of nasion above men	0.053	5.3x10 <sup>-8</sup>
n-men (1D dist)	z	14.698	2.386	prominence of nasion relative to men	0.046	4.4x10 <sup>-9</sup>
n-men (2D dist)	yz	17.492	2.344	prominence and height of nasion	0.047	3.1x10 <sup>-16</sup>
n-men (z.yz angle)	yz	32.032	7.817	angle between the yz vector and z axis	0.171	0.036

**Means and standard deviations (SDs) are in mm; angles are in degrees;  
SE: standard error; D: dimension**

Conditional analyses showed that the associations in the y and z dimensions were independent of each other and that there was only weak evidence of association between the SNP and yz angle between nasion and men. These results suggest that the association between rs7559271 and the 3D n-men distance is being mostly driven by the distance in the yz plane (Figure 7.2).

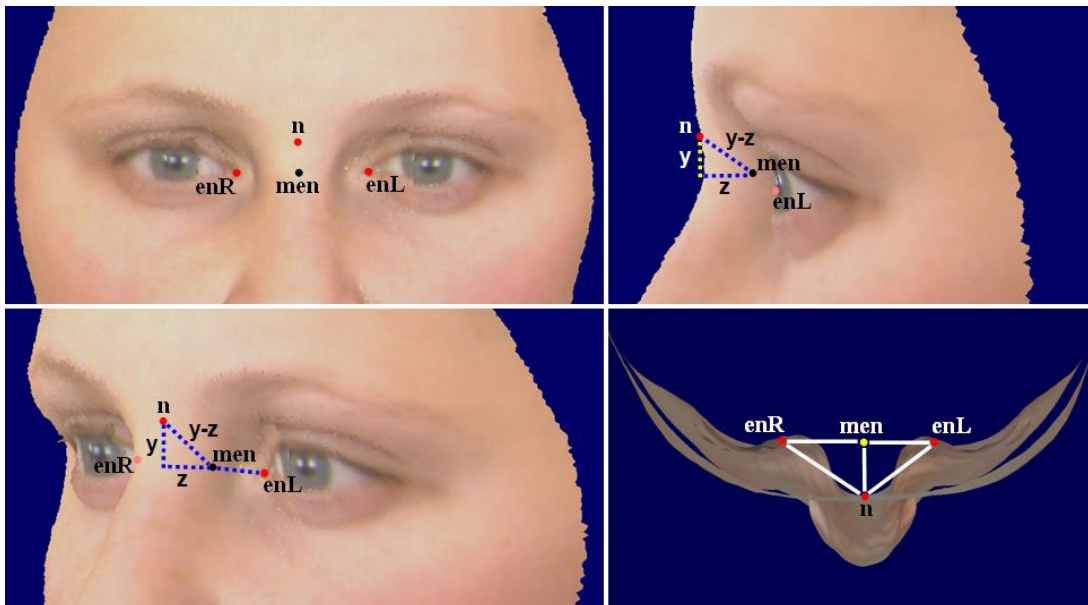


Figure 7.2.

Deconstruction of the 3D n-men phenotype into its constituent dimensional distances,

The mid-endocanthion (men) is defined as the midpoint between left and right endocanthi (en) and is therefore not a surface point. The 3D (n-men) distance was deconstructed into the three 1D distances: the x (the lateral distance between nasion and men, a measure of how off-center nasion is relative to men), the y (the vertical distance between nasion and men), and the z (the prominence of nasion relative to men). The 2D yz distance was also constructed as the angle between yz and z components.

Table 7.3 shows the association between rs7559271 and the *scaled* n-men distance in the combined sample (n=3807). The association analysis gave very similar results ( $p = 1.0 \times 10^{-17}$ ) to the unscaled data analysis.

<b>Table 7.3. The association between rs7559271 and the scaled n-men distance in the combined sample (n=3807)</b>				
<b>Phenotype</b>	<b>Dimension</b>	<b>Mean</b>	<b>SD</b>	<b>p-value</b>
n-men (3D dist)	xyz	17.517	2.144	$1.0 \times 10^{-17}$
n-men (1D dist)	x	0.575	0.453	0.7549
n-men (1D dist)	y	9.197	2.299	$2.8 \times 10^{-4}$
n-men (1D dist)	z	14.701	2.217	$1.4 \times 10^{-7}$

**Means and standard deviations (SDs) are in mm**

### **7.3.2 Visualizing facial phenotypic variation influenced by genetic effect**

- i) A total of 14 average faces (7 for females, 7 for males) were constructed to show the effect of variation of the n-men 3D distance on the face shape. The average faces of the normal group ( $-0.5$  SD to  $+0.5$  SD) and the extremes ( $<-2.5$  SD and  $>+2.5$  SD) were superimposed for visual comparison of facial shape, as shown in Figure 7.3. It is obvious that *PAX3* gene affects “nasal bridge prominence phenotype”. Videos (*saved on a CD enclosed with this thesis*) were generated for females and males showing the variation effect at 0.1 SD change in the n-men 3D distance, from  $-3$  SD to  $+3$  SD.

- ii) Average faces were also constructed for subjects with *PAX3* different genotypes (G allele): genotype 0 (1417 individuals), genotype 1 (1658 individuals), and genotype 2 (564 individuals). Figure 7.4 shows superimposition of average phenotypes for genotypes 0 and 1 (top); and 0 and 2 (bottom). The colour maps indicate the surface distances between the average facial shells (colour scale is shown). Green indicates no difference  $\pm 0.1$ mm; blue  $-0.1$  to  $-0.2$ mm; yellow  $0.1$  to  $0.2$ mm; orange  $0.2$  to  $0.4$ mm and deep orange  $0.4$  to  $0.8$ mm. The different genotypes show slight influences not only on the nose but also on the forehead, upper lip and chin areas. The maximum surface distances were observed between genotypes 0 and 2 with a difference of  $0.6$ mm at the nasal bridge area.

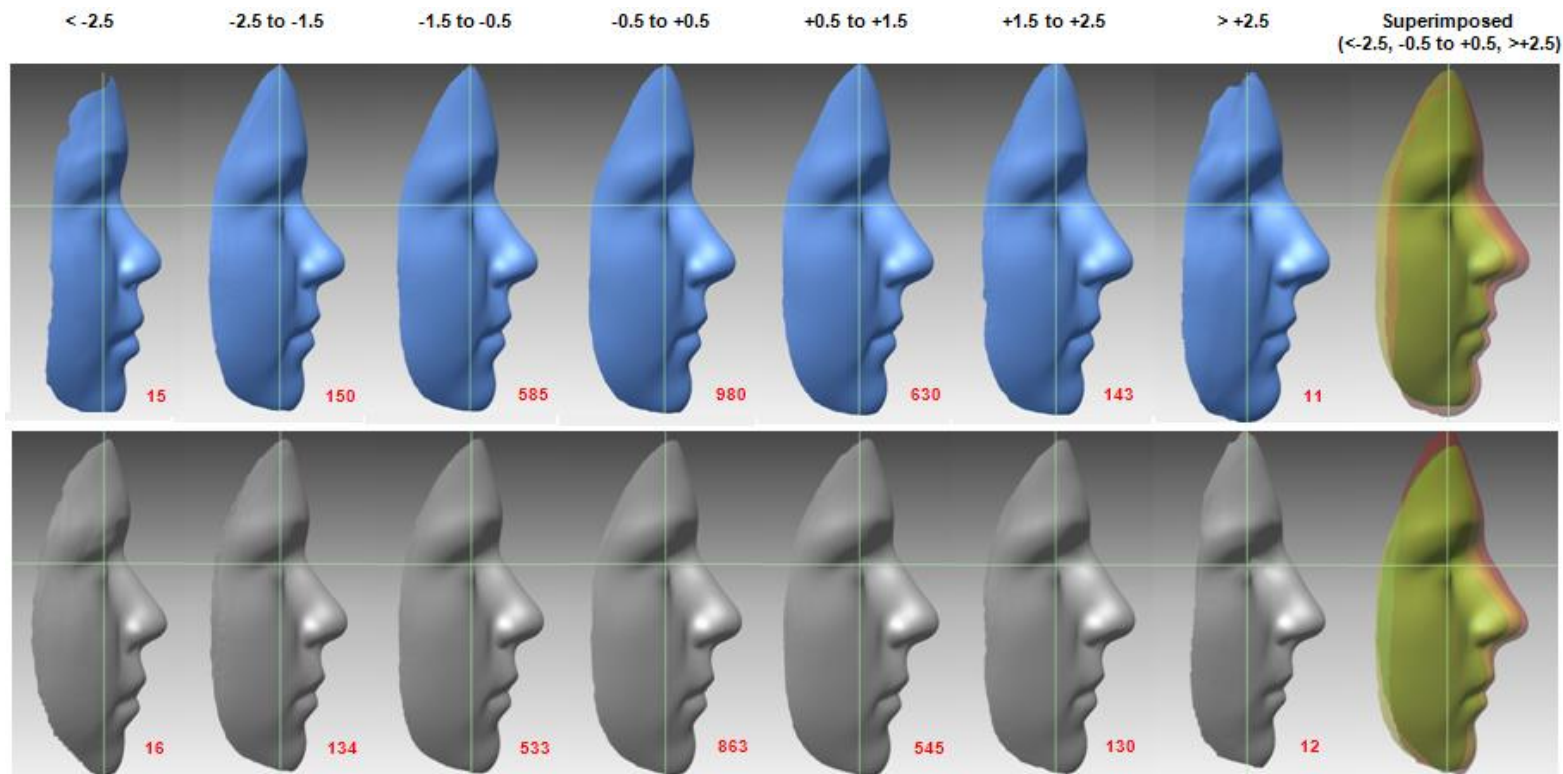


Figure 7.3.

The average faces constructed to show the effect of variation of the n-men 3D distance on the face shape (blue, females; grey, males; the red numbers indicate the number of individuals contributed to each average face). The average faces of the normal group (-0.5 to +0.5 SD) and the extremes (<-2.5 and >+2.5 SD) were superimposed for visual comparison of facial shape (right column), showing that *PAX3* gene affects the nasal bridge prominence phenotype.

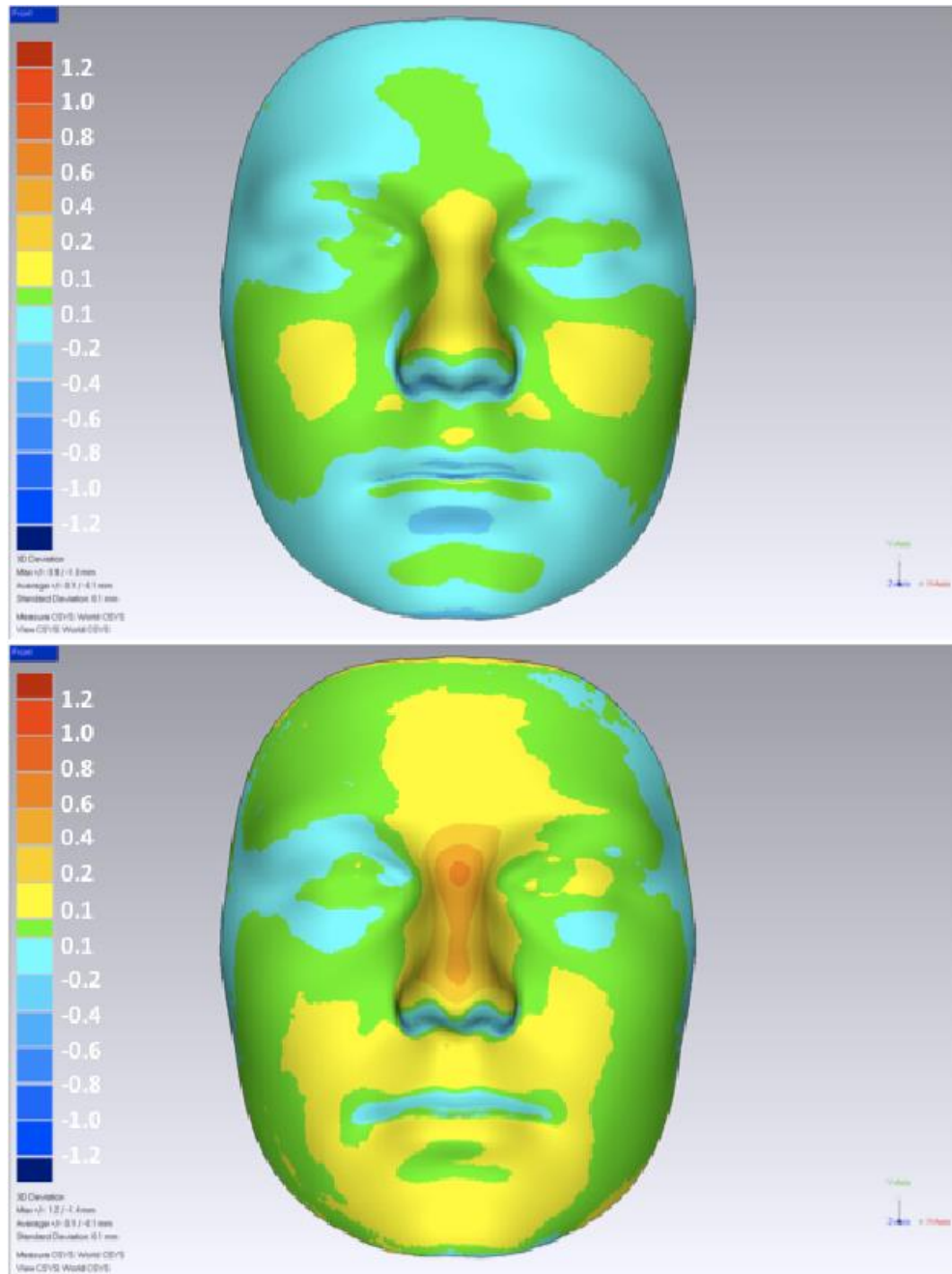


Figure 7.4.  
Superimposition of average phenotypes for *PAX3* different genotypes (G allele): 0 and 1 (top); 0 and 2 (bottom),  
The colour maps indicate the surface distances between the average facial shells (colour scale is shown). The green indicates no difference +/- 0.1mm; blue -0.1 to -0.2mm; yellow 0.1 to 0.2mm; orange 0.2 to 0.4mm and deep orange 0.4 to 0.8mm. The different genotypes show slight influences not only on the nose but also on the forehead, upper lip and chin areas.

## 7.4 Discussion

Twin, family, and animal studies have consistently found that inheritance plays an important role in determining craniofacial morphology. The influence of genetics on facial features is obvious in many families, and familial resemblances for craniofacial structures have been documented in numerous studies as highlighted in Table 2.3. However, good evidence is still lacking in the literature on the association between facial morphological features and genes in a normal population. In genetic studies evaluating the heritability of craniofacial structures, linear and angular measurements have been widely used. These studies have been undertaken using different techniques available to capture and analyse the craniofacial morphology. The traditional 2D measuring techniques using photographs or lateral skull radiographs (cephalometry) tend to be imprecise as facial landmarks are subject to rotational, positional and magnification errors (Houston *et al.*, 1986; Benson and Richmond, 1997). However, the recent innovations in this field have led to the development of non-invasive, optically based, high resolution 3D digitization techniques which have provided the opportunity to better capture the spatial relationship between facial landmarks. In addition, usually the heritability of bone structures (hard tissues) was investigated, and little is known about the influence of genetic factors on facial soft tissue morphology.

Therefore, the current study, which uses a novel 3D measuring technology, provides the opportunity to better capture facial soft tissue structures and determine which genetic variants may influence these structures.

Furthermore, most of the studies reported in Table 2.3 recruited quite small samples of different age and ethnic groups for their analyses in comparison to our study (4747 British adolescents), which is one of the very few studies that use a large sample of one age and one ethnic group to carry out the association analyses. Another issue is the low significant level (p-value) that was adopted by these studies in comparison to our study that considered only genetic associations with a p-value threshold of less than  $5 \times 10^{-8}$ . In addition, the *Bonferroni* correction, which is a conservative method for multiple testing was applied in this study.

Here I would like to refer to the following two recent studies. The first one is by Boehringer *et al.* (2011) who reported that genetic loci involved in non-syndromic cleft lip and palate are also associated with normal variation. The authors found a genetic association with inter-alar width (as measured by 2D photographs,  $p = 6 \times 10^{-4}$ ) in one sample and another association with bizygomatic distance (determined by magnetic resonance imaging,  $p = 0.017$ ) in a separate sample. However, their results were not replicated in the reciprocal populations, which may be due to the difficulty in identifying the same facial landmarks with two different image-capture techniques. The second study is by Liu *et al.* (2012) who identified independent genetic loci associated with different facial phenotypes, suggesting the involvement of 5 candidate genes (*PRDM16*, *PAX3*, *TP63*, *C5orf50*, and *COL17A1*) in the determination of the human face. Their findings at *PAX3* influencing the position of nasion replicate our findings.

In our study, the sample was registered using Procrustes analysis; with this technique, the landmark 3D coordinates were placed in the same space reducing confounding errors (rotation and translation). The scaled n-men distance was generated and the association analysis with the SNP “rs7559271” gave similar results to the un-scaled data analysis indicating that the association does not appear to be driven by size. In addition, the n-men 3D distance was further investigated to determine in which dimension(s) and/or plane(s) the associations were having an effect, and the association was mostly driven by the distance in the yz plane.

Average faces were also used in this study to visualize facial phenotypic variations influenced by genes in the European population. The effect of *PAX3* gene on facial morphology was clearly shown as variation of the nasal bridge prominence phenotype. Short videos were generated to track the effect of variation of the n-men 3D distance on the face shape.

No genome-wide significant associations were observed for any of the principal components. Although principal components capture information on covariance between traits and would be successful in identifying genes that influence these correlated traits, if a genetic variant has a very specific localized effect (as in rs7559271), then this effect will be diluted in a PC analysis. Similar results were obtained by Liu *et al.* (2012).

As mentioned earlier, the reason why we did not include all possible facial parameters in the GWAS study was to avoid being accused of data fishing; however, further GWAS analyses are planned for the future.

Generally, researchers believe that all *PAX3* gene mutations have the same effect: they destroy the ability of the *PAX3* protein to bind to DNA and regulate the activity of other genes to form bones, in addition to other activities. In this study, the SNP rs7559271 in *PAX3* gene was found to be associated with nasal bridge prominence phenotype (n-men distance), rs7559271 is an intronic SNP (common genetic variant) in *PAX3* (paired box 3, MIM 606597). This gene encodes a transcription factor that plays crucial role in fetal development including craniofacial bones (as explained in details in the Literature Review, section **2.10.2.1** Genetic expression in craniofacial development). "*PAX3* is expressed longitudinally down the length of the neural tube from the hindbrain, but only in mitotically active cells of the alar and roof plates, dorsal to the sulcus limitans. These cells are the source of the neural crest. Among neural crest derivatives, *PAX3* expression was seen in the spinal ganglia and some craniofacial cells (*nasal process* and some first and second branchial arch derivatives) (Gerard *et al.*, 1995; Read and Newton, 1997; Terzic and Saraga-Babic, 1999). In general, *PAX* genes are a family of genes coding for tissue specific transcription factors containing a paired domain and usually a partial or complete homeodomain. An octapeptide may also be present. *PAX* proteins are important in development for the specification of specific tissues. Murine *PAX3* (479 amino acids) contains two DNA-binding domains, a paired-box domain (PD) and a homeodomain (HD) (Goulding *et al.*, 1991). The protein made from *PAX3* gene directs the activity of other genes that signal neural crest cells to form specialized tissues or cell

types such as some nerve tissue, bones in the face and skull (craniofacial bones), and pigment-producing cells called melanocytes. *PAX3* gene mutations, e.g. mutations leading to truncation of the paired-box domain (PD) or loss of the homeodomain (HD) (Guo *et al.*, 2010) and mutations producing aberrantly spliced mRNA transcripts (Epstein *et al.*, 1993), eventually may lead to non-functional *PAX3* polypeptides and destroy the ability of the *PAX3* proteins to bind to DNA and regulate the activity of other genes to form bones and other specific tissues". *PAX3* was identified as being involved in Waardenburg syndrome (WS) Type I (MIM 193500) after the identification of a patient with a de novo inversion (inv[2][q35q37.3]) (Tsukamoto *et al.*, 1992). Approximately 85 different *PAX3* point mutations have now been identified in Type I and Type III (MIM 148820) WS patients, approximately half of which are missense and half of which are truncating variants, and most of which are extremely rare (Pingault *et al.*, 2010). This syndrome affects ~1 in 42,000 births (Waardenburg, 1951) and is characterized by deafness; hair, skin, and eye pigmentation abnormalities; as well as (specifically for Type I WS) characteristic facial features like broad, high nasal root and wide spacing of the endocanthi of the eyes "telecanthus" (Read and Newton, 1997).

In summary, in this genome-wide association study of facial morphology, we have identified an association between rs7559271 and nasion position in a population cohort of 15-year-old adolescents. This SNP is within an intron of *PAX3*. Many rare variants in this gene have been associated with Waardenburg syndrome, which has symptoms including wide spacing of

the endocanthi. Therefore, it is of interest that we now report that common variants in this gene are also associated with prominence and vertical position of “nasion” in the general population, although these facial characteristics are different to those reported in Waardenburg syndrome.

Further discussion of the successes and failures in identifying genes influencing facial morphology including likely hits identified in this study but did not reach significance, and the pleiotropic nature of genes will be highlighted in the next chapter (General Discussion).

## **7.5 Conclusions**

A strong genetic association was identified between the common ‘intronic’ SNP rs7559271 in *PAX3* gene on chromosome 2 and the 3D facial distance ‘nasion to mid-endocanthion’ (n-men). Variation in n-men distance reflects variation in the nasal bridge prominence phenotype. Rare variants in this gene have been reported to be associated with Waardenburg syndrome, which presents with facial malformations; therefore, it is now of interest to report that common variants in this gene are also associated with normal variation in facial morphology of the general population. The effect of smooth variation of the n-men 3D distance on the average face shape has been visualised as a set of 61 frames (video) represented by average faces of appropriate statistical groups.

# Chapter 8

## General Discussion

## 8. General Discussion

### 8.1 *Genome-wide association studies: failures and successes*

Looking at the history of research into the genetic basis of common diseases and different observable traits (like height, eye colour, facial features...etc): prior to 2005, the field was largely a scientific wasteland scattered with many un-replicated genetic association studies, with barely a handful of well-validated genetic association hits have been identified. However, in 2005, the first genome-wide association studies (GWAS) emerged from the combination of the hugely successful HapMap project with a new technology for testing hundreds of thousands of single-base genetic variants (SNPs); from 2005 until today, GWAS have rapidly grown in scale and complexity, with studies now looking at over a million genetic markers in cohorts approaching a hundred thousand individuals.

From the outset, the aim of GWAS has been two-fold:

1. Identifying potential genetic markers (SNPs) that can be used to predict individual disease risk and/or observable physical traits; and
2. Highlighting the main molecular pathways underlying common diseases, thereby providing potential targets for therapy.

There is little disagreement in the scientific community that the appearance of GWAS has changed the face of genetic associations: from that handful of genuine associations in 2005, we now have somewhere in the vicinity of 400 regions of the genome displaying replicated associations with around 70 common diseases and complex physical traits.

However, the experts may differ on the issue of whether continuing to increase the scale of GWAS to ever-larger sample sizes is worth the substantial costs, and whether current personal genomics companies like 23andMe, who use GWAS results to provide various genetic associations, are really providing a reliable and valuable service to the community.

Although GWAS have been “strikingly successful” in identifying sites of common genetic variation associated with complex diseases or physical traits, the variants that have been found – both individually and altogether – explain just a small fraction of the overall genetic contribution to common disease risk and physical traits. The major response from researchers performing GWAS has been to continually increase sample sizes, giving them power to reveal variants with ever-smaller effect sizes. However, experts argue that this approach is doomed to failure. Based on what is known about the distribution of effect sizes of risk variants, researchers argue that if common risk variants underlie the totality of genetic risk there must be a ridiculously large number of them; and that means that these variants will provide little useful insight into the biology of a condition. For example, if common variants are responsible for most genetic components of type 2 diabetes, height, and similar traits, then genetics will provide relatively little guidance about the biology of these conditions, because most genes are “height genes” or “type 2 diabetes genes”. However, other experts argue that despite the failure to uncover the majority of the genetic disease risk or physical traits, GWAS have in fact contributed substantially to our understanding of the mechanisms behind these conditions.

Regarding genes influencing facial morphology, only recently GWAS have identified few genes associated with normal variation in facial morphology. The current study (started in October 2008) was the first genome-wide association study of three-dimensional facial morphology to identify genes influencing normal facial variation in the general population, followed by two studies (Boehringer *et al.*, 2011; Liu *et al.*, 2012) highlighted in the previous chapter.

In this study, likely hits (modest associations) were also found in the first round GWAS we carried out for the 14 unscaled principal components. The associations between the common SNP (rs7559271) in *PAX3* gene (associated with n-men distance) and each of the principal components were examined to see whether this SNP was just below the genome-wide significant threshold for any of the PCs. The SNP (rs7559271) showed modest associations with PC5 ( $p = 2 \times 10^{-4}$ ) and PC11 ( $p = 6 \times 10^{-6}$ ). These PCs describe prominence of the eyes relative to the nasal bridge (PC5), and prominence of the upper eyelids (PC11), and so are relevant, but a GWAS of these PCs alone would fail to identify this SNP from the noise further down in the p value distribution.

Although PCs capture information on covariance between traits and would be successful in identifying genes that influence these correlated traits, if a genetic variant has a very specific localized effect (as in rs7559271), then this effect will be diluted in a PC analysis.

Further genetic associations were investigated; the *scaled* PC2 describing ratio of nasion and glabella prominence (relative to eyes) to inner canthi height was shown to be associated with the SNP (rs791623) in *FAM44B* gene (discovery phase,  $p = 5.9 \times 10^{-8}$ ). Unfortunately, this association did not replicate strongly ( $p = 0.4341$ ).

Moreover, in a second round GWAS where all ALSPAC individuals were combined into a discovery set and analysed using additive, dominant and recessive models, more facial parameters were included in this analysis (Table 3, Appendix) in addition to the principal components. Initial findings indicate some exciting associations:

*PAX3*: associated with four nasal bridge traits – additive –  $p = 7 \times 10^{-16}$ , these traits include: distances n-men (the association ‘QQ’ plot is shown in Figure 7 of the Appendix) and sn-men.z, and ratios n-men.z/lis-men.z and n-men.z/li-men.z;

*SKAP2*: associated with six mouth width traits – dominant –  $p = 1 \times 10^{-12}$ , these traits include: unscaled PC10 (Philtrum-to-nose width ratio) and scaled PC17 (philtrum width), distances ls-cphL and cphL-cphR, and ratios ls-cphR/exR-enR and cphL-cphR.x/chL-chR.x – SKAP2 gene is involved in developmental regulation and cellular differentiation; and

*KIF13B*: associated with two nose shape traits – additive –  $p = 2 \times 10^{-10}$ , these traits include: angles n-all-sn and n-all-sn.xy. KIF13B gene may be involved in reorganization of the cortical cytoskeleton.

However, the above genetic associations are still to be validated in further replication studies with other cohorts using: (*Future Work*)

- Exact same measures from 3D data
- Representative measures from 2D data

## **8.2 Pleiotropic nature of genes**

Pleiotropy occurs when one gene (or gene cluster) influences multiple, seemingly unrelated phenotypic traits, consequently, a mutation in a pleiotropic gene may have an effect on some or all traits simultaneously. An example is when a mutation in a gene causes a disease with a wide range of symptoms. Pleiotropy is frequently revealed when the possible genetic contributions to behavioural dysfunctions or manifestations are identified, particularly clearest when a single gene or a small aggregation of genes is affected and relatively diverse consequences are manifested. Pleiotropy has been clearly identified in a wide range of species including humans. Pleiotropic gene action can limit the rate of multivariate evolution when a natural, sexual or artificial selection on one trait favours one specific version of the gene (allele), while selection on other traits favours a different allele.

The underlying mechanism of pleiotropy in most cases is the effect of a gene on metabolic pathways that contribute to different phenotypes. The genetic correlations and hence correlated responses to various selections are most often caused by pleiotropy.

The term 'Polygenic Trait' refers to a trait that can result from the actions of multiple genes; that is when a gene whose individual effect on the phenotype of a single organism is too small to be observed, but which can act together with other genes to produce observable phenotypic variation.

Genome-wide association studies have identified many genetic variants that each affects multiple traits, particularly across autoimmune diseases, cancers and neuropsychiatric disorders, suggesting that pleiotropic effects on human complex traits may be widespread. However, the systematic detection of such effects is challenging and requires new methodologies and frameworks for interpreting cross-phenotype results.

In a recent genome-wide association study of primary tooth eruption, pleiotropic loci have been found associated with height and craniofacial distances (Fatemifar *et al*, 2013). In this study, the authors identified a total of 15 independent loci, with 10 loci reaching a genome-wide significance ( $P < 5 \times 10^{-8}$ ) for 'age at first tooth' and 11 loci for 'number of teeth'. The identified loci included eight previously unidentified loci, some containing genes known to play a role in tooth and other developmental pathways. Three of these loci, containing the genes *HMGA2*, *AJUBA* and *ADK*, also showed evidence of association with craniofacial distances, particularly those indexing facial width. Their results suggest that the genome-wide association approach is a powerful strategy for detecting variants involved in tooth eruption, and potentially craniofacial growth and more generally organ development.

What is particularly important about that study is the number of loci displaying large effect sizes. Typically, GWASs of quantitative traits require tens of thousands of individuals to identify common variants of small effect. However, the tooth eruption phenotype appears to be influenced by some loci of comparably large effect (i.e. >1% of the phenotypic variance), implying that the genome-wide study of primary tooth eruption might be a powerful strategy not only at detecting variants involved in dentition, but also SNPs that may exert pleiotropic actions on other aspects of growth and facial development.

Generally speaking, SNPs with large effect size that found to meet the criteria for genome-wide significance ( $P < 5 \times 10^{-8}$ ) should be investigated for further genetic associations with other related phenotypes (e.g. craniofacial measurements) to find whether these genetic variants exhibit pleiotropic effects on craniofacial morphology in general.

In this study, the intronic SNP rs7559271 (common genetic variant) in *PAX3* (paired box 3, MIM 606597) was found to be associated with nasal bridge prominence phenotype (n-men distance). This gene encodes a transcription factor that plays crucial role in fetal development including craniofacial bones (as explained in details in the Literature Review, section **2.10.2.1** Genetic expression in craniofacial development). Murine *PAX3* (479 amino acids) contains two DNA-binding domains, a paired-box domain (PD) and a homeodomain (HD) (Goulding *et al.*, 1991). The protein made from *PAX3* gene directs the activity of other genes that signal neural crest

cells to form specialized tissues or cell types such as some nerve tissue, bones in the face and skull (craniofacial bones), and pigment-producing cells called melanocytes. *PAX3* gene mutations, e.g. mutations leading to truncation of the paired-box domain (PD) or loss of the homeodomain (HD) (Guo *et al.*, 2010) and mutations producing aberrantly spliced mRNA transcripts (Epstein *et al.*, 1993), eventually may lead to non-functional *PAX3* polypeptides and destroy the ability of the *PAX3* proteins to bind to DNA and regulate the activity of other genes to form bones and other specific tissues.

# Chapter 9

## Conclusions

## Conclusions

- The reproducibility of identifying facial landmarks varies between landmarks. For good reproducibility, a landmark must be unambiguously defined and its definition well understood by the examiner. Landmarks placed on clearly defined contours show higher reproducibility than those placed on flat areas; this may be gender specific.
- To be of clinical use, it must be ensured that the reproducibility of each landmark in all three spatial dimensions (x, y, and z) is sufficiently high.
- Poorer reproducibility was observed in the inter-examiner assessment than intra-examiner assessment.
- The examiner must become familiar with the software program used to view and process the 3D facial scans in order to improve reproducibility of some landmarks (e.g. those associated with the eyes).
- The majority of the x, y, and z coordinates were reproducible to less than 1mm (51% intra-examiner, 45% inter-examiner), which is clinically acceptable. The precision of identifying the 21 facial landmarks ranged from 0.29mm to 1.26mm (error).
- The fact that different facial landmarks show different reproducibility levels should be considered when analysing facial morphology variation. Also landmark variation will affect sample size estimation in determining various differences between population groups.
- 14 PCs were identified for the total ALSPAC sample of 4747 subjects (unscaled dataset), which explained 82% of the total variance in facial form, with the first three components accounting for 46% of the variance and describing face height, width and convexity.

- 15 PCs were identified for males and 16 for females (unscaled dataset). The results generally showed that males and females had similar modes or patterns of facial variation, suggesting that the major components of facial variation do not differ between the genders. However, different PCs positions between males and females indicate different levels of significance of the variation exhibited by different facial features for males and females, though both genders present the same components of facial variation. In addition, size variation between genders was obvious for most derived facial parameters specially face height.
- 17 PCs were identified for the total ALSPAC sample of 4747 subjects (scaled dataset), which explained 82% of the total variance in facial shape, with the first three components accounting for 35% of the variance. Ratios explained most of the shape variance revealed by the first few components (PCs 1, 2, and 4). 18 PCs were identified for males and females, separately.
- The variation in facial form and shape can be accurately quantified and visualized as a multidimensional statistical continuum with respect to the principal components.
- This study presented a novel surface-based method to visualize facial morphology variation using accurate average faces where the individual faces, prior to averaging, were scaled based on the average centroid size.
- This method of facial assessment has the potential to identify and classify faces and facial changes that occur as a result of physical anomalies affecting the growth and development of the face, and inform clinicians of appropriate healthcare interventions for specific facial types.

- This study has demonstrated to what extent gender prediction can be achieved on the sole basis of facial metric information.
- 24 facial parameters were found to provide gender prediction efficiency of over 70%, 23 of these parameters are distances that describe variation in facial height, nose width, and prominence of facial structures (forehead, eyes, nasal bridge, tip of the nose, lips and mouth, and chin). 13 of these distances are related to mid-endocanthion point (men), which suggests it is an important landmark.
- The highest prediction efficiency was provided by the 3D distance ls-men: 80.1% (females), 75.6% (males), and 78% (total prediction efficiency).
- None of the angles were found to predict gender, and only 1 ratio gave prediction efficiency of over 70% in females only.
- These parameters provide a good source of different facial characteristics that can be used in the future for automatic recognition of faces.
- A strong genetic association was identified between the common 'intronic' SNP rs7559271 in *PAX3* gene on chromosome 2 and the 3D facial distance 'nasion to mid-endocanthion' (n-men). Variation in n-men distance reflects variation in the nasal bridge prominence phenotype. Rare variants in this gene have been reported to be associated with Waardenburg syndrome, which presents with facial malformations; therefore, it is now of interest to report that common variants in this gene are also associated with normal variation in facial morphology of the general population. The effect of smooth variation of the n-men 3D distance on the average face shape has been visualised as a set of 61 frames (video) represented by average faces of appropriate statistical groups.

# Chapter 10

## Future Work

### Future Work

- Replicate the genetic associations that were identified in the second round GWAS of all ALSPAC individuals (aged 15 year old) using 3D and 2D measures obtained from other cohorts.
- Explore facial variation among ALSPAC individuals (currently aged 24-25 year olds).
- Explore genotype/phenotype associations in the ALSPAC population (currently aged 24-25 year olds) and try replicating these associations with other cohorts.
- Undertake some gene expression studies to validate the genetic and developmental origin of facial morphology variation, these also include studying the molecular changes in *PAX3* gene caused by different mutations (intronic and exonic SNPs, common and rare) and what these molecular changes might be doing to the structure and function of the encoded protein (transcription factors) that lead to the specific variation in facial morphology.

# Chapter 11

## References

## References

- Abdi H, Valentin D, Edelman B, O'Toole AJ (1995) More about the difference between men and women: evidence from linear neural networks and the principal-component approach. *Perception* 24:539-562
- Abdi H, Williams LJ (2010) Principal component analysis. Wiley Interdisciplinary Reviews: *Computational Statistics* 2:433-459
- Ackermann RR (1997) Three-dimensional imaging in forensic anthropology: a test study using the Macintosh. *Journal of Forensic Sciences* 42:93-99
- Acs N, Banhidy F, Puho E, Czeizel AE (2005) Maternal influenza during pregnancy and risk of congenital abnormalities in offspring. *Birth Defects Research* 73:989-996
- Ahlqvist J, Eliasson S, Welander U (1986) The effect of projection errors on cephalometric length measurements. *European Journal of Orthodontics* 8:141-148
- Al Ali A, Richmond S, Popat H, Toma AM, Playle R, Pickles T, Zhurov AI, Marshall D, Rosin PL, Henderson J (2013) A three-dimensional analysis of the effect of atopy on face shape. *European Journal of Orthodontics*, 2013 Jan 28 [Epub]
- Al Ali A, Richmond S, Popat H, Toma AM, Playle R, Zhurov AI, Marshall D, Rosin PL, Henderson J (2012) The influence of asthma on face shape: a three-dimensional study. *European Journal of Orthodontics*, 2012 Oct 4 [Epub]
- Alavi DG, BeGole EA, Schneider BJ (1988) Facial and dental arch asymmetries in Class II subdivision malocclusion. *American Journal of Orthodontics & Dentofacial Orthopedics* 93:38-46
- Allanson JE (1997) Objective techniques for craniofacial assessment: what are the choices? *American Journal of Medical Genetics* 70:1-5
- Allanson JE, Cole TR (1996) Sotos syndrome: evolution of facial phenotype subjective and objective assessment. [Erratum appears in

*American Journal of Medical Genetics*, 1998; 79:229-230]. *American Journal of Medical Genetics* 65:13-20

- Allanson JE, Hall JG, Hughes HE, Preus M, Witt RD (1985) Noonan syndrome: the changing phenotype. *American Journal of Medical Genetics* 21:507-514
- Allanson JE, Hennekam RC (1997) Rubinstein-Taybi syndrome: objective evaluation of craniofacial structure. *American Journal of Medical Genetics* 71:414-419
- Allanson JE, O'Hara P, Farkas LG, Nair RC (1993) Anthropometric craniofacial pattern profiles in Down syndrome. *American Journal of Medical Genetics* 47:748-752
- Amos CI, Wu X, Broderick P, Gorlov IP, Gu J, Eisen T, Dong Q, Zhang Q, Gu X, Vijayakrishnan J, Sullivan K, Matakidou A, Wang Y, Mills G, Doheny K, Tsai YY, Chen WV, Shete S, Spitz MR, Houlston RS (2008) Genome-wide association scan of tag SNPs identifies a susceptibility locus for lung cancer at 15q25.1. *Nature Genetics* 40:616-622
- Arridge S, Moss JP, Linney AD, James DR (1985) Three dimensional digitization of the face and skull. *Journal of Maxillofacial Surgery* 13:136-143
- Astley SJ, Clarren SK (1996) A case definition and photographic screening tool for the facial phenotype of fetal alcohol syndrome. *Journal of Pediatrics* 129:33-41
- Attanasio C, Nord AS, Zhu Y, Blow MJ, Li Z, Liberton DK, Morrison H, Plajzer-Frick I, Holt A, Hosseini R, Phouanavong S, Akiyama JA, Shoukry M, Afzal V, Rubin EM, FitzPatrick DR, Ren B, Hallgrimsson B, Pennacchio LA, Visel A (2013) Fine tuning of craniofacial morphology by distant-acting enhancers. *Science* 342:1241006
- Aung SC, Ngim RCK, Lee ST (1995) Evaluation Of The Laser Scanner As A Surface Measuring Tool And Its Accuracy Compared With Direct Facial Anthropometric Measurements. *British Journal Of Plastic Surgery* 48:551-558

- Ayoub A, Garrahy A, Hood C, White J, Bock M, Siebert JP, Spencer R, Ray A (2003) Validation of a vision-based, three-dimensional facial imaging system. *Cleft Palate-Craniofacial Journal* 40:523-529
- Ayoub AF, Siebert P, Moos KF, Wray D, Urquhart C, Niblett TB (1998) A vision-based three-dimensional capture system for maxillofacial assessment and surgical planning. *British Journal of Oral & Maxillofacial Surgery* 36:353-357
- Ayoub AF, Wray D, Moos KF, Jin J, Niblett TB, Urquhart C, Mowforth P, Siebert P (1997) A three-dimensional imaging system for archiving dental study casts: a preliminary report. *International Journal of Adult Orthodontics & Orthognathic Surgery* 12:79-84
- Ayoub AF, Wray D, Moos KF, Siebert P, Jin J, Niblett TB, Urquhart C, Mowforth R (1996) Three-dimensional modeling for modern diagnosis and planning in maxillofacial surgery. *International Journal of Adult Orthodontics & Orthognathic Surgery* 11:225-233
- Badam RK, Manjunath M, Rani MS (2012) Determination of Sex by Discriminant Function Analysis of Lateral Radiographic Cephalometry. *Journal of Indian Academy of Oral Medicine & Radiology* 23:179-183
- Baik HS, Jeon JM, Lee HJ (2007) Facial soft-tissue analysis of Korean adults with normal occlusion using a 3-dimensional laser scanner. *American Journal of Orthodontics & Dentofacial Orthopedics* 131:759-766
- Baik HS, Lee HJ, Lee KJ (2006) A proposal for soft tissue landmarks for craniofacial analysis using 3-dimensional laser scan imaging. *World Journal of Orthodontics* 7:7-14
- Balding DJ (2006) A tutorial on statistical methods for population association studies. *Nature Reviews Genetics* 7:781-791
- Barr FG, Galili N, Holick J, Biegel JA, Rovera G, Emanuel BS (1993) Rearrangement of the PAX3 paired box gene in the paediatric solid tumour alveolar rhabdomyosarcoma. *Nature Genetics* 3:113-117
- Barrett JC, Fry B, Maller J, Daly MJ (2005) Haploview: analysis and visualization of LD and haplotype maps. *Bioinformatics* 21:263-265

- Baumrind S (2001) Integrated three-dimensional craniofacial mapping: background, principles, and perspectives. *Seminars in Orthodontics* 7:223-232
- Baumrind S, Frantz RC (1971a) The reliability of head film measurements. 1. Landmark identification. *American Journal of Orthodontics* 60:111-127
- Baumrind S, Frantz RC (1971b) The reliability of head film measurements. 2. Conventional angular and linear measures. *American Journal of Orthodontics* 60:505-517
- Baumrind S, Moffitt F (1972) Mapping the skull in 3-d. *Journal - California Dental Association* 48:22-31
- Baumrind S, Moffitt FH, Curry S (1983a) The geometry of three-dimensional measurement from paired coplanar x-ray images. *American Journal of Orthodontics* 84:313-322
- Baumrind S, Moffitt FH, Curry S (1983b) Three-dimensional x-ray stereometry from paired coplanar images: a progress report. *American Journal of Orthodontics* 84:292-312
- Baydas B, Erdem A, Yavuz I, Ceylan I (2007) Heritability of facial proportions and soft-tissue profile characteristics in Turkish Anatolian siblings. *American Journal of Orthodontics & Dentofacial Orthopedics* 131:504-509
- Beales PL, Warner AM, Hitman GA, Thakker R, Flintner FA (1997) Bardet-Biedl syndrome: a molecular and phenotypic study of 18 families. *Journal of Medical Genetics* 34:92-98
- Beaty TH, Murray JC, Marazita ML, Munger RG, Ruczinski I, Hetmanski JB, Liang KY, Wu T, Murray T, Fallin MD et al (2010) A genome-wide association study of cleft lip with and without cleft palate identifies risk variants near MAFB and ABCA4. *Nature Genetics* 42:525-529
- Benson PE, Richmond S (1997) A critical appraisal of measurement of the soft tissue outline using photographs and video. *European Journal of Orthodontics* 19:397-409

- Beraldin J-A, El-Hakim SF, Blais F (1995) Performance evaluation of three active vision systems built at the National Research Council of Canada. *In Proceedings of the Optical 3D Measurement Techniques III*, NRC Technical Report 39165. Vienna: pp. 352–361
- Berkowitz S, Cuzzi J (1977) Biostereometric analysis of surgically corrected abnormal faces. *American Journal of Orthodontics* 72:526-538
- Bernardini F, Rushmeier H (2002) The 3D Model Acquisition Pipeline. *Computer Graphics Forum* 21:149–172
- Berrios GE (2003) The face in medicine and psychology: A conceptual history. In Katsikitis M (Ed) *The human face: Measurement and meaning*, Springer Science+Business Media New York, pp 49–62
- Besl PJ, McKay ND (1992) A method for registration of 3-D shapes. *IEEE Transactions on Pattern Analysis and Machine Intelligence* 14:239-256
- Biggerstaff RH (1977) Craniofacial characteristics as determinants of age, sex, and race in forensic dentistry. *Dental Clinics of North America* 21:85-97
- Bill JS, Reuther JF, Dittmann W, Kubler N, Meier JL, Pistner H, Wittenberg G (1995) Stereolithography in oral and maxillofacial operation planning. *International Journal of Oral & Maxillofacial Surgery* 24:98-103
- Binnal A, Devi BKY (2012) Identification of Sex using Lateral Cephalogram: Role of Cephalofacial Parameters. *Journal of Indian Academy of Oral Medicine and Radiology* 24:280-283
- Birkeland K, Boe OE, Wisth PJ (2000) Relationship between occlusion and satisfaction with dental appearance in orthodontically treated and untreated groups. A longitudinal study. *European Journal of Orthodontics* 22:509-518
- Bjorn H, Lundquist C, Hjelstrom P (1954) A photogrammetric method of measuring the volume of facial swellings. *Journal of Dental Research* 33:295-308
- Bland JM, Altman DG (1986) Statistical methods for assessing agreement between two methods of clinical measurement. [Reprint in

- International Journal of Nursing Studies*, 2010; 47:931-936]. *Lancet* 1:307-310
- Bland JM, Altman DG (2010) Statistical methods for assessing agreement between two methods of clinical measurement. *International Journal of Nursing Studies* 47:931-936
  - Blumenbach JF (1776) MD thesis, De generis humani varietate nativa [On the Natural Varieties of Mankind], University of Göttingen, first published in 1776.
  - Boehringer S, van der Lijn F, Liu F, Gunther M, Sinigerova S, Nowak S, Ludwig KU, Herberz R, Klein S, Hofman A, Uitterlinden AG, Niessen WJ, Breteler MM, van der Lugt A, Wurtz RP, Nothen MM, Horsthemke B, Wieczorek D, Mangold E, Kayser M (2011) Genetic determination of human facial morphology: links between cleft-lips and normal variation. *European Journal of Human Genetics* 19:1192-1197
  - Bookstein FL (1986) Size and shape spaces for landmark data in two dimensions. *Statistical Science* 1:181–242
  - Bookstein FL (1989) Principal Warps: Thin-Plate Splines and the Decomposition of Deformations", *IEEE Transactions on Pattern Analysis and Machine Intelligence* 11:567-585
  - Bookstein FL (1991a) Four metrics for image variation. *Progress in Clinical & Biological Research* 363:227-240
  - Bookstein FL (1991b) Morphometric tools for landmark data, Cambridge University Press, Cambridge
  - Bookstein FL, Grayson B, Cutting CB, Kim HC, McCarthy JG (1991) Landmarks in three dimensions: reconstruction from cephalograms versus direct observation. *American Journal of Orthodontics & Dentofacial Orthopedics* 100:133-140
  - Borman H, Ozgur F, Gursu G (1999) Evaluation of soft-tissue morphology of the face in 1,050 young adults. *Annals Of Plastic Surgery* 42:280-288
  - Bourgeois P, Bolcato-Bellemin AL, Danse JM, Bloch-Zupan A, Yoshida K, Stoetzel C et al (1998) The variable expressivity and incomplete penetrance of the twist-null heterozygous mouse phenotype resemble

- those of human Saethre-Chotzen syndrome. *Human Molecular Genetics* 7:945-957
- Bourne C, Kerr W, Ayoub A (2001) Development of a three-dimensional imaging system for analysis of facial change. *Clinical Orthodontics & Research* 4:105-111
  - Bozic M, Kau CH, Richmond S, Hren NI, Zhurov A, Udovic M, Melink S, Ovsenik M (2009) Facial morphology of Slovenian and Welsh white populations using 3-dimensional imaging. *Angle Orthodontist* 79:640-645
  - Bozic M, Kau CH, Richmond S, Ovsenik M, Hren NI (2010) Novel method of 3-dimensional soft-tissue analysis for Class III patients. *American Journal of Orthodontics & Dentofacial Orthopedics* 138:758-769
  - Bresolin D, Shapiro PA, Shapiro GG, Chapko MK, Dassel S (1983) Mouth breathing in allergic children: its relationship to dentofacial development. *American Journal of Orthodontics* 83:334-340
  - Brewster U, Trivedi SS, Tuy HK, Udupa JK (1984) Interactive surgical planning. *IEEE Computer Graphics And Applications* 4:31-40
  - Broadbent BH (1931) A new X-ray technique and its application to orthodontia. *Angle Orthodontist* 1:45-66
  - Broadbent BH, Broadbent BJ, Golden WH (1975) Bolton standards of dentofacial developmental growth, CV Mosby Co., St Louis
  - Brown T, Abbott AH (1989) Computer-assisted location of reference points in three dimensions for radiographic cephalometry. *American Journal of Orthodontics & Dentofacial Orthopedics* 95:490-498
  - Bruce V, Burton AM, Hanna E, Healey P, Mason O, Coombes A, Fright R, Linney A (1993) Sex discrimination: how do we tell the difference between male and female faces? *Perception* 22:131-152
  - Bugaighis I, Mattick CR, Tiddeman B, Hobson R (2013) Three-dimensional gender differences in facial form of children in the North East of England. *European Journal of Orthodontics* 35:295-304
  - Bugaighis I, O'Higgins P, Tiddeman B, Mattick C, Ben Ali O, Hobson R (2010) Three-dimensional geometric morphometrics applied to the

- study of children with cleft lip and/or palate from the North East of England. *European Journal of Orthodontics* 32:514-521
- Bugaighis I, Tiddeman B, Mattick CR, Hobson R (2012) 3D comparison of average faces in subjects with oral clefts. *European Journal of Orthodontics*, 2012 Nov 20 [Epub]
  - Burke PH, Beard FH (1967a) Stereophotogrammetry of the face. A preliminary investigation into the accuracy of a simplified system evolved for contour mapping by photography. *American Journal of Orthodontics* 53:769-782
  - Burke PH, Beard LF (1967b) Stereo-photogrammetry of the face. Report of the Congress; *European Orthodontic Society*:279-293
  - Burton AM, Bruce V, Dench N (1993) What's the difference between men and women? Evidence from facial measurement. *Perception* 22:153-176
  - Bush K, Antonyshyn O (1996) Three-dimensional facial anthropometry using a laser surface scanner: validation of the technique. *Plastic & Reconstructive Surgery* 98:226-235
  - Callaerts P, Halder G, Gehring WJ (1997) PAX-6 in development and evolution. *Annual Review of Neuroscience* 20:483-532
  - Caloss R, Atkins K, Stella JP (2007) Three-dimensional imaging for virtual assessment and treatment simulation in orthognathic surgery. *Oral & Maxillofacial Surgery Clinics of North America* 19:287-309
  - Camper P (1770) Two lectures to the Amsterdam Drawing society on the facial angle. Facial Angles refers to the content of two lectures on this subject by the Amsterdam professor of anatomy Peter Camper on the 1st and 8 August in 1770 to the Amsterdam Drawing Academy called the Teken-akademie
  - Cao D, Chen C, Piccirilli M, Adjeroh D, Bourlai T, Ross A (2011) Can facial metrology predict gender? *In International Joint Conference on Biometrics (IJCB)*, 2011, pp 1-8. Washington DC, USA
  - Cardon LR, Bell JI (2001) Association study designs for complex diseases. *Nature Reviews Genetics* 2:91-99

- Carels C, Van Cauwenberghe N, Savoye I, Willems G, Loos R, Derom C, Vlietinck R (2001) A quantitative genetic study of cephalometric variables in twins. *Clinical Orthodontics & Research* 4:130-140
- Cargill M, Altshuler D, Ireland J, Sklar P, Ardlie K, Patil N, Shaw N, Lane CR, Lim EP, Kalyanaraman N, Nemesh J, Ziaugra L, Friedland L, Rolfe A, Warrington J, Lipshutz R, Daley GQ, Lander ES (1999) Characterization of single-nucleotide polymorphisms in coding regions of human genes. [Erratum appears in *Nature Genetics*, 1999; 23:373]. *Nature Genetics* 22:231-238
- Cavalcanti Mde G, Antunes JL (2002) 3D-CT imaging processing for qualitative and quantitative analysis of maxillofacial cysts and tumors. *Pesquisa Odontologica Brasileira = Brazilian Oral Research* 16:189-194
- Chanock SJ, Manolio T, Boehnke M, Boerwinkle E, Hunter DJ *et al.* (2007) Replicating genotype-phenotype associations. *Nature* 447:655-660
- Chen LH, Iizuka T (1995) Evaluation and prediction of the facial appearance after surgical correction of mandibular hyperplasia. *International Journal of Oral & Maxillofacial Surgery* 24:322-326
- Chen W, Liang L, Abecasis GR (2009) GWAS GUI: graphical browser for the results of whole-genome association studies with high-dimensional phenotypes. *Bioinformatics* 25:284-285
- Claes P, Liberton DK, Daniels K, Rosana KM, Quillen EE, Pearson LN, McEvoy B, Bauchet M, Zaidi AA, Yao W *et al* (2014) Modeling 3D facial shape from DNA. *PLoS Genetics* 10:e1004224
- Cleall JF, BeGole EA, Chebib FS (1979) Craniofacial morphology: a principal component analysis. *American Journal of Orthodontics* 75:650-666
- Cliff N (1988) The eigenvalues-greater-than-one rule and the reliability of components. *Psychological Bulletin* 103:276-279
- Coblentz A, Mollard R, Ignazi G (1991) 3-Dimensional Face Shape-Analysis Of French Adults, And Its Application To The Design Of Protective Equipment. *Ergonomics* 34:497-517

- Cobourne MT (2000) Construction for the modern head: current concepts in craniofacial development. *Journal of Orthodontics* 27:307-314
- Cohen MM, Jr, Richieri-Costa A, Guion-Almeida ML, Saavedra D (1995) Hypertelorism: interorbital growth, measurements, and pathogenetic considerations. *International Journal of Oral & Maxillofacial Surgery* 24:387-395
- Compton MT, Brudno J, Kryda AD, Bollini AM, Walker EF (2007) Facial measurement differences between patients with schizophrenia and non-psychiatric controls. *Schizophrenia Research* 93:245-252
- Cookson W, Liang L, Abecasis G, Moffatt M, Lathrop M (2009) Mapping complex disease traits with global gene expression. *Nature Reviews Genetics* 10:184-194
- Corruccini RS (1991) Anthropological aspects of orofacial and occlusal variations and anomalies. In: Kelley MA and Larsen CS (eds.) *Advances in Dental Anthropology*. New York, NY: Wiley-Liss Inc.; 295-323
- Corruccini RS (1999) How Anthropology Informs the Orthodontic Diagnosis of Malocclusion's Causes. Lewiston, NY: The Edwin Mellen Press.
- Corruccini RS, Flander LB, Kaul SS (1985) Mouth breathing, occlusion, and modernization in a north Indian population. An epidemiologic study. *Angle Orthodontist* 55:190-196
- Coward TJ, Watson RM, Scott BJJ (1997) Laser scanning for the identification of repeatable landmarks of the ears and face. *British Journal Of Plastic Surgery* 50:308-314
- Cutting C, Bookstein FL, Grayson B, Fellingham L, McCarthy JG (1985) Three-dimensional computer-assisted optimization and interaction with cephalometric and CT-based models. *Plastic & Reconstructive Surgery* 77:877-885
- Cutting CB, McCarthy JG, Karron DB (1988) Three-dimensional input of body surface data using a laser light scanner. *Annals of Plastic Surgery* 21:38-45

- Dalal AB, Phadke SR (2007) Morphometric analysis of face in dysmorphology. *Computer Methods & Programs in Biomedicine* 85:165-172
- De Greef S, Willems G (2005) Three-dimensional cranio-facial reconstruction in forensic identification: Latest progress and new tendencies in the 21st century. *Journal Of Forensic Sciences* 50:12-17
- DeCarlo D, Metaxas D, Stone M (1998) An Anthropometric Face Model using Variational Techniques. *In Proceedings SIGGRAPH 1998*. pp. 67-74
- Deli R, Di Gioia E, Galantucci LM, Percoco G (2010) Automated landmark extraction for orthodontic measurement of faces using the 3-camera photogrammetry methodology. *Journal of Craniofacial Surgery* 21:87-93
- Deng J, Newton NM, Hall-Craggs MA, Shirley RA, Linney AD, Lees WR, Rodeck CH, McGrouther DA (2000) Novel technique for three-dimensional visualisation and quantification of deformable, moving soft-tissue body parts. *Lancet* 356:127-131
- DiLiberti JH, Olson DP (1991) Photogrammetric evaluation in clinical genetics: theoretical considerations and experimental results. *American Journal of Medical Genetics* 39:161-166
- Dixon AL, Liang L, Moffatt MF, Chen W, Heath S, Wong KC, Taylor J, Burnett E, Gut I, Farrall M, Lathrop GM, Abecasis GR, Cookson WO (2007) A genome-wide association study of global gene expression. *Nature Genetics* 39:1202-1207
- Djordjevic J, Lewis BM, Donaghy CE, Zhurov AI, Knox J, Hunter L, Richmond S (2012) Facial shape and asymmetry in 5-year-old children with repaired unilateral cleft lip and/or palate: an exploratory study using laser scanning. *European Journal of Orthodontics*, 2012 Oct 4 [Epub]
- Dohmoto A, Shimizu K, Asada Y, Maeda T (2002) Quantitative trait loci on chromosomes 10 and 11 influencing mandible size of SMXA RI mouse strains. *Journal of Dental Research* 81:501-504

- Dollfus H, Verloes A (2004) Dysmorphology and the orbital region: a practical clinical approach. *Survey of Ophthalmology* 49:547-561
- Dooley M (1982) Anthropometric Modeling Programs - A Survey. *IEEE Computer Graphics And Applications* 2:17-25
- Duffy S, Noar JH, Evans RD, Sanders F (2000) Three-dimensional analysis of the child cleft face. *Cleft Palate-Craniofacial Journal* 37:137-144
- Edelman B, Valentin D, Abdi H (1998) Sex Classification of Face Areas: How Well Can a Linear Neural Network Predict Human Performance? *Journal of Biological Systems* 6:241-263
- Eguchi S, Townsend GC, Richards LC, Hughes T, Kasai K (2004) Genetic contribution to dental arch size variation in Australian twins. *Archives of Oral Biology* 49:1015-1024
- El-Bialy T, Aboul-Azm SF, El-Sakhawy M (2000) Study of craniofacial morphology and skeletal maturation in juvenile diabetics (Type I). *American Journal of Orthodontics & Dentofacial Orthopedics* 118:189-195
- Elliott M, Maher ER (1994) Beckwith-Wiedemann syndrome. *Journal of Medical Genetics* 31:560-564
- Enciso R, Shaw A, Neumann U, Mah J (2003) 3D head anthropometric analysis. SPIE Medical Imaging, San Diego, CA
- Enlow DH (1982) Handbook of facial growth. Philadelphia, PA: W B Saunders
- Epstein CJ (1995) The new dysmorphology: application of insights from basic developmental biology to the understanding of human birth defects. *Proceedings of the National Academy of Sciences of the United States of America* 92:8566-8573
- Epstein DJ, Vogán KJ, Trasler DG, Gros P (1993) A mutation within intron 3 of the Pax-3 gene produces aberrantly spliced mRNA transcripts in the splotch (Sp) mouse mutant. *Proceedings of the National Academy of Sciences of the United States of America* 90:532-536

- Ercan I, Ozdemir ST, Etoz A, Sigirli D, Tubbs RS, Loukas M, Guney I (2008) Facial asymmetry in young healthy subjects evaluated by statistical shape analysis. *Journal of Anatomy* 213:663-669
- Eriksson N, Do CB, Tung JY, Kiefer AK, Hinds DA, Mountain JL, Francke U (2012) Over 250 novel associations with human morphological traits. 23andMe, Mountain View, CA. [In: *American Society of Human Genetics Annual Meeting*, 2012 Nov, San Francisco, CA]
- Farkas LG (1994) Anthropometry of the head and face. New York: Raven Press (2nd edition)
- Farkas LG, Cheung G (1981) Facial asymmetry in healthy North American Caucasians. An anthropometrical study. *Angle Orthodontist* 51:70-77
- Farkas LG, Forrest CR, Litsas L (2000) Revision of neoclassical facial canons in young adult Afro-Americans. *Aesthetic Plastic Surgery* 24:179-184
- Farkas LG, Hajnis K, Posnick JC (1993) Anthropometric and anthroposcopic findings of the nasal and facial region in cleft patients before and after primary lip and palate repair. *Cleft Palate-Craniofacial Journal* 30:1-12
- Farkas LG, Katic MJ, Forrest CR, Alt KW, Bagic I, Baltadjiev G, Cunha E, Cvicelová M, Davies S, Erasmus I *et al.* (2005) International anthropometric study of facial morphology in various ethnic groups/races. *Journal Of Craniofacial Surgery* 16:615-646
- Farkas LG, Kolar JC (1987a) Anthropometric guidelines in cranio-orbital surgery. *Clinics in Plastic Surgery* 14:1-16
- Farkas LG, Kolar JC (1987b) Anthropometrics and art in the aesthetics of women's faces. *Clinics in Plastic Surgery* 14:599-616
- Farkas LG, Munro IR (1987) Anthropometric facial Proportions in Medicine. Springfield, IL: Thomas Books
- Farkas LG, Ross RB, Posnick JC, Indech GD (1989) Orbital measurements in 63 hypertelorhic patients. Differences between the

- anthropometric and cephalometric findings. *Journal of Cranio-Maxillo-Facial Surgery* 17:249-254
- Farrell K (2011) A critical evaluation of facial characteristics and their association with anti-social behaviour and psychosis. Thesis (MScD), Cardiff University
  - Fatemifar G, Hoggart CJ, Paternoster L, Kemp JP, Prokopenko I, Horikoshi M, Wright VJ, Tobias JH, Richmond S, Zhurov AI, Toma AM *et al.* (2013) Genome-wide association study of primary tooth eruption identifies pleiotropic loci associated with height and craniofacial distances. *Human Molecular Genetics* 22:3807-3817
  - Feingold M, Bossert WH (1974) Normal values for selected physical parameters: an aid to syndrome delineation. *Birth Defects: Original Article Series* 10:1-16
  - Fellous JM (1997) Gender discrimination and prediction on the basis of facial metric information. *Vision Research* 37:1961-1973
  - Ferrario VF, Sforza C, Ciusa V, Dellavia C, Tartaglia GM (2001) The effect of sex and age on facial asymmetry in healthy subjects: a cross-sectional study from adolescence to mid-adulthood. *Journal of Oral & Maxillofacial Surgery* 59:382-388
  - Ferrario VF, Sforza C, Pizzini G, Vogel G, Miani A (1993) Sexual dimorphism in the human face assessed by euclidean distance matrix analysis. *Journal of Anatomy* 183:593-600
  - Ferrario VF, Sforza C, Poggio CE, Schmitz JH (1997) Three-dimensional study of growth and development of the nose. *Cleft Palate-Craniofacial Journal* 34:309-317
  - Ferrario VF, Sforza C, Poggio CE, Schmitz JH (1998a) Craniofacial growth: a three-dimensional soft-tissue study from 6 years to adulthood. *Journal of Craniofacial Genetics & Developmental Biology* 18:138-149
  - Ferrario VF, Sforza C, Poggio CE, Schmitz JH (1998b) Facial volume changes during normal human growth and development. *Anatomical Record* 250:480-487

- Ferrario VF, Sforza C, Poggio CE, Schmitz JH (1999a) Soft-tissue facial morphometry from 6 years to adulthood: a three-dimensional growth study using a new modeling. *Plastic & Reconstructive Surgery* 103:768-778
- Ferrario VF, Sforza C, Poggio CE, Serrao G (1996a) Facial three-dimensional morphometry. *American Journal of Orthodontics & Dentofacial Orthopedics* 109:86-93
- Ferrario VF, Sforza C, Poggio CE, Tartaglia G (1994a) Distance from symmetry: a three-dimensional evaluation of facial asymmetry. *Journal of Oral & Maxillofacial Surgery* 52:1126-1132
- Ferrario VF, Sforza C, Puleo A, Poggio CE, Schmitz JH (1996b) Three-dimensional facial morphometry and conventional cephalometrics: a correlation study. *International Journal of Adult Orthodontics & Orthognathic Surgery* 11:329-338
- Ferrario VF, Sforza C, Schmitz JH, Santoro F (1999b) Three-dimensional facial morphometric assessment of soft tissue changes after orthognathic surgery. *Oral Surgery Oral Medicine Oral Pathology Oral Radiology & Endodontics* 88:549-556
- Ferrario VF, Sforza C, Serrao G, Ciusa V, Dellavia C (2003) Growth and aging of facial soft tissues: A computerized three-dimensional mesh diagram analysis. *Clinical Anatomy* 16:420-433
- Ferrario VF, Sforza C, Serrao G, Colombo A, Ciusa V (1999c) Soft tissue facial growth and development as assessed by the three-dimensional computerized mesh diagram analysis. *American Journal of Orthodontics & Dentofacial Orthopedics* 116:215-228
- Ferrario VF, Sforza C, Serrao G, Puletto S, Bignotto M, Tartaglia G (1994b) Comparison of soft tissue facial morphometry in children with Class I and Class II occlusions. *International Journal of Adult Orthodontics & Orthognathic Surgery* 9:187-194
- Firnberg N, Neubuser A (2002) FGF signaling regulates expression of Tbx2, Erm, Pea3, and Pax3 in the early nasal region. *Developmental Biology* 247:237-250

- Frayling TM, Timpson NJ, Weedon MN, Zeggini E, Freathy RM, Lindgren CM, Perry JR, Elliott KS, Lango H, Rayner NW *et al.* (2007) A common variant in the FTO gene is associated with body mass index and predisposes to childhood and adult obesity. *Science* 316:889-894
- Gerard M, Abitbol M, Delezoide AL, Dufier JL, Mallet J, Vekemans M (1995) PAX-genes expression during human embryonic development, a preliminary report. *Comptes Rendus de L'Academie des Sciences - Serie Iii, Sciences de la Vie* 318:57-66
- Gnanaprakasam C, Sumathi S, Malini RR (2010) Average-half-face in 2D and 3D using wavelets for face recognition. *In Proceedings of the 9th WSEAS international conference on Signal processing*. Catania, Italy, World Scientific and Engineering Academy and Society (WSEAS), pp 107-112
- Golding J, Pembrey M, Jones R, Team AS (2001) ALSPAC--the Avon Longitudinal Study of Parents and Children. I. Study methodology. *Paediatric and Perinatal Epidemiology* 15:74-87
- Gordon C (1989) 1988 anthropometric survey of U.S. Army personnel: methods and summary statistics. *In, United States Army Natick Research, Development and Engineering Center*
- Gorlin RJ, Cohen MM, Hennekam RCM (2001) Syndromes of the head and neck. Oxford University Press, New York
- Goulding MD, Chalepakis G, Deutsch U, Erselius JR, Gruss P (1991) Pax-3, a novel murine DNA binding protein expressed during early neurogenesis. *EMBO Journal* 10:1135-1147
- Graber TM (1946) Patient Photography in Orthodontics\*. *The Angle Orthodontist* 16:17-43
- Graham R, Sampson R (1973) Moire Topography. *British Journal of Photography* 120:864-867
- Grayson B, Cutting C, Bookstein FL, Kim H, McCarthy JG (1988) The three-dimensional cephalogram: theory, technique, and clinical application. *American Journal of Orthodontics & Dentofacial Orthopedics* 94:327-337
- Gruss P, Walther C (1992) Pax in development. *Cell* 69:719-722

- Guan W, Liang L, Boehnke M, Abecasis GR (2009) Genotype-based matching to correct for population stratification in large-scale case-control genetic association studies. *Genetic Epidemiology* 33:508-517
- Guo J, Mei X, Tang K (2013) Automatic landmark annotation and dense correspondence registration for 3D human facial images. *BMC Bioinformatics* 14:232
- Guo XL, Ruan HB, Li Y, Gao X, Li W (2010) Identification of a novel nonsense mutation on the Pax3 gene in ENU-derived white belly spotting mice and its genetic interaction with c-Kit. *Pigment Cell & Melanoma Research* 23:252-262
- Guttman L (1954) Some necessary conditions for common factor analysis. *Psychometrika* 19:149-161
- Gwilliam JR, Cunningham SJ, Hutton T (2006) Reproducibility of soft tissue landmarks on three-dimensional facial scans. *European Journal of Orthodontics* 28:408-415
- Hajeer MY, Ayoub AF, Millett DT (2004a) Three-dimensional assessment of facial soft-tissue asymmetry before and after orthognathic surgery. *British Journal of Oral & Maxillofacial Surgery* 42:396-404
- Hajeer MY, Ayoub AF, Millett DT, Bock M, Siebert JP (2002) Three-dimensional imaging in orthognathic surgery: the clinical application of a new method. *International Journal of Adult Orthodontics & Orthognathic Surgery* 17:318-330
- Hajeer MY, Millett DT, Ayoub AF, Siebert JP (2004b) Applications of 3D imaging in orthodontics: part I. *Journal of Orthodontics* 31:62-70
- Hajeer MY, Millett DT, Ayoub AF, Siebert JP (2004c) Applications of 3D imaging in orthodontics: part II. *Journal of Orthodontics* 31:154-162
- Halazonetis DJ (2007) Morphometric evaluation of soft-tissue profile shape. *American Journal of Orthodontics & Dentofacial Orthopedics* 131:481-489
- Halushka MK, Fan JB, Bentley K, Hsie L, Shen N, Weder A, Cooper R, Lipshutz R, Chakravarti A (1999) Patterns of single-nucleotide

polymorphisms in candidate genes for blood-pressure homeostasis. *Nature Genetics* 22:239-247

- Hammond P, Hindocha N, Hutton TJ, Beales PL (2003a) 3D dense surface modeling defines a characteristic facial phenotype in Bardet-Biedl syndrome [Proceedings paper]. *In 53rd Annual Meeting of the American Society of Human Genetics*, Los Angeles, Nov 2003, *American Journal of Human Genetics* 73:284
- Hammond P, Hutton TJ, Allanson JA, Smith ACM (2003b) The 3D face of Smith-Magenis syndrome (SMS): a study using dense surface models [Proceedings paper]. *In European Human Genetics Conference 2003*, Birmingham, *European Journal of Human Genetics* 11:102
- Hammond P, Hutton TJ, Allanson JE, Buxton B, Campbell LE, Clayton-Smith J, Donnai D, Karmiloff-Smith A, Metcalfe K, Murphy KC *et al.* (2005) Discriminating power of localized three-dimensional facial morphology. *American Journal of Human Genetics* 77:999-1010
- Hammond P, Hutton TJ, Allanson JE, Campbell LE, Hennekam RC, Holden S, Patton MA, Shaw A, Temple IK, Trotter M, Murphy KC, Winter RM (2004) 3D analysis of facial morphology. *American Journal of Medical Genetics Part A* 126:339-348
- Hammond P, Suttie M (2012) Large-scale objective phenotyping of 3D facial morphology. *Human Mutation* 33:817-825
- Haraguchi S, Takada K, Yasuda Y (2002) Facial asymmetry in subjects with skeletal Class III deformity. *Angle Orthodontist* 72:28-35
- Hardie S, Hancock P, Rodway P, Penton-Voak I, Carson D, Wright L (2005) The enigma of facial asymmetry: is there a gender-specific pattern of facedness? *Laterality* 10:295-304
- Harris EF, Johnson MG (1991) Heritability of craniometric and occlusal variables: a longitudinal sib analysis. *American Journal of Orthodontics & Dentofacial Orthopedics* 99:258-268
- Harrison JA, Nixon MA, Fright WR, Snape L (2004) Use of hand-held laser scanning in the assessment of facial swelling: a preliminary study. *British Journal Of Oral & Maxillofacial Surgery* 42:8-17

- He S, Hartsfield JK, Jr., Guo Y, Cao Y, Wang S, Chen S (2012) Association between CYP19A1 genotype and pubertal sagittal jaw growth. *American Journal of Orthodontics & Dentofacial Orthopedics* 142:662-670
- Heike CL, Cunningham ML, Hing AV, Stuhaug E, Starr JR (2009) Picture perfect? Reliability of craniofacial anthropometry using three-dimensional digital stereophotogrammetry. *Plastic & Reconstructive Surgery* 124:1261-1272
- Hell B (1995) 3D sonography. *International Journal of Oral & Maxillofacial Surgery* 24:84-89
- Henneberg M, Simpson E, Stephan C (2003) Human Face in Biological Anthropology: Craniometry, Evolution and Forensic Identification. In Katsikitis M (Ed) *The human face: Measurement and meaning*, Springer Science+Business Media New York, pp 29-48
- Hennessy RJ, Baldwin PA, Browne DJ, Kinsella A, Waddington JL (2010) Frontonasal dysmorphology in bipolar disorder by 3D laser surface imaging and geometric morphometrics: comparisons with schizophrenia. *Schizophrenia Research* 122:63-71
- Hennessy RJ, Baldwin PA, Browne DJ, Kinsella A, Waddington JL (2007) Three-dimensional laser surface imaging and geometric morphometrics resolve frontonasal dysmorphology in schizophrenia. *Biological Psychiatry* 61:1187-1194
- Hennessy RJ, Kinsella A, Waddington JL (2002) 3D laser surface scanning and geometric morphometric analysis of craniofacial shape as an index of cerebro-craniofacial morphogenesis: initial application to sexual dimorphism. *Biological Psychiatry* 51:507-514
- Hennessy RJ, Lane A, Kinsella A, Larkin C, O'Callaghan E, Waddington JL (2004) 3D morphometrics of craniofacial dysmorphology reveals sex-specific asymmetries in schizophrenia. *Schizophrenia Research* 67:261-268
- Hennessy RJ, McLearnie S, Kinsella A, Waddington JL (2005) Facial surface analysis by 3D laser scanning and geometric morphometrics in

- relation to sexual dimorphism in cerebral--craniofacial morphogenesis and cognitive function. *Journal of Anatomy* 207:283-295
- Hennessy RJ, Moss JP (2001) Facial growth: separating shape from size. *European Journal of Orthodontics* 23:275-285
  - Hide T, Hatakeyama J, Kimura-Yoshida C, Tian E, Takeda N, Ushio Y et al (2002) Genetic modifiers of otocephalic phenotypes in Otx2 heterozygous mutant mice. *Development* 129:4347-4357
  - Hinrichs AS, Karolchik D, Baertsch R, Barber GP, Bejerano G, Clawson H, Diekhans M, Furey TS, Harte RA, Hsu F et al. (2006) The UCSC Genome Browser Database: update 2006. *Nucleic Acids Research* 34:D590-598
  - Hochheiser H, Aronow BJ, Artinger K, Beaty TH, Brinkley JF, Chai Y, Clouthier D, Cunningham ML, Dixon M, Donahue LR et al. (2011) The FaceBase Consortium: A comprehensive program to facilitate craniofacial research. *Developmental Biology* 355:175-182
  - Hotelling H (1933) Analysis of a complex of statistical variables into principal components. *Journal of Educational Psychology* 24:417-441 and 498-520
  - Hotelling H (1936) Relations between two sets of variates. *Biometrika* 27:321-77
  - Houston WJ, Maher RE, McElroy D, Sherriff M (1986) Sources of error in measurements from cephalometric radiographs. *European Journal of Orthodontics* 8:149-151
  - Hovis CL, Butler MG (1997) Photoanthropometric study of craniofacial traits in individuals with Williams syndrome. *Clinical Genetics* 51:379-387
  - Howells WW (1973) Cranial variation in man. *Papers of the Peabody Museum Cambridge: Harvard University* (Vol 67)
  - Hrdlicka A (1972) *Practical Anthropometry*, AMS Press
  - Hsiao TH, Chang HP, Liu KM (1996) Sex determination by discriminant function analysis of lateral radiographic cephalometry. *Journal of Forensic Sciences* 41:792-795

- Huang D, Yan H (2003) NURBS curve controlled modelling for facial animation. *Computers & Graphics* 27:373-385
- Hunt N, Shah R, Sinanan A, Lewis M (2006) Northcroft Memorial Lecture 2005: muscling in on malocclusions: current concepts on the role of muscles in the aetiology and treatment of malocclusion. *Journal of Orthodontics* 33:187-197
- Hunter WS, Balbach DR, Lamphiear DE (1970) The heritability of attained growth in the human face. *American Journal of Orthodontics* 58:128-134
- Ismail SF, Moss JP (2002) The three-dimensional effects of orthodontic treatment on the facial soft tissues--a preliminary study. *British Dental Journal* 192:104-108
- Ismail SF, Moss JP, Hennessy R (2002) Three-dimensional assessment of the effects of extraction and nonextraction orthodontic treatment on the face. *American Journal of Orthodontics & Dentofacial Orthopedics* 121:244-256
- Jackson DA (1993) Stopping rules in principal components analysis: a comparison of heuristical and statistical approaches. *Ecology* 74:2204-2214
- James D (1985) Maxillofacial injuries in children. In: Rowe NL, Williams JL (eds) *Maxillofacial injuries*, Churchill Livingstone, Ann Arbor, pp 538-558
- Johannsdottir B, Thorarinsson F, Thordarson A, Magnusson TE (2005) Heritability of craniofacial characteristics between parents and offspring estimated from lateral cephalograms. *American Journal of Orthodontics & Dentofacial Orthopedics* 127:200-207; quiz 260-201
- Jones KL (1997) Smith's recognizable patterns of human malformation. 5th ed, Philadelphia, PA: W B Saunders Company
- Jones KL, Smith DW (1973) Recognition of the fetal alcohol syndrome in early infancy. *Lancet* 302:999-1001

- Joss SK, Paterson W, Donaldson MD, Tolmie JL (2002) Cleft palate, hypotelorism, and hypospadias: Schilbach-Rott syndrome. *American Journal of Medical Genetics* 113:105-107
- Kaiser HF (1958) The varimax criterion for analytic rotation in factor analysis. *Psychometrika* 23:187-200
- Kau CH (2007) A Three-Dimensional Study of Facial Changes in Children Aged 11-14 Years. PhD Thesis. In Department of Dental Health and Biological Sciences. Cardiff, Wales, UK, Cardiff University, School of Dentistry
- Kau CH, Hunter LM, Hingston EJ (2007) A different look: 3-dimensional facial imaging of a child with Binder syndrome. *American Journal of Orthodontics & Dentofacial Orthopedics* 132:704-709
- Kau CH, Knox J, Zhurov AI, Richmond S (2004a) Validity and reliability of a portable 3D optical scanning device for field studies. *In Proceedings of the 7th European Craniofacial Congress; 2004; Bologna: Monduzzi Editore – Int Proc Division:41-45*
- Kau CH, Olim S, Nguyen JT (2011) The Future of Orthodontic Diagnostic Records. *Seminars in orthodontics* 17:39-45
- Kau CH, Richmond S (2008) Three-dimensional analysis of facial morphology surface changes in untreated children from 12 to 14 years of age. *American Journal of Orthodontics & Dentofacial Orthopedics* 134:751-760
- Kau CH, Richmond S, Palomo JM, Hans MG (2005a) Three-dimensional cone beam computerized tomography in orthodontics. *Journal of Orthodontics* 32:282-293
- Kau CH, Richmond S, Zhurov A, Ovsenik M, Tawfik W, Borbely P, English JD (2010) Use of 3-dimensional surface acquisition to study facial morphology in 5 populations. *American Journal of Orthodontics & Dentofacial Orthopedics* 137:S56.e51-59; discussion S56-57
- Kau CH, Richmond S, Zhurov AI, Knox J, Chestnutt I, Hartles F, Playle R (2005b) Reliability of measuring facial morphology with a 3-dimensional

- laser scanning system. *American Journal of Orthodontics & Dentofacial Orthopedics* 128:424-430
- Kau CH, Zhurov A, Richmond S, Bibb R, Sugar A, Knox J, Hartles F (2006) The 3-dimensional construction of the average 11-year-old child face: a clinical evaluation and application. *Journal of Oral & Maxillofacial Surgery* 64:1086-1092
  - Kau CH, Zhurov A, Scheer R, Bouwman S, Richmond S (2004b) The feasibility of measuring three-dimensional facial morphology in children. *Orthodontics & Craniofacial Research* 7:198-204
  - Kawai T, Natsume N, Shibata H, Yamamoto T (1990a) Three-dimensional analysis of facial morphology using moire stripes. Part II. Analysis of normal adults. *International Journal of Oral & Maxillofacial Surgery* 19:359-362
  - Kawai T, Natsume N, Shibata H, Yamamoto T (1990b) Three-dimensional analysis of facial morphology using moire stripes. Part I. Method. *International Journal of Oral & Maxillofacial Surgery* 19:356-358
  - Keith T (2007) Human Genome-Wide Association Studies: Achieving Sufficient Power to Detect Disease Genes with the Quebec Founder Population [Tutorial]. *Genetic Engineering & Biotechnology News* 27
  - Kendall J, Liu Q, Bakleh A, Krasnitz A, Nguyen KC, Lakshmi B, Gerald WL, Powers S, Mu D (2007) Oncogenic cooperation and coamplification of developmental transcription factor genes in lung cancer. *Proceedings of the National Academy of Sciences of the United States of America* 104:16663-16668
  - Kerr WJ, McWilliam JS, Linder-Aronson S (1989) Mandibular form and position related to changed mode of breathing--a five-year longitudinal study. *Angle Orthodontist* 59:91-96
  - Klingenberg CP, Leamy LJ, Routman EJ, Cheverud JM (2001) Genetic architecture of mandible shape in mice: effects of quantitative trait loci analyzed by geometric morphometrics. *Genetics* 157:785-802
  - Kobayashi T, Ueda K, Honma K, Sasakura H, Hanada K, Nakajima T (1990) Three-dimensional analysis of facial morphology before and

- after orthognathic surgery. *Journal of Cranio-Maxillo-Facial Surgery* 18:68-73
- Koenderink JJ, Vandoorn AJ (1992) Surface Shape And Curvature Scales. *Image And Vision Computing* 10:557-564
  - Kohn LAP (1991) The Role of Genetics in Craniofacial Morphology and Growth. *Annual Review of Anthropology* 20:261-278
  - Kolar J, Salter E (1996) Craniofacial Anthropometry: Practical Measurement of the Head and Face for Clinical, Surgical and Research Use, Charles C. Thomas Publisher, LTD
  - Kowalski CJ, Nasjleti CE (1976) Upper face height-total face height ratio in adult American black males. *Journal of Dental Research* 55:913
  - Kranioti EF, Iscan MY, Michalodimitrakis M (2008) Craniometric analysis of the modern Cretan population. *Forensic Science International* 180:110.e111-115
  - Kreiborg S, Cohen MM, Jr. (2010) Ocular manifestations of Apert and Crouzon syndromes: qualitative and quantitative findings. *Journal of Craniofacial Surgery* 21:1354-1357
  - Krey KF, Dannhauer KH (2008) Morphometric analysis of facial profile in adults. *Journal of Orofacial Orthopedics* 69:424-436
  - Krneta B, Primožic J, Zhurov A, Richmond S, Ovsenik M (2012) Three-dimensional evaluation of facial morphology in children aged 5-6 years with a Class III malocclusion. *European Journal of Orthodontics*, 2012 Apr 6 [Epub]
  - Kruglyak L, Nickerson DA (2001) Variation is the spice of life. *Nature Genetics* 27:234-236
  - Kumar M, Lone MM, Patnaik VVG (2013) Determination of sex by discriminant function analysis: A cephalometric study. *International Journal of Pure and Applied Bioscience* 1:18-21
  - Laestadius ND, Aase JM, Smith DW (1969) Normal inner canthal and outer orbital dimensions. *Journal of Pediatrics* 74:465-468

- Lanctot C, Moreau A, Chamberland M, Tremblay ML, Drouin J (1999) Hindlimb patterning and mandible development require the Ptx1 gene. *Development* 126:1805-1810
- Lang D, Lu MM, Huang L, Engleka KA, Zhang M, Chu EY, Lipner S, Skoultchi A, Millar SE, Epstein JA (2005) Pax3 functions at a nodal point in melanocyte stem cell differentiation. *Nature* 433:884-887
- Langlois JH, Roggman LA (1990) Attractive Faces Are Only Average. *Psychological Science* 1:115-121
- Langlois JH, Roggman LA, Musselman L (1994) What Is Average and What Is Not Average About Attractive Faces? *Psychological Science* 5:214-220
- Lauweryns I, Carels C, Vlietinck R (1993) The use of twins in dentofacial genetic research. *American Journal of Orthodontics & Dentofacial Orthopedics* 103:33-38
- Lee JK, Park JW, Kim YH, Baek SH (2012a) Association between PAX9 single-nucleotide polymorphisms and nonsyndromic cleft lip with or without cleft palate. *Journal of Craniofacial Surgery* 23:1262-1266
- Lee WC, Yamaguchi T, Watanabe C, Kawaguchi A, Takeda M, Kim YI, Haga S, Tomoyasu Y, Ishida H, Maki K, Park SB, Kimura R (2012b) Association of common PAX9 variants with permanent tooth size variation in non-syndromic East Asian populations. *Journal of Human Genetics* 57:654-659
- Leivesley WD (1983) The reliability of contour photography for facial measurements. *British Journal of Orthodontics* 10:34-37
- Li WH, Sadler LA (1991) Low nucleotide diversity in man. *Genetics* 129:513-523
- Lill W, Solar P, Ulm C, Watzek G, Blahout R, Matejka M (1992) Reproducibility of three-dimensional CT-assisted model production in the maxillofacial area. *British Journal of Oral & Maxillofacial Surgery* 30:233-236
- Linder-Aronson S (1970) Adenoids. Their effect on mode of breathing and nasal airflow and their relationship to characteristics of the facial skeleton

and the dentition. A biometric, rhino-manometric and cephalometro-radiographic study on children with and without adenoids. *Acta Oto-Laryngologica Supplement* 265:1-132

- Linder-Aronson S (1979) Respiratory function in relation to facial morphology and the dentition. *British Journal of Orthodontics* 6:59-71
- Linder-Aronson S, Woodside DG, Lundstrom A (1986) Mandibular growth direction following adenoidectomy. *American Journal of Orthodontics* 89:273-284
- Linney AD, Coombes AM (1998) Computer modeling of facial form. In, Clement JG, Ransom DL (eds): *Craniofacial identification in forensic medicine*. Edward Arnold, London, pp. 187-199
- Liu F, van der Lijn F, Schurmann C, Zhu G, Chakravarty MM, Hysi PG, Wollstein A, Lao O, de Bruijne M, Ikram MA *et al.* (2012) A genome-wide association study identifies five Loci influencing facial morphology in europeans. *PLoS Genetics* 8:e1002932
- Loos HS, Wiczorek D, Wurtz RP, von der Malsburg C, Horsthemke B (2003) Computer-based recognition of dysmorphic faces. *European Journal of Human Genetics* 11:555-560
- Lowe AA, Santamaria JD, Fleetham JA, Price C (1986) Facial morphology and obstructive sleep apnea. *American Journal of Orthodontics & Dentofacial Orthopedics* 90:484-491
- Lu KH (1965) Harmonic analysis of the human face. *Biometrics* 21:491-505
- Lumsden A, Sprawson N, Graham A (1991) Segmental origin and migration of neural crest cells in the hindbrain region of the chick embryo. *Development* 113:1281-1291
- Lundström A (1948) Tooth size and occlusion in twins. Thesis, (Uppsala). 2nd edn. S. Karger, Basle and New York.
- Lundström A (1954) The Importance of Genetic and Non-Genetic Factors in the Facial Skeleton Studied in 100 Pairs of Twins. *European Orthodontic Society, The Hague*:92-102

- Lundström A (1984) Nature versus nurture in dento-facial variation. *European Journal of Orthodontics* 6:77-91
- Lundström A, McWilliam J (1988) Comparison of some cephalometric distances and corresponding facial proportions with regard to heritability. *European Journal of Orthodontics* 10:27-29
- Lundström A, McWilliam JS (1987) A comparison of vertical and horizontal cephalometric variables with regard to heritability. *European Journal of Orthodontics* 9:104-108
- MacGregor AR, Newton I, Gilder RS (1971) A stereophotogrammetric method of investigating facial changes following the loss of teeth. *Medical & Biological Illustration* 21:75-82
- Machado AF, Martin LJ, Collins MD (2001) Pax3 and the splotch mutations: structure, function, and relationship to teratogenesis, including gene-chemical interactions. *Current Pharmaceutical Design* 7:751-785
- Mäkinen E, Raisamo R (2008a) Evaluation of gender classification methods with automatically detected and aligned faces. *IEEE Transactions on Pattern Analysis & Machine Intelligence* 30:541-547
- Mäkinen E, Raisamo R (2008b) An experimental comparison of gender classification methods. *Pattern Recognition Letters* 29:1544-1556
- Manfredi C, Martina R, Grossi GB, Giuliani M (1997) Heritability of 39 orthodontic cephalometric parameters on MZ, DZ twins and MN-paired singletons. *American Journal of Orthodontics & Dentofacial Orthopedics* 111:44-51
- Mann I (1957) *Developmental Abnormalities of the Eye*. 2nd ed. British Medical Association: London.
- Mansouri A, Stoykova A, Torres M, Gruss P (1996) Dysgenesis of cephalic neural crest derivatives in Pax7<sup>-/-</sup> mutant mice. *Development* 122:831-838
- Mao Z, Ju X, Siebert JP, Cockshott WP, Ayoub AF (2006) Constructing Dense Correspondences for the Analysis of 3D Facial Morphology. *Pattern Recognition Letters* 27:597-608

- Marsh JL, Vannier MW, Stevens WG, Warren JO, Gayou D, Dye DM (1985) Computerized imaging for soft tissue and osseous reconstruction in the head and neck. *Clinics in Plastic Surgery* 12:279-291
- Martin R (1913) Lehrbuch der anthropologie. Stuttgart: Fisher
- Mass E, Belostoky L (1993) Craniofacial morphology of children with Williams syndrome. *Cleft Palate-Craniofacial Journal* 30:343-349
- McCallum BC, Fright WR, Nixon MA, Price NB (1996) A feasibility study of hand-held laser surface scanning. *Proceedings, Image and Vision Computing*. University of Auckland, New Zealand, pp. 103-108
- McCallum BC, Nixon MA, Price NB, Fright WR (1998) Hand-held laser scanning in practice. *Proceedings, Image and Vision Computing*. University of Auckland, New Zealand, pp. 17-22
- McCance AM, Moss JP, Fright WR, James DR, Linney AD (1992a) A three dimensional analysis of soft and hard tissue changes following bimaxillary orthognathic surgery in skeletal III patients. *British Journal of Oral & Maxillofacial Surgery* 30:305-312
- McCance AM, Moss JP, Fright WR, James DR, Linney AD (1993) A three-dimensional analysis of bone and soft tissue to bone ratio of movements in 17 Skeletal II patients following orthognathic surgery. *European Journal of Orthodontics* 15:97-106
- McCance AM, Moss JP, Fright WR, Linney AD (1997a) Three-dimensional analysis techniques--Part 3: Color-coded system for three-dimensional measurement of bone and ratio of soft tissue to bone: the analysis. *Cleft Palate-Craniofacial Journal* 34:52-57
- McCance AM, Moss JP, Fright WR, Linney AD, James DR (1997b) Three-dimensional analysis techniques--Part 1: Three-dimensional soft-tissue analysis of 24 adult cleft palate patients following Le Fort I maxillary advancement: a preliminary report. *Cleft Palate-Craniofacial Journal* 34:36-45
- McCance AM, Moss JP, Fright WR, Linney AD, James DR (1997c) Three-dimensional analysis techniques--Part 2: Laser scanning: a

- quantitative three-dimensional soft-tissue analysis using a color-coding system. *Cleft Palate-Craniofacial Journal* 34:46-51
- McCance AM, Moss JP, Fright WR, Linney AD, James DR, Coghlan K, Mars M (1997d) Three-dimensional analysis techniques--Part 4: Three-dimensional analysis of bone and soft tissue to bone ratio of movements in 24 cleft palate patients following Le Fort I osteotomy: a preliminary report. *Cleft Palate-Craniofacial Journal* 34:58-62
  - McCance AM, Moss JP, Wright WR, Linney AD, James DR (1992b) A three-dimensional soft tissue analysis of 16 skeletal class III patients following bimaxillary surgery. *British Journal of Oral & Maxillofacial Surgery* 30:221-232
  - McCulley M (2000) Classification and genetic analysis of human facial features. Thesis. In, University of London
  - McNamara JA (1981) Influence of respiratory pattern on craniofacial growth. *Angle Orthodontist* 51:269-300
  - Medic S, Ziman M (2010) PAX3 expression in normal skin melanocytes and melanocytic lesions (naevi and melanomas). *PLoS ONE* [Electronic Resource] 5:e9977
  - Meerdink JE, Garbin CP, Leger DW (1990) Cross-gender perceptions of facial attributes and their relation to attractiveness: do we see them differently than they see us? *Perception and Psychophysics* 48:227-233
  - Meintjes EM, Douglas TS, Martinez F, Vaughan CL, Adams LP, Stekhoven A, Viljoen D (2002) A stereo-photogrammetric method to measure the facial dysmorphology of children in the diagnosis of fetal alcohol syndrome. *Medical Engineering & Physics* 24:683-689
  - Mercan E, Shapiro LG, Weinberg SM, Lee SI (2013) The use of pseudo-landmarks for craniofacial analysis: A comparative study with L1-regularized logistic regression. *Conference Proceedings, IEEE Engineering in Medicine & Biology Society* 2013:6083-6086
  - Miamoto CB, Soares RL, de Carvalho EM, Pereira LJ, Marques LS (2011) Ocular hypertelorism in an orthodontic patient. *American Journal of Orthodontics & Dentofacial Orthopedics* 139:544-550

- Midtgard J, Bjork G, Linder-Aronson S (1974) Reproducibility of cephalometric landmarks and errors of measurements of cephalometric cranial distances. *Angle Orthodontist* 44:56-61
- Mishima K, Sugahara T, Mori Y, Sakuda M (1996) Application of a new method for anthropometric analysis of the nose. *Plastic & Reconstructive Surgery* 98:637-644
- Moawad HA, Sinanan ACM, Lewis MP, Hunt NP (2012) Grouping patients for masseter muscle genotype-phenotype studies. *Angle Orthodontist* 82:261-266
- Moffatt MF, Kabesch M, Liang L, Dixon AL, Strachan D, Heath S, Depner M, von Berg A, Bufe A, Rietschel E *et al.* (2007) Genetic variants regulating ORMDL3 expression contribute to the risk of childhood asthma. *Nature* 448:470-473
- Morecroft L (2009) A Statistical Approach to Facial Identification. PhD Thesis. Department of Probability and Statistics, University of Sheffield, UK.
- Marrant DG, Shaw WC (1996) Use of standardized video recordings to assess cleft surgery outcome. *Cleft Palate-Craniofacial Journal* 33:134-142
- Moss JP (2006) The use of three-dimensional imaging in orthodontics. *European Journal Of Orthodontics* 28:416-425
- Moss JP, Coombes AM, Linney AD, Campos J (1991) Methods of three dimensional analysis of patients with asymmetry of the face. *Proceedings of the Finnish Dental Society* 87:139-149
- Moss JP, Goodwin PM, Linney AD (1996) The use of three dimensional techniques in the monitoring of the growth of facial anomalies. *Opus Honorarium*, Benito Miotti, Edizioni Libreria Progetto, Padova:pp. 205-214
- Moss JP, Grindrod SR, Linney AD, Arridge SR, James D (1988) A computer system for the interactive planning and prediction of maxillofacial surgery. *American Journal of Orthodontics & Dentofacial Orthopedics* 94:469-475

- Moss JP, Hennessey RJ (2002) [Lasers in dentistry 7. The use of 3D imaging in dentistry]. *Nederlands Tijdschrift voor Tandheelkunde* 109:378-382
- Moss JP, Ismail SF, Hennessy RJ (2003) Three-dimensional assessment of treatment outcomes on the face. *Orthodontics & Craniofacial Research* 6 Suppl 1:126-131; discussion 179-182
- Moss JP, James DR (1984) An investigation of a group of 35 consecutive patients with a first arch syndrome. *British Journal of Oral & Maxillofacial Surgery* 22:157-169
- Moss JP, Linney AD, Grindrod SR, Arridge SR, Clifton JS (1987) Three-dimensional visualization of the face and skull using computerized tomography and laser scanning techniques. *European Journal of Orthodontics* 9:247-253
- Moss JP, Linney AD, Grindrod SR, Mosse CA (1989) A Laser Scanning System For The Measurement Of Facial Surface-Morphology. *Optics And Lasers In Engineering* 10:179-190
- Moss JP, Linney AD, James DR (1990) The three dimensional analysis and treatment of patients with Hemifacial Microsomia. *Transactions Nederlandse Vereniging voor Orthodontische Studie* 8:262-275
- Moss JP, McCance AM, Fright WR, Linney AD, James DR (1994) A three-dimensional soft tissue analysis of fifteen patients with Class II, Division 1 malocclusions after bimaxillary surgery. *American Journal of Orthodontics & Dentofacial Orthopedics* 105:430-437
- Moss JP, McDonagh SM, Lee RT, Morris DO, Goodwin PM (1997) A three dimensional study of the effects of functional appliance therapy in a randomized study of class II/1 patients. *Transactions of the 14th International Congress of SIDO*, Published by Societa Italiana di Ortodonzia:pp. 35-42
- Mossey PA (1999a) The heritability of malocclusion: Part 1--Genetics, principles and terminology. *British Journal of Orthodontics* 26:103-113
- Mossey PA (1999b) The heritability of malocclusion: part 2. The influence of genetics in malocclusion. *British Journal of Orthodontics* 26:195-203

- Motoyoshi M, Namura S, Arai HY (1992) A three-dimensional measuring system for the human face using three-directional photography. *American Journal of Orthodontics & Dentofacial Orthopedics* 101:431-440
- Mu YD, Xu Z, Contreras CI, McDaniel JS, Donly KJ, Chen S (2013) Mutational analysis of AXIN2, MSX1, and PAX9 in two Mexican oligodontia families. *Genetics and Molecular Research* 12:4446-4458
- Nagasao T, Miyamoto J, Jiang H, Kaneko T, Tamaki T (2011) Biomechanical analysis of the effect of intracranial pressure on the orbital distances in trigonocephaly. *Cleft Palate-Craniofacial Journal* 48:190-196
- Naikmasur VG, Shrivastava R, Mutalik S (2010) Determination of sex in South Indians and immigrant Tibetans from cephalometric analysis and discriminant functions. *Forensic Science International* 197:122.e121-126
- Naini FB, Moss JP (2004) Three-dimensional assessment of the relative contribution of genetics and environment to various facial parameters with the twin method. *American Journal of Orthodontics & Dentofacial Orthopedics* 126:655-665
- Nair P, Cavallaro A (2009) 3-D Face Detection, Landmark Localization, and Registration Using a Point Distribution Model. *IEEE Transactions on Multimedia* 11:611-623
- Nakajima A, Sameshima GT, Arai Y, Homme Y, Shimizu N, Dougherty H (2005) Two- and three-dimensional orthodontic imaging using limited cone beam-computed tomography. *Angle Orthodontist* 75:895-903
- Nakata N, Yu PI, Davis B, Nance WE (1973) The use of genetic data in the prediction of craniofacial dimensions. *American Journal of Orthodontics* 63:471-480
- Nanda RS, Ghosh J, Bazakidou E (1996) Three-dimensional facial analysis using a video imaging system. *Angle Orthodontist* 66:181-188
- Nasjleti CE, Kowalski CJ (1975) Stability of upper face height-total face height ratio with increasing age. *Journal of Dental Research* 54:1241

- Nichols DH (1981) Neural crest formation in the head of the mouse embryo as observed using a new histological technique. *Journal of Embryology & Experimental Morphology* 64:105-120
- Nie X, Luukko K, Kettunen P (2006) FGF signalling in craniofacial development and developmental disorders. *Oral Diseases* 12:102-111
- Ning R, Tang X, Conover D, Yu R (2003) Flat panel detector-based cone beam computed tomography with a circle-plus-two-arcs data acquisition orbit: preliminary phantom study. *Medical Physics* 30:1694-1705
- Nishina S, Kohsaka S, Yamaguchi Y, Handa H, Kawakami A, Fujisawa H, Azuma N (1999) PAX6 expression in the developing human eye. *British Journal of Ophthalmology* 83:723-727
- Noden DM (1975) An analysis of migratory behavior of avian cephalic neural crest cells. *Developmental Biology* 42:106-130
- Nute SJ, Moss JP (2000) Three-dimensional facial growth studied by optical surface scanning. *Journal of Orthodontics* 27:31-38
- Oh J, Wang CJ, Poole M, Kim E, Davis RC, Nishimura I et al (2007) A genome segment on mouse chromosome 12 determines maxillary growth. *Journal of Dental Research* 86:1203-1206
- Opdebeeck H, Bell WH (1978) The short face syndrome. *American Journal of Orthodontics* 73:499-511
- Opdebeeck H, Bell WH, Eisenfeld J, Mischelevich D (1978) Comparative study between the SFS and LFS rotation as a possible morphogenic mechanism. *American Journal of Orthodontics* 74:509-521
- Opitz JM (1982) The developmental field concept in clinical genetics. *Journal of Pediatrics* 101:805-809
- O'Rahilly R, Muller F (2007) The development of the neural crest in the human. *Journal of Anatomy* 211:335-351
- Othman SA, Ahmad R, Mericant AF, Jamaludin M (2013) Reproducibility of facial soft tissue landmarks on facial images captured on a 3D camera. *Australian Orthodontic Journal* 29:58-65

- Palmer LJ, Cardon LR (2005) Shaking the tree: mapping complex disease genes with linkage disequilibrium. *Lancet* 366:1223-1234
- Palmer SE (1977) Hierarchical structure in perceptual representation. *Cognitive Psychology* 9:441-474
- Palomo JM, Kau CH, Palomo LB, Hans MG (2006) Three-dimensional cone beam computerized tomography in dentistry. *Dentistry Today* 25:130, 132-135
- Park HK, Chung JW, Kho HS (2006) Use of hand-held laser scanning in the assessment of craniometry. *Forensic Science International* 160:200-206
- Park JW, McIntosh I, Hetmanski JB, Jabs EW, Vander Kolk CA, Wu-Chou YH, Chen PK, Chong SS, Yeow V, Jee SH, Park BY, Fallin MD, Ingersoll R, Scott AF, Beaty TH (2007) Association between IRF6 and nonsyndromic cleft lip with or without cleft palate in four populations. *Genetics in Medicine* 9:219-227
- Paternoster L, Zhurov AI, Toma AM, Kemp JP, St Pourcain B, Timpson NJ, McMahon G, McArdle W, Ring SM, Smith GD, Richmond S, Evans DM (2012) Genome-wide association study of three-dimensional facial morphology identifies a variant in PAX3 associated with nasion position. *American Journal of Human Genetics* 90:478-485
- Patil KR, Mody RN (2005) Determination of sex by discriminant function analysis and stature by regression analysis: a lateral cephalometric study. *Forensic Science International* 147:175-180
- Pearson H (2006) Genetics: what is a gene? *Nature* 441:398-401
- Pearson K (1901) On lines and planes of closest fit to systems of points in space. *Philosophical Magazine* 2:559-572
- Peck S, Peck L, Kataja M (1991) Skeletal asymmetry in esthetically pleasing faces. *Angle Orthodontist* 61:43-48
- Pennisi E (2007) Genomics. DNA study forces rethink of what it means to be a gene. *Science* 316:1556-1557

- Perakis P, Passalis G, Theoharis T, Kakadiaris IA (2010) "3d facial landmark detection and face registration". Tech Rep, University of Athens, Greece
- Pereira TV, Salzano FM, Mostowska A, Trzeciak WH, Ruiz-Linares A, Chies JA, Saavedra C, Nagamachi C, Hurtado AM, Hill K, Castro-de-Guerra D, Silva-Junior WA, Bortolini MC (2006) Natural selection and molecular evolution in primate PAX9 gene, a major determinant of tooth development. *Proceedings of the National Academy of Sciences of the United States of America* 103:5676-5681
- Peyton WT, Ritchie HP (1936) Quantitative studies on congenital clefts of the lip. *Archives of Surgery* 33:1035-1046
- Pierson WR (1961) Monophotogrammetric determination of body volume. *Ergonomics* 4:213-217
- Pingault V, Ente D, Dastot-Le Moal F, Goossens M, Marlin S, Bondurand N (2010) Review and update of mutations causing Waardenburg syndrome. *Human Mutation* 31:391-406
- Pirttiniemi P (1992) Associations of Mandibulofacial Asymmetries, with Special Reference to Glenoid Fossa Remodelling. Oulu, Finland: University of Oulu.
- Pirttiniemi P, Kantomaa T, Lahtela P (1990) Relationship between craniofacial and condyle path asymmetry in unilateral cross-bite patients. *European Journal of Orthodontics* 12:408-413
- Pollefeys M, Koch R, Vergauwen M, Gool LV (1999) Hand-held acquisition of 3D models with a video camera. *In Proceedings of the 2nd international conference on 3-D digital imaging and modeling*. Ottawa, Canada, *IEEE Computer Society*. pp. 14–23
- Popat H, Richmond S, Playle R, Marshall D, Rosin P, Cosker D (2008a) Three-dimensional motion analysis - an exploratory study. Part 1: assessment of facial movement. *Orthodontics & Craniofacial Research* 11:216-223
- Popat H, Richmond S, Playle R, Marshall D, Rosin P, Cosker D (2008b) Three-dimensional motion analysis - an exploratory study. Part 2:

reproducibility of facial movement. *Orthodontics & Craniofacial Research* 11:224-228

- Popovich F, Thompson GW (1977) Craniofacial templates for orthodontic case analysis. *American Journal of Orthodontics* 71:406-420
- Proffit WR, Fields HW, Jr., Moray LJ (1998) Prevalence of malocclusion and orthodontic treatment need in the United States: estimates from the NHANES III survey. *International Journal of Adult Orthodontics & Orthognathic Surgery* 13:97-106
- Proffit WR, White RP, Sarver DM (2003) Contemporary Treatment of Dentofacial Deformity, St Louis, Mo: Mosby
- Rabey G (1968) Morphanalysis. HK Lewis & Co Ltd, 136 Gower Street, London
- Rabey G (1971) Craniofacial morphanalysis. *Proceedings of the Royal Society of Medicine* 64:103-111
- Rabey GP (1977) Current principles of morphanalysis and their implications in oral surgical practice. *British Journal of Oral Surgery* 15:97-109
- Randolph JC, Sokol JA, Lee HB, Nunery WR (2011) Orbital manifestations of Noonan syndrome. *Ophthalmic Plastic & Reconstructive Surgery* 27:e160-3
- Ras F, Habets LL, van Ginkel FC, PrahI-Andersen B (1996) Quantification of facial morphology using stereophotogrammetry--demonstration of a new concept. *Journal of Dentistry* 24:369-374
- Rayleigh L (1874) On the Manufacture and Theory of Diffraction-Gratings. *Philosophical Magazine* 47:81-93 and 193-205
- Read AP, Newton VE (1997) Waardenburg syndrome. *Journal of Medical Genetics* 34:656-665
- Reich DE, Gabriel SB, Altshuler D (2003) Quality and completeness of SNP databases. *Nature Genetics* 33:457-458
- Rhodes G, Sumich A, Byatt G (1999) Are Average Facial Configurations Attractive Only Because of Their Symmetry? *Psychological Science* 10:52-58

- Richardson A (1966) An investigation into the reproducibility of some points, planes, and lines used in cephalometric analysis. *American Journal of Orthodontics* 52:637-651
- Richman JM, Lee SH (2003) About face: signals and genes controlling jaw patterning and identity in vertebrates. *Bioessays* 25:554-568
- Risch N, Merikangas K (1996) The future of genetic studies of complex human diseases. *Science* 273:1516-1517
- Robinson GW, Mahon KA (1994) Differential and overlapping expression domains of Dlx-2 and Dlx-3 suggest distinct roles for Distal-less homeobox genes in craniofacial development. *Mechanisms of Development* 48:199-215
- Robinson MS, Bidmos MA (2009) The skull and humerus in the determination of sex: reliability of discriminant function equations. *Forensic Science International* 186:86.e81-85
- Rocchini C, Cignoni P, Montani C, Scopigno R (1999) Multiple textures stitching and blending on 3D objects. *In Proceedings of the 10th Eurographics conference on Rendering*. Granada, Spain, Eurographics Association. pp. 127–138
- Rogers S (1984) *Personal Identification from Human Remains*, Charles C. Thomas Publisher, LTD
- Romero-Huertas M, Pears N (2008) 3D Facial Landmark Localisation by Matching Simple Descriptors. *In 2nd IEEE International Conference on Biometrics: Theory, Applications and Systems*, 2008, pp 1–6.
- Ronchi V (1923) Combination fringes in the study of surfaces and optical systems. *Journal of Optics and Precision Mechanics* 2:9-35
- Ronchi V (1927) Two new methods for the study of surfaces and optical systems. *Annali della Scuola Normale Superiore di Pisa - Classe di Scienze, Series 1*, 15:1-50
- Ronchi V (1964) "Forty Years of History of a Grating Interferometer." *Applied Optics* 3:437-451

- Rose JC, Roblee RD (2009) Origins of Dental Crowding and Malocclusions: An Anthropological Perspective. *Compendium* 30(5), Published by AEGIS Communications
- Sampson PD, Streissguth AP, Bookstein FL, Barr HM (2000) On categorizations in analyses of alcohol teratogenesis. *Environmental Health Perspectives* 108 Suppl 3:421-428
- Sanna S, Jackson AU, Nagaraja R, Willer CJ, Chen WM, Bonnycastle LL, Shen H, Timpson N, Lettre G, Usala G *et al.* (2008) Common variants in the GDF5-UQCC region are associated with variation in human height. *Nature Genetics* 40:198-203
- Sarkar S, Plutynski A (2008) A Companion to the Philosophy of Biology. Oxford: Blackwell
- Savara BS (1965a) Applications of photogrammetry for quantitative study of tooth and face morphology. *American Journal of Physical Anthropology* 23:427-434
- Savara BS (1965b) A method for measuring facial bone growth in three dimensions. *Human Biology* 37:245-255
- Savoye I, Loos R, Carels C, Derom C, Vlietinck R (1998) A genetic study of anteroposterior and vertical facial proportions using model-fitting. *Angle Orthodontist* 68:467-470
- Schendel SA, Eisenfeld J, Bell WH, Epker BN, Mishelevich DJ (1976) The long face syndrome: vertical maxillary excess. *American Journal of Orthodontics* 70:398-408
- Schmid W, Mongini F, Felisio A (1991) A computer-based assessment of structural and displacement asymmetries of the mandible. *American Journal of Orthodontics & Dentofacial Orthopedics* 100:19-34
- Scholl FA, Kamarashev J, Murmann OV, Geertsen R, Dummer R, Schafer BW (2001) PAX3 is expressed in human melanomas and contributes to tumor cell survival. *Cancer Research* 61:823-826
- Scott LJ, Mohlke KL, Bonnycastle LL, Willer CJ, Li Y, Duren WL, Erdos MR, Stringham HM, Chines PS, Jackson AU *et al.* (2007) A genome-

- wide association study of type 2 diabetes in Finns detects multiple susceptibility variants. *Science* 316:1341-1345
- Scuteri A, Sanna S, Chen WM, Uda M, Albai G, Strait J, Najjar S, Nagaraja R, Orru M, Usala G *et al.* (2007) Genome-wide association scan shows genetic variants in the FTO gene are associated with obesity-related traits. *PLoS Genetics* 3:e115
  - Seeram E (1997) 3-D imaging: basic concepts for radiologic technologists. [Erratum appears in *Radiologic Technology*, 1998; 69:208]. *Radiologic Technology* 69:127-144; quiz 145-128
  - Serbedzija GN, Bronner-Fraser M, Fraser SE (1992) Vital dye analysis of cranial neural crest cell migration in the mouse embryo. *Development* 116:297-307
  - Severt TR, Proffit WR (1997) The prevalence of facial asymmetry in the dentofacial deformities population at the University of North Carolina. *International Journal of Adult Orthodontics & Orthognathic Surgery* 12:171-176
  - Shah SM, Joshi MR (1978) An assessment of asymmetry in the normal craniofacial complex. *Angle Orthodontist* 48:141-148
  - Shaner DJ, Peterson AE, Beattie OB, Bamforth JS (2000) Assessment of soft tissue facial asymmetry in medically normal and syndrome-affected individuals by analysis of landmarks and measurements. *American Journal of Medical Genetics* 93:143-154
  - Sharland M, Morgan M, Patton MA (1993) Photoanthropometric study of facial growth in Noonan syndrome. *American Journal of Medical Genetics* 45:430-436
  - Shaw PJA (2003) *Multivariate statistics for the Environmental Sciences*, Hodder-Arnold. ISBN 0-340-80763-6
  - Shepherd J (1989) The face and social attribution. *In Handbook of Research on Face Processing*, Young AW and Ellis HD (Eds); Amsterdam: North-Holland; pp. 289-320.
  - Shi J, Samal A, Marx D (2006) How effective are landmarks and their geometry for face recognition? *CVIU* 102:117–133

- Shih H-C (2013) Robust gender classification using a precise patch histogram. *Pattern Recognition* 46:519-528
- Shum L, Takahashi K, Takahashi I, Nagata M, Tanaka O, Semba I, Tan DP, Nuckolls GH, Slavkin HC (2000) Embryogenesis and the Classification of Craniofacial Dysmorphogenesis. *In Oral and Maxillofacial Surgery*, Vol 6 (eds Baker, SB and Fonseca, RJ), Philadelphia: WB Saunders Co, pp149-157
- Siebert JP, Marshall SJ (2000) Human body 3D imaging by speckle texture projection photogrammetry. *Sensor Review* 20:218-226
- Smith WM (2000) Hemispheric and facial asymmetry: gender differences. *Laterality* 5:251-258
- Sokol RJ, Chik L, Martier SS, Salari V (1991) Morphometry of the neonatal fetal alcohol syndrome face from 'snapshots'. *Alcohol & Alcoholism Supplement* 1:531-534
- Sorek R (2007) The birth of new exons: mechanisms and evolutionary consequences. *Rna-A Publication of the Rna Society* 13:1603-1608
- Souccar NM, Kau CH (2012) Methods of Measuring the Three-Dimensional Face. *Seminars in Orthodontics* 18:187-192
- Stein KF, Kelley T, Wood E (1956) Influence of heredity in the etiology of malocclusion. *American Journal of Orthodontics* 42:125-141
- Stern M, Moss JP (1994) 3D measurement of palatal dimensions and area using a linear laser scanner. *Journal Dental Research* 73:839-850
- Steyn M, Iscan MY (1998) Sexual dimorphism in the crania and mandibles of South African whites. *Forensic Science International* 98:9-16
- Stockton DW, Das P, Goldenberg M, D'Souza RN, Patel PI (2000) Mutation of PAX9 is associated with oligodontia. *Nature Genetics* 24:18-19
- Stuart ET, Kioussi C, Gruss P (1994) Mammalian Pax genes. *Annual Review of Genetics* 28:219-236
- Takasaki H (1970) Moire Topography. *Applied Optics* 9:1457-1472

- Tassopoulou-Fishell M, Deeley K, Harvey EM, Sciote J, Vieira AR (2012) Genetic variation in myosin 1H contributes to mandibular prognathism. *American Journal of Orthodontics & Dentofacial Orthopedics* 141:51-59
- Terzic J, Saraga-Babic M (1999) Expression pattern of PAX3 and PAX6 genes during human embryogenesis. *International Journal of Developmental Biology* 43:501-508
- Thaller SR, McDonald WS (2004) Facial Trauma. CRC Press, Print ISBN: 978-0-8247-4625-4
- Thompson MM (1966) Manual of Photogrammetry. In, ed. 3, Falls Church, VA: *American Society of Photogrammetry*
- Tie Y, Guan L (2013) Automatic landmark point detection and tracking for human facial expressions. *EURASIP Journal on Image and Video Processing* 2013:8
- Toma AM, Zhurov A, Playle R, Ong E, Richmond S (2009) Reproducibility of facial soft tissue landmarks on 3D laser-scanned facial images. *Orthodontics & Craniofacial Research* 12:33-42
- Toma AM, Zhurov A, Playle R, Richmond S (2008) A three-dimensional look for facial differences between males and females in a British-Caucasian sample aged 15½ years old. *Orthodontics & Craniofacial Research* 11:180-185
- Toma AM, Zhurov AI, Playle R, Marshall D, Rosin PL, Richmond S (2012) The assessment of facial variation in 4747 British school children. *European Journal of Orthodontics* 34:655-664
- Tomoyasu Y, Yamaguchi T, Tajima A, Nakajima T, Inoue I, Maki K (2009) Further evidence for an association between mandibular height and the growth hormone receptor gene in a Japanese population. *American Journal of Orthodontics & Dentofacial Orthopedics* 136:536-541
- Townsend G, Bockmann M, Hughes T, Brook A (2012) Genetic, environmental and epigenetic influences on variation in human tooth number, size and shape. *Odontology* 100:1-9

- Townsend G, Brook A (2008) Genetic, epigenetic and environmental influences on the human dentition. *Orthodontic Tribune* 3:3-6
- Townsend GC, Aldred MJ, Bartold PM (1998) Genetic aspects of dental disorders. *Australian Dental Journal* 43:269-286
- Townsend GC, Brook AH (2013) Genetic, Epigenetic and Environmental Influences on Human Tooth Size, Shape and Number. In eLS. John Wiley & Sons, Ltd
- Townsend GC, Richards L, Hughes T, Pinkerton S, Schwerdt W (2005) Epigenetic influences may explain dental differences in monozygotic twin pairs. *Australian Dental Journal* 50:95-100
- Trask GM, Shapiro GG, Shapiro PA (1987) The effects of perennial allergic rhinitis on dental and skeletal development: a comparison of sibling pairs. *American Journal of Orthodontics & Dentofacial Orthopedics* 92:286-293
- Treil J, Faure J, Braga J, Casteigt J, Borianne P (2002) [Three-dimensional imaging and cephalometry of cranio-facial asymmetry]. *Orthodontie Francaise* 73:179-197
- Tremblay P, Dietrich S, Mericskay M, Schubert FR, Li Z, Paulin D (1998) A crucial role for Pax3 in the development of the hypaxial musculature and the long-range migration of muscle precursors. *Developmental Biology* 203:49-61
- Tremblay P, Kessel M, Gruss P (1995) A transgenic neuroanatomical marker identifies cranial neural crest deficiencies associated with the Pax3 mutant *Spotch*. *Developmental Biology* 171:317-329
- Tsukamoto K, Tohma T, Ohta T, Yamakawa K, Fukushima Y, Nakamura Y, Niikawa N (1992) Cloning and characterization of the inversion breakpoint at chromosome 2q35 in a patient with Waardenburg syndrome type I. *Human Molecular Genetics* 1:315-317
- Tuncay OC, Nuveen MJ, Nguyen CX, Slattery J (2000) The Development of a System for Three-dimensional Imaging and Animation of the Craniofacial Complex. In, *Greater Philadelphia Society of Orthodontists - GPSO*

- Udupa J, Herman G (1991) 3D Imaging in Medicine, Boca Raton: CRC Press
- Vanezis P, Blowes RW, Linney AD, Tan AC, Richards R, Neave R (1989) Application of 3-D computer graphics for facial reconstruction and comparison with sculpting techniques. *Forensic Science International* 42:69-84
- Vig PS, Hewitt AB (1975) Asymmetry of the human facial skeleton. *Angle Orthodontist* 45:125-129
- Visel A, Rubin EM, Pennacchio LA (2009) Genomic views of distant-acting enhancers. *Nature* 461:199-205
- Visel A, Taher L, Girgis H, May D, Golonzhka O, Hoch RV, McKinsey GL, Pattabiraman K, Silberberg SN, Blow MJ *et al.* (2013) A high-resolution enhancer atlas of the developing telencephalon. *Cell* 152:895-908
- Waardenburg PJ (1951) A new syndrome combining developmental anomalies of the eyelids, eyebrows and nose root with pigmentary defects of the iris and head hair and with congenital deafness. *American Journal of Human Genetics* 3:195-253
- Waddington CH (1957) The strategy of the genes. London: George Allen and Unwin.
- Waddington JL, Lane A, Scully P, Meagher D, Quinn J, Larkin C, O'Callaghan E (1999) Early cerebro-craniofacial dysmorphogenesis in schizophrenia: a lifetime trajectory model from neurodevelopmental basis to 'neuroprogressive' process. *Journal of Psychiatric Research* 33:477-489
- Wallin J, Mizutani Y, Imai K, Miyashita N, Moriwaki K, Taniguchi M, Koseki H, Balling R (1993) A new Pax gene, Pax-9, maps to mouse chromosome 12. *Mammalian Genome* 4:354-358
- Walther C, Gruss P (1991) Pax-6, a murine paired box gene, is expressed in the developing CNS. *Development* 113:1435-1449
- Walther C, Guenet JL, Simon D, Deutsch U, Jostes B, Goulding MD, Plachov D, Balling R, Gruss P (1991) Pax: a murine multigene family of paired box-containing genes. *Genomics* 11:424-434

- Wang DG, Fan JB, Siao CJ, Berno A, Young P, Sapolsky R, Ghandour G, Perkins N, Winchester E, Spencer J *et al.* (1998) Large-scale identification, mapping, and genotyping of single-nucleotide polymorphisms in the human genome. *Science* 280:1077-1082
- Wang J, Xu Y, Chen J, Wang F, Huang R, Wu S, Shu L, Qiu J, Yang Z, Xue J, Wang R, Zhao J, Lai W (2013) PAX9 polymorphism and susceptibility to sporadic non-syndromic severe anodontia: a case-control study in southwest China. *Journal of Applied Oral Science* 21:256-264
- Ward RE (1989) Facial morphology as determined by anthropometry: keeping it simple. *Journal of Craniofacial Genetics & Developmental Biology* 9:45-60
- Ward RE, Jamison PL (1991) Measurement precision and reliability in craniofacial anthropometry: implications and suggestions for clinical applications. *Journal of Craniofacial Genetics & Developmental Biology* 11:156-164
- Ward RE, Jamison PL, Allanson JE (2000) Quantitative approach to identifying abnormal variation in the human face exemplified by a study of 278 individuals with five craniofacial syndromes. *American Journal of Medical Genetics* 91:8-17
- Watnick SS (1972) Inheritance of craniofacial morphology. *Angle Orthodontist* 42:339-351
- Weedon MN, Lango H, Lindgren CM, Wallace C, Evans DM, Mangino M, Freathy RM, Perry JR, Stevens S, Hall AS *et al.* (2008) Genome-wide association analysis identifies 20 loci that influence adult height. *Nature Genetics* 40:575-583
- Weinberg SM, Parsons TE, Marazita ML, Maher BS (2013) Heritability of face shape in twins: a preliminary study using 3D stereophotogrammetry and geometric morphometrics. *Dentistry 3000* 1:a004
- Wigginton JE, Abecasis GR (2005) PEDSTATS: descriptive statistics, graphics and quality assessment for gene mapping data. *Bioinformatics* 21:3445-3447

- Willer CJ, Sanna S, Jackson AU, Scuteri A, Bonnycastle LL, Clarke R, Heath SC, Timpson NJ, Najjar SS, Stringham HM *et al.* (2008) Newly identified loci that influence lipid concentrations and risk of coronary artery disease. *Nature Genetics* 40:161-169
- Williamson EH, Simmons MD (1979) Mandibular asymmetry and its relation to pain dysfunction. *American Journal of Orthodontics* 76:612-617
- Winter RM (1998) Animal models for dysmorphology. *Current Opinion in Genetics & Development* 8:293-297
- Wong JY, Oh AK, Ohta E, Hunt AT, Rogers GF, Mulliken JB, Deutsch CK (2008) Validity and reliability of craniofacial anthropometric measurement of 3D digital photogrammetric images. *Cleft Palate-Craniofacial Journal* 45:232-239
- WTCCC 'Wellcome Trust Case Control Consortium': Burton PR, Clayton DG, Cardon LR, Craddock N, Deloukas P, Duncanson A, Kwiatkowski DP, McCarthy MI, Ouwehand WH, Samani NJ *et al.* (2007) Genome-wide association study of 14,000 cases of seven common diseases and 3,000 shared controls. *Nature* 447:661-678
- Wu J, Smith WAP, Hancock ER (2010) Facial gender classification using shape-from-shading. *Image and Vision Computing* 28:1039-1048
- Wu J, Smith WAP, Hancock ER (2011) Gender discriminating models from facial surface normals. *Pattern Recognition* 44:2871-2886
- Wylie WL (1944) A quantitative method for the comparison of craniofacial patterns in different individuals: Its application to a study of parents and offspring. *American Journal of Anatomy* 74:39-60
- Xue F, Rabie ABM, Luo G (2014) Analysis of the association of COL2A1 and IGF-1 with mandibular prognathism in a Chinese population. *Orthodontics & Craniofacial Research*, 2014 Jan 5 [Epub]
- Xue F, Wong R, Rabie AB (2010a) Identification of SNP markers on 1p36 and association analysis of EPB41 with mandibular prognathism in a Chinese population. *Archives of Oral Biology* 55:867-872
- Xue F, Wong RW, Rabie AB (2010b) Genes, genetics, and Class III malocclusion. *Orthodontics & Craniofacial Research* 13:69-74

- Yamada T, Mori Y, Minami K, Mishima K, Tsukamoto Y (2002) Three-dimensional analysis of facial morphology in normal Japanese children as control data for cleft surgery. *Cleft Palate-Craniofacial Journal* 39:517-526
- Yamada T, Sugahara T, Mori Y, Minami K, Sakuda M (1999) Development of a 3-D measurement and evaluation system for facial forms with a liquid crystal range finder. *Computer Methods And Programs In Biomedicine* 58:159-173
- Yu TH, Moon YS (2008) A Novel Genetic Algorithm for 3D Facial Landmark Localization. In *2nd IEEE International Conference on Biometrics: Theory, Applications and Systems*, 2008, pp 1–6.
- Zacharopoulos GV, Manios A, De Bree E, Kau CH, Petousis M, Zacharopoulou I, Kouremenos N (2012) Neoclassical facial canons in young adults. *Journal of Craniofacial Surgery* 23:1693-1698
- Zankl A, Eberle L, Molinari L, Schinzel A (2002) Growth charts for nose length, nasal protrusion, and philtrum length from birth to 97 years. *American Journal of Medical Genetics* 111:388-391
- Zelditch ML, Lundrigan BL, Garland T, Jr. (2004) Developmental regulation of skull morphology. I. Ontogenetic dynamics of variance. *Evolution & Development* 6:194-206
- Zhang MQ (1998) Statistical features of human exons and their flanking regions. *Human Molecular Genetics* 7:919-932
- Zhao S, Zhang X, Gao Y (2008) A comparative evaluation of Average Face on holistic and local face recognition approaches. In *19th International Conference on Pattern Recognition (ICPR)*, 2008, pp 1-4.
- Zheng JY (1994) Acquiring 3-D Models from Sequences of Contours. *IEEE Transactions on Pattern Analysis and Machine Intelligence* 16:163-178
- Zhou J, Lu Y, Gao XH, Chen YC, Lu JJ, Bai YX et al (2005) The growth hormone receptor gene is associated with mandibular height in a Chinese population. *Journal of Dental Research* 84:1052-1056

- Zhu H, Kartiko S, Finnell RH (2009) Importance of gene-environment interactions in the etiology of selected birth defects. *Clinical Genetics* 75:409-423
- Zhurov AI, Kau CH, Richmond S (2005) Computer methods for measuring 3D facial morphology. In, Middleton J, Shrive MG, Jones ML (eds). *Computer Methods in Biomechanics and Biomedical Engineering-5*. Cardiff: FIRST Numerics Ltd; ISBN 0-9549670-0-3
- Zhurov AI, Richmond S, Kau CH, Toma AM (2010) Averaging facial images. In, Kau CH, Richmond S (eds). *Three-dimensional imaging for orthodontics and maxillofacial surgery*. Wiley-Blackwell, London, pp 126-144
- Zitnick C, Webb JA (1996) Multi-baseline stereo using surface extraction. *In Technical Report CMU-CS-96-196*. Computer Science Department, Carnegie Mellon University, Pittsburgh, PA.

# Contributions

## Contributions

Work from this thesis has appeared in the following publications:

### Articles

**Toma AM**, Zhurov AI, Playle R, Marshall D, Rosin PL and Richmond S (2012) The assessment of facial variation in 4747 British school children. *European Journal of Orthodontics* 34 (6):655-664

**Toma AM**, Zhurov AI, Playle R, Ong E and Richmond S (2009) Reproducibility of facial soft tissue landmarks on 3D laser-scanned facial images. *Orthodontics and Craniofacial Research* 12 (1):33-42

**Toma AM**, Zhurov AI, Playle R and Richmond S (2008) A three-dimensional look for facial differences between males and females in a British-Caucasian sample aged 15½ years old. *Orthodontics and Craniofacial Research* 11 (3):180-185

Paternoster L, Zhurov AI, **Toma AM**, Kemp JP, St. Pourcain B, Timpson NJ, McMahon G, McArdle W, Ring SM, Smith GD, Richmond S and Evans DM (2012) Genome-wide Association Study of Three-Dimensional Facial Morphology Identifies a Variant in PAX3 Associated with Nasion Position. *American Journal of Human Genetics* 90 (3):478-485

Fatemifar G, Hoggart CJ, Paternoster L, Kemp JP, Prokopenko I, Horikoshi M, Wright VJ, Tobias JH, Richmond S, Zhurov AI, **Toma AM**, Pouta A *et al.* (2013) Genome-wide association study of primary tooth eruption identifies pleiotropic loci associated with height and craniofacial distances. *Human Molecular Genetics* 22 (18):3807-3817

Richmond S, Al Ali A, Beldie L, Chong YT, Cronin AJ, Djordjevic J, Drage N, Evans DM, Jones DK, Lu Y, Marshall D, Middleton J, Parker G, Paternoster L, Playle R, Popat H, Rosin PL, Sidorov K, **Toma AM**, Walker B, Wilson C and Zhurov AI (2012) Detailing Patient Specific Modeling to Aid Clinical Decision-Making. *Lecture Notes in Computational Vision and Biomechanics* 5:105-131

Djordjevic J, Lawlor DA, Zhurov AI, **Toma AM**, Playle R and Richmond S (2013) A population-based cross-sectional study of the association between facial morphology and cardiometabolic risk factors in adolescence. *BMJ Open* 3 (5):e002910

Richmond S, **Toma AM** and Zhurov AI (2009) New perspectives on craniofacial growth. *L'Orthodontie Française*. 80 (4):359-369 [Article in French]

Wilson C, Playle R, **Toma AM**, Zhurov AI, Ness A and Richmond S (2013) The prevalence of lip vermilion morphological traits in a 15-year-old population. *American Journal of Medical Genetics Part A* 161 (1):4-12

Popat H, Zhurov AI, **Toma AM**, Richmond S, Marshall D and Rosin PL (2012) Statistical modelling of lip movement in the clinical context. *Orthodontics and Craniofacial Research* 15 (2):92-102

Djordjevic J, Jadallah M, Zhurov AI, **Toma AM** and Richmond S (2013) Three-dimensional analysis of facial shape and symmetry in twins using laser surface scanning. *Orthodontics and Craniofacial Research* 16 (3):146-160

Djordjevic J, Pirttiniemi P, Harila V, Heikkinen T, **Toma AM**, Zhurov AI and Richmond S (2013) Three-dimensional longitudinal assessment of facial symmetry in adolescents. *European Journal of Orthodontics* 35 (2):143-151

Djordjevic J, **Toma AM**, Zhurov AI and Richmond S (2014) Three-dimensional quantification of facial symmetry in adolescents using laser surface scanning. *European Journal of Orthodontics* 36 (2):125-132

Al Ali A, Richmond S, Popat H, **Toma AM**, Playle R, Zhurov AI, Marshall D, Rosin PL and Henderson J. The influence of asthma on face shape: a three-dimensional study. *European Journal of Orthodontics*, first published online October 4, 2012 doi:10.1093/ejo/cjs067

Al Ali A, Richmond S, Popat H, **Toma AM**, Playle R, Pickles T, Zhurov AI, Marshall D, Rosin PL and Henderson J. A three-dimensional analysis of the effect of atopy on face shape. *European Journal of Orthodontics*, first published online January 28, 2013 doi:10.1093/ejo/cjs107

Pound N, Lawson DW, Toma AM, Richmond S, Zhurov A and Penton-Voak I. Facial fluctuating asymmetry is not associated with childhood ill-health in a large British cohort study. *Proceedings of the Royal Society B* [In Press]

### **Book Chapters**

Richmond S, Zhurov AI and **Toma AM** (2012) Three-dimensional facial imaging. In: Wilkinson C and Rynn C (eds.) *Craniofacial Identification*, Cambridge: Cambridge University Press, pp. 154-165

Zhurov AI, Richmond S, Kau CH and **Toma AM** (2010) Averaging facial images. In: Kau CH and Richmond S (eds.) *Three-Dimensional Imaging for Orthodontics and Maxillofacial Surgery*, London: Wiley-Blackwell, pp. 126-144

Richmond S, Zhurov AI, **Toma AM**, Kau CH and Hartles F (2010) Visualizing facial growth. In: Kau CH and Richmond S (eds.) *Three-Dimensional Imaging for Orthodontics and Maxillofacial Surgery*, London: Wiley-Blackwell, pp. 207-225

**Commentary:** from the editor in chief (Anne Marie Kuijpers-Jagtman) of the journal of Orthodontics and Craniofacial Research regarding the article:

**Toma AM**, Zhurov AI, Playle R, Marshall D, Rosin PL and Richmond S (2012) The assessment of facial variation in 4747 British school children. *European Journal of Orthodontics* 34 (6):655-664

Kuijpers-Jagtman AM (2012) Facial variation: from visual assessment to three-dimensional quantification. *European Journal of Orthodontics* 34 (6): 665-666

**Participation:**

The 86th congress of the European Orthodontic Society (EOS), June 15-19, 2010, Portoroz, Slovenia. (Oral Presentation: Categorization of Facial Form)

# Appendix

## Appendix

Total Sample (n=120)		Registration Data L/R				Superimposition (%)		
No	ID Number	Scan	AD mm	SD mm	0.5 mm %	0.5 mm %	0.75 mm %	1.0 mm %
1	70142849	a	0.22	0.22	91.2	81.1	94.2	98.8
		b	0.26	0.23	87.0			
2	70150497	a	0.27	0.30	85.0	77.4	88.3	94.3
		b	0.36	0.29	74.5			
3	70210679	a	0.20	0.18	94.1	71.2	82.8	88.9
		b	0.27	0.32	88.2			
4	70212424	a	0.28	0.29	83.2	71.2	77.7	80.9
		b	0.34	0.42	82.2			
5	70212591	a	0.33	0.35	81.3	85.9	94.9	98.4
		b	0.25	0.29	85.0			
6	70226869	a	0.35	0.43	78.8	73.0	82.0	87.2
		b	0.29	0.27	83.7			
7	70229605	a	0.40	0.35	71.1	83.9	93.6	96.9
		b	0.25	0.25	89.1			
8	70249479	a	0.36	0.41	76.4	73.4	84.0	89.6
		b	0.33	0.29	80.9			
9	70259863	a	0.34	0.34	78.0	83.4	95.2	97.9
		b	0.25	0.22	87.6			
10	70260617	a	0.28	0.26	83.0	96.1	99.8	100
		b	0.23	0.25	87.7			
11	70283911	a	0.30	0.29	83.7	84.1	92.8	97.5
		b	0.23	0.23	87.6			
12	70321343	a	0.23	0.21	89.6	76.2	91.8	95.0
		b	0.29	0.25	80.6			
13	70364414	a	0.33	0.24	75.6	81.3	92.2	97.0
		b	0.19	0.18	93.8			
14	70399320	a	0.31	0.41	85.3	72.6	90.4	96.0
		b	0.23	0.21	88.4			
15	70428043	a	0.29	0.26	82.9	82.1	95.1	97.6
		b	0.33	0.34	79.3			
16	70440646	a	0.25	0.23	88.1	80.4	95.9	99.5
		b	0.26	0.26	87.1			
17	70445908	a	0.31	0.32	78.3	78.3	89.8	94.5
		b	0.24	0.22	89.2			
18	70452021	a	0.25	0.22	88.1	82.4	93.9	97.7
		b	0.26	0.21	89.4			
19	70454547	a	0.38	0.29	71.5	84.0	91.0	96.0
		b	0.22	0.19	93.2			
20	70489830	a	0.35	0.30	78.8	80.7	86.6	89.9
		b	0.20	0.20	93.0			
21	70521149	a	0.23	0.24	90.1	88.1	97.2	99.3
		b	0.21	0.24	91.3			
22	70522684	a	0.34	0.38	79.3	85.0	95.8	98.5
		b	0.34	0.30	77.0			
23	70523131	a	0.29	0.28	83.7	88.3	97.0	99.5
		b	0.22	0.22	89.5			
24	70536348	a	0.24	0.28	86.1	82.0	93.3	98.1
		b	0.17	0.17	95.2			
25	70536655	a	0.27	0.26	84.0	77.2	89.1	96.1
		b	0.39	0.37	73.6			
26	70547039	a	0.27	0.30	85.2	88.1	97.0	99.5
		b	0.20	0.21	93.6			
27	70567807	a	0.19	0.18	95.3	89.9	98.0	99.9
		b	0.24	0.24	88.3			
28	70577437	a	0.35	0.38	78.3	70.2	84.0	91.1
		b	0.36	0.36	78.5			
29	70609133	a	0.25	0.22	88.7	97.4	99.9	100
		b	0.20	0.20	92.7			
30	70610054	a	0.24	0.16	93.3	90.1	98.6	99.5
		b	0.21	0.20	90.8			

**AD: Average Distance, SD: Standard Deviation, L/R: Left/Right (Facial Shells)**

<b>Total Sample (n=120)</b>			<b>Registration Data L/R</b>			<b>Superimposition (%)</b>		
<b>No</b>	<b>ID Number</b>	<b>Scan</b>	<b>AD mm</b>	<b>SD mm</b>	<b>0.5 mm %</b>	<b>0.5 mm %</b>	<b>0.75 mm %</b>	<b>1.0 mm %</b>
31	70625867	a	0.27	0.28	85.2	82.5	91.0	95.3
		b	0.33	0.27	78.9			
32	70645030	a	0.28	0.35	85.2	98.1	99.4	99.6
		b	0.23	0.18	93.6			
33	70674367	a	0.26	0.25	83.2	92.9	97.3	99.3
		b	0.22	0.21	89.0			
34	70693083	a	0.26	0.24	87.3	85.7	93.0	96.2
		b	0.24	0.24	87.0			
35	70749134	a	0.19	0.17	94.2	88.0	96.1	98.5
		b	0.29	0.25	84.2			
36	70753879	a	0.20	0.21	92.7	76.0	86.9	91.8
		b	0.31	0.30	80.1			
37	70766552	a	0.28	0.30	84.6	98.6	99.8	99.9
		b	0.19	0.18	93.6			
38	70777620	a	0.37	0.30	72.9	78.1	86.6	93.0
		b	0.36	0.27	72.4			
39	70790153	a	0.25	0.20	90.6	81.8	92.3	97.8
		b	0.36	0.30	77.3			
40	70791758	a	0.27	0.28	85.9	76.2	90.9	97.4
		b	0.27	0.23	87.4			
41	70793293	a	0.30	0.24	84.2	98.0	99.6	99.9
		b	0.17	0.19	96.4			
42	70813517	a	0.31	0.29	79.6	87.6	94.3	97.5
		b	0.30	0.24	81.2			
43	70828646	a	0.34	0.34	77.5	82.5	90.8	94.4
		b	0.34	0.33	76.3			
44	70849414	a	0.39	0.34	73.5	86.9	93.6	96.1
		b	0.28	0.29	83.8			
45	70854396	a	0.26	0.21	87.3	77.4	89.8	95.7
		b	0.36	0.38	77.2			
46	70866078	a	0.24	0.22	91.0	88.1	94.1	96.5
		b	0.22	0.23	90.4			
47	70867753	a	0.37	0.35	74.6	85.5	94.9	97.9
		b	0.27	0.26	83.1			
48	70879742	a	0.29	0.21	85.0	94.6	99.0	99.9
		b	0.17	0.20	94.8			
49	70905018	a	0.27	0.30	85.6	72.1	86.6	92.9
		b	0.42	0.36	71.5			
50	70913350	a	0.24	0.19	92.2	88.2	95.6	99.5
		b	0.26	0.22	84.4			
51	70915639	a	0.29	0.31	82.2	74.6	88.7	93.6
		b	0.21	0.19	92.5			
52	70921752	a	0.26	0.23	85.7	84.1	92.6	95.2
		b	0.22	0.21	90.2			
53	70926707	a	0.18	0.20	93.3	87.7	97.3	99.6
		b	0.26	0.25	84.7			
54	70928312	a	0.24	0.23	91.3	83.9	93.0	97.0
		b	0.32	0.27	81.1			
55	70932443	a	0.29	0.30	82.9	86.2	93.1	97.7
		b	0.27	0.30	86.7			
56	70941389	a	0.29	0.32	83.7	71.8	87.5	96.6
		b	0.27	0.31	84.7			
57	70942687	a	0.22	0.20	89.9	94.6	99.6	100
		b	0.25	0.23	86.8			
58	70948256	a	0.29	0.27	84.1	86.7	95.3	98.9
		b	0.34	0.32	80.7			
59	71013937	a	0.24	0.20	91.8	75.5	87.4	93.3
		b	0.33	0.37	78.9			
60	71052807	a	0.22	0.23	90.3	91.2	96.8	98.4
		b	0.30	0.29	83.0			

**AD: Average Distance, SD: Standard Deviation, L/R: Left/Right (Facial Shells)**

Table 1 (c) Subjects 61-90								
Total Sample (n=120)			Registration Data L/R			Superimposition (%)		
No	ID Number	Scan	AD mm	SD mm	0.5 mm %	0.5 mm %	0.75 mm %	1.0 mm %
61	71061683	a	0.28	0.25	84.3	80.1	91.7	97.0
		b	0.28	0.25	83.0			
62	71084056	a	0.23	0.23	90.9	75.1	93.6	98.1
		b	0.39	0.31	70.9			
63	71114217	a	0.16	0.20	95.4	95.2	99.8	100
		b	0.16	0.17	97.7			
64	71126680	a	0.19	0.19	93.6	87.7	96.1	98.9
		b	0.26	0.28	85.7			
65	71138292	a	0.18	0.17	94.4	96.7	99.8	100
		b	0.25	0.25	85.6			
66	71145606	a	0.28	0.23	87.2	72.4	82.8	87.3
		b	0.26	0.38	87.3			
67	71151412	a	0.34	0.30	75.6	72.7	90.3	97.3
		b	0.22	0.22	91.8			
68	71152947	a	0.16	0.21	97.1	72.5	88.1	96.0
		b	0.35	0.39	79.1			
69	71206402	a	0.32	0.27	77.7	76.4	89.3	95.3
		b	0.24	0.24	87.2			
70	71220093	a	0.26	0.29	84.1	95.5	99.1	99.5
		b	0.38	0.37	74.1			
71	71225732	a	0.17	0.15	97.6	99.5	100	100
		b	0.20	0.17	95.4			
72	71240317	a	0.32	0.32	79.7	73.5	86.6	93.2
		b	0.32	0.30	79.6			
73	71247965	a	0.31	0.30	80.3	84.6	96.1	99.2
		b	0.34	0.32	77.1			
74	71292571	a	0.20	0.20	92.5	86.0	96.0	99.2
		b	0.21	0.17	93.7			
75	71305788	a	0.26	0.27	84.5	93.3	98.9	99.8
		b	0.18	0.16	96.5			
76	71334958	a	0.27	0.22	88.7	89.2	96.4	98.7
		b	0.21	0.20	92.7			
77	71344044	a	0.18	0.21	94.3	82.5	92.3	96.2
		b	0.23	0.23	90.7			
78	71359787	a	0.29	0.24	80.7	89.4	98.5	99.7
		b	0.27	0.26	85.9			
79	71360778	a	0.18	0.19	93.1	94.4	98.5	99.8
		b	0.28	0.24	84.8			
80	71387115	a	0.26	0.27	87.5	85.3	94.6	99.2
		b	0.38	0.40	73.6			
81	71437387	a	0.26	0.22	86.8	97.8	99.9	100
		b	0.31	0.23	84.0			
82	71468092	a	0.27	0.24	86.7	93.9	98.2	99.1
		b	0.28	0.28	83.2			
83	71475950	a	0.27	0.27	84.6	96.9	99.1	99.7
		b	0.38	0.38	74.1			
84	71504673	a	0.25	0.30	88.5	89.8	95.9	97.9
		b	0.37	0.38	78.1			
85	71524520	a	0.33	0.37	78.6	84.4	91.7	95.3
		b	0.35	0.26	74.8			
86	71621520	a	0.37	0.37	76.9	80.0	91.8	97.0
		b	0.25	0.23	88.5			
87	71628317	a	0.20	0.19	93.5	88.8	98.2	99.8
		b	0.17	0.16	96.8			
88	71642385	a	0.30	0.28	81.4	76.9	84.8	89.6
		b	0.25	0.26	87.0			
89	71661478	a	0.25	0.27	87.1	83.4	92.4	95.8
		b	0.37	0.38	76.2			
90	71670257	a	0.24	0.21	89.9	91.8	97.2	99.0
		b	0.34	0.41	80.4			

AD: Average Distance, SD: Standard Deviation, L/R: Left/Right (Facial Shells)

Table 1 (d) Subjects 91-120								
Total Sample (n=120)			Registration Data L/R			Superimposition (%)		
No	ID Number	Scan	AD mm	SD mm	0.5 mm %	0.5 mm %	0.75 mm %	1.0 mm %
91	71676063	a	0.42	0.38	70.0	78.5	91.1	95.0
		b	0.36	0.31	75.0			
92	71681492	a	0.29	0.21	84.3	97.5	99.6	99.9
		b	0.14	0.14	98.6			
93	71688052	a	0.23	0.23	92.6	88.4	96.2	98.0
		b	0.19	0.21	95.0			
94	71705777	a	0.33	0.33	80.0	93.2	98.8	99.7
		b	0.29	0.32	84.1			
95	71706531	a	0.31	0.31	83.0	91.8	96.8	98.9
		b	0.15	0.14	97.4			
96	71733886	a	0.29	0.31	81.8	76.0	91.3	95.9
		b	0.32	0.37	80.1			
97	71735868	a	0.32	0.28	79.7	77.8	87.4	92.7
		b	0.39	0.38	71.3			
98	71748918	a	0.32	0.33	79.6	78.4	86.7	91.3
		b	0.33	0.31	80.9			
99	71771081	a	0.19	0.19	94.6	72.1	79.7	86.9
		b	0.32	0.32	78.7			
100	71778562	a	0.20	0.19	91.9	82.2	93.2	97.0
		b	0.36	0.32	74.2			
101	71820265	a	0.29	0.30	83.5	86.0	95.5	99.0
		b	0.33	0.35	77.1			
102	71881061	a	0.26	0.18	92.2	79.2	91.0	98.4
		b	0.29	0.30	79.9			
103	71883113	a	0.25	0.22	88.7	87.9	95.4	98.4
		b	0.32	0.29	78.9			
104	71897181	a	0.19	0.20	92.0	89.3	98.0	99.5
		b	0.18	0.17	94.4			
105	71898312	a	0.27	0.23	86.3	90.9	99.0	99.9
		b	0.30	0.28	82.7			
106	71930552	a	0.22	0.19	92.5	75.4	85.6	92.1
		b	0.34	0.27	78.3			
107	71935297	a	0.23	0.20	91.8	83.3	90.5	94.2
		b	0.34	0.35	78.4			
108	71946435	a	0.39	0.29	70.0	82.8	91.8	95.4
		b	0.30	0.38	82.6			
109	71991962	a	0.21	0.24	90.2	85.5	95.6	98.4
		b	0.18	0.19	95.0			
110	72002583	a	0.22	0.24	87.5	74.8	90.4	98.3
		b	0.21	0.22	92.2			
111	72010064	a	0.28	0.24	84.1	75.3	84.6	88.8
		b	0.34	0.31	77.4			
112	72047943	a	0.26	0.25	86.5	90.0	98.1	99.9
		b	0.27	0.24	86.3			
113	72052451	a	0.19	0.19	94.7	94.7	98.5	100
		b	0.20	0.21	92.8			
114	72072158	a	0.24	0.24	88.4	85.9	98.2	99.7
		b	0.26	0.21	90.2			
115	72082849	a	0.20	0.22	90.9	96.3	99.9	100
		b	0.24	0.19	91.1			
116	72083770	a	0.19	0.18	94.9	94.6	99.6	100
		b	0.22	0.22	90.2			
117	72089716	a	0.29	0.25	86.3	81.8	93.4	97.5
		b	0.32	0.28	78.4			
118	72158607	a	0.26	0.19	91.1	98.8	99.9	100
		b	0.18	0.18	93.7			
119	72177183	a	0.19	0.23	92.3	76.4	94.1	99.4
		b	0.28	0.31	82.2			
120	72185725	a	0.37	0.33	73.4	96.4	99.1	99.7
		b	0.28	0.23	85.1			

AD: Average Distance, SD: Standard Deviation, L/R: Left/Right (Facial Shells)

Table 2. Records taken for posture adoption study (Group 2)									
Total Sample (n=20)			Registration Data L/R Shells			Days Between Scans	Superimposition (%)		
No	ID Number	Scan	AD mm	SD mm	0.5mm %		0.5mm %	0.75mm %	1.0mm %
1	72201091	a	0.47	0.42	63.6	40	79.3	91.2	95.8
		b	0.24	0.19	91.3				
2	72195969	a	0.30	0.26	80.9	26	70.7	82.8	89.6
		b	0.24	0.22	90.9				
3	70758220	a	0.22	0.23	90.2	42	83.4	92.9	97.7
		b	0.28	0.27	83.2				
4	70907544	a	0.33	0.30	79.5	41	64.3	79.6	87.7
		b	0.17	0.17	95.2				
5	72203757	a	0.34	0.37	78.2	39	84.4	92.1	95.1
		b	0.14	0.16	98.5				
6	72191838	a	0.29	0.35	84.0	32	72.4	82.9	88.5
		b	0.26	0.32	86.2				
7	72192689	a	0.35	0.39	82.7	35	82.8	94.9	98.1
		b	0.24	0.27	88.4				
8	70912806	a	0.21	0.21	94.7	42	66.2	78.3	85.6
		b	0.39	0.51	78.6				
9	71359787	a	0.29	0.24	80.8	32	86.9	94.7	97.7
		b	0.37	0.41	77.8				
10	72190917	a	0.25	0.24	88.7	23	74.6	89.5	95.1
		b	0.31	0.32	82.3				
11	71951180	a	0.41	0.32	69.3	15	78.5	90.1	94.8
		b	0.25	0.26	87.9				
12	72197644	a	0.32	0.30	81.4	20	90.4	96.4	97.6
		b	0.37	0.37	76.4				
13	71051816	a	0.23	0.22	90.6	36	66.1	82.6	89.3
		b	0.25	0.27	87.3				
14	71093142	a	0.31	0.30	79.0	35	78.9	87.4	90.9
		b	0.30	0.24	82.9				
15	71438211	a	0.31	0.33	80.7	32	70.2	82.9	88.7
		b	0.62	0.78	65.3				
16	71812170	a	0.30	0.35	85.9	35	80.5	87.4	89.8
		b	0.24	0.25	86.9				
17	70846441	a	0.24	0.24	89.0	26	72.8	83.1	89.9
		b	0.30	0.24	80.7				
18	72051083	a	0.11	0.16	98.5	42	85.3	91.7	95.3
		b	0.31	0.31	81.3				
19	72205292	a	0.18	0.17	95.5	31	75.0	86.7	93.2
		b	0.37	0.38	75.4				
20	70122458	a	0.43	0.55	74.2	21	78.2	90.9	94.6
		b	0.33	0.39	79.8				

AD: Average Distance, SD: Standard Deviation, L/R: Left/Right (Facial Shells)

**Table 3. 250 facial parameters and their gender prediction efficiency  
(Females: n = 2514; Males: n = 2233; Total: n = 4747)**

No	Facial Parameters	Females (Average)	Females (SD)	Males (Average)	Males (SD)	Females (Pred.)	Males (Pred.)	Total (Pred.)
<b>Distances (n = 90)</b>								
1	en-men.x	16.81	1.38	17.39	1.43	59.3%	56.7%	58.0%
2	psL-men.y	8.27	1.42	7.40	1.56	62.2%	60.7%	61.5%
3	psR-men.y	8.17	1.44	7.26	1.56	64.2%	61.0%	62.7%
4	piL-men.y	3.25	1.11	3.54	1.18	55.6%	54.7%	55.2%
5	piR-men.y	3.21	1.10	3.55	1.17	58.2%	56.1%	57.2%
6	psL-sn.y	49.72	3.01	51.22	3.50	60.7%	57.7%	59.3%
7	psR-sn.y	49.62	3.00	51.09	3.52	58.9%	57.9%	58.4%
8	men-chL.x	25.92	2.06	26.59	2.21	57.5%	56.3%	57.0%
9	men-chR.x	26.57	2.14	27.10	2.25	55.8%	53.6%	54.8%
10	men-cphL.x	5.79	1.16	6.45	1.25	62.4%	59.9%	61.2%
11	men-cphR.x	6.42	1.13	7.10	1.28	62.6%	60.5%	61.7%
12	<b>men-g.z</b>	<b>14.76</b>	<b>2.12</b>	<b>17.23</b>	<b>2.37</b>	<b>72.0%</b>	<b>70.4%</b>	<b>71.2%</b>
13	men-n.x	-0.15	0.69	-0.17	0.74	49.4%	50.5%	49.9%
14	men-n.y	9.22	2.27	9.15	2.38	50.2%	51.1%	50.7%
15	<b>men-n.z</b>	<b>13.54</b>	<b>1.93</b>	<b>16.00</b>	<b>2.17</b>	<b>73.8%</b>	<b>72.2%</b>	<b>73.1%</b>
16	men-psL.z	3.69	1.66	4.91	1.69	64.3%	65.0%	64.6%
17	men-psR.z	3.68	1.64	4.82	1.66	65.4%	65.4%	65.4%
18	<b>men-all.x</b>	<b>15.84</b>	<b>1.35</b>	<b>17.12</b>	<b>1.50</b>	<b>70.1%</b>	<b>66.9%</b>	<b>68.6%</b>
19	men-alR.x	16.57	1.44	17.84	1.57	68.5%	66.9%	67.7%
20	<b>men-prn.z</b>	<b>35.61</b>	<b>2.58</b>	<b>39.23</b>	<b>3.06</b>	<b>76.3%</b>	<b>73.6%</b>	<b>75.0%</b>
21	g-men.x	-0.43	0.78	-0.45	0.81	50.8%	49.9%	50.4%
22	prn-men.x	-0.12	1.06	-0.14	1.18	49.6%	49.3%	49.4%
23	mal-men.x	-0.37	0.79	-0.36	0.84	50.8%	51.3%	51.0%
24	sn-men.x	-0.11	0.86	-0.11	0.95	49.9%	48.8%	49.4%
25	ls-men.x	-0.29	0.74	-0.29	0.76	50.7%	50.7%	50.7%
26	mcph-men.x	-0.31	0.75	-0.32	0.78	49.5%	49.8%	49.6%
27	li-men.x	0.04	0.68	0.09	0.70	52.3%	51.5%	51.9%
28	mch-men.x	-0.32	0.77	-0.25	0.79	52.4%	51.1%	51.8%
29	pg-men.x	0.33	0.84	0.41	0.87	51.4%	52.8%	52.0%
30	<b>mal-men.z</b>	<b>15.88</b>	<b>1.93</b>	<b>18.19</b>	<b>2.16</b>	<b>73.3%</b>	<b>71.4%</b>	<b>72.4%</b>
31	<b>sn-men.z</b>	<b>21.10</b>	<b>2.07</b>	<b>24.03</b>	<b>2.38</b>	<b>76.1%</b>	<b>74.6%</b>	<b>75.4%</b>
32	<b>ls-men.z</b>	<b>22.14</b>	<b>1.75</b>	<b>24.80</b>	<b>2.00</b>	<b>78.6%</b>	<b>74.5%</b>	<b>76.7%</b>
33	li-men.z	18.65	1.65	20.36	1.87	69.5%	67.4%	68.5%
34	<b>mcph-men.z</b>	<b>21.25</b>	<b>1.69</b>	<b>23.85</b>	<b>1.91</b>	<b>77.9%</b>	<b>75.1%</b>	<b>76.6%</b>
35	<b>mch-men.z</b>	<b>6.63</b>	<b>1.81</b>	<b>8.42</b>	<b>1.80</b>	67.7%	<b>70.0%</b>	68.8%
36	pg-men.z	14.47	2.76	14.60	2.97	50.6%	51.1%	50.8%
37	g-men	26.37	1.97	27.04	2.02	56.6%	56.2%	56.4%
38	g-n	12.59	2.61	11.63	2.60	56.0%	58.5%	57.2%
39	enL-enR	33.65	2.76	34.81	2.86	59.2%	56.7%	58.0%
40	exL-exR	86.75	3.84	88.40	4.08	57.9%	56.6%	57.3%
41	psL-psR	61.23	3.28	62.40	3.41	57.8%	54.4%	56.2%
42	piL-piR	61.87	3.23	63.07	3.37	58.2%	55.2%	56.8%
43	enL-exL	27.04	1.92	27.22	1.97	52.7%	52.5%	52.6%
44	enR-exR	27.32	1.88	27.48	1.89	51.6%	52.5%	52.1%
45	psL-piL	11.79	1.34	11.53	1.40	54.9%	51.6%	53.4%
46	psR-piR	11.63	1.35	11.38	1.38	54.7%	51.6%	53.2%
47	exL-XZ	-0.38	1.69	1.29	1.90	69.0%	67.2%	68.1%
48	<b>exR-XZ</b>	<b>-0.53</b>	<b>1.68</b>	<b>1.45</b>	<b>1.92</b>	<b>72.2%</b>	<b>70.0%</b>	<b>71.2%</b>
49	exL-XY	-4.53	1.41	-5.66	1.54	66.7%	64.9%	65.9%
50	exR-XY	-4.75	1.43	-5.92	1.51	67.1%	64.4%	65.9%
51	exL-YZ	43.29	1.98	44.11	2.13	59.1%	56.7%	58.0%
52	exR-YZ	-43.45	2.00	-44.27	2.09	57.0%	57.5%	57.2%
53	<b>enL-XZ</b>	<b>-0.91</b>	<b>1.46</b>	<b>1.29</b>	<b>1.66</b>	<b>77.0%</b>	<b>74.9%</b>	<b>76.0%</b>
54	<b>enR-XZ</b>	<b>-1.11</b>	<b>1.46</b>	<b>0.98</b>	<b>1.66</b>	<b>76.1%</b>	<b>72.5%</b>	<b>74.4%</b>
55	<b>enL-XY</b>	<b>0.57</b>	<b>1.13</b>	<b>-1.01</b>	<b>1.19</b>	<b>75.8%</b>	<b>74.5%</b>	<b>75.2%</b>
56	<b>enR-XY</b>	<b>0.87</b>	<b>1.10</b>	<b>-0.60</b>	<b>1.22</b>	<b>75.7%</b>	<b>72.5%</b>	<b>74.2%</b>
57	enL-YZ	16.82	1.46	17.38	1.51	58.9%	55.5%	57.3%
58	enR-YZ	-16.80	1.45	-17.40	1.51	59.6%	56.2%	58.0%
59	n-men	16.54	2.02	18.59	2.20	68.9%	68.1%	68.5%
60	<b>sn-men</b>	<b>46.55</b>	<b>2.79</b>	<b>50.03</b>	<b>3.30</b>	<b>73.3%</b>	<b>70.0%</b>	<b>71.7%</b>

61	n-prn	43.82	3.39	46.27	3.83	64.2%	62.6%	63.4%
62	n-sn	51.26	3.54	53.63	3.91	64.2%	61.6%	63.0%
63	n-all	44.19	2.89	47.00	3.18	69.6%	66.0%	67.9%
64	n-alR	44.39	2.90	47.20	3.18	69.4%	66.8%	68.2%
65	<b>alL-alR</b>	<b>32.44</b>	<b>2.30</b>	<b>35.00</b>	<b>2.56</b>	<b>73.0%</b>	69.0%	<b>71.1%</b>
66	prn-sn	19.45	1.87	20.08	1.96	59.1%	55.4%	57.4%
67	<b>prn-all</b>	<b>25.70</b>	<b>1.51</b>	<b>27.60</b>	<b>1.78</b>	<b>74.6%</b>	<b>70.5%</b>	<b>72.7%</b>
68	<b>prn-alR</b>	<b>25.95</b>	<b>1.52</b>	<b>27.77</b>	<b>1.77</b>	<b>73.9%</b>	<b>70.5%</b>	<b>72.3%</b>
69	sn-all	19.46	1.32	20.63	1.46	68.1%	64.8%	66.5%
70	sn-alR	19.84	1.33	20.99	1.46	68.5%	65.2%	66.9%
71	sn-ls	13.78	2.09	15.60	2.24	67.2%	66.2%	66.7%
72	ls-li	15.49	2.31	16.31	2.70	58.7%	55.0%	57.0%
73	li-pg	20.35	2.50	21.84	3.05	64.1%	57.5%	61.0%
74	ls-pg	35.68	3.13	37.96	3.77	66.8%	60.6%	63.9%
75	ls-cphL	6.45	0.95	7.15	1.10	66.2%	62.2%	64.3%
76	ls-cphR	6.52	0.98	7.25	1.12	64.9%	62.7%	63.9%
77	cphL-cphR	12.23	1.74	13.56	1.99	66.1%	62.6%	64.5%
78	chL-chR	52.52	3.92	53.72	4.17	56.8%	55.4%	56.1%
79	chL-cphL	26.61	2.31	27.17	2.48	55.8%	54.5%	55.2%
80	chL-li	29.68	2.54	30.36	2.69	57.0%	53.2%	55.3%
81	chR-cphR	26.64	2.33	27.07	2.47	54.9%	53.3%	54.2%
82	chR-li	30.31	2.62	30.95	2.69	56.6%	52.4%	54.6%
83	<b>ls-men</b>	<b>59.37</b>	<b>2.97</b>	<b>64.26</b>	<b>3.42</b>	<b>80.1%</b>	<b>75.6%</b>	<b>78.0%</b>
84	<b>li-men</b>	<b>72.52</b>	<b>3.80</b>	<b>77.55</b>	<b>4.36</b>	<b>75.2%</b>	<b>71.6%</b>	<b>73.5%</b>
85	<b>pg-men</b>	<b>90.92</b>	<b>4.47</b>	<b>96.76</b>	<b>5.32</b>	<b>74.4%</b>	<b>70.6%</b>	<b>72.6%</b>
86	pg-g	111.46	5.33	116.32	6.17	67.6%	64.9%	66.3%
87	<b>pg-n</b>	<b>98.98</b>	<b>5.18</b>	<b>104.82</b>	<b>6.02</b>	<b>70.5%</b>	68.0%	69.3%
88	<b>pg-sn</b>	<b>48.86</b>	<b>3.96</b>	<b>52.78</b>	<b>4.61</b>	<b>70.2%</b>	65.9%	68.2%
89	pg-chL	38.49	2.88	39.85	3.12	61.2%	56.7%	59.1%
90	pg-chR	39.40	2.96	40.75	3.09	62.7%	56.4%	59.7%
<b>Angles (n = 118)</b>								
1	ex-ps-enL.xy	118.41	6.80	123.27	8.06	66.7%	58.8%	63.0%
2	ex-ps-enR.xy	118.37	7.18	124.06	8.07	68.9%	61.6%	65.5%
3	ex-pi-enL.xy	149.22	7.00	149.01	7.01	50.4%	51.3%	50.8%
4	ex-pi-enR.xy	151.31	7.28	149.73	7.36	54.7%	54.5%	54.6%
5	cph-ls-cph.xy	145.65	9.76	145.26	9.19	53.1%	49.3%	51.3%
6	n-exL-pg.yz	102.10	7.83	101.77	7.77	50.6%	50.3%	50.5%
7	n-exR-pg.yz	102.10	7.78	101.02	7.67	52.2%	51.8%	52.0%
8	men-exL-pg.yz	71.06	17.14	77.50	19.54	59.2%	56.1%	57.7%
9	men-exR-pg.yz	72.70	15.81	75.51	17.90	54.8%	51.5%	53.3%
10	g-enL-enR	56.76	3.07	56.48	3.06	52.7%	51.9%	52.3%
11	g-enL-enR.XY	51.65	3.82	49.34	4.08	63.0%	60.6%	61.9%
12	g-enR-enL	58.09	3.15	57.92	3.20	50.8%	51.1%	50.9%
13	g-enR-enL.XY	52.63	3.88	50.21	4.14	64.0%	61.1%	62.6%
14	enL-g-enR	65.15	5.30	65.60	5.26	52.5%	50.2%	51.4%
15	enL-g-enR.XY	75.72	7.12	80.44	7.69	64.5%	60.2%	62.5%
16	g-enL-sn	100.54	5.41	95.45	5.56	67.9%	68.0%	68.0%
17	g-enL-sn.XY	119.10	5.26	117.09	5.54	58.7%	56.3%	57.6%
18	g-enR-sn	102.04	5.44	97.09	5.61	67.3%	67.0%	67.2%
19	g-enR-sn.XY	120.95	5.37	119.09	5.61	57.9%	56.1%	57.0%
20	g-exL-sn	63.61	3.59	62.47	3.71	56.2%	56.7%	56.5%
21	g-exL-sn.XY	69.79	3.63	69.44	3.76	51.5%	51.9%	51.7%
22	g-exR-sn	63.83	3.57	62.55	3.61	57.4%	57.5%	57.4%
23	g-exR-sn.XY	70.24	3.61	69.79	3.68	52.4%	52.8%	52.6%
24	men-g-exL	55.94	2.42	55.27	2.41	55.2%	55.3%	55.2%
25	men-g-exL.XY	63.16	3.17	64.10	3.38	56.3%	54.8%	55.6%
26	men-g-exR	57.15	2.38	56.70	2.42	52.8%	54.4%	53.6%
27	men-g-exR.XY	64.91	3.19	66.41	3.51	60.7%	58.4%	59.6%
28	prn-sn-ls	126.89	8.48	127.51	9.23	51.2%	51.5%	51.3%
29	prn-sn-ls.YZ	126.96	8.50	127.57	9.26	51.2%	51.3%	51.2%
30	n-sn-pg	163.61	5.45	161.01	5.59	58.4%	61.0%	59.6%
31	n-sn-pg.YZ	163.74	5.57	161.11	5.64	57.9%	61.3%	59.5%
32	n-sn-pg.XY	180.48	1.72	180.52	1.78	49.1%	50.4%	49.7%
33	n-prn-sn	101.20	4.66	100.36	4.67	53.1%	53.6%	53.3%
34	n-prn-sn.YZ	101.22	4.66	100.38	4.67	53.3%	53.7%	53.5%
35	n-prn-sn.XY	180.00	3.12	180.04	3.28	50.6%	49.8%	50.2%
36	n-prn-all	73.78	3.67	74.22	3.65	52.7%	51.3%	52.1%

37	n-prn-aIL.YZ	69.04	4.50	69.54	4.46	52.3%	50.9%	51.7%
38	n-prn-aIL.XY	101.46	5.72	101.81	5.70	49.6%	50.2%	49.9%
39	n-prn-aIR	74.08	3.76	74.54	3.78	52.6%	51.0%	51.8%
40	n-prn-aIR.YZ	69.23	4.69	69.76	4.70	51.9%	51.4%	51.7%
41	n-prn-aIR.XY	101.20	5.82	101.58	5.70	51.1%	51.1%	51.1%
42	n-aIL-sn	99.98	5.52	97.18	5.68	60.5%	60.3%	60.4%
43	n-aIL-sn.YZ	154.19	8.93	150.27	9.30	57.4%	59.6%	58.4%
44	n-aIL-sn.XY	99.62	5.62	96.82	5.79	60.3%	59.8%	60.1%
45	n-aIR-sn	98.65	5.57	96.06	5.76	57.9%	59.6%	58.7%
46	n-aIR-sn.YZ	154.59	9.25	151.08	9.71	56.5%	58.5%	57.4%
47	n-aIR-sn.XY	98.23	5.69	95.62	5.87	58.2%	59.4%	58.7%
48	aIL-prn-aIR	77.95	5.45	78.55	5.61	53.0%	51.2%	52.1%
49	aIL-prn-aIR.XZ	78.86	5.61	79.53	5.77	53.6%	51.3%	52.5%
50	aIL-prn-aIR.XY	157.34	10.44	156.61	10.26	50.6%	51.7%	51.1%
51	aIL-sn-aIR	111.70	7.88	115.03	8.44	58.8%	57.1%	58.0%
52	aIL-sn-aIR.XZ	144.32	8.96	143.06	9.05	52.1%	53.3%	52.7%
53	aIL-sn-aIR.XY	118.95	8.83	123.72	9.21	60.7%	61.1%	60.9%
54	prn-aIL-sn	48.58	4.72	46.42	4.56	56.0%	61.2%	58.5%
55	prn-aIL-sn.YZ	70.40	8.24	67.33	8.33	54.9%	59.0%	56.8%
56	prn-aIL-sn.XZ	32.82	4.29	31.76	4.19	52.7%	58.5%	55.4%
57	prn-aIL-sn.XY	42.39	5.64	40.30	5.52	56.4%	58.9%	57.6%
58	prn-aIR-sn	47.97	4.67	46.04	4.56	54.8%	61.7%	58.0%
59	prn-aIR-sn.YZ	70.86	8.52	68.17	8.85	54.3%	59.7%	56.8%
60	prn-aIR-sn.XZ	32.64	4.18	31.77	4.16	51.4%	57.8%	54.4%
61	prn-aIR-sn.XY	41.32	5.64	39.38	5.54	55.7%	58.3%	56.9%
62	cphL-ls-cphR	141.79	8.79	141.57	8.28	53.7%	48.2%	51.1%
63	cphL-ls-cphR.XY	145.65	9.76	145.26	9.19	53.1%	49.3%	51.3%
64	cphL-li-cphR	39.73	7.51	41.67	8.28	59.0%	51.2%	55.4%
65	cphL-li-cphR.XY	40.31	7.64	42.61	8.52	60.0%	52.2%	56.3%
66	ls-chR-li	29.05	4.58	29.81	5.16	54.7%	51.4%	53.1%
67	ls-chR-li.XY	31.67	5.07	32.14	5.77	53.0%	50.5%	51.8%
68	ls-chL-li	29.25	4.63	29.93	5.21	54.3%	51.1%	52.8%
69	ls-chL-li.XY	32.13	5.17	32.51	5.84	52.3%	50.0%	51.2%
70	chR-ls-chL	113.57	5.34	112.36	5.56	55.8%	53.6%	54.8%
71	chR-ls-chL.XY	148.94	7.55	149.59	7.96	51.3%	51.5%	51.4%
72	chR-li-chL	122.72	6.14	122.92	6.45	51.6%	50.5%	51.1%
73	chR-li-chL.XY	147.27	7.96	145.75	8.66	52.9%	54.5%	53.7%
74	chR-sn-chL	91.67	6.57	88.31	6.28	58.7%	61.2%	59.8%
75	chR-sn-chL.XY	103.10	8.70	99.69	8.47	56.0%	59.3%	57.6%
76	chR-pg-chL	85.10	6.32	83.96	6.91	53.7%	53.6%	53.7%
77	chR-pg-chL.XY	87.70	6.76	85.60	7.33	56.0%	55.3%	55.7%
78	pg-li-chL	98.77	4.57	98.06	4.68	52.8%	52.2%	52.5%
79	pg-li-chL.XY	105.70	4.55	106.40	4.82	52.7%	53.6%	53.2%
80	pg-li-chR	100.11	4.47	99.48	4.59	52.7%	52.7%	52.7%
81	pg-li-chR.XY	107.13	5.78	107.96	6.22	54.5%	53.0%	53.8%
82	cphR-pg-cphL	18.70	3.04	19.50	3.35	57.8%	52.3%	55.2%
83	cphR-pg-cphL.XY	19.07	3.08	20.11	3.44	59.0%	53.6%	56.5%
84	exR-pg-exL	50.31	2.48	48.67	2.64	62.5%	62.7%	62.6%
85	exR-pg-exL.XY	51.38	2.64	49.58	2.78	63.1%	63.1%	63.1%
86	enR-pg-enL	20.99	1.78	20.42	1.83	55.3%	56.6%	55.9%
87	enR-pg-enL.XY	21.26	1.82	20.66	1.86	55.7%	56.8%	56.2%
88	sn-pg-chL	47.57	4.05	46.58	4.37	56.0%	53.3%	54.8%
89	sn-pg-chL.XY	43.69	3.66	42.69	3.92	55.8%	54.9%	55.4%
90	sn-pg-chR	47.74	3.93	46.69	4.24	55.4%	54.5%	55.0%
91	sn-pg-chR.XY	44.01	3.52	42.92	3.80	56.1%	55.4%	55.8%
92	pg-sn-chL	51.05	4.80	48.62	4.52	57.8%	63.0%	60.3%
93	pg-sn-chL.XY	50.78	4.46	49.10	4.38	55.8%	59.8%	57.7%
94	pg-sn-chR	52.42	4.82	49.94	4.45	57.9%	62.7%	60.2%
95	pg-sn-chR.XY	52.32	4.51	50.59	4.34	56.0%	59.4%	57.6%
96	enL-exL-chL	72.02	3.46	73.85	3.58	60.7%	60.9%	60.8%
97	enL-exL-chL.XY	73.45	3.35	75.26	3.45	60.7%	61.3%	61.0%
98	enR-exR-chR	72.10	3.36	72.98	3.51	55.8%	54.1%	55.0%
99	enR-exR-chR.XY	73.71	3.25	74.60	3.38	56.3%	54.7%	55.6%
100	g-exL-chL	95.43	3.76	94.41	3.86	55.5%	55.7%	55.6%
101	g-exL-chL.XY	100.29	3.59	99.91	3.67	51.8%	51.9%	51.8%
102	g-exL-chL.YZ	125.82	6.08	121.64	6.52	63.6%	63.5%	63.6%
103	g-exR-chR	96.00	3.81	94.63	3.82	57.5%	57.6%	57.6%
104	g-exR-chR.XY	101.18	3.61	100.44	3.62	54.4%	53.8%	54.1%
105	g-exR-chR.YZ	125.47	6.06	120.86	6.40	63.8%	64.8%	64.3%

106	men-prn-pg	109.65	4.48	107.31	4.52	59.6%	60.1%	59.8%
107	men-prn-pg.XY	180.68	3.04	180.75	3.15	49.7%	49.8%	49.8%
108	men-prn-pg.YZ	109.68	4.48	107.34	4.52	59.6%	60.2%	59.9%
109	g-prn-pg	138.38	4.90	136.04	5.10	59.4%	59.8%	59.6%
110	g-prn-pg.XY	180.07	1.87	180.13	2.00	50.0%	50.9%	50.4%
111	g-prn-pg.YZ	138.42	4.90	136.07	5.10	59.5%	59.7%	59.6%
112	exL-pg-exR	50.31	2.48	48.67	2.64	62.5%	62.7%	62.6%
113	exL-pg-exR.XY	51.38	2.64	49.58	2.78	63.1%	63.1%	63.1%
114	exL-men-exR	165.56	3.96	166.76	3.77	55.1%	56.4%	55.7%
115	exL-men-exR.XZ	166.01	4.03	167.23	3.84	55.7%	56.0%	55.8%
116	g-men-pg	136.51	6.05	131.39	6.41	66.1%	65.4%	65.8%
117	g-men-pg.XY	179.31	2.38	179.28	2.57	53.3%	46.1%	49.9%
118	g-men-pg.YZ	136.55	6.06	131.42	6.42	66.2%	65.6%	65.9%
<b>Ratios (n = 42)</b>								
1	g-n/prn-pg.z	0.0629	0.0657	0.0549	0.0637	46.0%	59.2%	52.2%
2	g-n/prn-mch.z	0.0438	0.0436	0.0422	0.0474	46.0%	56.4%	50.9%
3	en/ch.x	0.6437	0.0677	0.6510	0.0681	54.3%	49.3%	52.0%
4	Inv.en/ch.x	1.5706	0.1649	1.5530	0.1622	49.9%	53.6%	51.6%
5	en/al.x	1.0409	0.0938	0.9983	0.0922	57.6%	60.8%	59.1%
6	Inv.en/al.x	0.9686	0.0884	1.0103	0.0937	62.0%	56.8%	59.6%
7	ex-enL/ls-cphL.x	4.4476	0.7268	4.0651	0.6983	57.4%	66.0%	61.5%
8	Inv.ex-enL/ls-cphL.x	0.2308	0.0373	0.2529	0.0416	65.0%	59.3%	62.4%
9	ex-enR/ls-cphR.x	4.4520	0.7367	4.0450	0.7116	56.9%	67.3%	61.8%
10	Inv.ex-enR/ls-cphR.x	0.2306	0.0371	0.2541	0.0411	63.6%	60.5%	62.1%
11	en-exL/al.x	0.8203	0.0750	0.7680	0.0704	63.0%	66.1%	64.4%
12	Inv.en-exL/al.x	1.2293	0.1126	1.3131	0.1215	66.6%	61.8%	64.4%
13	en-exR/al.x	0.8256	0.0723	0.7722	0.0686	63.7%	66.5%	65.0%
14	Inv.en-exR/al.x	1.2205	0.1069	1.3052	0.1168	67.7%	62.6%	65.3%
15	men-sn/men-pg.z	1.5216	0.3829	1.7278	0.4666	69.4%	51.4%	60.9%
16	Inv.men-sn/men-pg.z	0.6934	0.1550	0.6138	0.1409	59.2%	62.9%	60.9%
17	men-sn/men-pg.y	0.4624	0.0265	0.4589	0.0280	51.9%	53.8%	52.8%
18	Inv.men-sn/men-pg.y	2.1697	0.1254	2.1874	0.1334	54.1%	52.0%	53.1%
19	n/cph.x	2.8085	0.4608	2.6243	0.4646	54.0%	63.5%	58.5%
20	Inv.en/cph.x	0.3653	0.0580	0.3919	0.0641	61.1%	57.4%	59.3%
21	<b>sn-ls/g-n.y</b>	<b>1.1398</b>	<b>0.3142</b>	<b>1.4163</b>	<b>0.4186</b>	<b>73.2%</b>	58.2%	66.1%
22	Inv.sn-ls/g-n.y	0.9415	0.2524	0.7621	0.2087	61.1%	70.0%	65.3%
23	Ang.exL-chL/exR-chR	29.9762	3.8490	28.6215	3.8431	58.5%	57.9%	58.2%
24	Ang.exL-chL/exR-chR.XY	30.4613	3.9938	29.1440	3.9875	57.7%	57.6%	57.7%
25	Ang.exL-exR/chL-chR	2.0962	1.2116	2.0225	1.1560	45.3%	57.1%	50.8%
26	Ang.exL-exR/chL-chR.XY	1.2939	1.0305	1.2627	1.0082	42.3%	58.5%	49.9%
27	n-alL/n-alR	0.9957	0.0256	0.9961	0.0262	50.4%	49.3%	49.9%
28	n-chL/n-chR	0.9992	0.0182	0.9998	0.0169	52.1%	50.4%	51.3%
29	enL-enR/alL-alR	1.0407	0.0936	0.9982	0.0920	57.8%	61.0%	59.3%
30	enL-enR/chL-chR	0.6439	0.0677	0.6513	0.0681	54.2%	49.1%	51.8%
31	enL-sn/enR-sn	1.0079	0.0261	1.0101	0.0280	53.0%	49.2%	51.2%
32	exL-prn/exR-prn	1.0003	0.0326	0.9983	0.0335	51.0%	51.8%	51.3%
33	exL-sn/exR-sn	1.0011	0.0295	0.9982	0.0311	52.6%	51.6%	52.1%
34	exL-chL/exR-chR	1.0044	0.0308	0.9991	0.0297	53.6%	55.7%	54.6%
35	exL-pg/exR-pg	0.9976	0.0175	0.9947	0.0174	53.8%	53.9%	53.8%
36	exL-alL/exR-alR	1.0062	0.0399	1.0002	0.0405	53.0%	54.2%	53.6%
37	exL-exR/chL-chR	1.6595	0.1258	1.6536	0.1277	49.0%	54.2%	51.4%
38	prn-chL/prn-chR	0.9976	0.0315	0.9990	0.0305	51.9%	50.9%	51.4%
39	sn-chL/sn-chR	0.9938	0.0450	0.9966	0.0435	52.8%	49.4%	51.2%
40	alL-alR/chL-chR	0.6199	0.0507	0.6540	0.0558	65.9%	61.7%	63.9%
41	cphL-pg/cphR-pg	0.9914	0.0143	0.9911	0.0141	50.8%	51.0%	50.9%
42	chL-pg/chR-pg	0.9775	0.0328	0.9783	0.0318	52.5%	49.6%	51.1%

**Total number of facial parameters = 250**

**Distances (90)**

**Angles (118)**

**Ratios (42)**

**Highlighted cells indicate facial parameters with gender prediction efficiency >70% (23 distances, 1 ratio), explained and summarized in Chapter 6.**

**Three of the distances (their sequence number is shown in red) were needed to support the discussion of Chapter 4.**

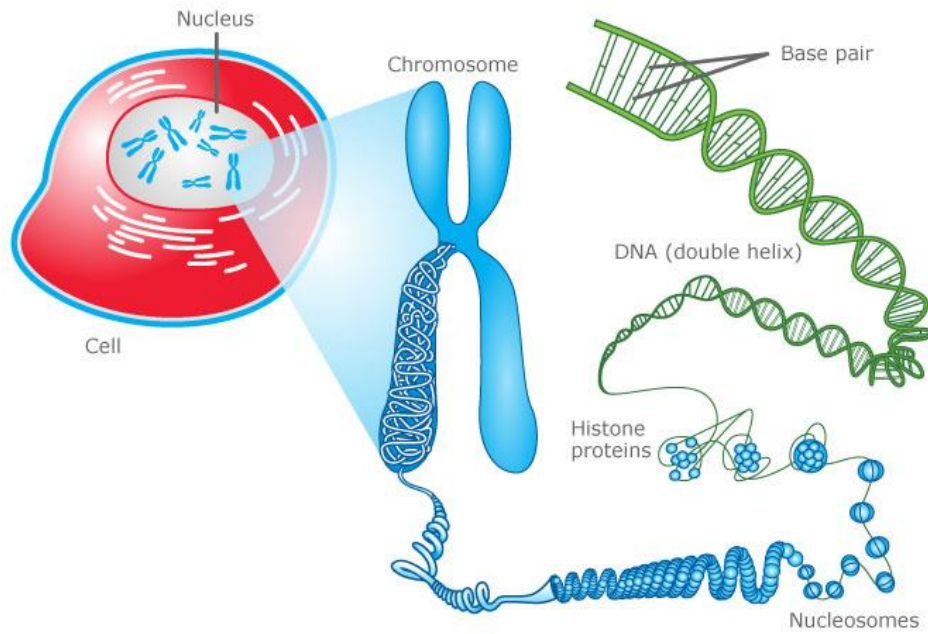


Figure 1  
Overview of the human cell nucleus, chromosome structure and DNA

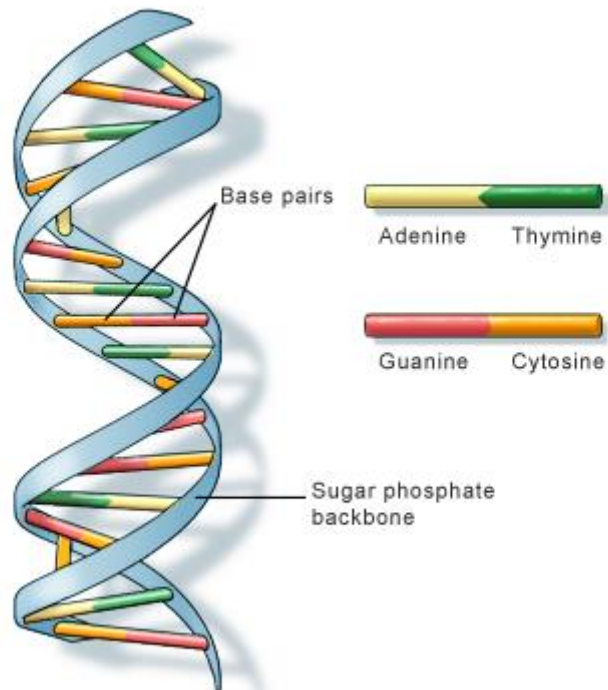


Figure 2  
The base pair structure of DNA

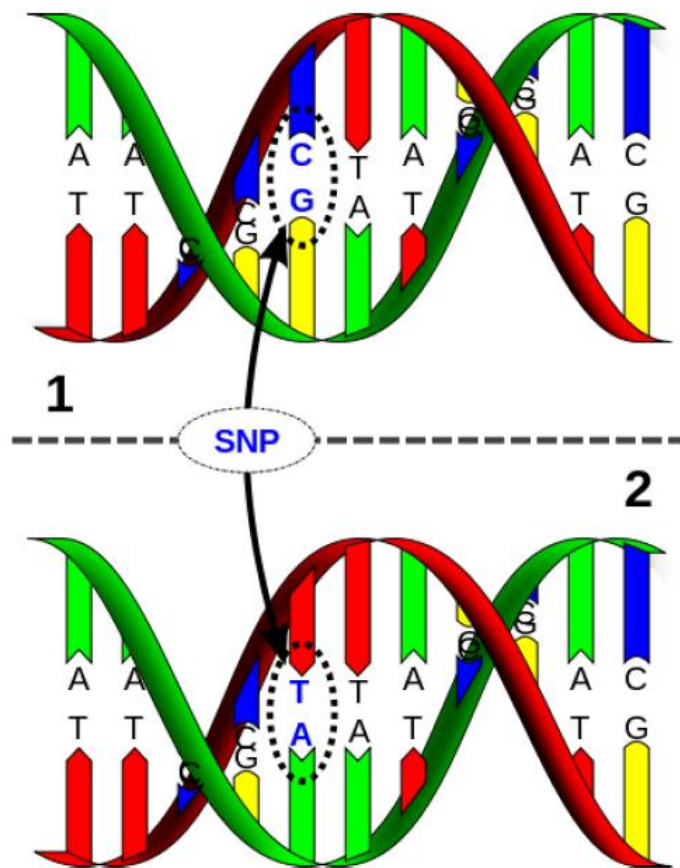


Figure 3  
A single-nucleotide polymorphism (SNP), a DNA sequence variation occurring in a single base pair over the human population

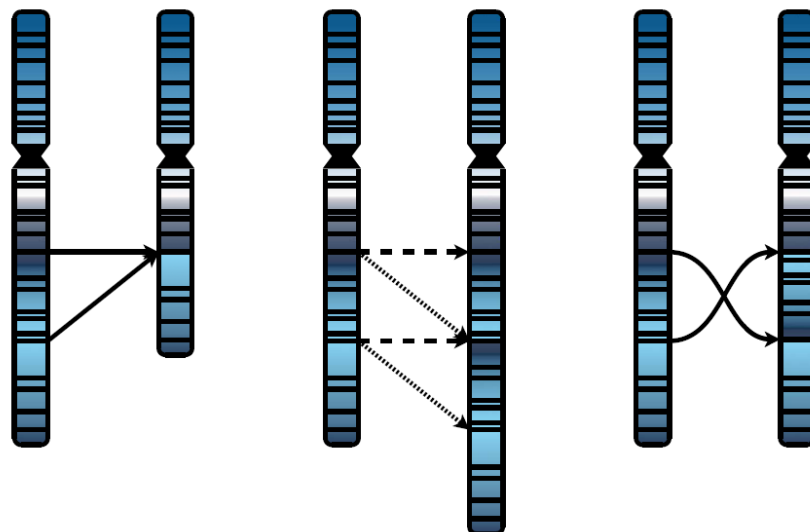


Figure 4  
Copy-number variation, showing from left (deletions, duplications, inversions)

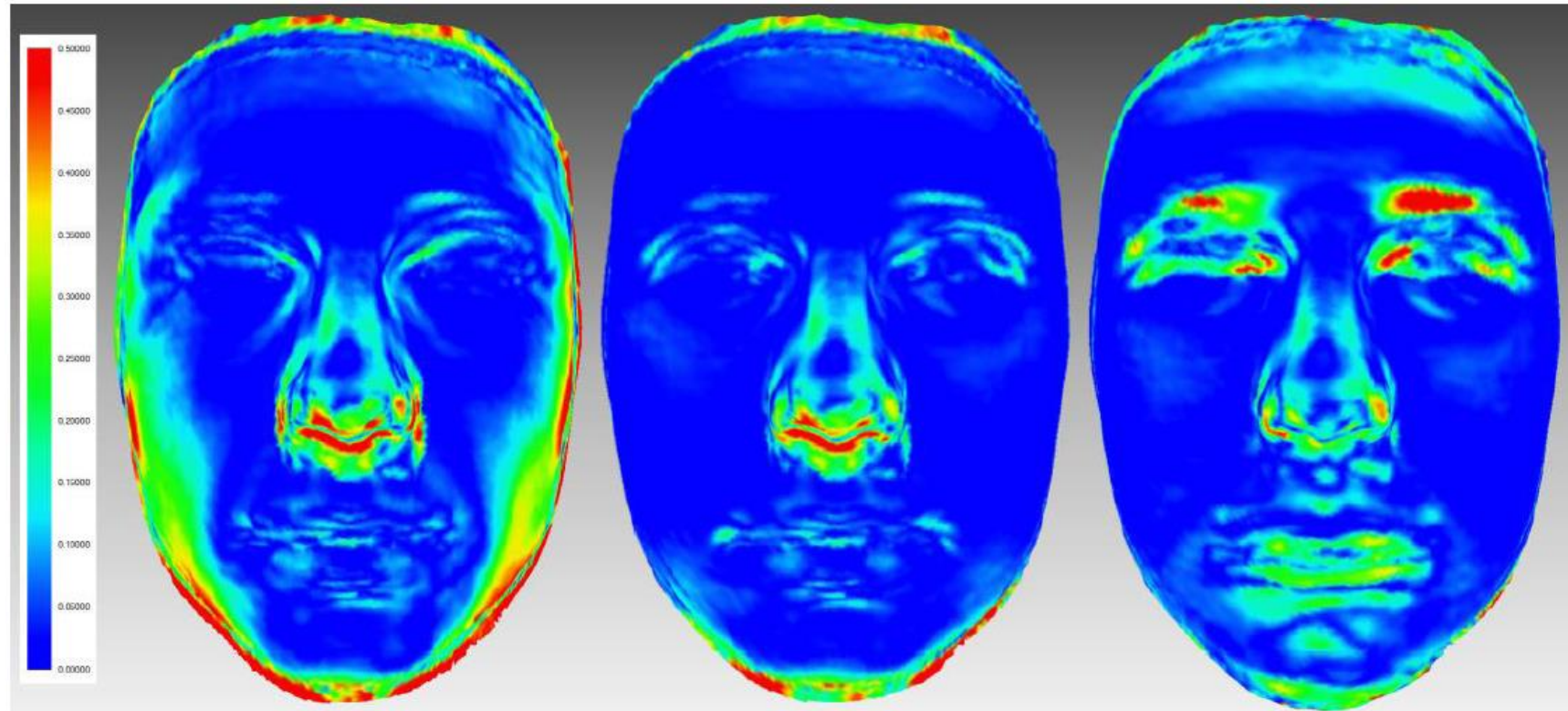


Figure 5

Comparison of the average faces obtained by the Z-coordinate, cylindrical radial and spherical radial averaging methods versus the one obtained by the iterative template averaging method. Absolute-colour deviation maps show respective differences (left to right); range of deviations from 0 to 0.5 mm (Zhurov *et al.*, 2010)

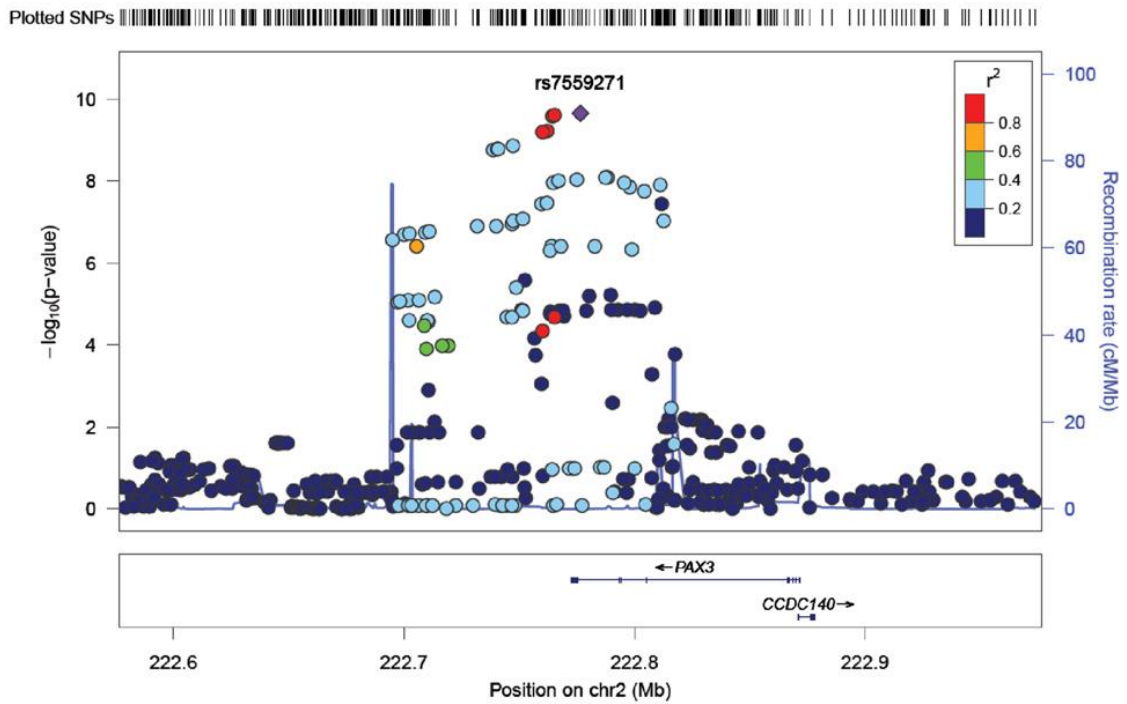


Figure 6  
Association 'Manhattan' plot of the region surrounding *PAX3* for the nasion-to-midendocanthion 3D distance in the discovery phase (rs7559271 and n-men genetic association)

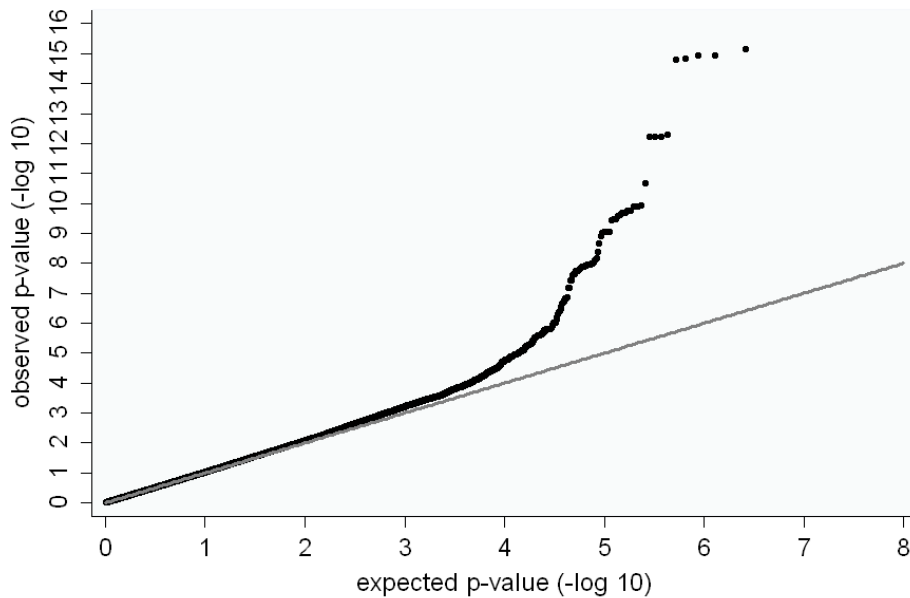


Figure 7  
Association 'QQ' plot for rs7559271 in *PAX3* gene and n-men 3D distance in the combined (all ALSPAC individuals) sample, 2nd round GWAS